Tropical paleoclimate reconstructions from stable isotopes of mangrove lipid biomarkers

Sarah Nemiah Ladd

A dissertation
submitted in partial fulfillment of the
requirements for the degree of

Doctor of Philosophy

University of Washington

2014

Reading Committee:

Julian Sachs, Chair

Anitra Ingalls

Paul Quay

Program Authorized to Offer Degree:

Oceanography

University of Washington

Abstract

Tropical paleoclimate reconstructions from stable isotopes of mangrove lipid biomarkers

Sarah Nemiah Ladd

Chair of the Supervisory Committee:

Prof. Julian Sachs, PhD
Oceanography

Tropical oceans play an integral role in global climate dynamics, yet past tropical hydrologic variability is poorly constrained, as many established climate proxies are better suited to higher latitudes. Hydrogen isotope ratios ($^{2}H/^{1}H$) of leaf waxes are a promising new proxy. Previous field assessments have been conducted in temperate regions or in continental interiors. On tropical coastlines, mangroves are a major source of organic matter to sediments. Unlike other higher plants, mangroves grow in saline water, which is known to influence ^{2}H fractionation in algal lipids. In order to use $^{2}H/^{1}H$ ratios of leaf lipids in coastal tropical sediments, it was thus necessary to assess salinity's effect on ^{2}H fractionation in mangroves.

In field calibrations of *Avicennia marina* from subtropical Australia and *Rhizophora* spp. from Micronesia, salinity strongly affected net ^{2}H fractionation in mangrove lipids. A unit increase in salinity resulted in an increase of 1.5 ± 0.3‰ in *n*-alkane fractionation in *A. marina*

(Chapter 2) and 0.9 ± 0.2‰ in the *Rhizophora* biomarker taraxerol (Chapter 4). In the same *A. marina n*-alkanes, carbon isotope fractionation decreased by 0.2 ± 0.05‰ PSU^{-1} (Chapter 3).

$^{2}H/^{1}H$ and $^{18}O/^{16}O$ ratios of leaf and xylem water from Micronesian *Rhizophora* and from a 9.5-month time series of 3 mangrove species from subtropical Australia were used to investigate mechanisms responsible for the H-isotope response. Salinity does not cause changes in leaf water enrichment. Rather, changes in net ^{2}H fractionation are best explained by biochemical responses to salinity, such as compatible solute production or increased use of stored carbohydrates, or by the timing of production of leaves and leaf lipids (Chapters 4 and 5).

Mangroves and algae have opposite H isotope responses to salinity. By pairing $^{2}H/^{1}H$ ratios of mangrove and algal biomarkers, it is possible to calculate past changes in salinity and water isotopes. Initial applications of this approach to an 800-year sedimentary record from Palau demonstrate significant drying during the Little Ice Age (~1400 - ~1800 AD) (Chapter 6).

Acknowledgements

First and foremost, I would like to thank my advisor, Julian Sachs, for his enthusiastic support of this project over the past five and half years. This work would not have been possible without Julian's belief in its importance and his tireless pursuit of the necessary funds. Julian was involved in all the fieldwork for this project and collected the Mobbs Bay sample set during his sabbatical in Australia. He has provided comments on multiple drafts of each chapter in this thesis, and has been intellectually engaged in this work throughout its completion.

My committee members – Anitra Ingalls, Paul Quay, Chuck Nittrouer, and Liz van Volkenburgh – have also contributed to intellectually to this project and help frame its scope. They have asked good questions and helped me stay focused on the main objectives. Each has brought their own unique insights from their diverse backgrounds and improved the quality of my work.

The Oceanography staff, in particular Su Tipple and April Timer, has been extremely helpful over the years. International fieldwork in remote locations, shipping samples around the globe, and submitting grant proposals appropriately would not be possible without the hard work of our staff. Miriam Bertram of the Program on Climate Change has enriched my time at UW by creating a vibrant, interdisciplinary community focused on all aspects of climate science.

The Sachs lab has been a collaborative place to work, and I have benefited from discussions and daily interactions with my fellow graduate students: Alyssa Atwood, Dan Nelson, Ashley Maloney, Tessa McGee, and Marta Wolfshorndl. Ines Mugler and Julie Richey were helpful mentors during their time as post-docs in our lab, and Julie oversaw most of the initial work on the Clear Lake sediment core. Our former lab manager Orest Kawka, and our

current lab manager Josh Gregersen, have kept our lab running and facilitated the analytical and field components of this project.

I was fortunate to have the opportunity to work with several fantastic undergraduates on various aspects of this project. In particular, Tory Johnson helped with much of the lab work for the Brisbane and Micronesian projects, while Ariel Townsend processed the majority of the Mobbs Bay samples. Johnny Huang assisted with the Clear Lake sediment core.

I am grateful to the fantastic community of graduate students within Oceanography and the Program on Climate Change. I have learned so much from all of my peers and developed great friendships with many of them. In particular, the inhabitants and frequent guests of 321 NE 54th St. have been an integral part of my graduate experience, and I cannot imagine completing a PhD without their ongoing support and companionship.

Ansgar Kahmen at the University of Basel hosted me during the final year of my graduate studies, and the leaf and xylem water extractions and analyses were completed in his laboratory. Ansgar also provided many useful insights for the interpretation of the Micronesian and Mobbs Bay data.

Finally, I would like to acknowledge my husband, Dan Nelson. Dan has engaged in many discussions about this project, helped me trouble shoot instruments and pack for the field, and provided moral support when things did not go as planned. He has helped me keep my perspective and enriched my life immeasurably.

Table of Contents:

List of Figures

Chapter 1: Introduction

1.1 Background and motivation

The tropics play an integral role in global climate dynamics. Radiative imbalances at low-latitudes provide the energy that drives Earth's global circulation, and deep convection in the tropics is a major source of moisture to the atmosphere (*Wang & Enfield, 2003; Chiang, 2009*). Small changes in tropical sea surface temperature (SSTs) and precipitation anomalies, such as those associated with the El Niño – Southern Oscillation, have far reaching effects (*Wallace & Gutzler, 1981; Pierrehumbert, 2000; Wang & Mehta, 2008; Chiang, 2009*). Climate models predict that global warming will influence precipitation patterns in the tropics, with regions that are currently wet becoming wetter and dry regions becoming drier (*Held & Soden, 2006*). Models also predict a weakening of Pacific Walker Circulation, resulting in a more "El Niño-Like" mean state in the tropical Pacific (*Vecchi et al., 2006).* However, models do not fully capture modern climate variability in the tropical Pacific.

Studying past climate change can improve understanding of the climate dynamics and better constrain natural variability of this system. Unfortunately, past tropical climate variability remains poorly understood, as many well-studied archives of past environmental conditions, such as tree rings and ice cores, are more commonly found at mid to high latitudes. Many climate records that do exist from marine tropical locations are from marine sediments (e.g. *Koutavas et al., 2002; Lea et al., 2006; Herbert et al, 2010*), where slow accumulation rates preclude reconstructions of centennial to decadal variability. Climate proxies that can be applied in more rapidly accumulating marine tropical locations, such as low elevation lakes and swamps on islands, are thus important for addressing this information gap.

1.2 Lipid hydrogen isotope proxy

Hydrogen isotope ratios ($^2H/^1H$, typically expressed as $\delta^2H = (((^2H/^1H_{Sample})/(^2H/^1H_{VSMOW}) - 1)$ of leaf waxes have recently been developed as a paleoclimate proxy (*Sachse et al., 2012,* and sources therein). Over large spatial gradients, leaf wax δ^2H values, δ^2H_{Wax}, are well correlated with those of precipitation, δ^2H_{Precip} (*Sachse et al., 2004; Polissar & Freeman, 2010; Sachse et al., 2012; Tipple & Pagani, 2013*). Sedimentary δ^2H_{Wax} can thus provide useful information about past environmental conditions, as δ^2H_{Precip} is strongly influenced by temperature, precipitation rates, and moisture sources (*Dansgaard, 1964; Craig & Gordon, 1965; Gat, 1996*). In marine tropical settings, the amount of precipitation is the dominant control on δ^2H_{Precip}, with low δ^2H_{Precip} values strongly correlated to wetter climates (*Dansgaard, 1964; Rozanski et al., 1993; Kurita et al., 2009; Conroy et al., 2013*).

The δ^2H values of leaf waxes and other lipids are typically depleted in ^2H relative to the plant's source water (*Sessions et al., 1999; Sauer et al., 2001; Chikaraishi & Naraoka, 2003; Sachse et al., 2012*). The difference between lipid and source water δ^2H values is expressed using the net fractionation factor $\alpha_{Lipid\text{-}Water} = (^2H/^1H_{Lipid})/(^2H/^1H_{Water}) = (\delta^2H_{Lipid} + 1000)/(\delta^2H_{Water} + 1000)$. While $\alpha_{Lipid\text{-}Water}$ encompasses the overall offset between source water and lipids, it is composed of several smaller fractionation factors. These include evaporative enrichment of leaf water ($\alpha_{LW\text{-}Water}$) and biosynthetic fractionation that occurs when lipids are synthesized using leaf water ($\alpha_{Lipid\text{-}LW}$).

A number of environmental variables influence the magnitude of $\alpha_{Lipid\text{-}Water}$ in trees and other vascular plants. These include relative humidity (*Feakins & Sessions, 2010; Kahmen et al., 2013a; Kahmen et al., 2013b; Tipple et al., 2014*), which reduces evaporative enrichment of leaf water (*Helliker & Ehrlinger, 2002a; Helliker & Ehlinger, 2002b; Farquhar & Cernusak, 2005*).

Plant type can also influence $\alpha_{Lipid\text{-}Water}$, with differences in isotope fractionation being observed between mosses and woody plants (*Sachse et al., 2006*), between woody plants and grasses (*Liu et al., 2006; Hou et al., 2007*), and between C_3 and C_4 plants (*Smith & Freeman, 2006; McInerney et al., 2011*). Light levels can also influence $\alpha_{Lipid\text{-}Water}$ (*Liu & Yang, 2008; Yang et al., 2009*).

Despite all these sources of variability in $\alpha_{Lipid\text{-}Water}$ for individual plants, large-scale field calibrations have consistently demonstrated that δ^2H_{Wax} is a good proxy for δ^2H_{Precip}. Past field assessments have been primarily based in mid-latitudes (e.g. *Sachse et al., 2004; Hou et al., 2008; Feakins & Sessions, 2010; Tipple & Pagani, 2013*). Those that have occurred in the tropics have been from continental interiors (*Polissar & Freeman, 2010; Kahmen et al., 2013a*).

Mangroves cover more than 15m hectares of tropical and subtropical coastlines (*Spalding, 2010*). Mangroves are highly productive ecosystems and have been estimated to contribute 10 – 15% of the total terrestrial carbon accumulating in modern marine sediments (*Jennerjahn & Ittekkot, 2002; Dittmar et al., 2006*). As such, they are likely a major contributor of leaf waxes and other plant lipids that are found in coastal sediments at low latitudes.

Unlike other higher plants, mangroves grow in brackish to hypersaline water. Increasing salinity results in less ^2H fractionation in algal lipids (*Schouten et al., 2006; Sachse & Sachs, 2008; Sachs & Schwab, 2011; Nelson & Sachs, 2014*). In order to use $^2H/^1H$ ratios of leaf lipids in coastal tropical sediments, it was thus necessary to assess salinity's effect on ^2H fractionation in mangroves. The major goals of this project were to (1) determine what, if any, effect salinity has on isotope fractionation in mangroves lipids, (2) investigate potential mechanisms for this response, and (3) use isotope ratios of mangroves lipids to reconstruct past hydrologic change in the Western Pacific Warm Pool over the past millennium.

1.3 Chapter Overview

Chapter 2 presents the results of an initial field calibration of the influence of salinity on ^{2}H fractionation in the mangrove *Avicennia marina*. Along a salinity gradient of 6-35 in the Brisbane River Estuary in southern Queensland, Australia, the magnitude of net fractionation in *A. marina* leaf wax *n*-alkanes increased by 1.5 ± 0.3‰ per unit increase in salinity. This is the opposite response of that seen in algae, where increasing salinity results in less net ^{2}H fractionation (*Schouten et al., 2006; Sachse & Sachs, 2008; Sachs & Schwab, 2011; Nelson & Sachs, 2014*). Three hypotheses to explain increased ^{2}H fractionation in mangroves were proposed: (1) preferential exclusion of ^{2}H by roots during water uptake, (2) increased compatible solute production, resulting in more relatively depleted H^{+} from NADPH being incorporated into lipids, or (3) increased salt secretion at high salinity, which could decrease the $\delta^{2}H_{LW}$ by creating a layer of isotopically depleted water hydrating the salt on the surface of leaves. A major goal of subsequent experiments was to evaluate these hypotheses by measuring the H isotope composition of intermediate xylem and leaf water pools.

Chapter 3 reports carbon isotopes measurements ($\delta^{13}C$ values) of the same leaf wax *n*-alkanes from Brisbane *A. marina*, as well as $\delta^{13}C$ values of bulk leaves and total lipid extracts. ^{13}C fractionation in bulk leaves and leaf wax *n*-alkanes decreases with salinity, most likely because of increased water use efficiency. For *n*-alkanes, a unit increase in salinity was associated with a 0.2 ± 0.05‰ increase in the $\delta^{13}C$ values of *A. marina n*-alkanes. Independent responses to salinity make it possible to quantitatively reconstruct salinity and $\delta^{2}H_{Water}$ by measuring $\delta^{13}C$ and $\delta^{2}H$ values of the same mangrove lipid.

Since it is impossible to identify the source of sedimentary *n*-alkanes in sediment, and since the controls on isotope fractionation in mangroves difference from terrestrial plants, this proxy is best applied with a mangrove specific lipid biomarker. Taraxerol is produced in high abundance *Rhizophora* spp. (red mangroves) (*Killops & Frewin, 1994; Koch et al., 2003; Versteegh et al., 2004*), covaries with *Rhizophora* pollen in coastal sediments (*Versteegh et al., 2004; Kim et al., 2005*), and is relatively refractory (*Koch et al., 2003*). Taraxerol is therefore a promising target lipid. Chapter 4 is a field calibration of salinity's influence on ^{2}H fractionation in taraxerol and *n*-alkanes produced by *Rhizophora* spp. growing along three estuaries on the Micronesian Island of Pohnpei and four marine lakes in Palau. *Rhizophora* displayed a similar hydrogen isotope response to Brisbane *A. marina*, with net ^{2}H fractionation in taraxerol increasing by 0.9 ± 0.2‰ per unit increase in salinity (Chapter 4).

While empirical calibrations are a necessary part of developing a paleoclimate proxy, understanding the mechanism(s) responsible for the observed signal is important for robust applications. In order to better understand the underlying causes that result in more ^{2}H fractionation in mangroves at high salinity, leaf and xylem water $\delta^{2}H$ and $\delta^{18}O$ values were measured in the Micronesian *Rhizophora* sample set (Chapter 4) and from a 9.5-month time series of 3 mangrove species from subtropical Australia (Chapters 5). These studies suggest that most of changes in net ^{2}H fractionation are due to changes in fractionation between leaf water and lipids. Changes in $\alpha_{Lipid\text{-}LW}$ could be due to biochemical responses to salinity, such as compatible solute production or increased use of stored carbohydrates, or by the timing of production of leaves and leaf lipids.

Chapter 6 demonstrates an application of this proxy to sediments from a brackish marine lake in Palau (7°N, 143°W) in the heart of the Western Pacific Warm Pool (WPWP).

Precipitation rates in Palau are influenced by the position of the Intertropical Convergence Zone (ITCZ), a region of deep convection that tracks the warmest SSTs (*Legates and Willmott, 1990; Spencer, 1993; Xie and Arkin, 1997*). Interanual precipitation anomalies are correlated with the Southern Oscillation Index (SOI) (*Xie & Arkin, 1997*).

During the Little Ice Age (LIA; ~1400 - ~1800 AD) δ^2H_{Lipid} values of dinosterol and palmitic acid from three marine lakes in Palau increased, indicate that the region was drier (*Sachs et al., 2009; Smittenberg et al., 2011; Richey & Sachs, in prep*). Since both increasing salinity and the higher δ^2H_{Water} values associated with less rain marine tropical locations such as Palau (*Dansgaard, 1964; Kurita et al., 2009; Smittenberg et al., 2011; Conroy et al., 2013*) will result in higher δ^2H_{Lipid} values of algae lipids, it is not possible to distinguish how much of the algal lipid signal is caused by changes in salinity and how much by changes in δ^2H_{Water}. Since mangroves growing around marine lakes in Palau use the same water as algae, but have an opposite ^2H fractionation response to salinity, it is possible to calculate past changes in salinity and water isotopes by pairing $^2H/^1H$ ratios of mangrove and algal biomarkers. In Chapter 6, I present an 800-year sedimentary record of paired taraxerol and dinosterol δ^2H values in a sediment core from Clear Lake, Palau. Reconstructed salinity and δ^2H_{Water} is complicated in this setting due to potential time-variable non-mangrove taraxerol inputs to the sediment. However, the observed decrease in taraxerol δ^2H values during the LIA is consistent with a reduction in precipitation rates during this time. This result demonstrates that Palau was drier during the LIA, which is consistent with a southward shift in the ITCZ, or strengthening of ENSO activity (defined here as either more frequent or strong El Niño events).

1.4 References

Chiang, J. C. H. (2009) The tropics in paleoclimate. *Annual Review of Earth and Planetary Sciences* 37, 263-297.

Chikaraishi, Y. & Naraoka, H., 2003. Compound-specific δD- δ13C analyses of *n*-alkanes extracted from terrestrial and aquatic plants. Phytochemistry 63, 361-371.

Conroy J. L., Cobb K. M. & Noone D. (2013) Comparison of precipitation isotope variability across the tropical Pacific in observations and SWING2 model simulations. *Journal of Geophysical Research: Atmospheres* 118, 5867-5892.

Craig H. & Gordon L. (1965) Deuterium and oxygen 18 variations in the ocean and the marine atmosphere. In *Proceedings of a Conference on Stable Isotopes in Oceanographic Studies and Paleotemperatures* (ed E. Tongiori). CNR-Laboratorio di Geologia Nucleare, Pisa. pp. 9-130.

Dansgaard W. (1964) Stable isotopes in precipitation. *Tellus* 16, 436-468.

Dittmar T., Hertkorn N., Kattner G. & Lara R.J. (2006) Mangroves, a major source of dissolved organic carbon to the oceans. *Global Biogeochemical Cycles* 20:GB1012, doi:10.1029/2005GB002570.

Farquhar, G. D. & Cernusak, L. A. (2005) On the isotopic composition of leaf water in the non-steady state. *Functional Plant Biology* 32, 293-303.

Feakins S. J. & Sessions A. L. (2010) Controls on the D/H ratios of plant leaf waxes in an arid ecosystem. *Geochimica Cosmochimica Acta* 74, 2128-2141.

Gat, J. R. (1996) Oxygen and hydrogen isotopes in the hydrologic cycle. *Annual Review in Earth and Planetary Sciences* 24, 225-262.

Held, I. M. & Soden, B. J. (2006) Robust responses of the hydrological cycle to global warming, *J. Clim*., 19, 5686–5698.

Helliker, B. R. & Ehleringer, J. R. (2002a) Differential ^{18}O enrichment of leaf cellulose in C_3 versus C_4 grasses. *Functional Plant Biology* 29, 435-442.

Helliker, B. R. & Ehleringer, J. R. (2002b) Grass blades as tree rings: environmentally induced changes in the oxygen isotope ratio of cellulose along the length of grass blades. *New Phytologist* 155, 417-424.

Herbert, T. D., Peterson, L. C., Lawrence, K. T. & Liu, Z. (2010) Tropical ocean temperatures over the past 3.5 million years. *Science* 328, 1530-1534.

Hou, J., D'Andrea, W. & Huang, Y., 2008. Can sedimentary leaf waxes record D/H ratios of continental precipitation? Field, model and experimental assessments. *Geochimica et Cosmochimica Acta* 72, 3503-3517.

Hou J., D'Andrea W., MacDonald D. & Huang Y. S. (2007) Hydrogen isotopic variability in leaf waxes among terrestrial and aquatic plants around Blood Pond, Massachusetts (USA). *Organic Geochemistry* 38, 977-984.

Jennerjahn T.C. & Ittekot V. (2002) Relevance of mangroves for the production and deposition of organic matter along tropical continental margins. *Naturwissenschaften* 89, 23-30.

Kahmen A., Hoffmann B., Schefuss E., Arndt S. K., Cernusak L. A., West J. B. & Sachse D. (2013a) Leaf water deuterium enrichment shapes leaf wax n-alkane dD values of angiosperm plants II: Observational evidence and global implications. *Geochimica et Cosmochimica Acta* 111, 50-63.

Kahmen A., Schefuss E. & Sachse D. (2013b) Leaf water deuterium enrichment shapes leaf wax *n*-alkane dD values of angiosperm plants I: Experimental evidence and mechanistic insights. *Geochimica et Cosmochimica Acta* 111, 39-49.
Killops S. D. & Frewin N. L. (1994) Triterpenoid diagenesis and cuticular preservation. *Organic Geochemistry* 21, 1193-1209.
Kim, J., Dupont, L., Behling, H., Versteegh, G., 2005. Impacts of rapid sea-level rise on mangrove deposit erosion: application of taraxerol and *Rhizophora* records. *Journal of Quaternary Science* 20, 221-225.
Koch B. P., Rullkotter J., & Lara R. J. (2003) Evaluation of triterpenols and sterols as organic matter biomarkers in a mangrove ecosystem in northern Brazil. *Wetlands Ecology and Management* 11, 257-263.
Koutavas, A., Lynch-Stieglitz, J., Marchitto, T.M., Sachs, J.P., 2002. El Nino-like pattern in ice age tropical Pacific sea surface temperature. *Science* 297, 226-230.
Kurita N., Ichiyanagi K., Matsumoto J., Yamanaka M. D. & Ohata T. (2009) The relationship between the isotopic content of precipitation and the precipitation amount in tropical regions. *Journal of Geochemical Exploration* 102, 113-122.
Lea, D. W., Pak, D. K., Belanger, C. L., Spero, H. J., Hall, M. A. & Shackleton, N. J. (2006) Paleoclimate history of Galapagos surface waters over the last 135,000 yr. *Quaternary Science Reviews* 25, 1152-1167.
Legates, D. R. & Willmott, C. J. (1990) Mean seasonal and spatial variability in gauge-corrected, global precipitation. *Int. J. Climatol*. 10, 111-127
Liu W. G. & Yang H. (2008) Multiple controls for the variability of hydrogen isotopic compositions in higher plant *n*-alkanes from modern ecosystems. *Global Change Biology* 14, 2166-2177.
Liu W. G., Yang H. & Li L. (2006) Hydrogen isotopic composition of *n*-alkanes from terrestrial plants correlate with their ecological life form. *Oecologia* 150, 330-338.
McInerney, F. A., Helliker, B. R. & Freeman, K. H. (2011) Hydrogen isotope ratios of leaf wax *n*-alkanes in grasses are insensitive to transpiration. *Geochimica et Cosmochimica Acta* 75, 541-554.
Nelson, D. B. & Sachs, J. P. (2014) The influence of salinity on D/H fractionation in dinosterol and brassicasterol from globally distributed saline and hypersaline lakes. *Geochimica et Cosmochimica Acta*, 133, 325-339.
Pierrehumbert R. T. (2000) Climate change and the tropical Pacific: The sleeping dragon wakes. *Proc. Natl. Acad. Sci.* 97, 1355–1358
Polissar P. J. & Freeman K. H. (2010) Effects of aridity and vegetation on plant-wax δD in modern lake sediments. *Geochimica et Cosmochimica Acta* 74, 5785-5797.
Richey, J. N. & Sachs, J. P. (in prep) "Precipitation in the western tropical Pacific over the past millenium."
Rozanski, K., Araguas-Araguas, L., and Gonfiantini, R., 1993. Isotopic patterns in modem global precipitation. In "Climate Change in Continental Isotopic Records - Geophysical Monograph 78." (P. K. Swart, K. C. Lohman, J. McKenzie, and S. Savin, Eds.), pp. 1-36. American Geophysical Union, Washington, D.C.
Sachs, J. P., Sachse, D., Smittenberg, R. H., Zhang, Z., Battisti, D. S. & Golubic, S. (2009) Southward movement of the Pacific intertropical convergence zone AD 1400–1850. *Nature Geoscience* 2, 519-525.
Sachs, J. P. & Schwab, V. F. (2011) Hydrogen isotopes in dinosterol from the Chesapeake Bay

estuary. *Geochimica et Cosmochimica Acta* 75, 444-459.
Sachse D., Billault I., Bowen G. J., Chikaraishi Y., Dawson T. E., Feakins S. J., Freeman K. H., Magill C. R., McInerney F. A., van der Meer M. T. J., Polissar P., Robins R. J., Sachs J. P., Schmidt H. L., Sessions A. L., White J. W. C., West. J. B. & Kahmen A. (2012) Molecular paleohydrology: interpreting the hydrogen-isotopic composition of lipid biomarkers from photosynthesizing organisms. *Annual Review of Earth and Planetary Science* 40, 212-249.
Sachse D., Radke J. & Gleixner G. (2004) Hydrogen isotope ratios of recent lacustrine sedimentary *n*-alkanes record modern climate variability. *Geochimica et Cosmochimica Acta* 68, 4877-4889.
Sachse, D., Radke, J. & Gleixner, G. (2006) δD values of individual *n*-alkanes from terrestrial plants along a climatic gradient – Implications for the sedimentary biomarker record. Organic Geochemistry 37, 469-483.
Sachse, D., & Sachs, J. P. (2008) Inverse relationship between D/H fractionation in cyanobacterial lipids and salinity in Christmas Island saline ponds. *Geochimica et Cosmochimica Acta, 72*(3), 793-806.
Sauer P. E., Eglinton T. I., Hayes J. M., Schimmelmann A., Sessions A. L. (2001) Compound-specific D/H ratios of lipid biomarkers from sediments as a proxy for environmental and climatic conditions. *Geochimica et Cosmochimica Acta* 65, 213-222.
Schouten, S., Ossebaar, J., Schreiber, K., Kienhuis, M. V. M., Langer, G., Benthien, A., Bijma & J. (2006) The effect of temperature, salinity and growth rate on the stable hydrogen isotopic composition of long chain alkenones produced by *Emiliania huxleyi* and *Gephyrocapsa oceanica*. *Biogeosciences* 3, 113-119.
Sessions A. L., Burgoyne T. W., Schimmelmann A. & Hayes J. M. (1999) Fractionation of hydrogen isotopes in lipid biosynthesis. *Organic Geochemistry* 30, 1193-1200.
Smith F. A. & Freeman K. H. (2006) Influence of physiology and climate on δD of leaf wax *n*-alkanes from C_3 and C_4 grasses. *Geochimica et Cosmochimica Acta* 70, 1172-1187.
Smittenberg, R. H., Saenger, C., Dawson, M. N. & Sachs, J. P. (2011). Compound-specific D/H ratios of the marine lakes of Palau as proxies for West Pacific Warm Pool hydrologic variability. *Quaternary Science Reviews* 30, 921-933.
Spalding, M., Kainuma, M., & Collins, L. (2010) *World atlas of mangroves*. Washington, D.C., Earthscan.
Spencer, R.W. (1993) Global oceanic precipitation from the MSU during 1979-91 and comparisons to other climatologies. *J. Clim*. 6, 1301-1326.
Tipple B. J., Berke M., Hambach B., Roden J. S. & Ehleringer J. R. (In Press) Predicting leaf wax *n*-alkane (2) H/(1) H ratios: controlled water source and humidity experiments with hydroponically grown trees confirm predictions of Craig-Gordon model. *Plant, Cell and Environment*. doi: 10.1111/pce.12457.
Tipple, B. J. & Pagani, M. (2013) Environmental control on eastern broadleaf forest species' leaf wax distributions and D/H ratios. *Geochimica et Cosmochimica Acta* 111, 64-77.
Versteegh, G. J. M, Schefub, E., Dupont, L., Marret, F., Sinninghe Damaste, J. & Jansen, J. H. F. (2002) Taraxerol and *Rhizophora* pollen as proxies for tracking past mangroves ecosystems. *Geochimica et Cosmochimica Acta* 68, 411-422.
Vecchi, G. A., Soden, B. J., Wittenberg, A. T., Held, I. M., Leetmaa, A. & Harrison, M. J. (2006) Weakening of tropical Pacific atmospheric circulation due to anthropogenic forcing. *Nature* 441, 73-76

Wallace, J. M. & Gutzler, D. S. (1981) Teleconnections in the geopotential height field during the Northern Hemisphere winter. *Mon. Weather Rev*. 109, 784–812.

Wang, C. & D. B. Enfield (2003) A Further Study of the Tropical Western Hemisphere Warm Pool. *Journal of Climate* 16, 1476-1493.

Wang, H. & Mehta, V. M. (2008) Decadal Variability of the Indo-Pacific Warm Pool and Its Association with Atmospheric and Oceanic Variability in the NCEP–NCAR and SODA Reanalyses. *Journal of Climate* 21, 5545-5565.

Xie, P. P. & Arkin, P. A. (1997) Global precipitation: A 17-year monthly analysis based on gauge observations, satellite estimates, and numerical model outputs. *Bull. Am. Meteorol. Soc.* 78, 2539–2558.

Yang, H., Pagani, M., Briggs, D. E. G., Equiza, M. A., Jagels, R., Leng Q. & LePage B. A. (2009) Carbon and hydrogen isotope fractionation under continuous light: implications for paleoenvironmental interpretations of the High Arctic during Paleogene warming. *Oecologia* 160, 461-470.

Chapter 2: Inverse relationship between salinity and *n*-alkane δD values in the mangrove *Avicennia marina*[1]

2.1 Abstract

Hydrogen isotope ratios in lipids derived from mangroves have the potential to be used for paleohydrologic reconstructions and could serve as a much needed tool for establishing past climate variability in the tropics. We assessed the effect of salinity on the apparent fractionation factor, α_a, between mangrove derived *n*-alkanes and their source water for *Avicennia marina* (gray mangrove) specimens collected along a 28 PSU salinity gradient in the Brisbane River Estuary. Our results indicate that there is an inverse relationship between the apparent fractionation factor and salinity. This salinity effect is large enough to override variability in the isotopic composition of source water, which plays a dominant role in determining the hydrogen isotope ratio of leaf waxes in other vascular plants. We suggest that this relationship may be due to (i) increased discrimination against deuterium during water uptake at high salinity, (ii) increased production of compatible solutes from D enriched pyruvate at high salinity, resulting in more hydrogen from D depleted NADPH being incorporated in leaf waxes, and/or (iii) increased secretion of salty brine by leaves at high salinity, resulting in (iii.a) higher relative humidity at the leaf surface, and (iii.b) introducing the possibility that D depleted water of hydration is absorbed by the leaf. Our results indicate that hydrogen isotope ratios of mangrove lipid biomarkers can be developed as a paleo-salinity indicator. They also imply that care must be taken when interpreting hydrogen isotopic variations in non-source specific higher plant lipids in sediments where both mangrove and non-mangrove plants contribute organic material.

[1] Previously published as Ladd S. N. and Sachs J. P. (2012) Inverse relationship between salinity and *n*-alkane δ

2.2 Introduction

Hydrogen isotopes of lipid biomarkers have recently emerged as a promising paleoclimate proxy. Compound specific hydrogen isotope measurements were made possible by analytical developments during the late 1990s (Burgoyne and Hayes, 1998; Hilkert et al., 1999) and the technique rapidly garnered considerable interest because lipids can be source specific and well preserved in sediment. Thus measuring hydrogen isotope ratios of lipids in marine and lacustrine sediments allows for paleoclimate reconstructions in a myriad of archives for which no robust proxies previously existed. The basic premise of such reconstructions is that lipids produced by autotrophic organisms will reflect the hydrogen isotopic signature of their source water, a relationship that has been established by both laboratory cultures and field calibrations (Sessions et al., 1999; Sauer et al., 2001; Huang et al., 2002, 2004; Chikaraishi and Naraoka, 2003; Sachse et al., 2004; Englebrecht and Sachs, 2005; Zhang and Sachs, 2007; Sachs and Schwab, 2011; Schwab and Sachs, 2011). Water isotopes, in turn, are closely linked to the hydrologic cycle (Craig, 1961; Craig and Gordon, 1965; Gat, 1996) and by serving as a proxy for the isotopic composition of ancient water, lipids can provide valuable insights into paleohydrology.

During the past decade, hydrogen isotopes of lipid biomarkers have been employed around the world to reconstruct paleohydrologic changes on 10^1–10^7 year time scales (Huang et al., 2002; Schefuss et al., 2005; Pagani et al., 2006; Makou et al., 2007; Pahnke et al., 2007; Vandermeer et al., 2007, 2008; Sachs et al., 2009) and they have demonstrated the potential to significantly enhance our understanding of paleoclimate variability in the tropics. The tropics are a region of considerable interest in climate dynamics, as the flux of heat and moisture poleward from the tropics drives much of Earth's atmospheric circulation. Reorganizations of

tropical climate thus have the potential to profoundly impact the rest of the planet (Chiang, 2009). However, our understanding of past variability in this important region has been limited by a dearth of high resolution paleoclimate records. Ice cores in this region are limited to a few high altitude locations. Likewise, tree rings are often difficult to interpret in the tropics and frequently do not exist in equatorial regions with no distinct dry season (Worbes, 1995; Jones et al., 2009). Marine sediments have been used to create long term records of climatic variability in the tropics using proxies such as alkenone Uk'_{37} (Ohkouchi et al., 1994; Lawrence et al., 2006; Koutavas and Sachs, 2008; Herbert et al., 2010), and $\delta^{18}O$ and Mg/Ca of foraminifera (Koutavas et al., 2002; Stott et al., 2002; Lea et al., 2006). However, given the slow accumulation rates typical of pelagic sediments, temporal resolution is often limited to 10^2–10^3 years. Varved sediment sequences are found in a few locations (such as the Cariaco Basin and the Arabian Sea), but are quite uncommon. $\delta^{18}O$ of coralline $CaCO_3$ has been used to generate annually resolved records of climate variability in the tropics (Hendy et al., 2002; Cobb et al., 2003; Linsley et al., 2006), but are limited in duration to decades to a few centuries. Recently, high resolution records from hydrogen isotopes of lipid biomarkers have been produced from high accumulation rate sediments in brackish ponds in Palau and the Line Islands (Sachs et al., 2009; Smittenberg et al., 2011) and the coastal margin of Indonesia (Tierney et al., 2010).

1.1 Potential for mangrove based δD studies

A tropical sedimentary archive that has been unexploited for lipid D/H studies is peat in mangrove swamps. Mangrove peat has accumulated at rates on the order of 1 m/kyr in the tropical Pacific over the past two millennia (Ellison and Stoddart, 1991; Fujimoto, 1997) and is comprised in large part of decaying leaf matter from mangroves (Kristensen et al., 2008) which

are woody trees and shrubs that have adapted to live in brackish or saline water along estuaries and intertidal flats.

The environment inhabited by mangroves is a harsh one, characterized by fluctuations in salinity and anoxic soils. As such, few higher plants are adapted to live in these waters, with only 20 genera existing worldwide (Hogarth, 2007). Nearly half of all mangrove species belong to either the Avicenniaceae or Rhizophoraceae families. This makes the mangrove forests in any given location relatively homogenous, with many prominent mangrove swamps dominated by 2 or 3 species (Polidoro et al., 2010). Because of the low species diversity in a mangrove swamp, there are very few potential sources of higher plant lipids to the peat that accumulates in the swamp, increasing the probability that a source specific biomarker for paleohydrologic reconstructions based on hydrogen isotopes can be exploited in the sediments.

1.2 Competing influences on leaf wax δD

It is beneficial to work with lipid biomarkers that can be attributed to a single species or to a small group of species when inferring past climate variability from hydrogen isotopes of leaf lipids. This is because a number of different studies have indicated that different groups of plants have different apparent fractionation factors between their source water and the leaf wax (Sachse et al., 2006; Smith and Freeman, 2006; Hou et al., 2007; Liu and Yang, 2008; Feakins and Sessions, 2010; Romero and Feakins, 2011). In this case, the apparent fractionation factor, hereafter referred to as α_a, is a measure of the isotopic difference between environmental water and lipids and is defined as $\alpha_a = (\delta D_{lipid} + 1000)/(\delta D_{water} + 1000)$, where $\delta D_{sample} = [(D/H)_{sample}/(D/H)_{VSMOW}-1]*1000$. It is important to note that α_a incorporates a number of steps during which fractionation might occur. In the case of terrigenous plants, these include enrichment of soil water due to evaporation (Riley et al., 2002; Eggemeyer et al., 2009), enrichment of leaf

water due to transpiration (Dawson et al., 2002; Kahmen et al., 2008), and D depletion due to enzymatically mediated fractionation during biosynthesis of lipids (Sessions et al., 1999; Sachse et al., 2006; Sessions, 2006; Feakins and Sessions, 2010). Differences in water use efficiencies, leaf morphology and transpiration have been cited as causes of differences in α_a that have been observed between mosses and woody plants (Sachse et al., 2006), between grasses and woody plants (Liu et al., 2006; Hou et al., 2007), and between C_3 and C_4 grasses (Smith and Freeman, 2006; McInerney et al., 2011). Feakins and Sessions (2010) observed considerable variations in α_a among species of the same general plant type growing at the same site, although the average δD of leaf waxes from all trees at each site along their southern California transect was well correlated with local precipitation. The discrepancies among α_a for different plants suggest that changes in downcore δD of non-source specific lipids, such as *n*-alkanes, *n*-alcohols, and *n*-fatty acids, may represent changes in plant community composition as well as hydrologic changes.

Other complications in interpreting δD of leaf waxes as an indicator of precipitation δD exist, for although the isotopic composition of precipitation plays a major role in determing that of lipids, a growing body of evidence suggests that other variables exert a significant influence on the δD values of lipid biomarkers. Results from a growth chamber study by Hou et al. (2008) suggested that relative humidity has a slight effect on α_a, presumably due to changes in evapotranspiration. However, no response to humidity was reported in a study of core tops along an aridity gradient in southwestern US, which Hou et al. (2008) attributed to changing contributions from grass and woody plants. More recently, Feakins and Sessions (2010), found little change in α_a along an aridity gradient in southern California. However, the magnitude of apparent enrichment values, ε_a, (where $\varepsilon_a = (\alpha_a - 1)*1000$) reported by both Feakins and Sessions (2010) and Hou et al. (2008) are significantly smaller (~-94‰($\alpha_a = 0.906$) and -99‰($\alpha_a = 0.901$),

respectively) compared to those reported in more humid regions such as the northeastern US (Hou et al., 2007) and Europe (Sachse et al., 2006), where ε_a is typically around -120‰ (α_a = 0.88) and has been reported to be as low as ~-160‰ (α_a = 0.84) (Sachse et al., 2006). A recent review suggests that relative humidity > 70% results in more depleted leaf wax δD values (Sachse et al., 2012).

Other variables that might affect leaf wax α_a are temperature and growth rate. Temperature has recently been proposed to affect D/H fractionation via evapotranspiration, although initial results do not suggest that it affects enzymatic fractionation (Zhou et al., 2011). The effect of growth rate on lipid α_a from plants has not been assessed, but cultures with algae suggest that it can have a significant effect on fractionation factors in algal lipids (Schouten et al., 2006; Zhang et al., 2009) and it is possible that similar effects may occur in higher plants.

Although the various controls on leaf wax δD described above complicate interpretation of this paleoclimate proxy, the majority of core-top studies show significant positive correlations between δD of precipitation and δD of leaf waxes (Sauer et al., 2001; Sachse et al., 2004; Hou et al., 2008; Polissar and Freeman, 2010). These empirical studies suggest that hydrogen isotopes of leaf waxes and other lipids are a viable paleoclimate proxy. Ideally, field calibrations will better constrain the factors influencing the leaf wax δD signal. If we wish to extend the use of leaf wax δD measurements to mangrove peat, it is important to assess the controls on δD values of leaf waxes from mangroves in the modern environment.

A major reason to evaluate mangrove derived lipids independently is that, unlike other higher plants, the salinity of a mangrove's source water is liable to change over time. Increasing salinity has been observed to increase δD values of lipids produced by phytoplankton and cyanobacteria by decreasing the apparent fractionation factor between the lipid and the source

water (Schouten et al., 2006; Sachse and Sachs, 2008; Sachs and Schwab, 2011). The goal of this study is to establish what effect, if any, variations in salinity have on the apparent fractionation factor between mangrove lipids and their source water and to assess the potential of using the δD values of mangrove lipids as a paleosalinity indicator. If successful, this technique will be beneficial to our efforts to reconstruct paleoclimate variability at low latitudes, since mangroves are ubiquitous to the tropics and often inhabit swamps with low species diversity.

2.3 Materials and methods

2.3.1. Sample collection

During a one week period in February 2010, whole *Avicennia marina* (gray mangrove) leaves were collected along the Brisbane River estuary and from Moretown Bay in Queensland, Australia (Fig. 1) (Table 1). Multiple leaves were collected from each tree and were immediately placed on ice and subsequently kept frozen during storage. *A. marina* was chosen for this study because it is one of the most salt tolerant species of mangroves (Ball, 1988; Ye et al., 2005) and as such, it was present along the entire length of the Brisbane River estuary from the coast to inland sites that had essentially freshwater at low tide.

At each site, surface water was collected adjacent to the sampled tree and the water temperature, conductivity and specific conductivity were measured using a YSI 85 conductivity probe (YSI Inc., Yellow Springs, OH, USA). When possible, multiple visits were made to the same site at different points in the tidal cycle in order assess the diurnal variation in salinity. For the six sites that were sampled near both high and low tide, the average tidal range of salinity was 4.2 ± 1.0 practical salinity units. Salinity in the Brisbane River estuary is correlated (R^2 = 0.84) with distance from the mouth of the river (Fig. 2), and the line of best fit relating measured

salinities to distance from the river mouth was used to infer the mean salinities used in Fig. 3, Fig. 4 and Table 1, which was deemed preferable to using the measured salinity at a single time point in the tidal cycle. The standard error of the regression in Fig. 2 is 2.9 PSU.

2.3.2. Analytical methods

2.3.2.1. Water δD

δD and $\delta^{18}O$ of water samples were measured in Brian Popp's laboratory at the University of Hawaii using a Picarro L1102-i Isotopic Liquid Water Analyzer in high precision mode and were normalized to VSMOW using lab standards. Each sample was analyzed 6 times and the first 3 analyses were discarded to avoid memory effects from the previous sample. The average precision of the water δD measurements was ±0.44‰.

2.3.2.2. Lipid extraction and purification

In order to avoid the significant isotopic differences that can occur from the base to the tip of a single leaf (Helliker and Ehleringer, 2000; Sessions, 2006), intact whole leaves from each tree were selected for analysis. In addition, in order to assess the isotopic variability among leaves from multiple locations on the same tree, five leaves each from two trees were prepared and treated as individual samples. Leaves were rinsed with DI water to remove debris and cut into small pieces using solvent cleaned scissors prior to freeze drying. Dry leaves were ground up with a solvent cleaned mortar and pestle and lipids were extracted using an Accelerated Solvent Extractor (ASE-200, Dionex Corp., Sunnyvale, CA, USA) with 9:1 dichloromethane:methanol (DCM:MeOH) at 100 °C and 1500 psi (10.3 MPa) for three five

minute static cycles. The resulting total lipid extract (TLE) was evaporated to dryness under a stream of nitrogen gas on a Turbovap system (Caliper, Hopkinton, MA, USA).

A small aliquot of the TLE was dissolved in 20 µl of pyridine and silylated with 20 µl of bis(trimethylsilyl)trifluoroacetamide (BSTFA, Sigma-Aldrich, St. Louis, MO, USA) at 60 °C for 60 minutes. An initial screening of lipids present in the TLEs was conducted by gas chromatography-mass spectrometry (GC-MS) using an Agilent (Santa Clara, CA, USA) 6890N gas chromatograph equipped with an Agilent 7683 autosampler, a split-splitless injector operated in splitless mode and an Agilent DB-5ms capillary column (60 m X 0.32 mm X 0.25 µm) interfaced to an Agilent 5975 quadrupole mass selective detector. The oven temperature was increased from 60 °C to 150 °C at 15 °C/min, then at 6 °C/min to 320 °C, where it was held for 28 minutes. Lipids were identified based on published EI spectra and comparisons to the mass spectra of laboratory standards. The composition of the TLEs did not vary significantly as a function of salinity, and the most abundant lipids included normal alkanes (*n*-C_{31} and *n*-C_{33} alkanes), normal alcohols (*n*-C_{26}, *n*-C_{28} and *n*-C_{30} alcohols), sterols (stigmasterol and β-sitosterol) and triterpenols (α-amyrin, β-amyrin, and lupeol), with lupeol being particularly abundant (Fig. S1).

Another aliquot of the TLE (~12 mg) was purified using two step column chromatography. During the first step, with a solid phase of 500 mg of amino propyl silica gel (Supelco, Lot # 2511301, Part # 5-7205) the neutral fraction was eluted with 8 ml of 3:1 DCM:isopropyl alcohol, acids with 6 ml 4% acetic acid in ethyl ether and other polar compounds with 6 ml of MeOH. The neutral fraction was further purified with a solid phase of 1 g of silica gel (EMD, Lot # 45169543, Part # 11567-2) that was 5% deactivated with water. Hydrocarbons

were eluted with 8 ml of hexane, sterols, alcohols and triterpenols with 6 ml of 4:1 hexane:ethyl acetate and remaining compounds with 4 ml of MeOH.

The hydrocarbon fraction was dominated by C_{31} and C_{33} *n*-alkanes, with relatively small amounts of *n*-C_{32} and other unidentified lipids (Fig. S2). Lipids in the hydrocarbon fraction were quantified with a gas chromatograph connected to a flame ionization detector (GC-FID). An Agilent 6890N gas chromatograph equipped with an Agilent 7683 autosampler, a programmable temperature vaporization inlet (PTV) operated in splitless mode and an Agilent DB-5ms capillary column (60 m X 0.32 mm X 0.25 μm) was used with helium as the carrier gas (2.4 ml/min). The oven temperature was increased from 60 °C to 150 °C at 15 °C/min, then at 6 °C/min to 320 °C, where it was held for 28 minutes. Quantification of *n*-alkanes was performed by comparing their integrated peak areas to that of a known amount of *n*-C_{37}, which had been added as a quantification standard. The hydrocarbon fractions were then dried under a gentle stream of nitrogen and brought up in toluene such that the concentration of the less abundant target compound (C_{31} or C_{33} *n*-alkane) was ~200 ng/μl.

2.3.2.3. Lipid δD

δD values of the C_{31} and C_{33} *n*-alkanes were measured by GC-IRMS on a Thermo DELTA V PLUS system (Thermo Scientific, Waltham, MA, USA). The gas chromatograph (Trace Ultra, Thermo) was equipped with a split-splitless injector operated in splitless mode at 300 °C, a TRIPLUS autosampler (Thermo Scientific), and a VF-17ms capillary column (60 m x 0.32 mm x 0.25 μm, Varian Inc., Middelburg, Nederlands). The GC was heated from 80 °C to 170 °C at 20 °C/min, then at 3 °C/min to 325 °C and then held at 325 °C for 20 min. Helium was used as the carrier gas at a constant flow of 1.3 ml/min. Compounds were pyrolyzed in a

ceramic reactor at 1400 °C. A 1 µl sample was injected along with 0.5 µl of *n*-C_{38} of known isotopic composition (A. Schimmelmann, Indiana University, Bloomington, Indiana). Four samples were also injected with a mixture of four coinjection standards (C_{21}, C_{26}, C_{38} and C_{40} *n*-alkanes from A. Schimmelmann), in order to assess the effect of different isotopic corrections. Thermo ISODAT software V.2.5 was used to control instrumentation and calculate δD values. Correcting the raw δD values of the *A. marina* hydrocarbons with one or multiple coinjection standards did not result in any significant change in final δD values and it had no impact on the overall trends reported here. The *n*-alkane δD values reported below were corrected using only the C_{38} coinjection standard. Additionally, instrument performance was monitored using a mix of lab standards, whose δD values had previously been established using TC/EA-IRMS. This standard mix was run in triplicate at the beginning and end of each sequence of samples, as well as in duplicate after every six analyses. The H_3^+ factor was determined each day using pulses of a reference gas of varying heights and ranged between 2.04 and 2.06. Each sample was measured in triplicate and the average standard deviation of triplicate analyses was 2.2‰.

2.4 Results

Water δD was positively correlated with salinity in the Brisbane River Estuary (R^2 = 0.88), reflecting the mixing of isotopically depleted freshwater and deuterium enriched seawater (Fig. 3). The overall range in water δD was 14.5‰ (values ranged from -10.2‰ to 4.3‰). The linear relationship between salinity and water δD implies that the fresh water end member of δD values (y-intercept) at the time of sampling was -12.7‰. From 1967–2002, mean February precipitation δD values in Brisbane averaged -15‰ ± 13.9‰, (1 s, IAEA, 2006), consistent with our estimate.

δD values were between -168‰ and -121‰ for *n*-C_{31}, a range of 47‰ and between -164‰ and -114‰ for *n*-C_{33}, a range of 50‰. δD values of *A. marina n*-alkanes were greatly depleted compared to that of their source water and were negatively correlated with salinity (Fig. 3). Linear regression analysis yielded correlation coefficients (R^2) of 0.52 for *n*-C_{31} vs. salinity (Fig. 3a) and 0.49 for *n*-C_{33} vs. salinity (Fig. 3b).

The apparent fractionation factor, α_a, was negatively correlated with salinity ($R^2 = 0.63$ for *n*-C_{31} and 0.59 for *n*-C_{33}) (Fig. 4). The apparent fractionation factors for the two lipids were highly correlated with each other ($R^2 = 0.93$), with *n*-C_{31} generally being 6‰ depleted relative to *n*-C_{33}.

Analysis of 5 leaves selected from a range of heights and sun exposure from the same tree generally yielded δD values within 4‰ of each other (Table 2). However, in one case, alkanes in one leaf were significantly enriched (>30‰) compared with the other 4 leaves from the same tree.

2.5 Discussion

2.5.1 Effect of salinity on mangroves and leaf wax δD values

2.5.1.1 Relationship between salinity and mangrove leaf wax δD values

The negative relationship between environmental water δD values and mangrove *n*-alkane δD values (Fig. 3) stands in sharp contrast with the positive correlation seen in studies with terrestrial plants (Sachse et al., 2006; Hou et al., 2007). It implies that environmental water δD values are not the main controlling variable of *n*-alkane δD in mangroves and, by extension, that sedimentary mangrove leaf wax δD values would not provide a proxy for water δD values. Rather, for reasons discussed below, environmental water salinity likely exerts a stronger control in determining δD values of leaf waxes produced by mangroves than environmental δD values.

Noteworthy is the fundamentally different relationship between salinity and lipid δD values in mangroves as compared to aquatic phytoplankton and cyanobacteria, in which δD values of lipids are positively correlated with salinity (Fig. 5) (Schouten et al., 2006; Sachse and Sachs, 2008; Sachs and Schwab, 2011). In field and laboratory based studies of phytoplankton and cyanobacteria, the difference between δD_{water} and δD_{lipid} is smaller at higher salinities. This has been attributed to either (i) diminished growth rate at higher salinity, (ii) deuterium enrichment of intracellular water resulting from enhanced water recycling within the cell, or (iii) production of D depleted osmolites that counter the greater osmotic gradient at high salinity (Sachs and Schwab, 2011).

Perhaps it is not surprising that single celled aquatic organisms and vascular plants respond differently to the same environmental change. A similar discrepancy was observed for the effect of temperature on α_a. For phytoplankton, increasing temperature has been demonstrated to result in greater apparent fractionation (Zhang et al., 2009). However, increasing temperature had no effect on net fractionation in a study of C_3 and C_4 vascular plants (Zhou et al., 2011).

Additionally, our results are not dissimilar to another study of leaf wax δD values from plants growing in a saline environment. Romero and Feakins (2011) measured xylem water, leaf water and leaf wax δD values for a variety of plants at four sites in a Californian salt marsh. They observed less apparent fractionation (α closer to 1) at the inland sites with more saline pore water, which seems to contrast with our results. However, by analyzing the xylem water of their plants, Romero and Feakins (2011) demonstrated that the plants at the more inland saline sites were using meteoric water, as the xylem water was depleted by 20‰ compared to the plants at the less saline sites, whose xylem water had δD values comparable to local seawater. Thus the

plants with the greatest apparent fractionation were those that were obtaining most of their water from seawater, similarly to the mangroves we studied in the Brisbane River Estuary.

Since α_a represents the combined fractionation factors of several different processes, it is possible that the fractionation associated with one or more of those processes is negatively related to salinity. In general, evapotranspiration causes leaf water to become enriched in D relative to environmental water (Leaney et al., 1985; Walker et al., 1989; Dawson et al., 2002; Kahmen et al., 2008) and biosynthesis results in lipids becoming depleted in D relative to leaf water (Sessions et al., 1999; Sachse et al., 2006; Feakins and Sessions, 2010; Romero and Feakins, 2011). Biosynthetic D depletion (α_b) has a greater magnitude than the D enrichment associated with evapotranspiration (α_e), resulting in net fractionations on the order of 0.90–0.84 (ε_a = -100‰ to -160‰) (Chikaraishi and Naraoka, 2003; Sachse et al., 2006, 2009; Feakins and Sessions, 2010). At 0.88 (ε_a = -120‰), the net fractionation for *A. marina* trees at low salinity sites in our study is comparable to the net fractionation observed in other C_3 dicots (growing at zero salinity). The greater negative apparent fractionation observed in *A. marina* growing at high salinity (α_a = 0.835; ε_a = -165‰) could be due to less enrichment of internal water, more D depletion during biosynthesis, or some combination of the two (Fig. 6).

Because salinity exerts a significant environmental challenge to mangroves, and because this is the primary difference between the trees in our study and those in other investigations of the controls on leaf wax δD values, it seems reasonable that our results can be explained in the context of the physiological responses of *A. marina* to increased salinity, and to the mechanisms *A. marina* has developed to manage salt contained in its water. In the following sections, we review the ways in which mangroves respond to increased salinity, including their strategies for dealing with salt, and assess the potential for these responses to impact α_e and α_b.

2.5.1.2 Physiological responses of mangroves to increased salinity

Salt imposes osmotic stress on plants and interferes with their enzymatic functions (Greenway and Osmond, 1972; Yeo, 1983; Morgan, 1984). Mangroves have evolved three strategies to manage salt. One strategy is to prevent salt from entering roots during water uptake (exclusion). Another strategy is to secrete salt from leaves (secretion). A final strategy is to accumulate salt in special vacuoles within the leaves (accumulation) (Hogarth, 2007; Parida and Jha, 2010). Although some species rely exclusively on one strategy, most mangroves employ two, or all three (Hogarth, 2007). The strategy employed by a mangrove can also vary as salinity changes. At low salinities, *A. marina* excludes 90% of the salt from its internal water (it both secretes and accumulates the remaining salt). As salinity increases, *A. marina* increases the fraction of salt its roots exclude, reaching a 97% exclusion rate when cultured in water with an NaCl concentration of 500 mol/m^3 (i.e., comparable to seawater; Ball, 1988).

Mangroves growing in saline water have also developed a number of adaptations to conserve water. These include smaller mature heights and lower growth rates (Ball, 1988; Lin and Sternberg, 1992; McKee et al., 2002; Naidoo, 2010), as well as lower concentrations of chlorophyll a and b (Naidoo, 2010), lower photosynthetic capabilities (Ball and Farquhar, 1984) and lower carbon assimilation rates (Ball and Farquhar, 1984; Lin and Sternberg, 1992). Increased salinity is also associated with lower stomatal conductance (Ball and Farquhar, 1984; Lin and Sternberg, 1992) and consequently diminished transpiration rates (Ball and Farquhar, 1984; Ye et al., 2005; Lopez-Hoffman et al., 2007).

2. 5.1.3 Potential for reduced stomatal conductance to affect α_a at high salinity

Numerous studies of the relationship between leaf wax δD values and environmental water δD values have suggested that changes in α_a are due to changes in evapotranspiration, with higher evapotranspiration rates resulting in greater isotope fractionation of the leaf water and enrichment of D and ^{18}O in that water (e.g. Sachse et al., 2006; Feakins and Sessions, 2010; Romero and Feakins, 2011). At first glance the *A. marina* δD data would seem to be consistent with this scenario, whereby higher salinity causes reduced rates of transpiration and less isotopic enrichment of leaf water and the leaf waxes produced from that water. But this overlooks the cause of the reduced transpiration rates when mangroves encounter more saline water, which, as stated, is diminished stomatal conductance.

Stomatal conductance is the rate at which water vapor or CO_2 pass through the stomata, which in turn is controlled by the aperture of the stomata. A reduction in the size of the stomatal aperture is thought to increase the isotope fractionation of water and cause isotopic enrichment of leaf water (Leaney et al., 1985; Walker et al., 1989; Barbour and Farquhar, 2000; Farquhar et al., 2007). Hence, since higher salinity causes mangroves to decrease their stomatal conductance (Ball and Farquhar, 1984; Lin and Sternberg, 1992), it ought to cause leaf water δD values to increase. This is opposite the dependence observed in *n*-alkanes from *A. marina* (Fig. 3), implying that lower transpiration rates brought on by diminished stomatal conductance in response to saltier water cannot explain the observed decrease in δD values.

2.5.1.4 Potential for mangrove salt tolerance strategies to affect α_a at high salinity

We have developed four hypotheses related to the salt tolerance mechanisms of *A. marina* that could explain some or all of the increased magnitude of α_a at high salinity: (i)

increased exclusion of salt at the roots could lead to more discrimination against deuterium during water uptake, (ii) salt secretion could increase the local relative humidity on the leaf surface, resulting in less enrichment of leaf water, (iii) depleted water of hydration could enter the leaves and result in less net enrichment of leaf water, or (iv) enhanced production of compatible solutes could use up pyruvate and cause more of the hydrogen in leaf waxes to come from relatively depleted NADPH. We will explore each of these possibilities below.

Although most plants do not fractionate water isotopes during uptake by the roots (White et al., 1985; Dawson and Ehleringer, 1991; Walker and Richardson, 1991), mangroves and other halophytic plants have been shown to discriminate against HDO (but not $H_2{}^{18}O$) during water uptake (Lin and Sternberg, 1993; Ellsworth and Williams, 2007). This fractionation has been attributed to the well developed Casparian band that is found on the roots of halophytic plants such as *A. marina* (Moon et al., 1986), which limits apoplastic transport (a bulk transfer process) of water into the roots, in favor of symplastic transport (which is a molecular transfer process). It is energetically favorable to disassociate H_2O rather than HDO from water aggregates, but there is little difference in the energy needed to disassociate $H_2{}^{16}O$ and $H_2{}^{18}O$ (Chacko et al., 2001). Therefore, increased symplastic transport could explain the fractionation of water isotopes that has been observed during water uptake by mangroves and other halophytes (Lin and Sternberg, 1993; Ellsworth and Williams, 2007). *Avicennia germinans*, a salt secreting mangrove that is closely related to *A. marina*, displayed less D discrimination when grown in freshwater than in saline water (Lin and Sternberg, 1993). The magnitude of the effect observed by Lin and Sternberg was <10‰, so at most, this mechanism accounts for less than 20% of the 50‰ implied change in α_a we observed for *A. marina* in the Brisbane River.

It is also possible that increased salt secretion at high salinity could partially explain the negative relationship between α_a and salinity. One way this could occur is by increasing the local relative humidity on the leaf surface. Saturated NaCl solutions maintain a constant relative humidity of 76% above them (O'Brien, 1948), greater than the mean annual humidity in Brisbane, which is 53% (http://www.bom.gov.au). Elevating relative humidity reduces transpiration rates due to a decreased gradient in vapor pressure across the leaf surface and reducing transpiration by this mechanism also results in reduced isotopic enrichment of leaf water (Helliker and Ehleringer, 2002a, 2002b; Farquhar and Cernusak, 2005). Helliker and Ehleringer (2002b) observed that leaf water in grass blades grown at a relative humidity of 76% had a $\delta^{18}O$ value ~7.5‰ less than grass growing at a relative humidity of 53%. Since the enrichment associated with evaporation is typically 5 times greater for hydrogen than oxygen, it is plausible that this increase in relative humidity could account for a ~35‰ decrease in δD_{leaf} water.

However, it is unclear whether changes in leaf water δD are captured in lipid δD, and some studies suggest that relative humidity may not have a large role in determining leaf wax δD (Hou et al. 2008; McInerney et al., 2011). A recent review (Sachse et al., 2012) concluded that relative humidity likely influences leaf wax δD, but the relationship is not straightforward and needs to be investigated further. It would be necessary to grow *A. marina* at different relative humidities (and constant salinity) in order to determine its impact on *n*-alkane δD values.

Another way that increased salt secretion at high salinity could result in more apparent fractionation is the potential for D depleted hydration water from exchange with atmospheric water vapor in secreted salts to mix with leaf water, lowering its δD value. Water of hydration in Na salts can be depleted in deuterium by 80‰ relative to source water at 25 °C (Matsuo et al.,

1972). If hydration water derived from the atmosphere in secreted salts exchanges with internal leaf water the latter would undergo isotopic depletion. In order to account for the entire ~50‰ variation we observed in *A. marina* leaf wax δD values, hydration water would need to account for more than 50% of the water in the leaf, which seems improbable.

Finally, it is possible that the increased production of compatible solutes at high salinity is responsible for some of the increased fractionation observed at high salinity. *A. marina* produces compatible solutes (predominantly asparagine, but also stachyose, glycine betaine, alanine, pinitol and proline) at high salinity, which reverse the osmotic gradient within the leaf and help the plant maintain isolation of salt ions in vacuoles (Ashihara et al., 1997; Hibino et al., 2001; Kathiresan and Bingham, 2001; Datta and Ghose, 2003). Amino acids, organic acids and soluble carbohydrates, such as the compatible solutes listed above, are enriched in D relative to pyruvate, a biosynthetic precursor of *n*-alkanes (Schmidt et al., 2003). The hydrogen in pyruvate is derived from two sources: water via soluble carbohydrates and NADPH via the pentose phosphate cycle (Schmidt et al., 2003). Of these, NADPH-derived hydrogen is significantly more depleted in D (δD ~-250‰) than that from carbohydrates (δD ~-70‰) (Luo et al., 1991; Hayes, 2001; Schmidt et al., 2003). Therefore, at high salinity it may be that a greater proportion of the H in pyruvate would, by necessity, be derived from NADPH due to the increased demand for compatible solutes to reverse the osmotic gradient. This would result in D depletion of the *n*-alkanes and other lipids synthesized from pyruvate (Schmidt et al., 2003; Zhou et al., 2010). Since the majority of hydrogen in lipids is derived from water in all cases, it seems unlikely that this mechanism could, in and of itself, account for the entire ~50‰ signal we observed in *A. marina n*-alkane δD values along the Brisbane River estuary.

Of the four mechanisms we propose that could contribute to the increased D/H fractionation in *A. marina n*-alkanes as salinity increases, none seems able to account for the entire signal independently. However, a combination of some or all of these mechanisms could be large enough to cause the overall observed reduction in δD values of *A. marina n*-alkanes along the salinity gradient.

2.5.1.5 Deviations from the linear relationship between salinity and α_a

There are a few outlying *n*-alkane δD values at the higher end of the salinity spectrum. One of those outliers is from a tree on the coast of Moreton Bay, outside the Brisbane River Estuary (site 16). The *n*-alkanes from this tree are enriched in D compared to the trend defined by the linear regression of *n*-alkane δD versus salinity. The mangrove sampled at this site was growing on the edge of a public park on a sandy intertidal flat. At a similar site further north on the coast, groundwater seepage was noted to be contributing to the water around a mangrove we sampled, which caused us to ultimately exclude that sample from this study, since groundwater seeps are often not constant through time. It is possible that a similar source of freshwater intermittently impacted the Moreton Bay site, causing the leaf *n*-alkanes to have higher δD values than predicted by the trend line in Fig. 3. Consistent with this notion, *A. germanins* trees growing on sand bars amidst hypersaline water in South America have been observed to utilize groundwater percolating through the sand as opposed to the more prevalent saline surface water (Lambs et al., 2008) and *R. mangle* trees from the Florida Everglades have been observed to switch their source water to ground water during the dry season (Ewe et al., 2007). It is possible that the tree sampled here was employing a similar strategy and thus was consuming less saline water than the surface water we measured.

It is also probable that much of the scatter observed in the relationship between salinity and α_a in *A. marina* shown in Fig. 4 is due to the wide range of maturities and microenvironments of the mangroves in the sample set. Plants in the sample set ranged from large mature trees to small saplings. Our results give some indication of how much this might have contributed to the scatter in Fig. 4. At the mouth of the river (site 14), we sampled a mature tree with a height of ~5 m as well as a small sapling that was <1 m tall. The δD and α_a values for *n*-alkanes in these two trees are plotted as separate data points in Fig. 3 and Fig. 4 and fall within 4‰ of one another for the *n*-C_{31} alkane. For the C_{33} *n*-alkane, the offset was 10‰.

Additionally, the amount of sunlight incident on sampled leaves was not controlled, contrary to many other studies (e.g. Sachse et al., 2009; Feakins and Sessions, 2010). It is possible that this could affect either the amount of transpiration in a leaf and the D/H fractionation during *n*-alkane biosynthesis (i.e., α_b). Low level continuous light (such as that during summer at polar latitudes) has been observed to result in a 40‰ enrichment of leaf waxes relative to leaf waxes in plants grown with diurnal light cycles, which could be due to more evapotranspiration under continuous light conditions (Yang et al., 2009). However, no systematic study of the effect of varying light intensity within a single tree has been published to date.

Finally, we did not control for the age of the leaf sampled. Seasonal variations in leaf wax δD have been observed in sea grasses and some trees (Sessions, 2006; Sachse et al., 2009), but not in other species of trees and some grasses (Sachse et al., 2010; Kahmen et al., 2011). It is unclear whether leaf waxes are continually produced in leaves, or whether they are predominantly produced when the leaf is young (Jetter et al., 2007; see discussion in McInerney

et al., 2011). In either case, leaf wax *n*-alkanes from older leaves may have a different isotopic signature than those from younger leaves if they formed during different times of year.

At most sites we measured *n*-alkane δD values in a single leaf. Multiple analyses of leaves from the same tree generally justified this approach, but there was one leaf that had *n*-alkanes that were greatly enriched (by >30‰) compared with the mean of the other 4 leaves from the same tree (which had δD values within 4‰ of one another) (Table 2). Future studies should seek to minimize the range of these variables in an effort to better isolate the effect of salinity on D/H fractionation. Despite the limitations of this particular sample set, there remains a significant negative correlation between salinity and the apparent fractionation factor between source water and mangrove *n*-alkanes, suggesting that salinity plays a major role in controlling leaf wax δD values in mangrove leaves.

We might expect that the relationship between salinity and α_a would not be strictly linear, because it is likely that the environmental challenge presented by salinity is non-linear and diminishes at lower salinity. Indeed, the relationship between salinity and growth rate is not strictly linear. Cultivation of *Avicennia* and *Rhizophora* in different salinity treatments has consistently shown that these genera of mangroves obtain their highest growth rates in brackish water with salinity between 5 and 15 PSU (Gordon et al., 1992; Ye et al., 2005; Patel et al., 2010).

2.5.2 Implications for paleoclimate reconstructions

If the relationship between salinity and *A. marina n*-alkane δD values observed here is characteristic of other lipids, in other mangrove species, and at other locations, it suggests that mangrove lipid δD may be used as a paleosalinity proxy. This would be useful in developing

records of past hydrologic change, especially in settings where mangrove biomarkers are found alongside biomarkers of other organisms that are more strongly influenced by source water δD. For example, the δD value of dinosterol, a sterol produced primarily by dinoflagellates, is controlled by both source water δD and salinity in roughly equal proportions (Sachs and Schwab, 2011). An independent measure of salinity variability could constrain dinosterol δD values and provide for a more robust measure of past changes in water δD values.

A paleosalinity proxy based on mangrove lipids could be applied in a variety of settings, including mangrove swamps. Advantages of working in mangrove swamps include their prevalence along tropical coastlines, their relatively high accumulation rates, and the fact that are dominated by relatively few higher plants. However, material within a swamp could be subject to lateral advection by currents, or vertical movement by roots or animals. The organic material in mangrove swamps comes both from the mangroves and from marine sources, with some swamps being influenced more by one source than the other (Bouillon et al., 2003). Contributions of lipids from inland terrestrial plants are less common in mangrove areas, even where a major river is present (Volkman et al., 2007).

Bioturbation within a mangrove swamp is most commonly due to mangrove crabs, who may disturb the upper portion of the sediment when burrowing (Hogarth, 2007). Additional vertical mixing may be caused by mangrove roots, which are shallow (typically < 1m deep) compared to other trees (Lin and Sternberg, 1994; Hogarth, 2007). The roots themselves contribute younger organic material to the surrounding sediment, but often contain different lipids than the leaves (Wannigama et al., 1981; Basyuni et al., 2007), making their avoidance possible. Complications from vertical and horizontal mixing need to be assessed individually for specific mangrove swamps, as, indeed, they do for any sedimentary archive.

Our results are pertinent not only to mangrove swamps, but also to brackish lakes and ponds surrounded by mangroves and to sediments along continental margins in the tropics and subtropics, with the caveat that a mangrove-specific lipid biomarker would be necessary for the paleosalinity proxy to work in such an environment. Leaf waxes, which include the *n*-alkanes measured in this study, are produced by a wide range of plants. In a depositional setting with mixed contributions of mangrove and non-mangrove leaf waxes, the δD values of *n*-alkanes and other common lipids would be difficult to interpret, since different variables would influence the δD value of similar lipids to varying degrees. Given the negative correlation between salinity and α_a of mangrove leaf wax *n*-alkanes, drier periods should result in lower δD values in mangrove lipids, a consequence of increased water salinity caused by higher evaporation relative to precipitation and less freshwater runoff. The same processes would be expected to result in D enrichment of the source water used by non-mangrove trees, thereby causing D enrichment of their leaf waxes. A sedimentary mixture of the leaf waxes from both types of trees, characterized by opposing slopes of α_a vs. salinity, would produce a muted signal at best, while down-core changes in leaf wax δD would be influenced to an unknown extent by changes in the relative amounts of mangrove versus non-mangrove leaf waxes.

A mix of mangrove and non-mangrove contributions to sediment leaf waxes could explain the small amplitude of variation in the hydrogen isotope ratios of leaf waxes in some published studies. For example, Smittenberg et al. (2011) measured δD of dinosterol, palmitic acid and long chain *n*-alkanes from Spooky Lake and OTM in Palau. These lakes are surrounded by mangroves, but in catchments characterized by a wide range of tropical non-mangrove trees. The dinosterol δD values during the last 500 years, produced exclusively by dinoflagellates within the lake, had a wide range of variability (~50‰) that correlated with the

instrumental record of precipitation from the region. Palmitic acid δD values showed variability of ~35‰ over the past century and generally agreed with the trends observed for the dinosterol δD values. However, the long chain *n*-alkane δD values, presumably produced by a mix of mangrove and non-mangrove trees, had a much smaller range (~10‰) of values.

Likewise, Tierney et al. (2010) produced a record of hydrologic variability from leaf wax fatty acids preserved in marine sediments off the coast of Sulawesi, Indonesia. δD values of the leaf waxes were well correlated with the instrumental record of precipitation δD. However, the range of δD in precipitation (~40‰) was much larger than the corresponding range in leaf wax δD (~8‰). Tierney et al. (2010) proposed that the high sediment accumulation rates at their site implied large amounts of terrigenous runoff. Coastal Indonesia has abundant mangrove swamps and it is probable that both mangrove and non-mangrove leaf waxes contributed to the sedimentary lipid pool. A contribution of mangrove leaf waxes could partly explain why the range of sedimentary leaf wax δD variability during the last century is just 20% of the precipitation δD variability.

2.6 Conclusions

We collected leaves from *Avicennia marina* along a salinity gradient in the Brisbane River estuary and measured δD values of their *n*-alkanes, as well as of their source water. These measurements allowed us to calculate the apparent fractionation factor, α_a, for leaf wax *n*-alkanes produced by *A. marina*. The *n*-alkane δD values had a range greater than three times that of the water δD values and the two were inversely correlated with salinity such that the deuterium depletion in *n*-alkanes compared to water was only about 15‰ at 5 PSU and 70‰ at 35 PSU. There was a significant negative correlation between α_a and salinity for the mangrove leaf wax *n*-

alkanes, the opposite of the trend observed for algal lipids. Additionally, δD values of mangrove leaf waxes differ from those of other vascular plants, in that they do not seem to be primarily controlled by source water δD. Rather, the stress of added salinity appears to result in increased discrimination against deuterium. We have suggested that this trend could be caused by increased fractionation against D in the roots during water uptake, increased relative humidity at the leaf surface due the secretion of salty brines, water of hydration of leaf salts being incorporated in leaf water, or increased contributions of isotopically depleted hydrogen from NADPH at a high salinity. Of these, only one of the mechanisms involving secreted salts appears large enough to independently cause the hydrogen isotope response we observe in *n*-alkanes from *A. marina*. But a combination of two or more of them seems ample.

Regardless of the mechanism, the empirical relationship between salinity and δD_{leaf} wax in mangroves suggests that hydrogen isotope measurements of source specific mangrove lipids may prove to be a valuable paleosalinity indicator. Likewise, our results indicate that caution must be applied in interpreting δD values of non-source specific higher plant leaf waxes, such as the *n*-alkanes measured here, in areas where both mangroves and non-mangrove trees contribute plant matter to the sediments.

2.7 References

Ashihara, H., Adachi, K., Otawa, M., Yasumoto, E., Fukushima, Y., Kato, M., Sano, H., Sasamoto, H., Baba, S., 1997. Compatible solutes and inorganic ions in the mangrove plant *Avicennia marina* and their effects on the activities of enzymes. Zeitschrift für Naturforschung 52, 433-440.

Ball, M., 1988. Salinity tolerance in the mangroves *Aegiceras corniculatum* and *Avicennia marina.* I. Water use in relation to growth, carbon partitioning, and salt balance. Functional Plant Biology 15, 447-464.

Ball, M.C., Farquhar, G.D., 1984. Photosynthetic and stomatal responses of two mangrove species, *Aegiceras corniculatum* and *Avicennia marina*, to long term salinity and humidity conditions. Plant Physiology 74, 1-6.

Barbour, M.M., Farquhar, G.D., 2000. Relative humidity- and ABA-induced variation in carbon and oxygen isotope ratios of cotton leaves. Plant, Cell & Environment 23, 473-485.
Basyuni, M., Oku, H., Baba, S., Takara, K., Iwasaki, H., 2007. Isoprenoids of Okinawan mangroves as lipid input into estuarine ecosystem. Journal of Oceanography 63, 601-608.
Bouillon, S., Dahdouh-Guebas, F., Rao, A.V.V.S., Koedam, N., Dehair, F., 2007. Sources of organic carbon in mangrove sediments: variability and possible ecological implications. Hydrobiologia 495, 33-39.
Burgoyne, T.W., Hayes, J.M., 1998. Quantitative production of H-2 by pyrolysis of gas chromatographic effluents. Analytical Chemistry 70, 5136-5141.
Chacko, T., Cole, D.R., Horita, J., 2001. Equilibrium oxygen, hydrogen and carbon isotope fractionation factors applicable to geologic systems. Reviews in Mineralogy and Geochemistry 43, 1-81.
Chiang, J.C.H., 2009. The tropics in paleoclimate. Annual Review of Earth and Planetary Sciences 37, 263-297.
Chikaraishi, Y., Naraoka, H., 2003. Compound-specific δD- δ13C analyses of *n*-alkanes extracted from terrestrial and aquatic plants. Phytochemistry 63, 361-371.
Cobb, K.M., Charles, C.D., Cheng, H., Edwards, R.L., 2003. El Nino/Southern Oscillation and tropical Pacific climate during the last millennium. Nature 424, 271-276.
Craig, H., 1961. Isotopic variations in meteoric waters. Science 133, 1702-1703.
Craig, H., Gordon, L., 1965. Deuterium and oxygen 18 variations in the ocean and the marine atmosphere. In: Tongiori, E. (Ed.), Proceedings of a Conference on Stable Isotopes in Oceanographic Studies and Paleotemperatures. CNR-Laboratorio di Geologia Nucleare, Pisa, pp. 9-130.
Datta, P.N., Ghose, M., 2003. Estimation of osmotic potential and free amino acids in some mangroves of the Sundarbans, India. Acta Botanica Croatica 62, 37-45.
Dawson, T.E., Ehleringer, J.R., 1991. Streamside trees that do not use stream water: Evidence from hydrogen isotope ratios. Nature 350, 335-337.
Dawson, T.E., Mambelli, S., Plamboeck, A.H., Templer, P.H., Tu, K.P., 2002. Stable isotopes in plant ecology. Annual Review of Ecology and Systematics 33, 507-559.
Eggemeyer, K.D., Awada, T., Harvey, F.E., Wedin, D.A., Zhou, X., Zanner, C.W., 2009. Seasonal changes in depth of water uptake for encroaching trees Juniperus virginiana and Pinus ponderosa and two dominant C-4 grasses in a semi-arid grassland. Tree Physiology 29, 157-169.
Ellison, J.C., Stoddart, D.R., 1991. Mangrove ecosystem collapse during predicted sea-level rise: Holocene analogues and implications. Journal of Coastal Research 7, 151-165.
Ellsworth, P., Williams, D., 2007. Hydrogen isotope fractionation during water uptake by woody xerophytes. Plant and Soil 291, 93-107.
Englebrecht, A.C., Sachs, J. P., 2005. Determination of sediment provenance at drift sites using hydrogen isotopes and unsaturation ratios in alkenones. Geochimica et Cosmochimica Acta 69, 4253-4265.
Ewe, S., Sternberg, L., Childers, D., 2007. Seasonal plant water uptake patterns in the saline southeast Everglades ecotone. Oecologia 152, 607-616.
Farquhar, G.D., Cernusak, L.A., 2005. On the isotopic composition of leaf water in the non-steady state. Functional Plant Biology 32, 293-303.

Farquhar, G.D., Cernusak, L.A., Barnes, B., 2007. Heavy water fractionation during transpiration. Plant Physiology 143, 11-18.
Feakins, S.J., Sessions, A.L., 2010. Controls on the D/H ratios of plant leaf waxes in an arid ecosystem. Geochimica Cosmochimica Acta 74, 2128-2141.
Fujimoto, K., 1997. Mangrove habitat evolution related to Holocene sea-level changes on Pacific islands. Tropics 6, 203-213.
Gat, J.R., 1996. Oxygen and hydrogen isotopes in the hydrologic cycle. Annual Review in Earth and Planetary Sciences 24, 225-262.
Gordon, N., Lin, G., Sternberg, L., 1992. Isotopic fractionation during cellulose synthesis in two mangrove species: salinity effects. Phytochemistry 31, 2623-2626.
Greenway, H., Osmond, C.B., 1972. Salt responses of enzymes from species differing in salt tolerance. Plant Physiology 49, 256-259.
Hayes, J.M., 2001. Fractionation of carbon and hydrogen isotopes in biosynthetic processes. Reviews in Mineralogy and Geochemistry 43, 225-277.
Helliker, B.R., Ehleringer, J.R., 2000. Establishing a grassland signature in veins: ^{18}O in the leaf water of C_3 and C_4 grasses. Proceedings of the National Academy of Sciences of the United States of America 97, 7894-7898.
Helliker, B.R., Ehleringer, J.R., 2002a. Differential ^{18}O enrichment of leaf cellulose in C_3 versus C_4 grasses. Functional Plant Biology 29, 435-442.
Helliker, B.R., Ehleringer, J.R., 2002b. Grass blades as tree rings: environmentally induced changes in the oxygen isotope ratio of cellulose along the length of grass blades. New Phytologist 155, 417-424.
Hendy, E.J., Gagan, M.K., Alibert, C.A., McCulloch, M.T., Lough, J.M., Isdale, P.J., 2002. Abrupt decrease in tropical Pacific sea surface salinity at end of Little Ice Age. Science 295, 1511-1514.
Herbert, T.D., Peterson, L.C., Lawrence, K.T., Liu, Z., 2010. Tropical ocean temperatures over the past 3.5 million years. Science 328, 1530-1534.
Hibino, T., Meng, Y.L., Kawamitsu, Y., Uehara, N., Matsuda, N., Tanaka, Y., Ishikawa, H., Baba, S., Takabe, T., Wada, K., Ishii, T., Takabe, T., 2001. Molecular cloning and functional characterization of two kinds of betaine-aldehyde dehydrogenase in betaine-accumulating mangrove *Avicennia marina* (Forsk.) Vierh. Plant Molecular Biology 45, 353-363.
Hilkert, A.W., Douthitt, C.B., Schlüter, H.J., Brand, W.A., 1999. Isotope ratio monitoring gas chromatography/mass spectrometry of D/H by high temperature conversion isotope ratio mass spectrometry. Rapid Communications in Mass Spectrometry 13, 1226-1230.
Hogarth, P., 2007. The Biology of Mangroves. Oxford University Press, New York.
Hou, J., D' Andrea, W., Huang, Y., 2008. Can sedimentary leaf waxes record D/H ratios of continental precipitation? Field, model and experimental assessments. Geochimica et Cosmochimica Acta 72, 3503-3517.
Hou, J., D' Andrea, W., MacDonald, D., Huang, Y.S., 2007. Hydrogen isotopic variability in leaf waxes among terrestrial and aquatic plants around Blood Pond, Massachusetts (USA). Organic Geochemistry 38, 977-984.
Huang, Y., Shuman, B., Wang, Y., Webb III, T., 2002. Hydrogen isotope ratios of palmitic acid in lacustrine sediments record late Quaternary climate variations. Geology 30, 1103-1106.

Huang, Y., Shuman, B., Wang, Y., Webb, T., 2004. Hydrogen isotope ratios of individual lipids in lake sediments as novel tracers of climatic and environmental change: a surface sediment test. Journal of Paleolimnology 31, 363-375.

Jetter, R., Kunst, L., Samuels, A. L., 2007. Composition of plant cuticular waxes. In: Reiderer, M., Muller, C. (Ed) Annual Plant Reviews Volume 23: Biology of the Plant Cuticle. Blackwell Publishing Ltd., Oxford, pp. 145-181.

Jones, P.D., Briffa, K.R., Osborn, T.J., Lough, J.M., van Ommen, T.D., Vinther, B.M., Luterbacher, J., Wahl, E.R., Zwiers, F.W., Mann, M., Schmidt, G.A., Ammann, C.M., Buckley, B.M., Cobb, K.M., Esper, J., Goosse, H., Graham, N., Jansen, E., Kiefer, T., Kull, C., Küttel, M., Mosley-Thompson, E., Overpeck, J.T., Riedwyl, N., Schulz, M., Tudhope, A.W., Villalba, R., Wanner, H., Wolff, E., Xoplaki, E., 2009. High-resolution palaeoclimatology of the last millennium: a review of current status and future prospects. The Holocene 19, 3-49.

Kahmen, A., Dawson, T.E., Vieth, A., Sachse, D., 2011. Leaf wax *n*-alkane δD values are determined early in the ontogeny of *Populus trichocarpa* leaves when grown under controlled environmental conditions. Plant, Cell and Environment 34, 1639-1651.

Kahmen, A., Simonin, K., Tu, K.P., Merchant, A., Callister, A., 2008. Effects of environmental parameters, leaf physiological properties and leaf water relations on leaf water delta ^{18}O enrichment in different Eucalyptus species. Plant, Cell & Environment 31, 738-751.

Kathiresan, K., Bingham, B.L., 2001. Biology of mangroves and mangrove ecosystems, Advances in Marine Biology 40, 81-251.

Koutavas, A., Lynch-Stieglitz, J., Marchitto, T.M., Sachs, J.P., 2002. El Nino-like pattern in ice age tropical Pacific sea surface temperature. Science 297, 226-230.

Koutavas, A., Sachs, J.P., 2008. Northern timing of deglaciation in the eastern equatorial Pacific from alkenone paleothermometry. Paleoceanography 23, PA4205, 10pp.

Kristensen, E., Bouillon, S., Dittmar, T., Marchand, C., 2008. Organic carbon dynamics in mangrove ecosystems: A review. Aquatic Botany 89, 201-219.

Lambs, L., Muller, E., Fromard, F., 2008. Mangrove trees growing in a very saline condition but not using seawater. Rapid Communications in Mass Spectrometry 22, 2835-2843.

Lawrence, K.T., Liu, Z., Herbert, T.D., 2006. Evolution of the Eastern Tropical Pacific Through Plio-Pleistocene Glaciation. Science 312, 79-83.

Lea, D.W., Pak, D.K., Belanger, C.L., Spero, H.J., Hall, M.A., Shackleton, N.J., 2006. Paleoclimate history of Galapagos surface waters over the last 135,000 yr. Quaternary Science Reviews 25, 1152-1167.

Leaney, F.W., Osmond, C.B., Allison, G.B., Ziegler, H., 1985. Hydrogen isotope composition of leaf Water in C_3 and C_4 Plants - Its relationship to the hydrogen isotope composition of dry matter. Planta 164, 215-220.

Lin, G., Sternberg, L., 1992. Effect of growth form, salinity, nutrient and sulfide on photosynthesis, carbon isotope discrimination and growth of red mangrove *Rhizophora mangle* L. Functional Plant Biology 19, 509-517.

Lin, G., Sternberg, L., 1993. Hydrogen isotopic fractionation by plant roots during water uptake in coastal wetland plants. In: Ehleringer, J., Hall, A., Farquhar, G., (Ed.) Stable isotopes and plant carbon/water relations. Academic Press, Inc., San Diego, pp. 497-510.

Lin, G., Sternberg, L., 1994. Utilization of surface water by red mangrov (*Rhizophora mangle* L.): An isotopic study. Bulletin of Marine Science 54, 94-102.

Linsley, B.K., Kaplan, A., Gouriou, Y., Salinger, J., deMenocal, P.B., Wellington, G. M., Howe, S.S., 2006. Tracking the extent of the South Pacific Convergence Zone since the early 1600s. Geochemistry Geophysics Geosystems 7, Q05003, 15pp.

Liu, W.G., Yang, H., 2008. Multiple controls for the variability of hydrogen isotopic compositions in higher plant n-alkanes from modern ecosystems. Global Change Biology 14, 2166-2177.

Liu, W.G., Yang, H., Li, L., 2006. Hydrogen isotopic composition of *n*-alkanes from terrestrial plants correlate with their ecological life form. Oecologia 150, 330-338.

Lopez-Hoffman, L., Anten, N.P.R., Martinez-Ramos, M., Ackerly, D.D., 2007. Salinity and light interactively affect neotropical mangrove seedings at the leaf and whole plant levels. Oecologia 150, 545-556.

Luo, Y.H., Steinberg, L., Suda, S., Kumazawa, S., Mitsui, A., 1991. Extremely low D/H ratios of photoproduced hydrogen by cyanobacteria. Plant and Cell Physiology 32, 897-900.

Makou, M.C., Hughen, K.A., Xu, L., Sylva, S.P., Eglinton, T.I., 2007. Isotopic records of tropical vegetation and climate change from terrestrial vascular plant biomarkers preserved in Cariaco Basin sediments. Organic Geochemistry 38, 1680-91.

Matsuo, S., Friedman, I., Smith, G.I., 1972. Studies of quaternary saline lakes – I. Hydrogen isotope fractionation in saline minerals. Geochimica et Cosmochimica Acta 36, 427-435.

McInerney, F.A., Helliker, B.R., Freeman, K.H., 2011. Hydrogen isotope ratios of leaf wax *n*-alkanes in grasses are insensitive to transpiration. Geochimica et Cosmochimica Acta 75, 541-554.

McKee, K.L., Feller, I.C., Popp, M., Wanek, W., 2002. Mangrove isotopic fractionation across a nitrogen vs phosphorus limitation gradient. Ecology 83, 1065-1075.

Moon, G., Clough, B., Peterson, C., Allaway, W., 1986. Apoplastic and symplastic pathways in *Avicennia marina* (Forsk.) Vierh. roots revealed by fluorescent tracer dyes. Functional Plant Biology 13, 637-648.

Morgan, J.M., 1984. Osmoregulation and water stress in higher plants. Plant Physiology 35, 299-319.

Naidoo, G., 2010. Ecophysiological differences between fringe and dwarf *Avicennia marina* mangroves. Trees 24, 667-673.

O'Brien, F.E.M., 1948. The control of humidity by saturated salt solutions. Journal of Scientific Instruments 25, 73.

Ohkouchi, N., Kawamura, K., Nakamura, T., Taira, A., 1994. Small changes in the sea surface temperature during the last 20,000 years: Molecular evidence from the western tropical Pacific. Geophysical Research Letters 21, 2207-2210.

Pagani, M., Pedentchouk, N., Huber, M., Sluijs, A., Schouten, S., Brinkhuis, H., Damste, J.S.S., Dickens, G.R., Scientists, E., 2006. Arctic hydrology during global warming at the Palaeocene/Eocene thermal maximum. Nature 442, 671-675.

Pahnke, K., Sachs, J.P., Keigwin, L.D., Timmermann, A., Xie, S.P., 2007. Eastern tropical Pacific hydrologic changes during the past 27,000 years from D/H ratios in alkenones. Paleoceanography 22, PA4214, 15pp.

Parida, A., Jha, B., 2010. Salt tolerance mechanisms in mangroves: a review. Trees - Structure and Function 24, 199-217.

Patel, N.T., Gupta, A.K., Pandey, A.N., 2010. Salinity tolerance of *Avicennia marina* (Forssk.) Vierh. from Gujarat coasts of India. Aquatic Botany 93, 9-16.

Polidoro, B.A., Carpenter, K.E., Collins, L., Duke, N.C., Ellison, A.M., Ellison, J.C., Farnsworth, E.J., Fernando, E.S., Kathiresan, K., Koedam, N., Livingston, S.R., Miyagi, T., Moore, G.E., Vien, N.N., Ong, J.E., Primavera, J.H., Salmo, S.G., Sanciangco., J.C., Sukardjo, S., Wang, Y., Yong, J.W.H., 2010. The loss of species: mangrove extinction risk and geographic areas of global concern. PLoS One 5, e10095, 10pp.

Polissar, P.J., Freeman, K.H., 2010. Effects of aridity and vegetation on plant-wax δD in modern lake sediments. Geochimica et Cosmochimica Acta 74, 5785-5797.

Riley, W.J., Still, C.J., Torn, M.S., Berry, J.A., 2002. A mechanistic model of (H2O)-O-18 and (COO)-O-18 fluxes between ecosystems and the atmosphere: Model description and sensitivity analysis. Global Biogeochemical Cycles 16, 1095, 14pp.

Romero, I.C., Feakins, S.J., 2011. Spatial gradients in plant leaf wax D/H across a coastal salt marsh in southern California. Organic Geochemistry 42, 618-629.

Sachs, J.P., Sachse, D., Smittenberg, R.H., Zhang, Z., Battisti, D.S., Golubic, S., 2009. Southward movement of the Pacific intertropical convergence zone AD 1400-1850. Nature Geoscience 2, 519-525.

Sachs, J.P., Schwab, V.F., 2011. Hydrogen isotopes in dinosterol from the Chesapeake Bay estuary. Geochimica et Cosmochimica Acta 75, 444-459.

Sachse, D., Billault, I., Bowen, G.J., Chikaraishi, Y., Dawson, T.E., Feakins, S.J., Freeman, K.H., Magill, C.R., McInerney, F.A., van der Meer, M.T.J., Polissar, P., Robins, R.J., Sachs, J.P., Schmidt, H.L., Sessions, A.L., White, J.W.C., West., J.B., Kahmen, A., 2012. Molecular paleohydrology: interpreting the hydrogen-isotopic composition of lipid biomarkers from photosynthesizing organisms. Annual Review of Earth and Planetary Science 40, 212-249.

Sachse, D., Gleixner, G., Wilkes, H., Kahmen, A., 2010. Leaf wax *n*-alkane δD values of field-grown barley reflect leaf water δD values at the time of leaf formation. Geochimica et Cosmochimica Acta 74, 6741-6750.

Sachse, D., Kahmen, A., Gleixner, G., 2009. Significant seasonal variation in the hydrogen isotopic composition of leaf-wax lipids for two deciduous tree ecosystems (*Fagus sylvativa* and *Acer pseudoplatanus*). Organic Geochemistry 40, 732-742.

Sachse, D., Radke, J., Gleixner, G., 2004. Hydrogen isotope ratios of recent lacustrine sedimentary *n*-alkanes record modern climate variability. Geochimica et Cosmochimica Acta 68, 4877-4889.

Sachse, D., Radke, J., Gleixner, G., 2006. δD values of individual *n*-alkanes from terrestrial plants along a climatic gradient – Implications for the sedimentary biomarker record. Organic Geochemistry 37, 469-483.

Sachse, D., Sachs, J., 2008. Inverse relationship between D/H fractionation in cyanobacterial lipids and salinity in Christmas Island saline ponds. Geochimica et Cosmochimica Acta 72, 793-806.

Sauer, P.E., Eglinton, T.I., Hayes, J.M., Schimmelmann, A., Sessions, A.L., 2001. Compound-specific D/H ratios of lipid biomarkers from sediments as a proxy for environmental and climatic conditions. Geochimica et Cosmochimica Acta 65, 213-222.

Schefuss, E., Schouten, S., Schneider, R.R., 2005. Climatic controls on central African hydrology during the past 20,000 years. Nature 437, 1003-1006.

Schmidt, H.L., Werner, R.A., Eisenreich, W., 2003. Systematics of ^{2}H patterns in natural compounds and its importance for the elucidation of biosynthetic pathways. Phytochemistry Reviews 2, 61-85.

Schouten, S., Ossebaar, J., Schreiber, K., Kienhuis, M.V.M., Langer, G., Benthien, A., Bijma, J., 2006. The effect of temperature, salinity and growth rate on the stable hydrogen isotopic composition of long chain alkenones produced by *Emiliania huxleyi* and *Gephyrocapsa oceanica*. Biogeosciences 3, 113-119.

Schwab, V., Sachs, J., 2011. Hydrogen isotopes in individual alkenones from the Chesapeake Bay estuary. Geochimica et Cosmochimica Acta.

Sessions, A., 2006. Seasonal changes in D/H fractionation accompanying lipid biosynthesis in Spartina alterniflora. Geochima et Cosmochimica Acta 70, 2153-2162.

Sessions, A.L., Burgoyne, T.W., Schimmelmann, A., Hayes, J.M., 1999. Fractionation of hydrogen isotopes in lipid biosynthesis. Organic Geochemistry 30, 1193-1200.

Sheshshayee, M.S., Bindumadhava, H., Ramesh, R., Prasad, T.G., Lakshminarayana, M.R., Udayakumar, M., 2005. Oxygen isotope enrichment (Delta O-18) as a measure of time-averaged transpiration rate. Journal of Experimental Botany 56, 3033-3039.

Smith, F.A., Freeman, K.H., 2006. Influence of physiology and climate on δD of leaf wax *n*-alkanes from C_3 and C_4 grasses. Geochimica et Cosmochimica Acta 70, 1172-1187.

Smittenberg, R.H., Saenger, C., Dawson, M.N., Sachs, J.P., 2011. Compound-specific D/H ratios of the marine lakes of Palau as proxies for West Pacific Warm Pool hydrologic variability. Quaternary Science Reviews 30, 921-933.

Stott, L., Poulsen, C., Lund, S., Thunell, R., 2002. Super ENSO and Global Climate Oscillations at Millennial Time Scales. Science 297, 222-226.

Tierney, J.E., Oppo, D.W., Rosenthal, Y., Russell, J.M., Linsley, B.K., 2010. Coordinated hydrological regimes in the Indo-Pacific region during the past two millennia. Paleoceanography 25, PA1102, 7pp.

Vandermeer, M., Baas, M., Rijpstra, W., Marino, G., Rohling, E., Damste, J.S.S., Schouten, S., 2007. Hydrogen isotopic compositions of long-chain alkenones record freshwater flooding of the Eastern Mediterranean at the onset of sapropel deposition. Earth and Planetary Science Letters 262, 594-600.

Vandermeer, M., Sangiorgi, F., Baas, M., Brinkhuis, H., Damste, J.S.S., and Schouten, S., 2008. Molecular isotopic and dinoflagellate evidence for Late Holocene freshening of the Black Sea. Earth and Planetary Science Letters 267, 426-434.

Volkman, J.K., Revill, A.T., Bonham, P.I., Clementson, L.A., 2007. Sources of organic matter in sediments from the Ord River in tropical northern Australia. Organic Geochemistry 38, 1039-1060.

Walker, C.D., Leaney, F.W., Dighton, J.C., Allison, G.B., 1989. The influence of transpiration on the equilibration of leaf water with atmospheric water vapour. Plant, Cell & Environment 12, 221-234.

Walker, C.D., Richardson, S.B., 1991. The use of stable isotopes of water in characterising the source of water in vegetation. Chemical Geology: Isotope Geoscience section 94, 145-158.

Wannigama, G.P., Volkman, J.K., Gillan, F.T., Nichols, P.D., Johns, R.B., 1981. A comparison of lipid components of the fresh and dead leaves and pneumatophores of the mangrove *Avicennia marina.* Phytochemistry 20, 659-666.

White, J.W.C., Cook, E.R., Lawrence, J.R., Broecker, W.S., 1985. The D/H ratios of sap in trees: Implications for water sources and tree ring D/H ratios. Geochimica et Cosmochimica Acta 49, 237-246.

Worbes, M., 1995. How to measure growth dynamics in tropical trees: a review. IAWA Journal 16, 227-351.
Yang, H., Pagani, M., Briggs, D.E.G., Equiza, M.A., Jagels, R., Leng, Q., LePage, B.A., 2009. Carbon and hydrogen isotope fractionation under continuous light: implications for paleoenvironmental interpretations of the High Arctic during Paleogene warming. Oecologia 160, 461-470.
Ye, Y., Tam, N.F.Y., Lu, C.Y., Wong, Y.S., 2005. Effects of salinity on germination, seedling growth and physiology of three salt-secreting mangrove species. Aquatic Botany 83, 193-205.
Yeo, A.R., 1983. Salinity resistance: physiologies and prices. Physiologia Plantarum 58, 214-222.
Zhang, Z. Sachs, J.P., 2007. Hydrogen isotope fractionation in freshwater algae: I. Variations among lipids and species. Organic Geochemistry 38, 582-608.
Zhang, Z., Sachs, J.P., Marchetti, A., 2009. Hydrogen isotope fractionation in freshwater and marine algae: II. Temperature and nitrogen limited growth rate effects. Organic Geochemistry 40, 428-439.
Zhou, Y., Grice, K., Chikaraishi, Y., Stuart-Williams, H., Farquhar, G.D., Ohkouchi, N., 2011. Temperature effect on leaf water deuterium enrichment and isotopic fractionation during leaf lipid biosynthesis: results from controlled growth of C3 and C4 land plants. Phytochemistry 72, 207-213.
Zhou, Y., Grice, K., Stuart-Williams, H., Farquhar, G.D., Hocart, C. H., Lu, H., Liu, W., 2010. Biosynthetic origin of the saw-toothed profile in $\delta^{13}C$ and $\delta^{2}H$ of n-alkanes and systematic isotopic differences between n-, iso-, and anteiso-alkanes in leaf waxes of land plants.

2.8 Figure Captions

Figure 1 Map of the Brisbane River Estuary. Sampling sites used for this study are marked with bold numbers, corresponding to data in Table 1.

Figure 2 Salinity versus distance from river mouth in the Brisbane River. The linear regression of this field data was used to calculate the mean salinity values shown in Fig. 1.

Figure 3 Leaf wax and water δD values in the Brisbane River versus salinity. **A** shows *n*-C_{31} alkanes; **B** shows *n*-C_{33} alkanes. Lipid δD scale for both plots is on the left-hand y-axis; the water δD scale for both plots is on the right-hand y-axis. The two δD axes have been scaled equivently, but are offset by 100‰.

Figure 4 Apparent fractionation factors, α_a, of mangrove *n*-C_{31} alkanes (**A**) and *n*-C_{33} alkanes (**B**) versus salinity.

Figure 5 Comparision of this study's results (α_{c31} and α_{c33} from Fig 4, solid symbols) with previously published comparisons of apparent fractionation in algal lipids with salinity (open symbols). Dinosterol data is from Sachs and Schwab (2011); other algal lipids are from Sachse and Sachs (2008). Linear regressions are continued beyond the salinity range of each study for illustrative purposes only.

Figure 6 Schematic representation of processes that contributed to the hydrogen isotope ratios of mangrove lipids. The left panel represents a mangrove growing in low salinity, and is comparable to a terrestrial tree. The right two panels represent two ways a mangrove growing in more saline water could display greater apparent fractionation. At present, we cannot determine which scenario is more appropriate.

Supplementary Figure Captions

Figure S1 GC-MS total ion chromatogram of total lipid extract of *A. marina* leaf. Alcohols were converted to TMS-ethers prior to analysis.

Figure S2 GC-MS total ion chromatogram of hydrocarbon fraction of *A. marina* leaf.

Figure 1 Map of the Brisbane River Estuary. Sampling sites used for this study are marked with bold numbers, corresponding to data in Table 1.

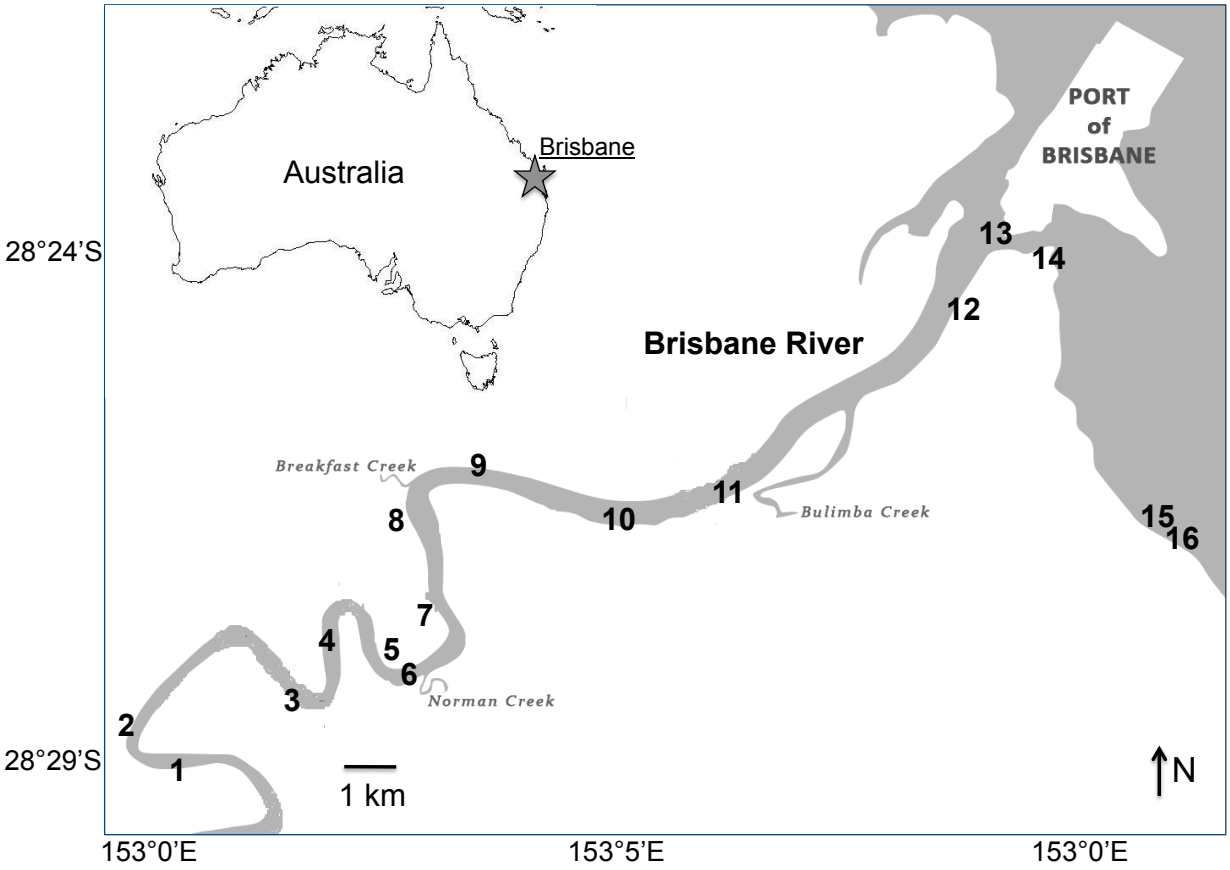

Figure 2 Salinity versus distance from river mouth in the Brisbane River. The linear regression of this field data was used to calculate the mean salinity values shown in Table 1.

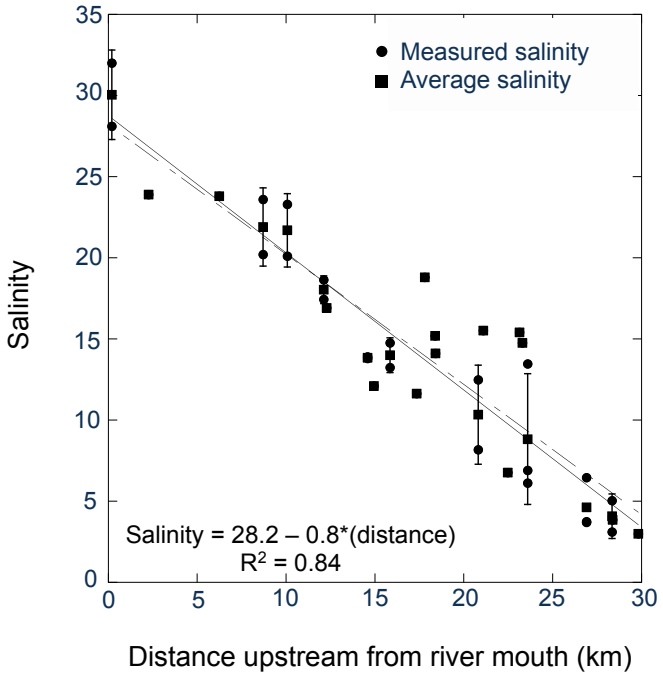

Figure 3 Leaf wax and water δD values in the Brisbane River versus salinity. **A** shows *n*-C_{31} alkanes; **B** shows *n*-C_{33} alkanes. Lipid δD scale for both plots is on the left-hand y-axis; the water δD scale for both plots is on the right-hand y-axis. The two δD axes have been scaled equivently, but are offset by 100‰.

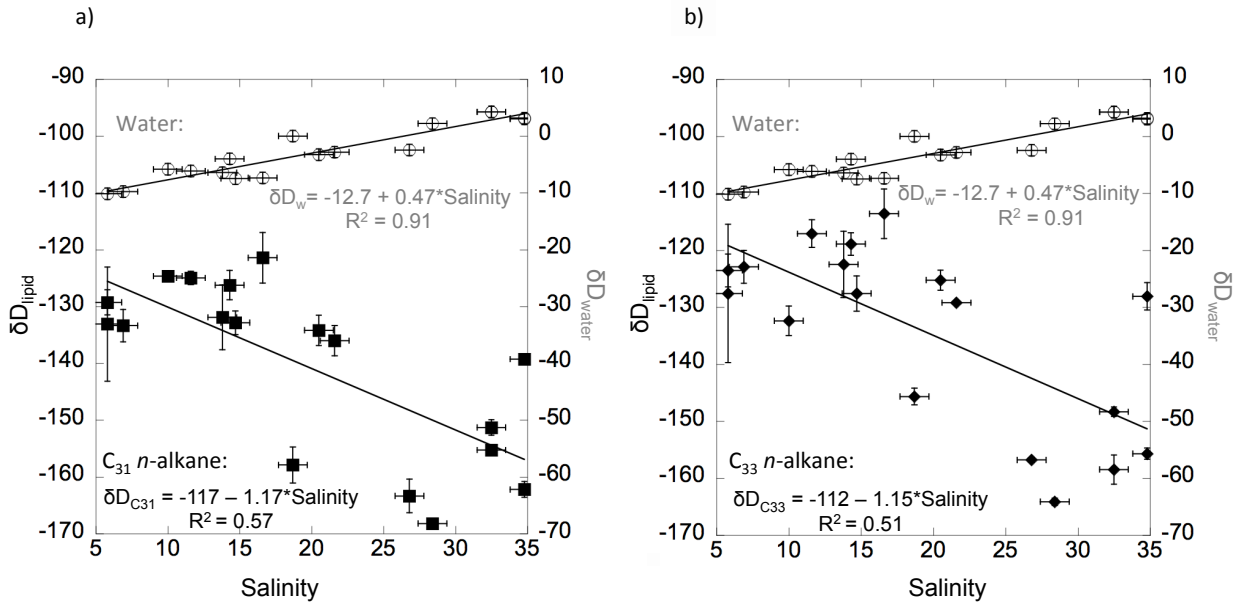

Figure 4 Apparent fractionation factors, α_a, of mangrove *n*-C_{31} alkanes (**A**) and *n*-C_{33} alkanes (**B**) versus salinity.

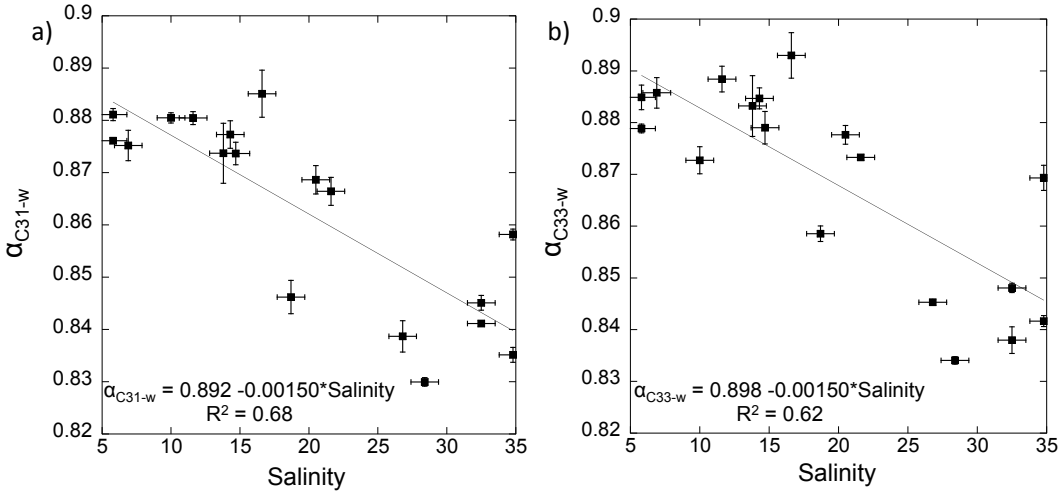

Figure 5 Comparision of this study's results (α_{c31} and α_{c33} from Fig 4, solid symbols) with previously published comparisons of apparent fractionation in algal lipids with salinity (open symbols). Dinosterol data is from Sachs and Schwab (2011); other algal lipids are from Sachse and Sachs (2008). Linear regressions are continued beyond the salinity range of each study for illustrative purposes only.

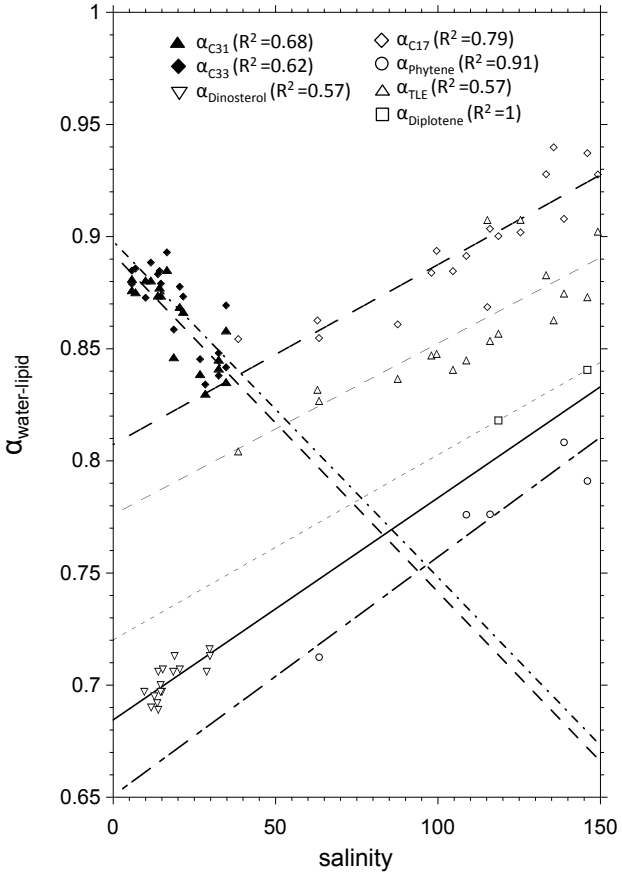

Figure 6 Schematic representation of processes that contributed to the hydrogen isotope ratios of mangrove lipids. The left panel represents a mangrove growing in low salinity, and is comparable to a terrestrial tree. The right two panels represent two ways a mangrove growing in more saline water could display greater apparent fractionation. At present, we cannot determine which scenario is more appropriate.

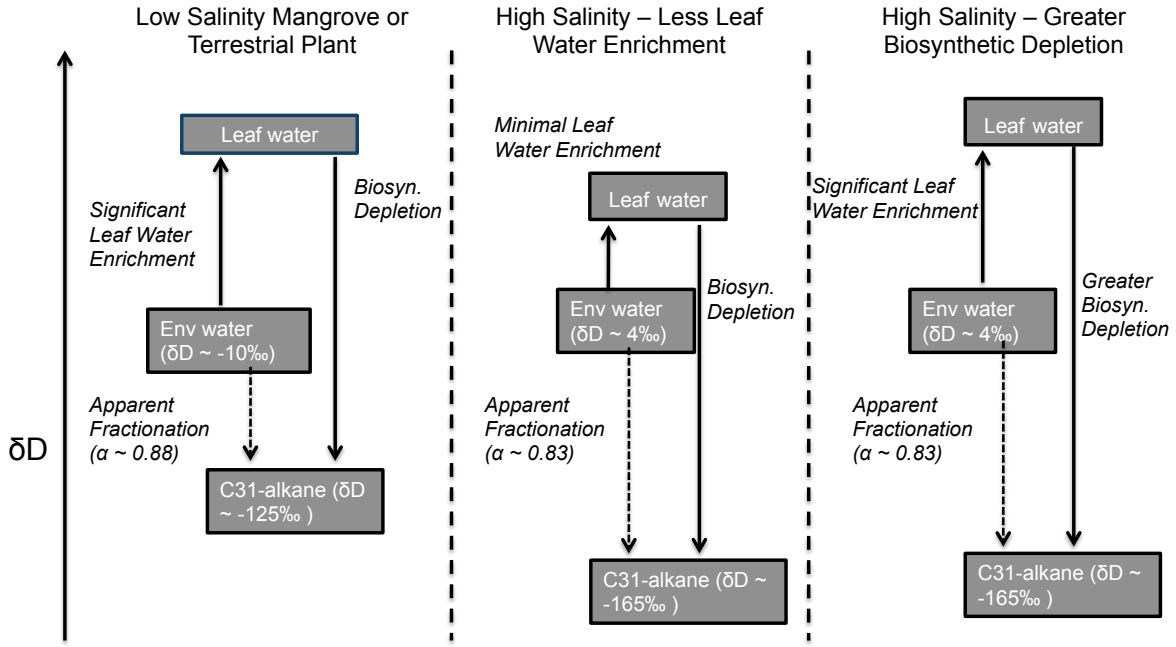

Figure S1 GC-MS total ion chromatogram of total lipid extract of *A. marina* leaf. Alcohols were converted to TMS-ethers prior to analysis.

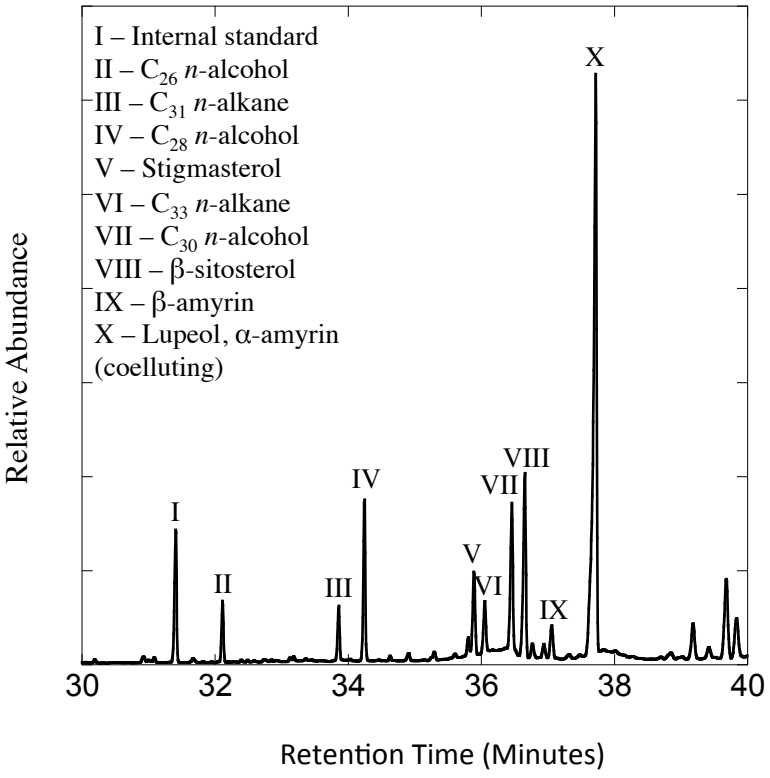

Figure S2 GC-MS total ion chromatogram of hydrocarbon fraction of *A. marina* leaf.

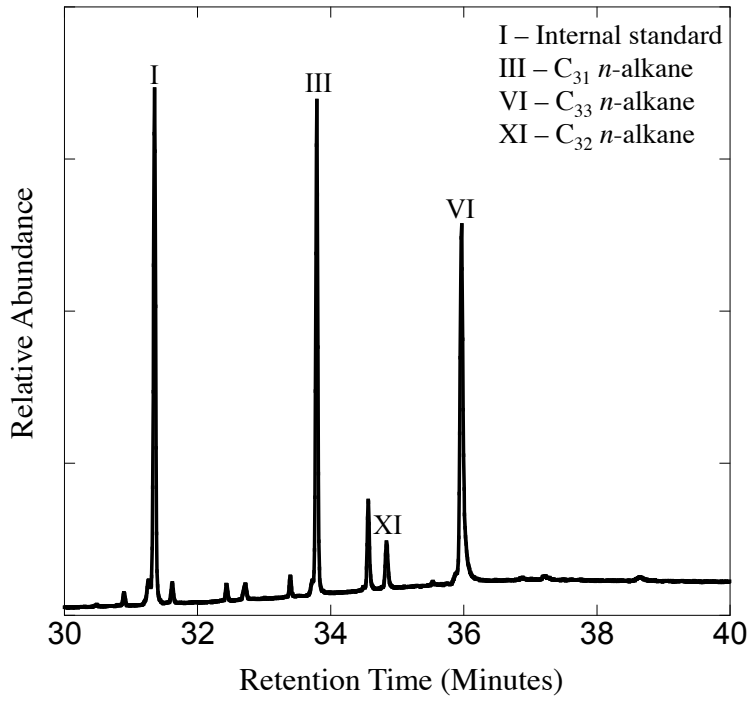

Chapter 3: Positive correlation between salinity and *n*-alkane $\delta^{13}C$ values in the mangrove *Avicennia marina*[2]

3.1 Abstract

Carbon isotope ratio ($\delta^{13}C$) values of lipid biomarkers from plants can be used to assess water use efficiency and reconstruct environmental conditions in the past. We assessed the effect of salinity on the $\delta^{13}C$ values for leaf wax *n*-C_{31}- and *n*-C_{33}-alkanes, bulk leaf matter and leaf total lipid extracts from *Avicennia marina* (gray mangrove) trees growing along the Brisbane River estuary in Queensland, Australia. We observed an increase of 0.19 ± 0.053‰ (R^2 =0.61, p =0.008) and 0.16 ± 0.052‰ (R^2 =0.55, p =0.01) per salinity unit for the two *n*-alkanes, respectively, and of 0.087 ± 0.028‰ (R^2 =0.41, p =0.009) for whole leaves per salinity unit, indicating that water use efficiency of *A. marina* increased with the salt content of water. There was no correlation between $\delta^{13}C$ values of total lipid extracts and salinity, perhaps because of a decrease in lipid concentration at higher salinity or because of varying contributions of different lipid classes to the extract. The robust relationship between salinity and $\delta^{13}C$ values of leaf wax lipids provides a means of quantitatively reconstructing past salinity from carbon isotope ratios of mangrove lipid biomarkers in sediments. When paired with measurements of the hydrogen isotope ratio values of the same compounds, the approach should facilitate quantitative reconstructions of the hydrogen isotope composition of environmental water. In order for this method to successfully reconstruct past salinity and water isotopes, a mangrove source for leaf-waxes would need to be confirmed by palynological or other evidence, or the isotopic composition of a more source specific biomarker, such as taraxerol, would need to be measured.

[2] Previously published as: Ladd S. N. & Sachs J. P. (2013) Positive correlation between salinity and *n*-alkane d13C values in the mangrove *Avicennia marina*. *Organic Geochemistry* 64, 1-8. Reprinted with permission from Elsevier.

3.2 Introduction

Water use efficiency (the ratio of carbon assimilation to stomatal conductance) is a dominant control of the carbon isotopic composition of plant matter (O'Leary, 1981; Farquhar et al., 1982a; Werner et al., 2012), and the bulk carbon isotope composition of plants has frequently been used as an indicator of water stress in plants (Ehleringer et al., 1992; Saurer et al., 2004; Shaheen and Hood-Nowotny, 2005). According to the model developed by O'Leary (1981), as stomatal conductance decreases there is a corresponding decrease in CO_2 entering the leaf and ribulose-1,5-bisphosphate carboxylase oxygenase (RuBisCo), the enzyme primarily responsible for carbon fixation, is forced to fix a greater proportion of $^{13}CO_2$ than under conditions where a greater supply of atmospheric CO_2 is available.

Under conditions of salt stress, plants typically increase their water use efficiency, reducing stomatal conductance relative to carbon assimilation rate (Farquhar et al., 1982b; Ball and Farquhar, 1984; Lin and Sternberg, 1992a; Krauss et al., 2008). It is no surprise, therefore, that, as salinity increases, the $\delta^{13}C$ value $\{[(^{13}C/^{12}C)_{sample}/(^{13}C/^{12}C)_{VPDB} - 1] \times 1000\}$ of bulk plant matter also increases (Farquhar et al., 1989 and references therein; Werner et al., 2012).

This relationship has been observed in halophillic plants such as mangroves, which are woody trees and shrubs that have adapted to live in brackish or saline water along estuaries and intertidal flats. Farquhar et al. (1982b) observed higher $\delta^{13}C$ values for *Avicennia marina* (gray mangrove) and *Aegiceras corniculatum* (river mangrove) cultivated in 50% seawater relative to those grown in freshwater. Subsequently, Lin and Sternberg (1992a) demonstrated a 3‰ decrease in discrimination against ^{13}C in *Rhizophora mangle* (red mangrove) cultivated in a 500 (~30 PSU) mM NaCl solution relative to those cultivated at 100 mM NaCl (~6 PSU).

The results of these culturing studies are consistent with measurements of $\delta^{13}C$ values of whole mangrove leaves in the field (Lin and Sternberg, 1992b; Medina and Francisco, 1996; McKee et al, 2002; Wei et al., 2008). However, no study has systematically determined the relationship between salinity and whole leaf $\delta^{13}C$ values in mangroves by sampling trees along a significant salinity gradient. Several studies (Lin and Sternberg, 1992b; Medina and Francisco, 1996; McKee et al, 2002) have compared the carbon isotopic composition of mangrove leaves between two sites and have observed $\delta^{13}C$ values that were as much as 4‰ greater at hypersaline sites. Wei et al. (2008) measured the $\delta^{13}C$ values of leaves from three mangrove species collected along a salinity gradient within a Chinese coastal swamp. While they observed a positive correlation between $\delta^{13}C$ and salinity for two of the three species, the results were not statistically significant for two of the species and the range in salinity was limited to 14-20 (PSU, practical salinity scale).

This study represents the first to establish a relationship between salinity and $\delta^{13}C$ values for mangrove leaf tissue and individual *n*-alkanes along a wide natural salinity gradient (6-35). The values for leaf wax were expected to covary with whole leaf values, as observed for other plants (Collister et al., 1994; Chikaraishi and Naraoka, 2007). We were particularly interested in the relationship between salinity and the $\delta^{13}C$ values of individual lipids because lipids are well preserved in sediments and could serve as a recorder of past fluctuation in salinity. We have previously demonstrated that leaf wax δD values are negatively correlated with salinity for *A. marina* growing in the Brisbane River Estuary (Ladd and Sachs, 2012). If $\delta^{13}C$ values of the same lipids covary with salinity, paired $\delta^{13}C$ and δD measurements of the same lipid could be used to create robust reconstruction of salinity and water isotopes over time.

3.3.Methods

3.3.1 Sample collection

During a one week period in February 2010, whole *A. marina* leaves were collected along the Brisbane River Estuary and Moretown Bay in Queensland, Australia (Fig. 1). Five to ten leaves were collected from various heights and aspects of each tree and were immediately placed on ice and subsequently kept frozen during storage. *A. marina* was chosen because it is one of the most salt tolerant species of mangroves (Ball, 1988; Ye et al., 2005) and so is present along the entire length of the Brisbane River estuary from the coast to inland sites where water is almost fresh at low tide.

At each site, surface water was collected adjacent to the sampled tree, and the water temperature, conductivity, and specific conductivity were measured using a YSI 85 conductivity probe (YSI Inc., Yellow Springs, OH, USA). When possible, multiple visits were made to the same site at different points in the tidal cycle in order assess tidal variation in salinity. For the six sites sampled near both high and low tide, the average tidal range of salinity was 4.2 ± 1.0 PSU. Salinity in the Brisbane River estuary was correlated (R^2 =0.86) with distance from the river mouth (Fig. 2). In order to minimize bias from salinity measured at one particular point in the tidal cycle we derived mean salinity for each sampling site from the linear regression relating salinity to distance from the mouth (Salinity = – 0.85 ± 0.058 x (distance) + 29 ± 1.1; Table 1, Fig. 2). The standard error of the regression in Fig. 2 is 2.9 salinity units.

3.3.2 Bulk leaf $\delta^{13}C$ values

Whole leaves were freeze-dried and ground to a homogenous powder. A small portion of the dry powder was wrapped in Sn capsules and analyzed using elemental analysis – isotope

ratio mass spectrometry (EA-IRMS). The EA instrument was a CE Instruments NC-2500 (CE Instruments, Wigan, UK) equipped with a 50 position carousel autosampler from CE instruments and attached to a Thermo Scientific Delta-XL IRMS instrument (Thermo Scientific, Waltham, MA, USA). Samples were dropped into a combustion reactor filled with Cr_2O_3 and Co_3O_4+Ag at 1040°C. The resulting CO_2 and H_2O were carried with He through a water removal trap filled with $Mg(ClO_4)_2$. The CO_2 continued through the ConFlow II capillary open split interface for transfer to the mass spectrometer. Measured isotope values were corrected to a CO_2 working standard, which had been corrected to an external standard of nicotinic acid. The standard error for these measurements was 0.06‰.

3.3.3 Lipid extraction and purification

Intact whole leaves from each tree were selected for analysis. They were rinsed with DI water to remove debris and cut into small pieces using solvent cleaned scissors prior to freeze drying. Dry leaves were ground with a solvent cleaned mortar and pestle, and lipids were extracted using accelerated solvent extraction (ASE-200, Dionex Corp., Sunnyvale, CA, USA) with 9:1 DCM:MeOH at 100 °C and 1500 psi for 3 x 5 min static cycles. The resulting total lipid extract (TLE) was evaporated to dryness under a stream of N_2 on a Turbovap system (Caliper, Hopkinton, MA, USA).

A small aliquot of the TLE was dissolved in 20 µl pyridine and silylated with 20 µl bis(trimethylsilyl)trifluoroacetamide (BSTFA, Sigma-Aldrich, St. Louis, MO, USA) at 60 °C for 60 min. An initial screening of the TLE was conducted using gas chromatography-mass spectrometry (GC-MS) with an Agilent (Santa Clara, CA, USA) 6890N gas chromatograph equipped with an Agilent 7683 autosampler, split-splitless injector operated in splitless mode and

an Agilent DB-5ms column (60 m x 0.32 mm x 0.25 μm) interfaced to an Agilent 5975 quadrupole mass selective detector. The oven temperature was increased from 60 to 150 °C at 15 °C/min, then at 6 °C/min to 320 °C (held 28 min). Lipids were identified based on published EI spectra and comparison with the spectra of laboratory standards. The composition of the TLE did not vary significantly as a function of salinity. The most abundant lipids included *n*-alkanes (*n*-C_{31} and *n*-C_{33}), *n*-alcohols (*n*-C_{26}, *n*-C_{28} and *n*-C_{30}), sterols (stigmasterol and β-sitosterol) and triterpenols (α-amyrin, β-amyrin, and lupeol), with lupeol particularly abundant (Fig. S1).

Another aliquot of the *A. marina* TLE (~12 mg) was purified using two-step column chromatography. During the first step, with a solid phase of 500 mg amino propyl silica gel (Supelco, Lot # 2511301, Part # 5-7205), the neutral fraction was eluted with 8 ml of 3:1 DCM:isopropanol, acids with 6 ml 4% $MeCO_2H$ in Et_2O and other polar compounds with 6 ml MeOH. The neutral fraction was further purified with a solid phase of 1g silica gel (EMD, Lot # 45169543, Part # 11567-2) deactivated (5%) with water. Hydrocarbons were eluted with 8 ml hexane, sterols, alcohols and triterpenols with 6 ml 4:1 hexane:EtOAc and remaining compounds with 4 ml MeOH.

The hydrocarbon fraction of *A. marina* was dominated by *n*-C_{31} and *n*-C_{33} alkanes, with relatively small amounts of *n*-C_{32} and other unidentified lipids (Fig. S2). Lipids in the hydrocarbon fraction were quantified with a GC instrument equipped with flame ionization detection (GC-FID). An Agilent 6890N gas chromatograph equipped with an Agilent 7683 autosampler, programmable temperature vaporization inlet (PTV) operated in splitless mode and an Agilent DB-5ms column (60 m x 0.32 mm x 0.25 μm) was used with He as carrier gas (2.4 ml/min). The oven temperature was increased from 60 to 150 °C at 15 °C/min, then at 6 °C/min

to 320 °C (held 28 min). Quantification of *n*-alkanes was performed by comparing integrated peak areas with a known amount of *n*-C_{37}, added to the sample just prior to GC-FID analysis.

3.3.4 Bulk lipid $\delta^{13}C$ values

An aliquot of the TLE was transferred to Sn capsule and evaporated to dryness under a gentle stream of N_2 before folding the capsule. Carbon isotopes were then measured using identical methods to those above.

3.3.5 Individual n-alkane $\delta^{13}C$ values

Values for a subset of ten samples were measured at the Woods Hole Oceanographic Institution (Woods Hole, MA). These ten samples were chosen to represent the full salinity gradient, and were selected so that the mean salinity difference between each subsequent site was ~3 PSU. An aliquot of the purified hydrocarbon fraction was injected using a PTV inlet (Gerstel, Mülheim an der Ruhr, Germany) operated in solvent venting mode. The temperature during the injection was held at 40°C for 15 s, then increased at 12 °C/s to 350 °C and held there for 3 min. Solvent was vented at 30 ml/min for 15 s, after which all flow was directed to the column. The sample dilution and injection volume were adjusted to deliver ca. 60-80 ng of the most abundant *n*-alkane of interest onto the column. Samples were injected using an HP 6890 autosampler.

The HP 6890 GC instrument was equipped with a CP-Sil 5CB low bleed-MS (60 m x 0.25 mm i.d. x 0.25 um phase) column, with flow at 1 ml/min He, programmed from 60 °C (3 min) then at 50°C/min to 180 °C (no hold), then at 3 °C/min to 340 °C (held as needed to fully elute all compounds). The GC instrument was interfaced to a Finnigan-MAT DeltaPlus IRMS instrument by a GC-Combustion III interface, modified after Goodman (1998) to an integral

fused silica combustion design. The reference gas value was calibrated against a suite of 9 compounds (of known isotopic values determined at numerous independent, external laboratories) injected on the above system. The standard error for this method was 0.3‰. Four samples were measured in triplicate, with an average standard deviation of 0.2‰. The remaining six samples were measured as single injections.

3.4 Results

3.4.1 Whole leaf $\delta^{13}C$ values

The values for leaf tissue were between -30.5‰ and -25.8‰, a range of 4.7‰ (Table 1), and ca. 20‰ less than atmospheric CO_2 (-8.25‰ in 2010; http://www.esrl.noaa.gov/gmd/ccgg/iadv/). Leaf values correlated positively with salinity (Fig. 3a). The one outlier was a leaf from a small seedling, which was depleted by 2.4‰ relative to the mature tree sampled at the same site. This was the only seedling sampled, and was excluded from subsequent analyses. Excluding this outlier, linear regression analysis yielded a correlation coefficient (R^2) of 0.41, indicating that the correlation was significant at the 95% confidence level ($p = 0.009$). The relationship between salinity and bulk leaf $\delta^{13}C$ values (excluding the sapling) was $\delta^{13}C_{leaf} = 0.087 \pm 0.028 \times \text{salinity} - 30.1 \pm 0.61$.

The net fractionation factor, $\alpha_{atm\text{-}leaf}$ [defined as $(^{13}C/^{12}C)_{leaf}/(^{13}C/^{12}C)_{atm}$), determined relative to atmospheric CO_2 ($\delta^{13}C$ -8.25‰ in 2010; http://www.esrl.noaa.gov/gmd/ccgg/iadv/), varied between 0.972 and 0.982 (Table 1). $\alpha_{atm\text{-}leaf}$ also correlated with salinity according to the relationship $\alpha_{atm\text{-}leaf} = 8.8 \times 10^{-5} \pm 2.85 \times 10^{-5} \times S - 0.978 \pm 0.000615$ (R^2 0.41; $p = 0.009$; Fig. 3b).

3.4.2 Bulk lipid $\delta^{13}C$ values

These varied between -35.6‰ and -29.2‰, a range of 6.3‰. They did not correlate with salinity (R^2 0.079, p = 0.29; Fig. 4).

3.4.3 Leaf wax n-alkane $\delta^{13}C$ values

The values were between -36.4‰ and -30.7‰ for *n*-C_{31}, a range of 5.7‰, and between -35.9‰ and -30.4‰ for *n*-C_{33}, a range of 5.5‰. The *A. marina n*-alkanes were depleted vs. the values for the whole leaf carbon and correlated positively with salinity (Fig. 5). Linear regression analysis yielded correlation coefficients (R^2) of 0.61 for *n*-C_{31} vs. salinity (Fig. 5a) and 0.55 for -*n*C_{33} vs. salinity (Fig. 5b). These relationships were significant at the 95% confidence level (p = 0.008 for *n*-C_{31} and 0.014 for *n*C_{33}). The relationship between salinity and leaf wax $\delta^{13}C$ values was $\delta^{13}C = 0.187 \pm 0.053$ x salinity – 37.7 ± 1.20 for *n*-C_{31}, and $\delta^{13}C = 0.163 \pm 0.052$ x salinity - 36.3 ± 1.48 for *n*-C_{33}.

Individual *n*-alkanes were always depleted in ^{13}C relative to bulk leaf material from the same leaf (Table 1). On average, *n*-C_{31} was depleted by 5.3‰ relative to whole leaf tissue, while *n*-C_{33} was depleted by 4.3‰ relative to leaves. The differences imply net biosynthetic fractionation ($\alpha_{leaf\text{-}wax}$) of 0.995 ± 0.001 and 0.996 ± 0.001, respectively, where $\alpha_{leaf\text{-}wax} = (^{13}C/^{12}C)_{wax}/(^{13}C/^{12}C)_{leaf}$.

Net fractionation from atmospheric CO_2 for each compound ($\alpha_{atm\text{-}nC31}$ and $\alpha_{atm\text{-}nC33}$) was between 0.972-0.977 for *n*C_{31}-alkanes, and between 0.972-0.978 for *n*C_{33}-alkanes (Table 1). Both fractionation factors were correlated with salinity according to the relationships $\alpha_{atm\text{-}nC31} = 1.9x10^{-4} \pm 5.30x10^{-5}*S - 0.970 \pm 1.21x10^{-3}$ ($R^2 = 0.61$, p = 0.008) and $\alpha_{atm\text{-}nC33} = 1.6x10^{-4} \pm 5.2x10^{-5}*S - 0.972 \pm 1.19x10^{-3}$ ($R^2 = 0.55$, p = 0.014) (Fig. 5d).

3.5 Discussion

3.5.1 Correlation between whole leaf $\delta^{13}C$ values and salinity

The positive relationship between whole leaf $\delta^{13}C$ values and salinity is similar to that reported for other mangroves (Farquhar et al., 1982b; Lin and Sternberg, 1992a; Wei et al., 2008) and halophytic plants (Guy et al., 1980; Ziegler et al., 1981; Neales et al., 1983). The relationship is best understood as a result of increased water use efficiency (the ratio of carbon assimilation to stomatal conductance) at high salinity, and can be explained by the leaf carbon isotope models of O'Leary (1981) and Farquhar et al. (1982a) for C_3 plants. The model is represented mathematically by :

$$\Delta^{13}C = a + (b - a)*(C_i / C_a) \quad (1)$$

where $\Delta^{13}C = (\delta^{13}C_{air} - \delta^{13}C_{plant})/(1 + \delta^{13}C_{plant}/1000)$, a the isotopic fractionation associated with the diffusion of CO_2 through the stomata (-4.4‰), b the net fractionation during carboxylation (ca. -27‰), and C_i/C_a the ratio of intercellular pCO_2 to ambient pCO_2.

As stomatal conductance decreases relative to carbon assimilation rates under conditions of salt or water stress, C_i/C_a will decrease, and the net fractionation expressed by Δ will be driven towards a, resulting in less discrimination against ^{13}C. In other words, as carbon is assimilated at a faster rate than it is replaced, the $\delta^{13}C$ value of CO_2 within the leaf will increase, and carbon that is subsequently fixed from that diminishing internal CO_2 pool will be relatively enriched vs. that fixed by plants with high stomatal conductance.

The magnitude of the salinity response of whole leaf $\delta^{13}C$ in Brisbane River *A. marina* is consistent with past studies of carbon isotopes in mangroves across a salinity gradient. Lin and

Sternberg (1992a) observed a 3‰ decrease in carbon isotope discrimination between *R. mangle* cultivated at 100 mM NaCl (ca. 7 PSU) and 500 mM NaCl (ca. 35 PSU), with $\delta^{13}C$ values for whole leaf matter increasing from ca. -30‰ to ca. -27‰. The regression for Brisbane River *A. marina* values as a function of salinity (Fig. 3) would predict an increase from -29.5‰ to -27.0‰ across the same salinity range, indicating a nearly identical carbon isotope response to increased salinity for both *R. mangle* and *A. marina*. This result is notable given that the two species belong to different families (Rhizophoraceae and Acanthaceae, respectively) and employ different strategies (Hogarth, 2007) for managing the salt in their water supply (exclusion by roots and vacuolization in *R. mangle*, and exclusion, vacuolization and secretion from leaves in *A. marina*). The similar carbon isotope response to changing salinity in the two species suggests that the relationship $\delta^{13}C_{leaf} = 0.087 \pm 0.028 \times s - 30.084 \pm 0.609$ may be applicable to a wide range of mangroves.

Additionally, the leaves used in this study were selected without controlling for aspect, height on the tree, or the age of the leaf, which likely accounts for some of observed scatter in the relationship between salinity and whole leaf $\delta^{13}C$. The fact that significant trends with salinity are still observed despite this non-systemic sampling suggests that the overall result is robust.

3.5.2 Lack of relationship between bulk lipid $\delta^{13}C$ values and salinity

In the light of the results for whole leaf tissue and leaf wax *n*-alkanes, the lack of correlation between bulk lipid $\delta^{13}C$ values and salinity (Fig. 4) was unexpected. Since relatively more ^{13}C is assimilated into the plant as a whole at high salinity, the isotopic composition of the

extractable lipids would be expected to track that of the whole plant (Hayes, 2001; Hobbie and Werner, 2004).

The most probable explanation for this discrepancy is that the lipid concentration in the leaves decreased with salinity ($R^2 = 0.26$; $p = 0.04$; Table S1; Fig. S3). As lipid concentrations increase, $\delta^{13}C$ values of bulk lipids increase as well (Park and Epstein, 1961; Hayes, 2001; Hobbie and Werner, 2004). This positive correlation is likely due to the fact that the biosynthesis of lipids discriminates against ^{13}C. As more and more carbon is partitioned into lipids, the $\delta^{13}C$ value of the remaining of pool of carbon from which new lipids can be produced increases, meaning that additional lipids are also relatively enriched in ^{13}C (Hayes, 2001; Hobbie and Werner, 2004). At low salinity, where relatively more carbon is allocated to lipids, one would therefore expect less net fractionation between the lipid and the whole leaf, somewhat increasing the $\delta^{13}C$ value of the TLE. Although the correlation between salinity and lipid concentration in our samples is not particularly strong, this trend would serve to counteract the positive relationship between whole leaf $\delta^{13}C$ values and salinity, and scatter in the relationship between TLE concentration and salinity only adds to scatter in the relationship between $\delta^{13}C_{TLE}$ values and salinity.

Another possible explanation comes from the variable concentrations of lipids produced via different biosynthetic pathways. Acetogenic lipids, such as *n*-alkanes, and triterpenoids, including sterols, are not only produced via different biosynthetic pathways, but also in different parts of the cell (chloroplast and cytosol, respectively). The differences can result in different $\delta^{13}C$ values among compound classes (Hayes, 2001). They are not systematic and vary with species, but can be as large as 8‰, with triterpenoids typically, although not always, enriched in ^{13}C relative to acetogenic lipids (Lockheart et al., 1997; Schouten et al., 1998; Hayes et al.,

2001). The contribution of acetogenic and isoprenoid lipids to the TLE from each leaf in our sample set was highly variable and did not correspond with salinity. A leaf with a higher proportion of isoprenoids might be expected to have a higher $\delta^{13}C$ value of its TLE than one with a low proportion of isoprenoids, regardless of the mean salinity where the plant grew.

A third, but far less likely, possibility is that the solvent (toluene) used to transfer the TLE to the Sn capsule did not completely evaporate, leaving a small amount of solvent-derived carbon in the capsule, which was subsequently analyzed along with the TLE carbon. The effect would be random, and could have been responsible for the uncorrelated relationship between bulk TLE $\delta^{13}C$ values and salinity. A procedural blank prepared with the samples contained unmeasurable (<1 μg) amounts of material. However, toluene may have been more likely to remain within the TLE matrix than in an empty capsule, in which case it could have altered our results.

3.5.3 Correlation between $\delta^{13}C$ values of n-alkanes and salinity

The positive correlation between $\delta^{13}C$ values of *A. marina n*-alkanes with salinity (Fig. 5) is most likely a direct result of the relative increase in ^{13}C fixed by the plants at higher salinity. This is expected and consistent with studies of compound specific carbon isotopes in leaves, which have shown that the carbon isotope ratio of leaf wax *n*-alkanes varies with bulk leaf $\delta^{13}C$ (Collister et al., 1994: Chikaraishi and Naraoka, 2003; Chikaraishi and Naraoka, 2007). Leaf wax *n*-alkanes are isotopically depleted relative to bulk leaf $\delta^{13}C$, with offsets for C_3 angiosperms reported to be -1.1 to -5.9‰ (Collister et al., 1994; Chikaraishi and Naraoka, 2003). The 4.3 to 5.3‰ ^{13}C depletion for *n*-alkanes here vs. whole *A. marina* leaves is consistent with this range.

Studies have reported significant differences in $\delta^{13}C$ values of homologous *n*-alkanes from leaves (Collister et al., 1994; Chikaraishi and Naraoka, 2007). However, there does not seem to be a common trend relating $\delta^{13}C$ of individual *n*-alkane homologues to chain length, even within specific plant groups such as C_3 angiosperm trees (Collister et al., 1994; Chikaraishi and Naraoka, 2007). In the case of *A. marina*, we observe that *n*-C_{33} appears to be enriched in ^{13}C vs. *n*-C_{31}, but that the difference is not statistically significant.

The higher correlation coefficients observed for the relationships between individual leaf wax *n*-alkanes and salinity may be an artifact of the smaller sample size used for these additional measurements. The p-values reported account for the fewer degrees of freedom in the *n*-alkane data set, and are comparable for *n*-C_{31} alkanes ($p = 0.008$) and whole leaves ($p = 0.009$), and slightly higher for *n*-C_{33} alkanes ($p = 0.014$).

3.5.4 Quantitative reconstruction of past salinity from paired $\delta^{13}C$ and δD in mangrove lipids

One of the most exciting applications of our results is the potential to reconstruct past variation in salinity using isotopic measurements of mangrove-derived lipids preserved in sediment. We previously demonstrated that hydrogen isotope fractionation in *A. marina* leaf wax is negatively correlated with salinity (Ladd and Sachs, 2012). The hydrogen isotope signature of the mangrove leaf wax is thus influenced by both salinity and the δD value of environmental water, making it impossible to determine the relative influence of salinity and source water isotopes by measuring only δD values of mangrove lipids. However, the systematic increase in hydrogen isotope fractionation with salinity, combined with the systematic decrease in carbon isotope fractionation presented here, provides two equations with two unknowns that can be solved. Quantitative reconstruction of past salinity (*S*) and water hydrogen isotopes

(*δDwater*) are thus possible from paired δD and $\delta^{13}C$ values of mangrove lipids preserved in sediment.

The approach begins with the empirical relationships determined here for carbon isotope variation in *A. marina*, and in our previous study of hydrogen isotope variation over the same salinity gradient (Ladd and Sachs, 2012). The empirical relationships between salinity and lipid isotopes can be described as:

$$^{2}\alpha = m_2 \text{ x } S + b_2 \quad (2)$$

$$^{13}\alpha = m_{13} \text{ x } S + b_{13} \quad (3)$$

where $^{2}\alpha$ is water-lipid D/H fractionation, $^{13}\alpha$ air-lipid $^{13}C/^{12}C$ fractionation, m_2 and b_2 -0.00151 and 0.892, respectively (Ladd and Sachs, 2012), and m_{13} and b_{13} 0.000188 and 0.970 respectively (Fig. 5c) for the *n*-C_{31} from *A. marina* in the Brisbane River estuary. We can then make use of the definitions of $^{2}\alpha$ and $^{13}\alpha$:

$$^{2}\alpha = \frac{\delta D_{lipid}+1000}{\delta D_{water}+1000} \quad (4)$$

$$^{13}\alpha = \frac{\delta^{13}C_{lipid}+1000}{\delta^{13}C_{atm}+1000} \quad (5)$$

where $\delta^{13}C_{atm}$ is the $\delta^{13}C$ value of atmospheric CO_2, which is well constrained from ice cores (Francey et al., 1999; Elsig et al., 2009)

After measuring δD_{lipid} and $\delta^{13}C_{lipid}$ directly, we are left with four equations and four unknowns (S, δD_{water}, $^{2}\alpha$, $^{13}\alpha$). After substituting the definitions of $^{2}\alpha$ and $^{13}\alpha$ into Eq. (2) and Eq. (3), and rearranging terms, we can solve for S and δD_{water}:

$$S = \left(\frac{\delta^{13}C_{lipid} + 1000}{\delta^{13}C_{atm} + 1000} - b_{13} \right) \times \frac{1}{m_{13}} \tag{6}$$

$$\delta D_{water} = \left[\frac{\delta D_{lipid} + 1000}{\frac{m_2}{m_{13}} \left(\frac{\delta^{13}C_{lipid} + 1000}{\delta^{13}C_{lipid} + 1000} - b_{13} \right) + b_2} \right] \tag{7}$$

An advantage of the approach is that it requires no assumptions about the relationship between salinity and δDwater, which is necessary when salinity or water δD are inferred from algal lipid δD values (Pahnke et al., 2007; van der Meer et al., 2007; Sachs et al., 2009; Smittenberg et al., 2011). Additionally, mangroves are widespread along low-latitude coastlines, and account for 10-20% of tropical wetlands (Bhattarai and Giri, 2011; Donato et al., 2011; Giri et al., 2011), so the approach can be applied to a wide range of tropical and subtropical locations.

The method for reconstructing salinity and δDwater should work best with lipids that can be unambiguously attributed to mangroves. An especially promising target compound is taraxerol, a pentacyclic triterpenoid produced in high abundance by *Rhizophora* mangroves (Killops and Frewin, 1994; Koch et al., 2003; Versteegh et al., 2004), and well-preserved in sediments (Koch et al., 2003). The *n*-alkanes studied here, and other ubiquitous leaf wax components, would not be suitable for such a study, unless pollen, concentration co-variance with a mangrove specific biomarker (Versteegh et al., 2004), or other evidence convincingly

suggested that mangroves were the dominant higher plant source for the sedimentary archive in question. As such, future work would profitably be focused on establishing empirical calibrations of mangrove-specific lipid $\delta^{13}C$ values as a function of salinity.

3.6 Conclusion

We measured the relationship between salinity and carbon isotopes in leaf wax *n*-alkanes, whole leaf tissue and lipid extracts from the mangrove *Avicennia marina* along a gradient of salinity from 6-35 PSU in the Brisbane River Estuary, Queensland, Australia. The $\delta^{13}C$ values of *n*-C_{31} and *n*-C_{33} varied systematically with salinity, increasing by 0.187 ± 0.053‰ and 0.163 ± 0.052‰, respectively.

Whole leaf tissue $\delta^{13}C$ values increased by 0.087 ± 0.028‰ per salinity unit, consistent with past culturing studies of mangroves and with field studies that compared bulk carbon isotopes of mangroves growing at a few locations. The study represents the first such calibration along a wide salinity gradient.

No consistent trend in $\delta^{13}C$ values of total lipid extracts from *A. marina* leaves with salinity was observed. Varying amounts of lipid carbon in leaves, or different lipid classes in the solvent-extracts may have caused this result.

When combined with our previous observation of increasing hydrogen isotope fractionation in *n*-alkanes from the same sample set of Brisbane River *A. marina* leaves, quantitative reconstruction of salinity and water isotopes are possible from paired measurements of δD and $\delta^{13}C$ of mangrove lipids. This method will work best with a lipid biomarker that is more source specific to mangroves, such as taraxerol, or in an environment where pollen or other

evidence suggests a mangrove source for more common compounds, such as the *n*-alkane leaf waxes studied here.

3.7 References

Ball, M., 1988. Salinity tolerance in the mangroves *Aegiceras corniculatum* and *Avicennia marina.* I. Water use in relation to growth, carbon partitioning, and salt balance. Functional Plant Biology 15, 447-464.

Ball, M.C., Farquhar, G.D., 1984. Photosynthetic and stomatal responses of two mangrove species, *Aegiceras corniculatum* and *Avicennia marina*, to long term salinity and humidity conditions. Plant Physiol. 74, 1-6.

Bhattarai, B., Giri, C., 2011. Assessment of mangrove forests in the Pacific region using Landsat imagery. Journal of Applied Remote Sensing 5, 053509 1-11.

Chikaraishi, Y., Naraoka, H., 2003. Compound-specific δD- δ13C analyses of *n*-alkanes extracted from terrestrial and aquatic plants. Phytochemistry 63, 361-371.

Chikaraishi, Y., Naraoka, H., 2007. $\delta^{13}C$ and δD relationships among three *n*-alkyl compound classes (*n*-alkanoic acid, *n*-alkane, and *n*-alcohol) of terrestrial higher plants. Organic Geochemistry 38, 198-215.

Collister, J.W., Rieley, G., Stern, B., Eglinton, G., Fry, B., 1994. Compound-specific $\delta^{13}C$ analyses of leaf lipids from plants wit differeing carbon dioxide metabolisms. Organic Geochemistry 21, 67-77.

Donato, D.C., Kauffman, J.B., Murdiyarso, D., Kurnianto, S., Stidham, M., Kanninen, M., 2011. Mangroves among the most carbon-rich forests in the tropics. Nature Geoscience 4, 293-297.

Ehleringer, J.R., Phillips, S.L., Comstock, J.P., 1992. Seasonal variation in the carbon isotopic composition of desert plants. Functional Ecology 6, 396-404.

Elsig, J., Schmitt, J., Leuenberger, D., Schneider, R., Eyer, M., Leuenberger, M., Joos, F., Fischer, H., Stocker, T.F., 2009. Stable isotope constraints on Holocene carbon cycle changes from an Antarctic ice core. Nature 461, 507-510.

Farquhar, G.D., Ball, M.C., von Caemmerer, S., Roksandic, Z., 1982b. Effect of salinity and humidity on $\delta^{13}C$ value of halophytes -- evidence for diffusional isotope fractionation determined by the raton of intercellular/atmospheric partial pressure of CO2 under different environmental conditions. Oecologia 52, 121-124.

Farquhar, G.D., Oleary, M.H., Berry, J.a., 1982a. On the relationship between carbon isotope discrimination and the inter-cellular carbon-dioxide concentration in leaves. Australian Journal of Plant Physiology 9, 121-137.

Farquhar, G.D., Ehleringer, J.R., Hubick, K.T., 1989. Carbon isotope discrimination and photosynthesis. Annual Review of Plant Physiology and Plant Molecular Biology 40, 503-537.

Francey, R.J., Allison, C.E., Etheridge, D.M., Trudinger, C.M., Enting, I.G., Leuenberger, M., Langenfelds, R.L., Michel, E., Steele, L.P., 1999. A 1000-year high precision record of $\delta^{13}C$ in atmospheric CO2. Tellus B 51, 170-193.

Giri, C., Ochieng, E., Tieszen, L.L., Zhu, Z., Singh, A., Loveland, T., Masek, J., Duke, N., 2011. Status and distribution of mangrove forests of the world using earth observation satellite data. Global Ecology and Biogeography 20, 154-159.

Guy, R.D., Reid, D.M., Krouse, H.R., 1980. Shifts in carbon isotope ratios of two C_3 halophytes under natural and artificial conditions. Oecologia 44, 241-247.

Hayes, J.M., 2001. Fractionation of carbon and hydrogen isotopes in biosynthetic processes. Reviews in Mineralogy and Geochemistry 43, 225-277.

Hobbie, E.A., Werner, R.A., 2004. Intramolecular, compound-specific, and bulk carbon isotope patterns in C_3 and C_4 plants: a review and synthesis. New Phytologist 161, 371-385.

Hogarth, P., 2007. The Biology of Mangroves. Oxford University Press, New York.

Killops, S.D., Frewin, N.L., 1994. Triterpenoid diagenesis and cuticular preservation. Organic Geochemistry 21, 1193-1209.

Koch, B.P., Rullkottter, J., Lara, R.J., 2003. Evaluation of triterpenols and sterols as organic matter biomarkers in a mangrove ecosystem in northern Brazil. Wetlands Ecology and Management 11, 257-263.

Koch, B.P., Harder, J., Lara, R.J., Kattner, G, 2005. The effect of selective microbial degradation on the composition of mangrove derived pentacyclic triterpenols in surface sediments. Organic Geochemistry 36, 273-285.

Krauss, K.W., Lovelock, C.E., McKee, K.L., Lopez-Hoffman, L., Ewe, S.M.L., Sousa, W.P., 2008. Environmental drivers in mangrove establishment and early development: A review. Aquatic Botany 89, 105-127.

Ladd, S.N., Sachs, J.P., 2012. Inverse relationship between salinity and n-alkane dD values in the mangrove Avicennia marina. Organic Geochemistry 48, 25-36.

Lin, G., Sternberg, L., 1992a. Effect of growth form, salinity, nutrient and sulfide on photosynthesis, carbon isotope discrimination and growth of red mangrove *Rhizophora mangle* L. Functional Plant Biology 19, 509-517.

Lin, G., da S.L. Sternberg, L., 1992b. Differences in morphology, carbon isotope ratios, and photosynthesis between scrub and fringe mangroves in Florida, USA. Aquatic Botany 42, 303-313.

Lockheart, M.J., VanBergen, P.F., Evershed, R.P., 1997. Variations in the stable carbon isotope compositions of individual lipids from the leaves of modern angiosperms: implications for the study of higher land plant-derived sedimentary organic matter. Organic Geochemistry 26, 733-736.

McKee, K.L., Feller, I.C., Popp, M., Wanek, W., 2002. Mangrove isotopic fractionation across a nitrogen vs phosphorus limitation gradient. Ecology 83, 1065-1075.

Medina, E., Francisco, M., 1997. Osmalality and $\delta^{13}C$ of leaf tissues of mangrove species from environments of contrasting rainfall and salinity. Estuarine, Coastal and Shelf Science 45, 337-344.

Neales, T.F., Fraser, M.S., Roksandic, Z., 1983. Carbon isotope composition of the halophyte *Disphyma clavellatum* (Haw.) Chinnock (Aizoaceae), as affected by salinity. Australian Journal of Plant Physiology 10, 437-444.

O'Leary, M.H., 1981. Carbon isotope fractionation in plants. Phytochemistry 20, 553-567.

Pahnke, K., Sachs, J.P., Keigwin, L.D., Timmermann, A., Xie, S.P., 2007. Eastern tropical Pacific hydrologic changes during the past 27,000 years from D/H ratios in alkenones. Paleoceanography 22, PA4214, 15pp.

Park, R., Epstein, S., 1961. Metabolic fractionation of C^{13} and C^{12} in plants. Plant Physiology 36, 133-138.

Sachs, J.P., Sachse, D., Smittenberg, R.H., Zhang, Z., Battisti, D.S., Golubic, S., 2009. Southward movement of the Pacific intertropical convergence zone AD 1400-1850. Nature Geoscience 2, 519-525.

Saurer, M., Siegwolf, R.T.W., Schweingruber, F.H., 2004. Carbon isotope discrimination indicates improving water-use efficiency of trees in northern Eurasia over the last 100 years. Global Change Biology 10, 2109-2120.

Schouten, S., Klein Breteler, W.C.M., Blokker, P., Schogt, N., Rijpstra, W.I.C., Grice, K., Bass, M., Sinninghe Damstée, J.S., 1998. Biosynthetic effects on the stable carbon isotopic compositions of algal lipids: Implications for deciphering the carbon isotopic biomarker record. Geochimica et Cosmochimica Acta 62, 1397-1406.

Shaheen, R., Hood-Nowotny, R.C., 2005. Carbon isotope discrimination: potential for screening salinity tolerance in rice at the seedling stage using hydroponics. Plant Breeding 124, 220-224.

Smittenberg, R.H., Saenger, C., Dawson, M.N., Sachs, J.P., 2011. Compound-specific D/H ratios of the marine lakes of Palau as proxies for West Pacific Warm Pool hydrologic variability. Quaternary Science Reviews 30, 921-933.

van der Meer, M., Baas, M., Rijpstra, W., Marino, G., Rohling, E., Sinninghe Damstée, J.S., Schouten, S., 2007. Hydrogen isotopic compositions of long-chain alkenones record freshwater flooding of the Eastern Mediterranean at the onset of sapropel deposition. Earth and Planetary Science Letters 262, 594-600.

Versteegh, G., Schefus, E., Dupont, L., Marret, F., Sinninghe Damste, J., Jansen, J., 2004. Taraxerol and *Rhizophora* pollen as proxies for tracking past mangrove ecosystems. Geochimica Et Cosmochimica Acta 68, 411-422.

Wei, L., Yan, C., Ye, B., Guo, X., 2008. Effects of salinity on leaf $\delta^{13}C$ in three dominant mangrove species along salinity gradients in an estuarine wetland, Southeast China. Journal of Coastal Research 24, 267-272.

Werner, C., Schnyder, H., Cuntz, M., Keitel, C., Zeemans, M.J., Dawson, T.E., Badeck, F.-W., Brugnolis, E., Ghashghaie, J., Grams, T.E.E., Kayler, Z.E., Lakatos, M., Lee, X., Maguas, C., Ogge, J., Rascher, K.G., Siegwolf, R.T.W., Unger, S., Welker, J., Wingate, L., Gessler, A., 2012. Progress and challenges in using stable isotopes to trace plant carbon and water relations across scales. Biogeosciences 9, 3083-3111.

Ye, Y., Tam, N.F.Y., Lu, C.Y., Wong, Y.S., 2005. Effects of salinity on germination, seedling growth and physiology of three salt-secreting mangrove species. Aquatic Botany 83, 193-205.

Zeigler, H., Batanouny, K.H., Sankhia, N., Vyas, O.P, Stichler, W., 1981. The photosynthetic pathway types of some desert plants from India, Saudi Arabia, Egypt, and Iraq. Oecologia 48, 93-99

3.8 Figure Captions

Figure 1 Map of the Brisbane River Estuary. Sampling sites used for this study are marked with bold numbers, corresponding to data in Table 1.

Figure 2 Salinity versus distance from river mouth in the Brisbane River. The linear regression of this field data was used to calculate the mean salinity values shown in Table 1.

Figure 3 Bulk leaf $\delta^{13}C$ values (a) and $\alpha_{atm\text{-}leaf}$ (b) of *A. marina* in the Brisbane River versus salinity. Dashed lines represent 95% confidence intervals. One outlier (a small seedling) is marked with an open triangle. Y error bars are ±0.06‰ and are too small to resolve from the measurement markers.

Figure 4 Total lipid extract (TLE) $\delta^{13}C$ values of *A. marina* in the Brisbane River versus salinity. Dashed lines represent 95% confidence intervals. Y error bars are ±0.06‰ and are too small to resolve from the measurement markers.

Figure 5 Leaf wax $\delta^{13}C$ values and $\alpha_{atm\text{-}n\text{-}alkane}$ of *A. marina* in the Brisbane River versus salinity. $\delta^{13}C$ values of nC_{31}-alkanes vs salinity are shown in **a**; $\delta^{13}C$ of nC_{33}-alkanes vs salinity are shown in **b**. Correspoinding $\alpha_{atm\text{-}nC31}$ and $\alpha_{atm\text{-}nC33}$ are shown in **c** and **d**, respectively. Dashed lines represent 95% confidence intervals.

Figure 1 Map of the Brisbane River Estuary. Sampling sites used for this study are marked with bold numbers, corresponding to data in Table 1.

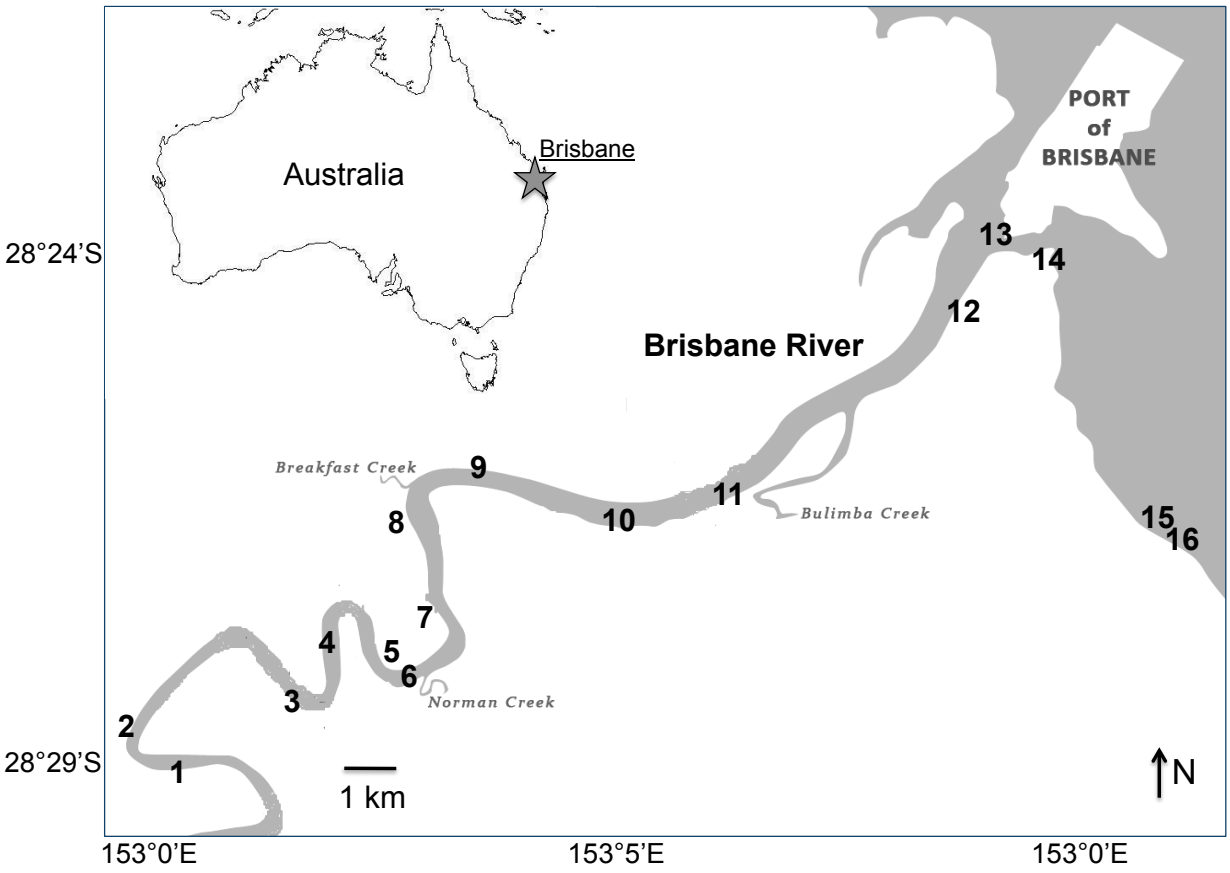

Figure 2 Salinity versus distance from river mouth in the Brisbane River. The linear regression of this field data was used to calculate the mean salinity values shown in Table 1.

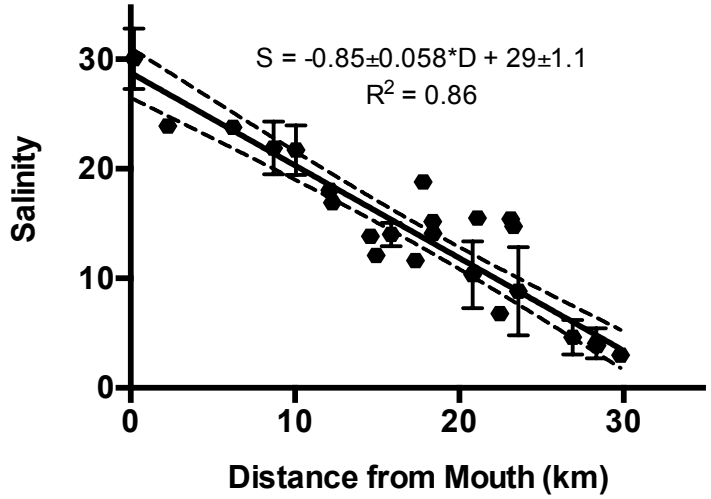

Figure 3 Bulk leaf $\delta^{13}C$ values (a) and $\alpha_{atm\text{-}leaf}$ (b) of *A. marina* in the Brisbane River versus salinity. Dashed lines represent 95% confidence intervals. One outlier (a small seedling) is marked with an open triangle. Y error bars are ±0.06‰ and are too small to resolve from the measurement markers.

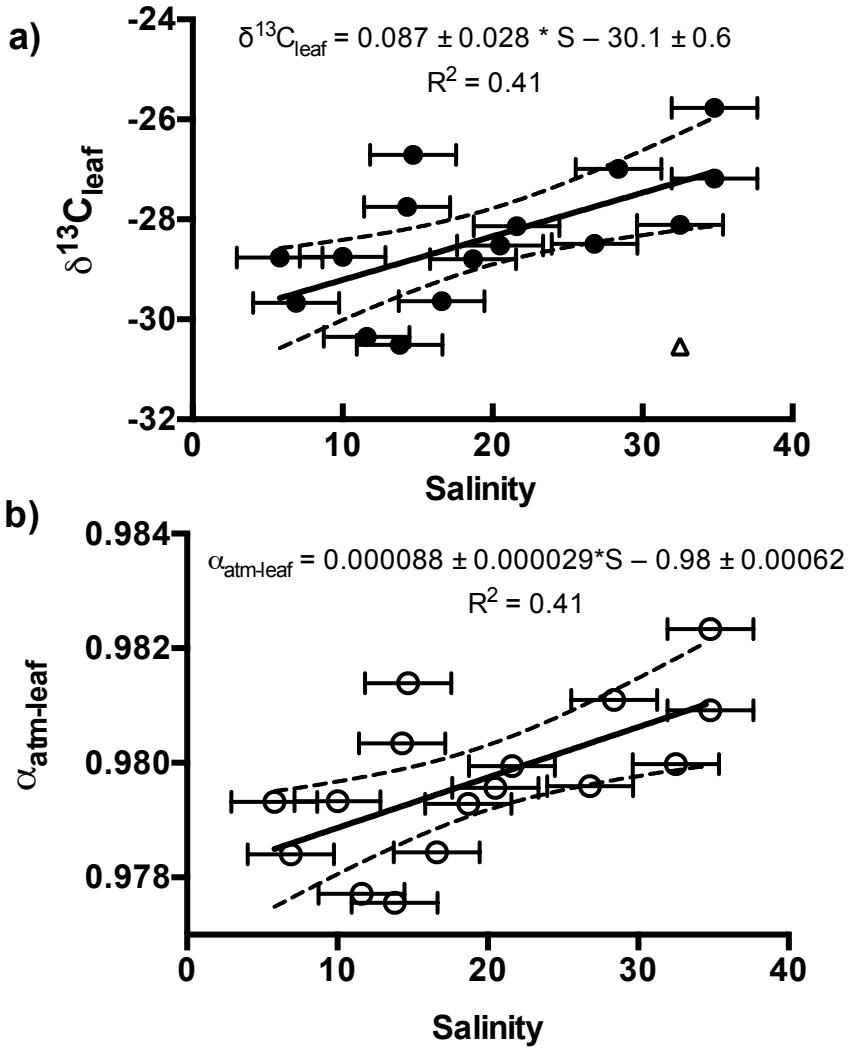

Figure 4 Total lipid extract (TLE) $\delta^{13}C$ values of *A. marina* in the Brisbane River versus salinity. Dashed lines represent 95% confidence intervals. Y error bars are ±0.06‰ and are too small to resolve from the measurement markers.

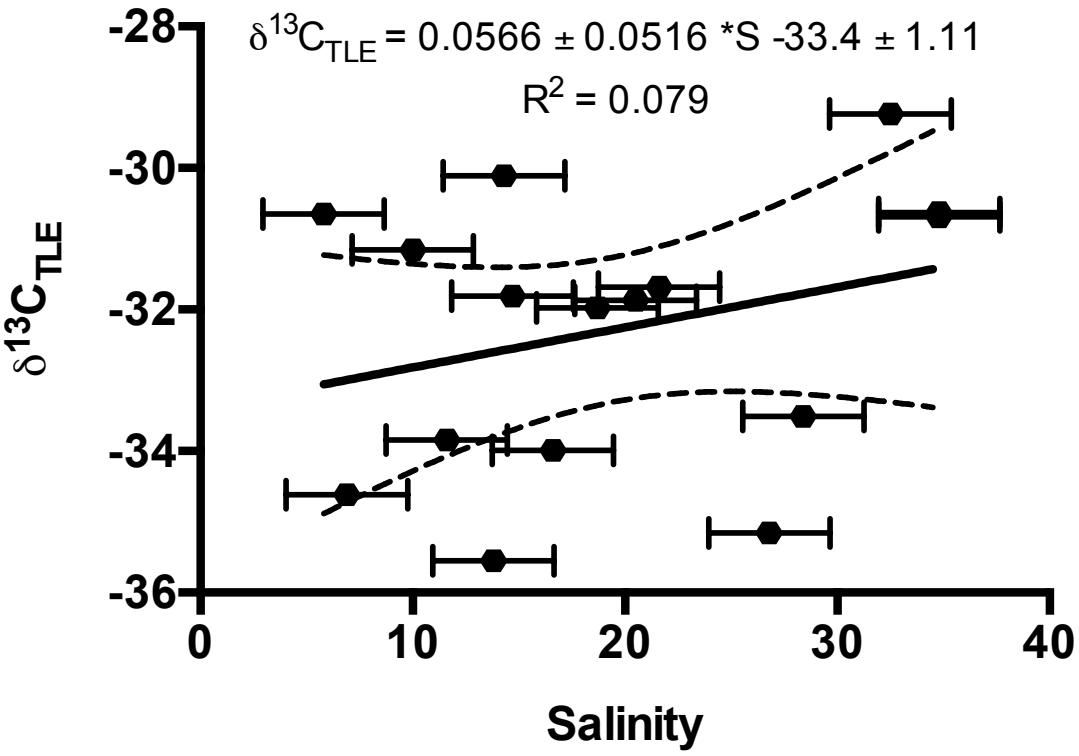

Figure 5 Leaf wax $\delta^{13}C$ values and $\alpha_{atm\text{-}n\text{-}alkane}$ of *A. marina* in the Brisbane River versus salinity. $\delta^{13}C$ values of nC_{31}-alkanes vs salinity are shown in **a**; $\delta^{13}C$ of nC_{33}-alkanes vs salinity are shown in **b**. Correspoinding $\alpha_{atm\text{-}nC31}$ and $\alpha_{atm\text{-}nC33}$ are shown in **c** and **d**, respectively. Dashed lines represent 95% confidence intervals.

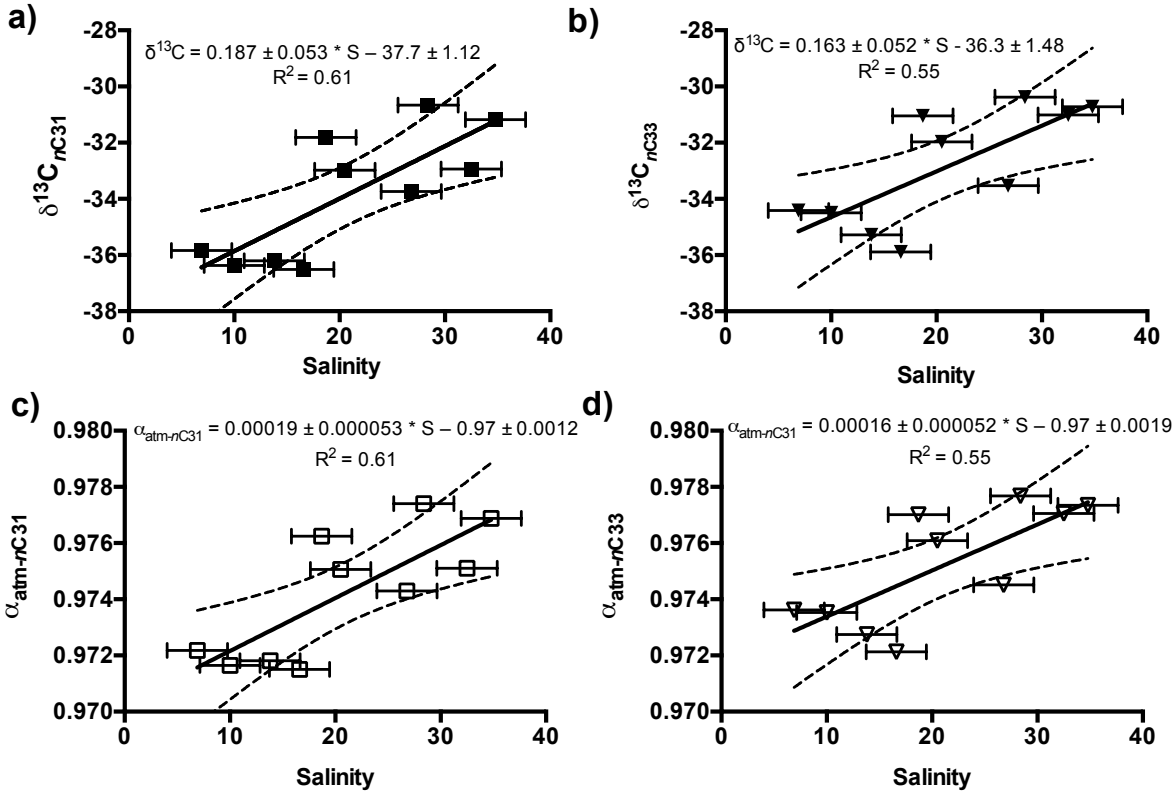

Table 1:

Site	Latitude (S)	Longitude (E)	Mean Salinity (PSS)	$\delta^{13}C_{leaf}$ (‰)	$\alpha_{atm\text{-}leaf}$	$\delta^{13}C_{TLE}$ (‰)	$\delta^{13}C_{nC31}$ (‰)	$\delta^{13}C_{nC33}$ (‰)	$\alpha_{atm\text{-}C31}$	$\alpha_{atn\text{-}C33}$	$\alpha_{leaf\text{-}C31}$	$\alpha_{leaf\text{-}C33}$
1	27°29.555’	153°0.12’	5.8	-28.76	0.9793	-30.65						
2	27°29.000’	152°59.783’	6.9	-29.67	0.9784	-34.62	-35.8	-34.4	0.972	0.974	0.994	0.995
3	27°28.579’	153°1.509’	10.0	-28.75	0.9716	-31.16	-36.4	-34.5	0.972	0.974	0.992	0.994
4	27°28.269’	153°2.048’	11.6	-30.35	0.9778	-33.84						
5	27°28.521’	153°2.625’	13.8	-30.51	0.9718	-35.55	-36.2	-35.3	0.972	0.972	0.994	0.995
6	27°28.568’	153°2.975’	14.3	-27.75	0.9803	-30.11						
7	27°28.294’	153°3.127’	14.7	-26.71	0.9814	-31.81						
8	27°27.19’	153°2.979’	16.6	-29.64	0.9784	-33.99	-36.5	-35.9	0.972	0.975	0.993	0.994
9	27°26.402’	153°3.731’	18.7	-28.80	0.9793	-31.98	-31.8	-31.1	0.976	0.977	0.997	0.998
10	27°26.949’	153°5.034’	20.5	-28.52	0.9796	-31.87	-33.0	-32.0	0.975	0.976	0.995	0.996
11	27°26.869’	153°5.967’	21.6	-28.14	0.9799	-31.68						
12	27°24.654’	153°8.95’	26.8	-28.49	0.9796	-35.16	-33.7	-33.5	0.974	0.975	0.995	0.995
13	27°23.969’	153°9.854’	28.4	-26.99	0.9811	-33.51	-30.7	-30.4	0.977	0.978	0.996	0.997
14a*	27°24.089’	153°10.079’	32.5	-28.11	0.9824	-29.24	-32.9	-31.0	0.975	0.977	0.995	0.997
14b*	27°24.089’	153°10.079’	32.5	-30.54		-41.56						
15	27°28.079’	153°11.616’	34.8	-25.77	0.9823	-30.69	-31.2	-30.7	0.977	0.977	0.994	0.995
16	27°28.108’	153°11.642’	34.8	-27.18	0.9809	-30.63						

*14a was a mature tree sampled at site 14, while 14b was a small seedling sampled at site 14

Chapter 4: Influence of salinity on hydrogen isotope fractionation in *Rhizophora* mangroves from Micronesia

4.1 Abstract

Hydrogen isotope ratios ($^2H/^1H$ or δ^2H) of plant leaf waxes typically covary with those of precipitation, and are therefore used as a proxy for past hydrologic variability. Mangroves present an important exception to this relationship, as salinity can have a strong effect on ^2H discrimination in leaf lipids. To better understand and calibrate this effect, δ^2H values of taraxerol and *n*-alkanes were measured in the leaves of *Rhizophora* spp. (red mangroves) from three estuaries and four brackish lakes on the Micronesian islands of Pohnpei and Palau, and compared to the δ^2H and $\delta^{18}O$ values of leaf water, xylem water and surface water. Net ^2H discrimination between surface water and taraxerol increased by 0.9 ± 0.2‰ ppt^{-1} over a salinity range 1-34 ppt. Xylem water was always depleted in ^2H relative to surface water, and the magnitude of this depletion increased with salinity, which is most likely due to a combination of greater ^2H discrimination by roots during water uptake and opportunistic use of freshwater. Changes in the ^2H content of xylem water can account for up to 43% of the change in net taraxerol fractionation with salinity. Leaf water isotopes were minimally enriched relative to xylem water and there were not significant changes in leaf water enrichment with salinity, which is consistent with a Péclet-modified Craig-Gordon model of leaf water enrichment. As leaf water enrichment is therefore unlikely to be responsible for increased $^2H/^1H$ fractionation in mangrove leaf lipids at elevated salinities, changes in biosynthetic fractionation in response to salt stress most likely explain the majority of this signal.

4.2 Introduction

Hydrogen isotope ratios of plant leaf waxes are increasingly used as a proxy for past hydrologic variability (*Sachse et al., 2012* and sources therein). This proxy is founded on the assumption that the hydrogen in leaf waxes and other plant lipids is derived from environmental water, and the observation that the δ^2H_{Lipid} values ($\delta^2H = (^2H/^1H)_{sample}/(^2H/^1H)_{VSMOW}$; $\delta^2H = \delta D$) are highly correlated with local $\delta^2H_{Precipitation}$ values (*Sachse et al., 2004; Polissar & Freeman, 2010; Sachse et al., 2012*). $\delta^2H_{Precipitation}$ values are determined by environmental parameters, including temperature, precipitation rate, and moisture source (*Dansgaard 1964; Craig & Gordon, 1965; Gat 1996*).

Leaf waxes and other lipids are typically very depleted in ^2H relative to the plant's source water (*Sessions et al., 1999; Sauer et al., 2001; Chikaraishi & Naraoka, 2003; Sachse et al., 2012)*. The difference between δ^2H_{Lipid} values and δ^2H_{Water} values is expressed using the net fractionation factor, $\alpha_{Lipid\text{-}Water} = (^2H/^1H)_{Lipid}/(^2H/^1H)_{Water}$. The magnitude of $\alpha_{Lipid\text{-}Water}$ is sensitive to variables such as plant type (*Luo et al., 2006; Smith & Freeman, 2006; Hou et al., 2007*), relative humidity (*Feakins & Sessions, 2010; Kahmen et al., 2013; Tipple et al., 2014*), and light levels (*Luo & Yang, 2008; Yang et al., 2009; Yang et al., 2011*). In order to reliably use sedimentary δ^2H_{Lipid} values to infer information about past changes in climate, it is important to better understand causes of variability in $\alpha_{Lipid\text{-}Water}$, which can result in changes to δ^2H_{Lipid} values that are not directly related to changes in $\delta^2H_{Precipitation}$ values alone.

Of particular importance for coastal sediments in the tropics and subtropics, the salinity of environmental water can influence $\alpha_{Lipid\text{-}Water}$ (*Romero & Feakins, 2011; Ladd & Sachs, 2012*). Mangrove trees are the dominant plant type in the intertidal zone of many low-latitude coastlines, and cover over 15 million hectare worldwide (*Spalding et al., 2010*). Mangroves are

highly productive ecosystems and have been estimated to contribute 10 –15% of the total terrestrial carbon accumulating in modern marine sediments (*Jennerjahn & Ittekkot, 2002; Dittmar et al., 2006*). Since this input is confined to regions where mangroves are present, their organic matter makes up a significant portion of that deposited in near shore, low-latitude sediments.

The influence of salinity on $\alpha_{Lipid\text{-}Water}$ in leaf wax *n*-alkanes produced by *Avicennia marina* (grey mangroves) was previously investigated along a salinity gradient of 6-35 PSU in the Brisbane River Estuary in Queensland, Australia (*Ladd & Sachs, 2012*). A decrease in $\alpha_{Lipid\text{-}Water}$ of 1.5‰ ± 0.3‰ PSU^{-1} was observed for both nC_{31}- and nC_{33}-alkanes. Several hypotheses were proposed that could explain this relationship: (1) preferential exclusion of ^2H during water uptake, (2) increased compatible solute production, preferentially using relatively enriched H^+ from the pentose phosphate cycle, and leaving relatively depleted H^+ from recent photosynthesis available for incorporation into lipids, or (3) increased salt secretion at high salinity, which could decrease the δ^2H value of leaf water (δ^2H_{LW}) by creating a layer of isotopically depleted water hydrating the salt on the surface of leaves. Because intermediate xylem water and leaf water pools were not analyzed in the Brisbane River study, it was not possible to definitively exclude or support any of these hypotheses.

The results of the Brisbane River calibration were significant for two reasons. First of all, they demonstrated a potential pitfall of using δ^2H values of generic leaf waxes to reconstruct climate in coastal tropical settings where mangroves contribute organic matter to the sediment. Leaf wax *n*-alkanes are ubiquitous in vascular plants, and it is impossible to distinguish nC_{31}-alkanes in a sediment sample from a mangrove or terrestrial plant source. If local climate became more arid, one would expect the δ^2H_{Wax} values of terrestrial plants to increase, since $\delta^2H_{Precipitation}$

values increase with decreasing precipitation amount in the tropics (*Dansgaard 1964; Gat 1996; Kurita et al., 2009; Conroy et al., 2013).*

Although mangrove trees in the region would also be using isotopically enriched water, the salinity of that water would be expected to increase as less freshwater was delivered through rain. Since increased salinity results in more net discrimination against ^{2}H during lipid biosynthesis by mangroves (*Ladd & Sachs, 2012*), the $\delta^{2}H_{Wax}$ from mangroves could actually decrease in more arid conditions. In Brisbane, for example, *Avicennia marina* growing at 35 PSU produced leaf wax lipids that were depleted by ~ 50‰ relative to trees growing at 6 PSU, even though the $\delta^{2}H_{Water}$ was enriched by ~15‰ (*Ladd & Sachs, 2012*). Opposing $\delta^{2}H_{Wax}$ responses to the same environmental shift would result in a muted signal in sediments that contain the molecular remains of both plant types. Relatively small $\delta^{2}H_{Wax}$ variability has in fact been observed in many coastal tropical records and could reflect this opposing hydrogen isotopic response (*Tierney et al., 2010; Smittenberg et al., 2011*).

While the inverse relationship between salinity and isotope fractionation in mangroves complicates the interpretation of $\delta^{2}H_{Wax}$ values in low-latitude coastal settings, it also forms the basis for quantitative reconstructions of both $\delta^{2}H_{Water}$ values and salinity. If the relationship between salinity and $\alpha_{Lipid\text{-}Water}$ observed in leaf waxes from the Brisbane River holds true for more mangrove-specific lipids, it will be possible to quantitatively reconstruct past salinity and $\delta^{2}H_{values}$ by measuring both $\delta^{2}H$ and $\delta^{13}C$ values in a single mangrove lipid, or by measuring $\delta^{2}H$ values of co-occurring lipids from phytoplankton and mangroves (*Ladd & Sachs, 2012; Ladd & Sachs, 2013*).

Required for both of these approaches is a robust calibration of the relationship between salinity and $\alpha_{Lipid\text{-}Water}$ for a mangrove specific lipid biomarker. Because the pentacyclic

triterpenoid taraxerol is produced in high abundance by *Rhizophora* spp. mangroves (*Killops & Frewin, 1994; Koch et al., 2003; Versteegh et al., 2004*), and because it is relatively refractory and well preserved in sediment (*Koch et al., 2003; Koch et al., 2005*), it is a promising target compound. The primary goal of this study was to assess the influence of salinity on net hydrogen isotope fractionation during the biosynthesis of taraxerol.

A related goal was to better understand the mechanisms by which isotopic fractionation occurs during lipid synthesis in mangroves. The only published study on the relationship between salinity and net H isotope fractionation in mangroves (*Ladd & Sachs, 2012*) presented δ^2H data from leaf wax *n*-alkanes and surface water. This allowed $\alpha_{Lipid\text{-}SW}$ to be calculated, but left the fractionation associated with several intermediate steps unconstrained. These steps include potential discrimination against ^2H during water uptake ($\alpha_{XW\text{-}SW}$; uncommon in most higher plants, but demonstrated to occur in halophytes by *Lin & Sternberg, 1993* and *Ellsworth & Williams, 2007*), enrichment of leaf water due to transpiration ($\alpha_{LW\text{-}XW}$; *Dawson et al., 2002; Kahmen et al., 2008*), and biosynthetic fractionation during the production of lipids from leaf water and carbon dioxide ($\alpha_{Lipid\text{-}LW}$). Analyzing δ^2H_{XW} and δ^2H_{LW} values, in addition to environmental water and lipids, is an effective method for determining fractionation associated with these intermediate steps (*Feakins & Sessions, 2010; Romero & Feakins, 2011; Kahmen et al., 2013; Tipple et al., 2013*).

4.3 Methods

4.3.1 Site description

This study focused on *Rhizophora* mangroves growing in two western Pacific sites: the island of Pohnpei (7°N, 158°E) in the Federated States of Micronesia, and the rock islands of

Palau (7°N, 134°E) (**Figure 1**). On Pohnpei, samples were collected from the banks of three estuaries, the Kamar (July 2011), the Sapwalap (August 2012) and the Soundau (August 2012) (**Figure 1**). Trees were sampled at five sites along the Kamar estuary, spanning a salinity range of 1-30 ppt, at eleven sites on the Sapwalap, spanning a salinity range of 1-34 ppt and at seven sites along the Soundau, spanning a salinity range of 4-33 ppt. Salinity was highly correlated with distance from the river mouth in each estuary (0.78 in Sapwalap, and 0.93 in Soundau) and the line of best fit relating measured salinities to distance from the river mouth was used to determine the mean salinities used in all figures and Table 1, which was deemed preferable to using the measured salinity at a single time point in the tidal cycle. The standard error of the regression between salinity and distance from the river mouth was 5.0 for Kamar, 4.4 for Sapwalap, and 2.8 for Soundau. These values are used for the salinity error bars in all tables and figures.

In Palau, trees were sampled in September and October of 2013 from Little Crocodile Lake and Big Crocodile Lake on Mecherchar Island and from Long Lake on Ngeruktabel Island **(Figure 1).** These meromictic marine lakes have been described in detail (*Hamner et al., 1982; Hamner & Hamner, 1998*). They are located in karst terrain and are connected at depth to the ocean through fissures in the surrounding bedrock. While dozens of lakes exist in the rock islands, *Rhizophora* is not present at the majority of them. The lakes for this study were chosen to represent the widest possible salinity range where *Rhizophora* is present.

Little Crocodile and Big Crocodile Lakes are highly stratified, and have a lens of brackish water above more saline deep water. The salinity of surface water in Little Crocodile Lake has been 8±2 ppt since monitoring began in the 1970's, and the surface water salinity in Big Crocodile Lake has been 20±3 ppt **(***Hamner & Hamner, 1998; Coral Reef Research*

*Foundation***)**. Surface water salinity in these lakes is constant through tidal cycles, but varies with amount of rainfall (*Hamner & Hamner, 1998*). Unlike the other two lakes, Long Lake is connected to the lagoon by a surface channel, and is not highly stratified. Salinity in this lake is near that of the local lagoon water, averaging 32±1 ppt. In addition to the three lakes, samples were also collected from fringing mangroves in the lagoon on the south coast of Koror, where salinity was 33±1 ppt.

At each site, salinity was measured with a refractometer (VeeGee Scientific, Kirkland, WA) with accuracy of ±1ppt. Specific conductance, water temperature, dissolved oxygen, and pH were measured using a Hydrolab Quanta data sonde (Hach, Loveland, CO). Multiple salinity measurements were made at each site over the sampling period, and at additional sites along each estuary at different points in the tidal cycle. 4mL of water was collected in a screw cap vial at each site for isotopic analysis. When possible, multiple water samples were collected from a site at different points in the tidal cycle to evaluate the range of surface salinities at individual sample locations along the estuaries.

4.3.2 Leaf and stem sampling

Leaves and stems were collected from as many as three species of *Rhizophora* at each site. *R. apiculata*, *R. stylosa*, and *R. mucronata* were present and sampled on Pohnpei. When two species were present at the same location, both were sampled. Typically *R. stylosa* and *R. mucronata* were found at the saltier sites and *R. apiculata* was found at the fresher sites, with *R. apiculata* present through a larger salinity range. In Palau, *R. apiculata* was sampled at Little Crocodile Lake and at one lagoon site. *R. mucronata* was sampled at Big Crocodile Lake, Long Lake, and two lagoon sites.

Stems for xylem water analyses were collected from sun exposed branches ~1 m above the lowest branches on the tree. On Palau, all of these samples came from the north shore of the lake and were south facing branches. ~5 cm of woody stem was collected and stored in an 11 mL glass screw cap vial. In Palau, the bark was stripped from the stem samples before they were placed in the vials.

Leaves for leaf water analyses were collected from the same branch as the xylem water samples. Sampled leaves were the second leaves from the distal end of the branch, which represent the youngest, fully mature leaves on the branch. Leaf water samples were also stored in 11 mL glass screw cap vials.

Leaves for lipids were collected from several additional branches. On Pohnpei, five leaves were collected from different sun exposed branches, ~1 m above the lowest branches on the tree. On Palau, one leaf each was collected from the south, west, and east aspects of the tree, and one leaf was collected from the most shaded interior branch present on the tree (trees on the north shore typically did not have any leaves on their north sides, as this aspect was totally shaded). All leaves for lipid analyses were the youngest fully mature leaf on their respective branches. All leaf and stem samples were placed on ice in the field and subsequently stored at -20°C prior to processing.

4.3.3 Leaf water and xylem water extraction

Leaf and xylem water samples were cryogenically extracted on a vacuum line. Samples were heated to 80°C while attached to a glass U-tube that was submerged in liquid Nitrogen. The sealed line was kept at a pressure below 60 mTorr for at least two hours. After this time, the U-tubes were removed from the liquid N_2, sealed, and the collected water was allowed to thaw. The

water was then filtered through a 0.45 μm PTFE filter to remove any particulate material and transferred to 2 mL screw cap vials, which were sealed with parafilm until analysis.

4.3.4 Water δ^2H and $\delta^{18}O$ analyses

Leaf and xylem water samples were analyzed by a Total Combustion Elemental Analyzer (TC/EA) coupled to a Delta V Isotope Ratio Mass Spectrometer (IRMS; Thermo Scientific, Waltham, MA) in the Sustainable Land Use Group in the Botany Department of the University of Basel, Switzerland. Each sample and standard was injected six times in sequence. In order to avoid any memory effects from the previous analysis, the first three injections of each sample were discarded. Thermo Isodat 3.0 software normalized raw isotopic ratios to the VSMOW (Vienna Standard Mean Ocean Water) scale using pulses of reference gas before and after the sample injection. Additionally, two in-house water standards of known isotopic composition were analyzed after every six samples throughout each sequence. The slope and intercept of the linear regression between the measured and known δ values of these samples was used to further normalize sample δ^2H and $\delta^{18}O$ values and to correct for any instrumental drift throughout the course of the sequence. An additional laboratory standard was analyzed after every 12 samples. This standard was not used for any of the isotopic corrections, but was used to assess instrument performance over time and the accuracy of the isotope corrections. Average absolute offset from the known isotopic value of this standard was 1.0‰ for δ^2H and 0.3‰ for $\delta^{18}O$. Average precision of triplicate sample injections was 0.80‰ for δ^2H and 0.2‰ for $\delta^{18}O$**.**

Surface water δ^2H and $\delta^{18}O$ values were measured by a Picarro Cavity Ring Down Spectroscopy (CRDS) L2130i Water Isotope Analyzer at the University of Washington. Measurements were normalized to the VSMOW scale using three laboratory standards of known

isotopic composition. The suite of standards was analyzed between every six samples throughout the run. All samples and standards were injected six times, and the first three measurements were discarded in order to avoid any memory effects from the previous analysis. Average precision of triplicate analyses was 0.2‰ for δ^2H and 0.05‰ for $\delta^{18}O$.

4.3.5 Leaf water model

Predicted δ^2H_{LW} and $\delta^{18}O_{LW}$ values of leaf water were calculated using a Péclet-Modified Craig-Gordon model of leaf water enrichment from Kahmen et al. (*2011*). The Craig-Gordon model of water enrichment is:

$$\Delta^2H_e = \varepsilon^+ + \varepsilon_k + (\Delta^2H_{WV} - \varepsilon_k)*(e_a/e_i) \quad (1)$$

where Δ^2H_e is evaporative enrichment of leaf water relative to xylem water at the site of evaporation, ε^+ is equilibrium fractionation between liquid water and water vapor, ε_k is kinetic fractionation associated with diffusion of water vapor from within the leaf to the atmosphere, Δ^2H_{WV} is the difference between water vapor δ^2H and δ^2H_{XW}, and e_a/e_i is the ratio of ambient to intercellular vapor pressures (*Craig & Gordon, 1965; Dongman et al., 1974*). The ratio of ambient to intercellular vapor pressure is dependent on relative humidity, air temperature and stomatal conductuctance. Relative humidity and air temperature were estimated from monthly averages for each site (www.nws.noaa.gov). Following observations in cultured *R. mangle* (*Lin & Sternberg, 1992*), stomatal conductance was set at 0.450 mol/m^{2}s for salinity < 15 PSU, and lowered by 0.015 mol/m^{2}s per PSU for salinities > 15 PSU. Internal leaf temperature was set at 0.5°C above air temperature, and the δ^2H and $\delta^{18}O$ values of water vapor were calculated

assuming equilibrium with precipitation during the study period. Each Pohnpei sampling campaign lasted no longer than 5 days, so the average precipitation isotopes from the entire time period were used to calculate equilibrium water vapor isotopes. Palau sampling took place over one month, and the water isotopes from the three nearest rain events were used to calculate equilibrium water vapor isotope values for Palau samples.

Following Kahmen et al. (*2011*), the Craig-Gordon model was modified to account for back diffusion of isotopically enriched water away from the site of evaporation using a Péclet effect ($\rho = L_M E/CD$, where L_M is the mixing path length, E is the transpiration stream, C is the molar concentration of water, and D is the diffusivity of $^1H^2HO$). L_M was set at 30.0 mm for all leaves, following Kahmen et al. (*2011*). The Péclet effect was used to calculate bulk leaf water enrichment, Δ^2H_{LW}, as follows:

$$\Delta^2 H_{LW} = \frac{\Delta^2 H_e(1-e^{-\rho})}{\rho} \quad (2)$$

Finally, δ^2H_{LW} was calculated as:

$$\delta^2 H_{LW} = (\Delta^2 H_{LW} + \delta^2 H_{XW}) + (\Delta^2 H_{LW} * \delta^2 H_{XW})/1000 \quad (3)$$

Calculations of $\delta^{18}O_{LW}$ followed the same equations, but used the equilibrium and kinetic fractionation factors associated with ^{18}O.

4.3.6 Lipid extraction and purification

Intact whole leaves from each tree from the Pohnpei estuaries were selected for analysis. From Palau sites, 4 leaves from different aspects of the tree were combined to form one sample. Leaves were rinsed with DI water to remove debris and cut into small (~0.5 cm) pieces using solvent-washed scissors prior to freeze-drying. Dry leaves were ground with a solvent-cleaned mortar and pestle, and lipids from ~0.5 g of dry leaf were extracted using accelerated solvent extraction (ASE-200, Dionex Corp., Sunnyvale, CA, USA) with 9:1 dichloromethane:methanol (DCM:MeOH)t 100 °C and 1500 psi for 3 x 5 min static cycles. The resulting total lipid extract (TLE) was evaporated to dryness under a stream of N_2 on a Turbovap system (Caliper, Hopkinton, MA, USA).

An aliquot of the *Rhizophora* TLE (~10 mg) was purified using silica gel column chromatography. Hydrocarbons were eluted with 8 mL hexane, sterols, alcohols and triterpenols with 8 ml 4:1 hexane:ethyl acetate and remaining compounds with 4 mL MeOH.

The alcohol fraction was acetylated at 70°C for 30 minutes with 25 μL of acetic anhydride of known δ^2H composition in 25 μL of pyridine. The alcohol fraction of *Rhizophora* leaves of all species was dominated by taraxerol, with relatively small amounts of β-sitosterol, β-amyrin, and *n*-alkanols. Lipids in the alcohol fraction were quantified by Gas Chromatography – Mass Spectrometry (GC-MS) using an Agilent (Santa Clara, CA, USA) 6890N gas chromatograph equipped with an Agilent 7683 autosampler, a split-splitless injector operated in splitless mode and an Agilent VF-17ms capillary column (60 m X 0.32 mm X 0.25 μm) interfaced to an Agilent 5975 quadrupole mass selective detector. The oven temperature was increased from 110°C to 320°C at 4°C/min, then held at 320°C for 10 minutes. Quantification of

taraxerol was performed by comparing integrated peak areas with a known amount of 5α-cholestane that was added to the sample just prior to GC-MS analysis.

The hydrocarbon fraction of *Rhizophora* leaves of all species was dominated by odd-numbered *n*-alkanes, with chain lengths ranging from C_{27}-C_{33}. In *R. apiculata* leaves from all locations, nC_{31} was the most abundant *n*-alkane, while in *R. mucronata* and *R. stylosa* leaves, nC_{29} was the most abundant *n*-alkane. The *n*-alkanes were quantified with a GC instrument equipped with flame ionization detection (GC-FID). An Agilent 6890N gas chromatograph equipped with an Agilent 7683 autosampler, programmable temperature vaporization inlet (PTV) operated in splitless mode and an Agilent DB-5ms column (60 m x 0.32 mm x 0.25 μm) was used with He as carrier gas (2.4 mL/min). The oven temperature was increased from 60 to 150 °C at 15 °C/min, then at 6 °C/min to 320 °C (held 28 min). Quantification of *n*-alkanes was performed by comparing integrated peak areas with a known amount of nC_{37}-alkane, added to the sample just prior to GC-FID analysis.

These quantifications were used to determine an appropriate amount of solvent in which to dissolve the sample so that it would produce a peak of ~20 V·s when analyzed by Gas Chromatrography – Isotope Ratio Mass Spectrometry (GC-IRMS).

4.3.7 Lipid δ^2H analyses

The δ^2H values of taraxerol, nC_{29}- and nC_{31}-alkanes were measured by GC-IRMS on a Thermo DELTA V PLUS system (Thermo Scientific, Waltham, MA, USA). The gas chromatograph (Trace Ultra, Thermo) was equipped with a split-splitless injector operated in splitless mode at 320 °C, a TRIPLUS autosampler (Thermo Scientific), and a VF-17ms capillary column (60 m x 0.25 mm x 0.25 μm, Agilent). For taraxerol analyses, the GC was heated from

120°C to 260°C at 20 °C/min, then at 1°C/min to 300°C, at 20 °C/min to 325°C and then held at 325 °C for 20 min. For *n*-alkane analyses, the GC was heated from 120°C to 250 °C at 20 °C/min, then at 6°C/min to 325 °C and then held at 325 °C for 12 min. Helium was used as the carrier gas at a constant flow of 1.1 mL/min. Compounds were pyrolyzed in a ceramic reactor at 1400 °C. 1 μL of sample was injected along with 0.5 μL of a mixture of *n*-alkanes of known isotopic composition (A. Schimmelmann, Indiana University, Bloomington, Indiana). For taraxerol analyses, this mixture included nC$_{26}$-, nC$_{28}$-, nC$_{32}$-, nC$_{34}$- and nC$_{41}$-alkanes. For *n*-alkane analyses, the co-injection standards were nC$_{21}$ and nC$_{23}$. At the beginning and end of a sequence, as well as after every 4-6 sample injections, a vial of additional *n*-alkane standards of known isotopic composition was analyzed with the co-injection standards, in place of a sample. For taraxerol sequences, this external standard was nC$_{38}$, which elutes within 1 minute of taraxerol using these GC conditions. For *n*-alkane sequences, nC$_{28}$-, nC$_{32}$- and nC$_{34}$-alkanes were used as external standards.

Thermo ISODAT software V.2.5 was used to control instrumentation and calculate δ^2H values. The slope and intercept of the relationship between measured and known δ^2H values of the *n*-alkane standards were used to calculate corrected δ^2H. Offsets between corrected and known δ^2H values of the standards were used to further correct for drift, retention time, and peak area on a sequence by sequence basis. Each sample was measured in triplicate. Reported analytical uncertainties are the standard error in the mean of the isotope standards, or the standard deviation of the triplicate sample analyses (whichever value was higher).

The H_{3+} factor was determined each day using pulses of a reference gas of varying heights and was 4.6±0.7 when analyzing Kamar samples in April, 2012, 4.2±0.3 when analyzing

Soundau and Sapwalap samples in Nov/Dec, 2012, and 1.71±0.01 when analyzing Palau samples in Feb/Mar 2014.

4.4 Results

4.4.1 Relationship between salinity and δ^2H and $\delta^{18}O$ values of different water pools

Surface water isotopes (δ^2H_{SW} and $\delta^{18}O_{SW}$) in all three estuaries and in the Palau lakes were highly correlated with salinity (R^2 = 0.96 and 0.98, respectively, for δ^2H_{SW}; R^2 = 0.97 and 0.96, respectively, for $\delta^{18}O_{SW}$) (**Figure 2; Table 1**). The slope of the relationship between salinity and both δ^2H_{SW} and $\delta^{18}O_{SW}$ was significantly different between the two islands ($p < 0.0001$). For δ^2H_{SW}, the slope was 0.81±0.03‰·ppt^{-1} on Pohnpei and 1.15±0.03‰·ppt^{-1} on Palau. For $\delta^{18}O_{SW}$, the slope was 0.142±0.003‰·ppt^{-1} for Pohnpei and 0.197±0.008‰·ppt^{-1} for Palau.

Rhizophora δ^2H_{XW} and $\delta^{18}O_{XW}$ values were positively correlated with salinity in both study sites (for δ^2H_{XW}, R^2 = 0.85 on Pohnpei and 0.89 on Palau; for $\delta^{18}O_{XW}$, R^2 = 0.81 for Pohnpei and 0.87 for Palau) (**Figure 2; Table 2**). However, the slopes of these relationships were shallower than those between the corresponding surface water isotopes and salinity (for δ^2H_{XW}, m = 0.54±0.05‰·ppt^{-1} on Pohnpei and 0.9±0.1‰·ppt^{-1} on Palau; for $\delta^{18}O_{XW}$, m = 0.10±0.01‰·ppt^{-1} on Pohnpei and 0.14±0.02‰·ppt^{-1} on Palau).

Rhizophora δ^2H_{LW} and $\delta^{18}O_{LW}$ values were positively correlated with salinity, but the relationships were much weaker (for δ^2H_{LW}, R^2 = 0.34 on Pohnpei and 0.11 on Palau; for $\delta^{18}O_{LW}$, R^2 = 0.36 on Pohnpei and 0.08 on Palau) **(Figure 2**). This relationship was not significant in the case of Palau ($p = 0.30$ for δ^2H_{LW} and 0.35 for $\delta^{18}O_{LW}$). On Pohnpei, the slope of the relationship between salinity and δ^2H_{LW} values was 0.4±0.1‰·ppt^{-1}. For $\delta^{18}O_{LW}$ values it was 0.11±0.03‰·PSU^{-1}.

Modeled δ^2H_{LW} and $\delta^{18}O_{LW}$ were well correlated with measured values ($R^2 = 0.71$ for δ^2H_{LW} and 0.68 for $\delta^{18}O_{LW}$; $p < 0.0001$ for both isotopes) (**Figure 3**). The slopes of the relationships between modeled and measured leaf water isotopes were close to unity (m = 1.0±0.1 for δ^2H_{LW} and 1.3±0.2 for $\delta^{18}O_{LW}$) and the y-intercepts were close to 0 (b = -3±2 for δ^2H_{LW} and -0.6±0.3 for $\delta^{18}O_{LW}$).

The fractionation factor between surface water and xylem water, $\alpha^2_{SW\text{-}XW}$, was always ≤ 1.0 and decreased with salinity (**Figures 4a and 4b; Table 2**). The correlation between $\alpha^2_{SW\text{-}XW}$ and salinity was moderate for Pohnpei ($R^2 = 0.41$) and weak for Palau ($R^2 = 0.07$) and was not statistically significant in Palau ($p = 0.39$). The fractionation factor between the xylem water and the leaf water, $\alpha^2_{LW\text{-}XW,}$ was uncorrelated with salinity at both sites (**Figures 5a and 5b; Table 2**).

For oxygen isotopes, the fractionation factor between surface water and xylem water, $\alpha^{18}_{SW\text{-}XW}$, was near 1.0 and decreased slightly with salinity (**Figures 4c and 4d; Table 2**). The correlation between $\alpha^{18}_{SW\text{-}XW}$ and salinity was moderate ($R^2 = 0.34$ for Pohnpei and 0.22 for Palau) and was not statistically significant on Palau ($p = 0.13$). There was essentially no trend between $\alpha^{18}_{LW\text{-}XW}$ and salinity ($p = 0.46$ for Pohnpei and 0.83 for Palau) (**Figures 5c and 5d; Table 2**).

4.4.2 Relationship between salinity and ^2H fractionation between mangrove leaf lipids and different water pools

There is a moderate negative correlation between salinity and $\alpha_{Tarax\text{-}SW}$ on Pohnpei and Palau ($R^2 = 0.27$ and 0.38, respectively; **Figures 6a and 6b**). The slope and intercept were not statistically different between the two sites (m = -0.0010±0.0003 ppt^{-1} for Pohnpei and -

$0.0007\pm0.0003 \cdot ppt^{-1}$ for Palau; b = 0.817±0.007 for Pohnpei and 0.806±0.007 for Palau). The linear regression describing the relationship between salinity and $\alpha_{Tarax\text{-}SW}$ for the pooled data set is $\alpha_{Tarax\text{-}SW} = (-0.0009\pm0.0002)*S + 0.814\pm0.006$. Separate linear regression analyses of the three species (*R. apiculata, R. mucronata, R. stylosa*) included in the sample set did not yield statistically different results.

Salinity was moderately correlated with $\alpha_{Tarax\text{-}XW}$ at both sites ($R^2 = 0.21$ on Pohnpei and 0.31 on Palau) although this relationship was not significant on Palau (p = 0.06). There was no correlation between $\alpha_{Tarax\text{-}LW}$ and salinity (p = 0.13 on Pohnpei and 0.87 on Palau).

Salinity is negatively correlated with net fractionation during the synthesis of nC$_{29}$-alkanes by *Rhizophora* spp. on both Pohnpei and Palau ($R^2 = 0.44$ and 0.28, respectively; **Figures 6c and 6d**), although this result was not statistically significant for Palau (p = 0.22), where many of the sampled leaves did not have enough nC$_{29}$-alkane for analysis. There were ample nC$_{31}$-alkanes for analysis in all leaves from Palau, and the negative correlation between $\alpha_{n\text{C31-SW}}$ and salinity was significant here ($R^2 = 0.37$, p = 0.04), although not on Pohnpei ($R^2 = 0.06$, p = 0.32) (**Figures 6e and 6f**).

The relationship between salinity and $\alpha_{nC29\text{-}XW}$ was negatively correlated on Pohnpei ($R^2 = 0.50$) and described by the relationship $\alpha_{nC29\text{-}XW} = (-0.0007\pm0.0001)*S + 0.875\pm0.004$. On Palau, these two variables were positively correlated ($R^2 = 0.25$), although this relationship was not significant (p = 0.26). There was a weak, insignificant negative relationship between salinity and $\alpha_{nC31\text{-}XW}$ on Pohnpei ($R^2 = 0.26$ and p = 0.12) and weak, insignificant positive relationship on Palau ($R^2 = 0.09$ and p = 0.36).

The relationship between salinity and $\alpha_{n\text{C29-LW}}$ was negatively correlated on Pohnpei ($R^2 = 0.55$) and described by the relationship $\alpha_{n\text{C29-LW}} = (-0.0009\pm0.0002)*S + 0.874\pm0.006$. On

Palau, these two variables were not correlated ($R^2 = 0.008$). There was essentially no relationship between salinity and $\alpha_{nC31\text{-}LW}$ at either site ($R^2 = 0.03$ on Pohnpei and 0.005 on Palau).

4.5 Discussion

4.5.1 Water sources and discrimination against ^2H during water uptake in Rhizophora mangroves

In most higher plants, δ^2H_{XW} and $\delta^{18}O_{XW}$ values are identical to those of the environmental water used by the plant, and can be used to determine water sources, since apoplastic water uptake by roots is a bulk process that does not result in isotopic fractionation (*White et al., 1985; Dawson and Ehleringer, 1991; Walker and Richardson, 1991; Dawson et al., 2002*). In the *Rhizophora* trees studied here, δ^2H_{XW} values were typically depleted relative to δ^2H_{SW} (**Figures 2 and 4; Table 2**). This implies that surface water was not the only water source for these plants and/or that the roots of these *Rhizophera* trees discriminate against water molecules containing ^2H during water uptake.

Previous studies indicate that mangroves and other salt tolerant plants discriminate against ^2H by as much as 11‰ during water uptake, but not against ^{18}O (*Lin & Sternberg, 1993; Ellsworth & Williams, 2007*). As such, $\delta^{18}O_{XW}$ values have been used to identify a plant's source water (*Lin & Sternberg, 1994; Ewe et al., 2007; Lambs et al., 2008; Wei et al., 2013*). In the estuaries on Pohnpei, the deviation of $\alpha^{18}_{SW\text{-}XW}$ from 1.000 was less than 0.001 (or 1‰) in 18 out of 22 plants, suggesting that the sampled surface water was the main water source for *Rhizophora* trees in those estuaries. The observed ^2H-depletions of xylem water are therefore consistent with ^2H-discrimination during water uptake by roots in Pohnpeian estuaries.

Lin and Sternberg (*1993*) observed that xylem water in *Avicennia germinans* was depleted by 1-2‰ relative to its source water when grown in freshwater, but was depleted by up to 8‰ relative to its source water when grown at a salinity of 28 ppt. Over the same salinity range, $\alpha_{SW\text{-}XW}$ in Pohnpeian *Rhizophora* trees decreased by 8‰ (**Figure 4a**), similar to that in the *A. germinans* measured by Lin and Sternberg (*1993*). In contrast to the *Rhizophora* from Pohnpei, Lin and Sternberg observed no difference in the magnitude of discrimination against ^{2}H by *Rhizophora mangle* from Florida growing in either freshwater or water with a salinity of 28 ppt.

Our results are consistent with the hypothesis that mangroves discriminate against ^{2}H during root water uptake, and that this discrimination increases as salinity increases. Increased ^{2}H-discrimination during water uptake could explain as much as 13‰ of the overall 30‰ decrease in both $\alpha_{Tarax\text{-}SW}$ and $\alpha_{nC29\text{-}SW}$ observed in *Rhizophora* spp. growing along estuaries in Pohnpei.

The situation is more complicated for *Rhizophora* growing around marine lakes in Palau, where the $\delta^{18}O_{XW}$ values were 1-3‰ lower than $\delta^{18}O_{SW}$ adjacent to the mangroves. This ^{18}O-depletion of xylem water suggests that the Palau mangroves had an additional water source. Potential alternative sources of water include subsurface water from the lakes, ground water, runoff during rain events, and foliar uptake of rain or dew.

It is highly unlikely that the sampled trees were using subsurface water, as this water was in all cases more saline than the surface water and had correspondingly enriched $\delta^{2}H$ and $\delta^{18}O$ values *(Smittenberg et al., 2011*). Due to the shallow root structure of *Rhizophora* (*Gill & Tomlinson, 1977; Hatchings & Saenger, 1987*), they are typically confined to water sources within the upper meter of substrate (*Lin & Sternberg, 1994)*. *R. mangle* in Florida has been

observed using relatively fresh groundwater seeps from a depth of 1 m during the dry season (*Ewe et al., 2007*). Since we did not sample and analyze groundwater from Palau, we cannot rule out the possibility that these trees had access to a fresher groundwater source, with correspondingly lower $\delta^{18}O$ values.

Some work suggests that mangroves may be able to opportunistically take up fresh water runoff during rain events (*Wei et al., 2013; Reef & Lovelock, 2014*). The light $\delta^{18}O_{XW}$ values from *Rhizophora* trees in Palau would be consistent with this strategy, since local meteroric freshwater had an average $\delta^{18}O$ value of -5‰ on Palau during the sampling period.

There is some evidence to suggest that mangroves may rely on foliar uptake of freshwater for a portion of their water (*Hoste et al., 2011; de Groote, 2013; Reef & Lovelock, 2014*). Foliar water uptake has been demonstrated to be an important water source for plants in cloud forests (*Johnson & Smith, 2008; Eller et al., 2013*) and foggy coastal areas (*Dawson, 1998; Burgess & Dawson, 2004*). Reverse xylem flow, which would be consistent with foliar water uptake, has been observed in mangroves at night (*Rada et al., 1989; Hao et al., 2008; Hoste et al, 2011*) and during rainfall events (*Hoste et al., 2011*). Foliar water uptake of rain or dew and corresponding reverse xylem flow would be also be consistent with relatively depleted $\delta^{18}O_{XW}$ values.

Measured $\delta^{2}H_{XW}$ values of Palau *Rhizophora* were less than would be expected based on their $\delta^{18}O_{XW}$ values and the local meteoric water line, which would predict $\delta^{2}H_{XW}$ values 6-14‰ higher than measured (**Figure 7**). This suggests that the measured $\delta^{2}H_{XW}$ values were offset from $\delta^{2}H_{SW}$ not only because the trees were using alternative water sources, but also because they were discriminating against ^{2}H during water uptake. Because symplastic water uptake by roots in halophytes is reported to discriminate against ^{2}H by 2-11‰ (*Lin & Sternberg, 1993; Ellsworth &*

Williams, 2007) the low δ^2H_{XW} values relative to surface water in *Rhizophora* mangroves is more consistent with water uptake by roots than with foliar uptake of water in leaves.

4.5.2 Leaf water enrichment in Rhizophora

Leaf water in *Rhizophora* was marginally enriched relative to xylem water across all sampled *Rhizophora* trees, and in 7 of 33 trees δ^2H_{LW} was slightly depleted relative to δ^2H_{XW} (**Figures 2 and 5; Table 2**). Measured δ^2H_{LW} values agreed well with the values predicted by the Péclet-Modified Craig-Gordon model of Kahmen et al. (*2011*; **Figure 3**). The model predicted ~70% of the variability in δ^2H_{LW} values, despite uncertainties in humidity and temperature. As such, the relatively small ^{2}H-enrichment of leaf water relative to xylem water can be ascribed to relatively high ambient relative humidity, resulting in a small vapor pressure gradient across the leaf surface (*Helliker & Ehrlinger, 2000; Farquhar et al., 2007*). δ^2H_{LW} values likely vary less with salinity than δ^2H_{XW} because of the plants experience the same relative humidity and water vapor isotopes, and this masks some of the variability in the δ^2H_{XW} values.

Because there was no correlation between salinity and $\alpha^2_{LW\text{-}XW}$ (**Figure 5)**, salinity-dependent changes in leaf water ^{2}H-enrichment cannot account for the negative correlation between $\alpha_{Lipid\text{-}SW}$ and salinity (**Figure 6**). Therefore the third hypothesis proposed to explain the inverse relationship between salinity and $\alpha_{Lipid\text{-}SW}$ in Ladd and Sachs (2012), that increased salt residue on the leaf surface at higher salinity reduces the vapor pressure gradient across the leaf surface and therefore decreases leaf water enrichment relative to xylem water, cannot be correct. At least in humid environments such as Pohnpei and Palau, where the average relative humidity of 82% (*www.nws.noaa.gov*) is greater than the relative humidity maintained above saturated salt

solutions (76%; *O'Brien, 1984*), alternate mechanisms must cause increased ^{2}H-discrimination in leaf lipids as salinity increases.

4.5.3 Relationship between salinity and biosynthetic ^{2}H fractionation in Rhizophora lipid

By measuring $\delta^{2}H_{LW}$ and $\delta^{2}H_{Lipid}$ values, the biosynthetic component of net fractionation, $\alpha_{Lipid\text{-}LW}$, can be calculated. For the most part, there were not significant correlations between salinity and $\alpha_{Lipid\text{-}LW}$. The one exception, $\alpha_{nC29\text{-}LW}$ from Pohnpei, had a slope identical to that of $\alpha_{nC29\text{-}SW}$, supporting the possibility that the entire change in $\alpha_{nC29\text{-}SW}$ over the salinity range 1-34 ppt could be due to changes in biosynthetic fractionation alone. Increased biosynthetic $^{2}H/^{1}H$ fractionation at higher salinity could be caused by increased compatible solute production, resulting in relatively more depleted NADPH from the pentane phosphate cycle being incorporated into lipids (as described in detail in *Ladd and Sachs, 2012*).

$\delta^{2}H_{Tarax}$ values were depleted relative to $\delta^{2}H_{n\text{-alkanes}}$ in both Pohnpei and Palau (**Figure 6; Table 2**). Increased biosynthetic fractionation during the synthesis of isoprenoids relative to acetogenic lipids has been previously observed and attributed to a greater proportion of hydride derived from NADPH in the former (*Sessions et al., 1999; Sessions, 2006; Zhang et al., 2009*).

4.5.4 Relationship between salinity and net ^{2}H fractionation in Rhizophora lipids

In both Pohnpei and Palau, the net fractionation between surface water and taraxerol, $\alpha_{Tarax\text{-}SW}$, decreased with salinity (**Figure 6**). This is the first assessment of environmental controls on $\delta^{2}H_{Tarax}$, and demonstrates that the hydrogen isotopic composition of this *Rhizophora* biomarker (*Killops & Frewin, 1994; Koch et al., 2003; Versteegh et al., 2004*) has a very similar relationship to salinity as leaf wax *n*-alkanes (*Ladd & Sachs, 2012*). Likewise, $\alpha_{nC29\text{-}SW}$ from

Pohnpei and $\alpha_{n\text{C31-SW}}$ from Palau were negatively correlated with salinity (**Figure 6**), suggesting that the negative correlation between salinity and $\alpha_{\text{Lipid-SW}}$ first observed in Brisbane *A. marina* (*Ladd & Sachs, 2012*) may be universal to leaf lipids from mangroves.

The results of the present study are important in that they demonstrate a relatively consistent negative relationship between salinity and $\alpha_{\text{Lipid-SW}}$ for lipids synthesized in different biosynthetic pathways (acetogenic *n*-alkanes and the isoprenoid taraxerol) and in very different climates (humid subtropics in Brisbane and equatorial tropics in Micronesia and Palau). They also demonstrate a similar relationship between salinity and $\alpha_{\text{Lipid-SW}}$ in mangroves from two genera with different salt management strategies. Both *Rhizophora* and *Avicennia* exclude salt from entering their roots, but this filtration is more efficient in *Rhizophora*, which lacks *Avicennia's* ability to secrete salt (*Scholander et al., 1962*).

However, $\alpha_{\text{Lipid-SW}}$ was less sensitive to salinity in Micronesian *Rhizophora* than it was in *A. marina* growing in the Brisbane River (*Ladd & Sachs, 2012*). In Brisbane, a slope of -1.5±0.3‰ PSU^{-1} was observed for both $n\text{C}_{31}$- and $n\text{C}_{33}$-alkanes from *A. marina*, while in this study the slopes of $\alpha_{\text{Lipid-SW}}$ for taraxerol and *n*-alkanes in *Rhizophora* spp. were between -0.0002 to -0.001 ppt^{-1} (**Figure 6**). The difference in sensitivity could be due to biological differences between the two types of mangroves, or to different environmental conditions.

It is possible that the lower relative humidity in Brisbane resulted in a stronger and steeper relationship between $\alpha_{\text{Lipid-SW}}$ and salinity than that observed in Micronesia. Saturated salt solutions maintain a relative humidity at their boundary layer of 76% (*O'Brien, 1984*). This is higher than the average relative humidity of 53% in Brisbane (http://www.bom.gov.au), but lower than the average relative humidity of 82% on both Pohnpei and Palau (www.nws.noaa.gov). Salt deposits on the leaf surface could therefore increase the relative

humidity along the leaf surface in Brisbane, and reduce vapor pressure differential (VPD) across the leaf surface. A lower VPD results in less leaf water enrichment (*Flanagan et al., 1991; Ripullone et al., 2008*).

This effect would be expected to be more pronounced for *Avicennia* spp. than for *Rhizophora* spp., as the former secretes salt from its leaves, but the latter does not (*Scholander et al., 1962; Parida & Jha, 2010*). However, some *Rhizophora* can be found with salt crystals on their leaves due to sea spray, and it has been suggested that the presence of such salt and the resulting decrease in VPD may help with its water management (*Reef & Lovelock, 2014*). This process would probably not contribute to $\alpha_{Lipid\text{-}SW}$ in Micronesia, since the ambient relative humidity is so high.

One biological difference that could account for the different sensitivities of $\alpha_{Lipid\text{-}SW}$ to salinity in *Rhizophora* and *Avicennia* could be differing residence times of leaves on the two types of trees. In studies from Phuket, Thailand, and Darwin, Australia *Rhizophora* leaves tended to persist longer on the tree, averaging 11.2±0.2 months, as compared to *Avicennia* leaves that persisted on average for 6.3±0.1 months (*Wium-Andersen & Christensen, 1978; Coupland et al., 2005*). These studies, both from continental regions with strong seasonality of precipitation, may not be representative of *Rhizophora* growing in regions with minimal seasonality, such as Pohnpei and Palau. Nevertheless, if this pattern does hold true for Micronesian mangroves, δ^2H_{Lipid} values from *Rhizophora* leaves might be more representative of long-term averages, while those in *Avicennia* may be more sensitive to seasonal conditions, and thereby more strongly influenced by salinity in the months just preceding sampling.

Another biological difference between *Avicennia* and *Rhizophora* is the compatible solutes they produce to maintain appropriate osmotic gradients. *A. marina* primarily uses the

amino acids asparagine and glycine betaine as compatible solutes (*Ashihara et al., 1997; Hibino et al., 2001*), while *Rhizophora* primarily produces soluble carbohydrates, including pinitol and manitol (*Hibino et al., 2001*). Soluble carbohydrates are relatively depleted in ^{2}H relative to amino acids (*Schmidt et al., 2003*). If the hypothesis that increased compatible solute production at high salinity causes the inverse relationship between salinity and $\alpha_{Lipid\text{-}SW}$ is correct, it would be more pronounced for *A. marina* than *Rhizophora*, since *A. marina* produces relatively ^{2}H-enriched compatible solutes, leaving increasingly more ^{1}H for lipid synthesis as salinity increases.

4.6 Conclusions

The relationship between salinity and net $^{2}H/^{1}H$ fractionation in leaf *n*-alkanes and taraxerol was calibrated in *Rhizophora* mangroves from three estuaries and four brackish lakes on the Micronesian islands of Pohnpei and Palau. As salinity increased from 1-34 ppt, net fractionation between both lipid classes and surface water increased by ~30‰. For the *Rhizophora* biomarker taraxerol, the relationship between isotope fractionation and salinity was $\alpha_{Tarax\text{-}SW} = (-0.0009\pm0.0002)*S + 0.814\pm0.006$ ($R^2=0.29$; $p=0.0005$; $n= 38$). Increased ^{2}H-discrimination during water uptake by roots can explain up to 43% of this signal.

Leaf water isotopes in the studied *Rhizophora* mangroves were not significantly enriched relative to xylem water, irrespective of salinity. Measured enrichment of both $\delta^{2}H_{LW}$ and $\delta^{18}O_{LW}$ were consistent with the predictions of a Péclet-Modified Craig-Gordon model of leaf water enrichment in terrestrial vascular plants that considers the effect of back diffusion in addition to ambient temperatures, humidity, stomatal conductance, xylem water $\delta^{2}H$ and $\delta^{18}O$, and water vapor $\delta^{2}H$ and $\delta^{18}O$. Therefore, mechanisms that invoke a change in $\delta^{2}H_{LW}$ in response to salinity

cannot explain the inverse relationship between salinity and isotope fractionation in mangrove lipids. Instead, more plausible causes are changes in xylem water isotopes associated with opportunistic freshwater use and changes in $^{2}H/^{1}H$ fractionation during lipid biosynthesis as a direct response to salt stress. The latter might result from increased compatible solute synthesis at high salinities and/or greater reliance on stored carbohydrates for lipid synthesis.

The observed 0.9‰ ppt^{-1} decrease *Rhizophora* leaf lipid $\delta^{2}H$ values supports the use of sedimentary taraxerol $\delta^{2}H$ values to reconstruct past changes in salinity. When combined with either $\delta^{2}H$ values of co-occurring algal lipids, or $\delta^{13}C$ values of taraxerol itself, both salinity and the $\delta^{2}H$ value of environmental water can be determined. Although the intercept of the linear least squares regression of $\alpha_{tarax\text{-}SW}$ with salinity is quite precise (+/-1%) the slope has an uncertainty of 22%. Estimates of salinity and water isotopes using the present field calibration will therefore be associated with moderately large uncertainties . Culturing mangroves at different salinities under controlled laboratory conditions ought to reduce those uncertainties.

4.7 References

Ashihara H., Adachi K., Otawa M., Yasumoto E., Fukushima Y., Kato M., Sano H., Sasamoto H. and Baba S. (1997) Compatible solutes and inorganic ions in the mangrove plant *Avicennia marina* and their effects on the activities of enzymes. *Zeitschrift für Naturforschung* **52**, 433-440.

Burgess S. S. O. and Dawson T. E. (2004) The contribution of fog to the water relations of Sequoia sempervirens (D. Don): foliar uptake and prevention of dehydration. *Plant, Cell & Environment* **27**, 1023–1034.

Chikaraishi Y. and Naraoka H., (2003) Compound-specific δD- δ13C analyses of *n*-alkanes extracted from terrestrial and aquatic plants. *Phytochemistry* **63**, 361-371.

Conroy J. L., Cobb K. M. and Noone D. (2013) Comparison of precipitation isotope variability across the tropical Pacific in observations and SWING2 model simulations. *Journal of Geophysical Research: Atmospheres* **118**, 5867-5892.

Coupland G. T., Paling E. I. and McGuinness, K. A. (2005) Vegetative and reproductive phenologies of four mangrove species from northern Australia. *Australian Journal of Botany* **53**, 109-117.

Craig H. and Gordon L. (1965) Deuterium and oxygen 18 variations in the ocean and the marine atmosphere. In *Proceedings of a Conference on Stable Isotopes in Oceanographic Studies and Paleotemperatures* (ed E. Tongiori). CNR-Laboratorio di Geologia Nucleare, Pisa. pp. 9-130.

Dansgaard W. (1964) Stable isotopes in precipitation. *Tellus* **16**, 436-468.

Dawson T. E. (1998) Fog in the California redwood forest: ecosystem inputs and use by plants. *Oecologia* **117**, 476-485.

Dawson T. E. and Ehleringer J. R. (1991) Streamside trees that do not use stream water: Evidence from hydrogen isotope ratios. *Nature* **350**, 335-337.

Dawson T. E., Mambelli S., Plamboeck A. H., Templer P. H. and Tu K.P. (2002) Stable isotopes in plant ecology. *Annual Review of Ecology and Systematics* **33**, 507-559.

De Groote S. (2013) Impact of dew and rain on the water relations of the mangrove species *Avicennia marina* (Forssk.) Vierh.Master's thesis, University Ghent, Faculty of Bioscience Engineering.

Dittmar T., Hertkorn N., Kattner G. and Lara R. J. (2006) Mangroves, a major source of dissolved organic carbon to the oceans. *Global Biogeochemical Cycles* **20**:GB1012, doi:10.1029/2005GB002570.

Dongmann G, Nornberg H. W., Forstel H. and Wagener K. (1974) On the enrichment of H^2 and ^{18}O in the leaves of transpiring plants. *Radiat Environ Biophys* **11**, 41–52.

Eller C. B., Lima A. L. and Oliveira R. S. (2013) Foliar uptake of fogwater and transport belowground alleviates drought effects in the cloud forest tree species, *Drimys brasiliensis* (Winteraceae). *New Phytologist* **199**, 151-162.

Ellsworth P. and Williams D. (2007) Hydrogen isotope fractionation during water uptake by woody xerophytes. *Plant and Soil* **291**, 93-107.

Ewe S., Sternberg L. and Childers, D. (2007) Seasonal plant water uptake patterns in the saline southeast Everglades ecotone. *Oecologia* **152**, 607-616.

Farquhar G. D., Cernusak L. A. and Barnes B., (2007) Heavy water fractionation during transpiration. *Plant Physiology* **143**, 11-18.

Feakins S. J. and Sessions A. L. (2010) Controls on the D/H ratios of plant leaf waxes in an arid ecosystem. *Geochimica Cosmochimica Acta* **74**, 2128-2141.

Flanagan L. B., Comstock J. P. and Ehleringer J. R. (1991) Comparison of modeled and observed environmental influences on the stable oxygen and hydrogen isotope composition of leaf water in *Phaseolus vulgaris* L. *Plant Physiol*. **96**, 588–596.

Gat, J. R. (1996) Oxygen and hydrogen isotopes in the hydrologic cycle. *Annual Review in Earth and Planetary Sciences* **24**, 225-262.

Gill A. M. and Tomlinson P. B. (1977) Studies on the growth of red mangrove *(Rhizophora mangle* L.). IV. The adult root system. *Biotropica* **9**,145-155.

Hamner W. M., Gilmer R. W. and Hamner P. P. (1982) The physical, chemical, and biological characteristics of a stratified, saline, sulfide lake in Palau. *Limnology and Oceanography* **27**, 896-909.

Hamner W. M. and Hamner P. P. (1998) Stratified marine lakes of Palau (Western Caroline Islands). *Physical Geography* **19**, 175-220.

Hao G. Y., Jones T. J., Luton C., Zhang Y. J., Manzane E., Scholz F. G., Bucci S. J., Cao K. F. and Goldstein G. (2009) Hydraulic redistribution in dwarf *Rhizophora mangle* trees driven by interstitial soil water salinity gradients: impacts on hydraulic architecture and gas exchange. *Tree Physiology* **29**, 697–705.

Hatchings P. and Saenger P. (1987) *Ecology of mangroves*. University of Queensland Press, New York..

Helliker B. R. and Ehleringer J. R. (2000) Establishing a grassland signature in veins: ^{18}O in the leaf water of C_3 and C_4 grasses. *Proceedings of the National Academy of Sciences* **97**, 7894-7898.

Hibino T., Meng Y. L., Kawamitsu Y., Uehara N., Matsuda N., Tanaka Y., Ishikawa H., Baba S., Takabe T., Wada K., Ishii T. and Takabe, T. (2001) Molecular cloning and functional characterization of two kinds of betaine-aldehyde dehydrogenase in betaine-accumulating mangrove *Avicennia marina* (Forsk.) Vierh. *Plant Molecular Biology* **45**, 353–363.

Hoste P. (2011) Ecophysiology of mangroves in Australia: hydraulic functioning. Master's thesis, University Ghent, Faculty of Bioscience Engineering.

Hou J., D' Andrea W., MacDonald D. and Huang Y. S. (2007) Hydrogen isotopic variability in leaf waxes among terrestrial and aquatic plants around Blood Pond, Massachusetts (USA). *Organic Geochemistry* **38**, 977-984.

Jennerjahn T. C. and Ittekot V. (2002) Relevance of mangroves for the production and deposition of organic matter along tropical continental margins. *Naturwissenschaften* **89**, 23-30.

Johnson D. M. and Smith W. K. (2008) Cloud immersion alters microclimate, photo- synthesis and water relations in *Rhododendron catawbiense* and *Abies fraseri* seedlings in the southern Appalachian Mountains, USA. *Tree Physiology* **28**, 385–392.

Kahmen A., Sachse D., Arndt S. K., Farrington H., Vitousek P. M. and Dawson T. E. (2011) Cellulose d^{18}O is an index of leaf to air vapor pressure difference (VPD) in tropical plants. *Proceedings of the National Academy of Sciences* **108**, 1981–1986.

Kahmen A., Schefuss E. and Sachse D. (2013) Leaf water deuterium enrichment shapes leaf wax *n*-alkane dD values of angiosperm plants I: Experimental evidence and mechanistic insights. *Geochimica et Cosmochimica Acta* **111**, 39-49.

Kahmen A., Simonin K., Tu K. P., Merchant A. and Callister A. (2008) Effects of environmental parameters, leaf physiological properties and leaf water relations on leaf water delta ^{18}O enrichment in different Eucalyptus species. *Plant, Cell & Environment* **31**, 738-751.

Killops S. D. and Frewin N. L. (1994) Triterpenoid diagenesis and cuticular preservation. *Organic Geochemistry* **21**, 1193-1209.

Koch B. P., Harder J., Lara R.J. and Kattner G. (2005) The effect of selective microbial degradation on the composition of mangrove derived pentacyclic triterpenols in surface sediments. *Organic Geochemistry* **36**, 273-285.

Koch B. P., Rullkotter J., and Lara R. J. (2003) Evaluation of triterpenols and sterols as organic matter biomarkers in a mangrove ecosystem in northern Brazil. *Wetlands Ecology and Management* **11**, 257-263.

Kurita N., Ichiyanagi K., Matsumoto J., Yamanaka M. D. and Ohata T. (2009) The relationship between the isotopic content of precipitation and the precipitation amount in tropical regions. *Journal of Geochemical Exploration* **102**, 113-122.

Ladd S. N. and Sachs J. P. (2012) Inverse relationship between salinity and *n*-alkane δ D values in the mangrove *Avicennia marina*. *Organic Geochemistry* **48**, 25-36.

Ladd S. N. and Sachs J. P. (2013) Positive correlation between salinity and *n*-alkane d13C values in the mangrove *Avicennia marina*. *Organic Geochemistry* **64**, 1-8

Lambs L., Muller E. and Fromard F. (2008) Mangrove trees growing in a very saline condition but not using seawater. *Rapid Communications in Mass Spectrometry* **22**, 2835-2843.

Lin G. and Sternberg L. (1992) Effect of growth form, salinity, nutrient and sulfide on photosynthesis, carbon isotope discrimination and growth of red mangrove *Rhizophora mangle* L. *Functional Plant Biology* **19**, 509-517.

Lin G. and Sternberg L. (1993) Hydrogen isotopic fractionation by plant roots during water uptake in coastal wetland plants. In *Stable Isotopes and Plant Carbon/Water Relations* (eds J. Ehleringer, A. Hall, and G. Farquhar), pp. 497-510. Academic Press, Inc., San Diego.

Lin G. and Sternberg L. (1994) Utilization of surface water by red mangrove (*Rhizophora mangle* L.): An isotopic study. *Bulletin of Marine Science* **54**, 94-102.

Liu W. G. and Yang H. (2008) Multiple controls for the variability of hydrogen isotopic compositions in higher plant *n*-alkanes from modern ecosystems. *Global Change Biology* **14**, 2166-2177.

Liu W. G., Yang H. and Li L. (2006) Hydrogen isotopic composition of *n*-alkanes from terrestrial plants correlate with their ecological life form. *Oecologia* **150**, 330-338.

O'Brien, F. E. M. (1948) The control of humidity by saturated salt solutions. *Journal of Scientific Instruments* **25**, 73.

Parida A. and Jha B. (2010) Salt tolerance mechanisms in mangroves: a review. *Trees - Structure and Function* **24**, 199-217.

Polissar P. J. and Freeman K. H. (2010) Effects of aridity and vegetation on plant-wax δ D in modern lake sediments. *Geochimica et Cosmochimica Acta* **74**, 5785-5797.

Rada F., Goldstein G., Orozco A., Montilla M., Zabala O., and Azócar A (1989) Osmotic and turgor relations of three mangrove ecosystem species. *Functional Plant Biology* **16** 477–486.

Reef R. and Lovelock C. E. (2014) Regulation of water balance in mangroves. *Annals of Botany* doi:10.1093/aob/mcu174

Ripullone F., Matsuo N., Stuart-Williams H., Wong S. C., Borghetti M., Tani M. and Farquhar G. (2008) Environmental effects on oxygen isotope enrichment of leaf water in cotton leaves. *Plant Physiology* **146**, 729-736.

Romero I. C. and Feakins S. J. (2011) Spatial gradients in plant leaf wax D/H across a coastal salt marsh in southern California. *Organic Geochemistry* **42**, 618-629.

Sachse D., Billault I., Bowen G. J., Chikaraishi Y., Dawson T. E., Feakins S. J., Freeman K. H., Magill C. R., McInerney F. A., van der Meer M. T. J., Polissar P., Robins R. J., Sachs J. P., Schmidt H. L., Sessions A. L., White J. W. C., West. J. B. and Kahmen A. (2012) Molecular paleohydrology: interpreting the hydrogen-isotopic composition of lipid biomarkers from photosynthesizing organisms. *Annual Review of Earth and Planetary Science* **40**, 212-249.

Sachse D., Radke J. and Gleixner G. (2004) Hydrogen isotope ratios of recent lacustrine sedimentary *n*-alkanes record modern climate variability. *Geochimica et Cosmochimica Acta* **68**, 4877-4889.

Sauer P. E., Eglinton T. I., Hayes J. M., Schimmelmann A., Sessions A. L. (2001) Compound-specific D/H ratios of lipid biomarkers from sediments as a proxy for environmental and climatic conditions. *Geochimica et Cosmochimica Acta* **65**, 213-222.

Schmidt H. L., Werner R. A. and Eisenreich W. (2003) Systematics of ^{2}H patterns in natural compounds and its importance for the elucidation of biosynthetic pathways. *Phytochemistry Reviews* **2**, 61-85.

Scholander P. F., Hammel H. T., Hemmingsen E. and Garey W. (1962) Salt Balance in Mangroves. *Plant Physiology* **37**, 722-729.

Sessions A. (2006) Seasonal changes in D/H fractionation accompanying lipid biosynthesis in Spartina alterniflora. *Geochima et Cosmochimica Acta* **70**, 2153-2162.

Sessions A. L., Burgoyne T. W., Schimmelmann A., Hayes J. M. (1999) Fractionation of hydrogen isotopes in lipid biosynthesis. *Organic Geochemistry* **30**, 1193-1200.

Smith F. A. and Freeman K. H. (2006) Influence of physiology and climate on δ D of leaf wax *n*-alkanes from C_3 and C_4 grasses. *Geochimica et Cosmochimica Acta* **70**, 1172-1187.

Smittenberg R. H., Saenger C., Dawson M. N. and Sachs J. P. (2011) Compound-specific D/H ratios of the marine lakes of Palau as proxies for West Pacific Warm Pool hydrologic variability. *Quaternary Science Reviews* **30**, 921-933.

Spalding M., Kainuma M. and Collins, L. (2010) *World atlas of mangroves*. Washington, D.C., Earthscan.

Tierney J. E., Oppo D. W., Rosenthal Y., Russell J. M. and Linsley B. K. (2010) Coordinated hydrological regimes in the Indo-Pacific region during the past two millennia. *Paleoceanography* **25**, PA1102, 7pp.

Tipple B. J., Berke M. A., Doman C. E., Khachaturyan S. and Ehleringer J. R. (2013) Leaf *n*-alkane record the plant-water environment at leaf flush. *Proceedings of the National Academy of Science* **110**, 2659-2664.

Tipple B. J., Berke M., Hambach B., Roden J. S. and Ehleringer J. R. (In Press) Predicting leaf wax *n*-alkane (2) H/(1) H ratios: controlled water source and humidity experiments with hydroponically grown trees confirm predictions of Craig-Gordon model. *Plant, Cell and Environment*. doi: 10.1111/pce.12457.

Versteegh G. J. M, Schefub E., Dupont L., Marret F., Sinninghe Damaste J., and Jansen J. H. F. (2002) Taraxerol and *Rhizophora* pollen as proxies for tracking past mangroves ecosystems. *Geochimica et Cosmochimica Acta* **68**, 411-422.

Walker C. D., and Richardson S. B., 1991. The use of stable isotopes of water in characterising the source of water in vegetation. *Chemical Geology* **94**, 145-158.

Wei L., Lockington D. A., Poh S. C., Gasparon M. and Lovelock C. E. (2013) Water use patterns of estuarine vegetation in a tidal creek system. *Oecologia* **172**, 485-494.

White, J. W. C., Cook E. R., Lawrence J. R., and Broecker W. S., 1985. The D/H ratios of sap in trees: Implications for water sources and tree ring D/H ratios. *Geochimica et Cosmochimica Acta* **49**, 237-246.

Wium-Andersen S. and Christensen B. (1978) Seasonal growth of mangrove trees in southern Thailand. II. Phenology of *Brugueira cylindrica, Ceriops tagal, Lumnitzera littoria* and *Avicennia marina. Aquatic Botany* **5**, 383-390.

Yang H., Pagani M., Briggs D. E. G., Equiza M. A., Jagels R., Leng Q. and LePage B. A. (2009) Carbon and hydrogen isotope fractionation under continuous light: implications for paleoenvironmental interpretations of the High Arctic during Paleogene warming. *Oecologia* **160**, 461-470.

Zhang Z., Sachs J. P., Marchetti A. (2009) Hydrogen isotope fractionation in freshwater and marine algae: II. Temperature and nitrogen limited growth rate effects. *Organic Geochemistry* **40**, 428-439.

Table 1: Sites included in this study.

Site	Latitude (N)	Longitude (E)	Mean Salinity (PSS)	Species sampled	Mean water δ^2H (‰)	Mean water $\delta^{18}O$ (‰)
			Pohnpei, Federated States of Micronesia			
Kamar 1	6°56.573'	158°13.591'	1 ± 5	*R. apiculata*	-24.3±1	-4.58±0.2
Kamar 2	6°57.276'	158°13.479'	4 ± 5	*R. apiculata*	-33.5±1	-4.13±0.2
Kamar 3	6°58.083'	158°13.317'	16 ± 5	*R. stylosa*	-12.0±1	-2.31±0.2
Kamar 4	6°58.849'	158°12.979'	23 ± 5	*R. stylosa*	-7.3±1	-1.58±0.2
Kamar 5	6°58.965'	158°13.054'	30 ± 5	*R. stylosa*	-6.7±1	-1.3±0.2
Sapwalap 1	6°53.204'	158°17.417'	2 ± 4.4	*R. apiculata*	-26.4±1	-5.12±0.02
Sapwalap 2	6°52.920'	158°17.768'	8 ± 4.4	*R. apiculata*	-21.4±1	-4.22±0.02
Sapwalap 3	6°52.935'	158°17.825'	10 ± 4.4	*R. apiculata*	-18.9±1	-3.77±0.02
Sapwalap 4	6°52.890'	158°18.109'	14 ± 4.4	*R. apiculata*	-16.5±1	-3.32±0.02
Sapwalap 5	6°52.733'	158°18.339'	19 ± 4.4	*R. apiculata*	-12.3±1	-2.42±0.02
Sapwalap 6	6°52.495'	158°18.536'	23 ± 4.4	*R. apiculata*	-9.0±1	-1.97±0.02
Sapwalap 7	6°52.448'	158°18.501'	25 ± 4.4	*R. apiculata, R. stylosa*	-6.6±1	-1.52±0.02
Sapwalap 8	6°52.232'	158°18.680'	29 ± 4.4	*R. stylosa*	-3.3±1	-0.92±0.02
Sapwalap 9	6°52.252'	158°18.604'	31 ± 4.4	*R. apiculata, R. mucronata*	-2.4±1	-0.77±0.02
Sapwalap 10	6°51.742'	158°19.475'	34 ± 4.4	*R. stylosa*	0.1±1	-0.77±0.02
Sapwalap 11	6°52.123'	158°20.313'	34 ± 4.4	*R. stylosa*	0.1±1	-0.32±0.02
Soundau 1	6°54.712'	158°08.952'	4 ± 2.8	*R. apiculata*	-23.1±1	-0.32±0.02
Soundau 2	6°54.507'	158°07.654'	14 ± 2.8	*R. apiculata*	-15.4±1	-4.39±0.13
Soundau 3	6°54.403'	158°07.517'	18 ± 2.8	*R. apiculata, R. mucronata*	-12.4±1	-3.03±0.13
Soundau 4	6°54.343'	158°07.332'	22 ± 2.8	*R. mucronata*	-9.3±1	-2.49±0.13
Soundau 5	6°54.187'	158°07.197'	26 ± 2.8	*R. stylosa*	-6.2±1	-1.94±0.13
Soundau 6	6°54.064'	158°06.945'	30 ± 2.8	*R. stylosa*	-3.1±1	-1.4±0.13
Soundau 7	6°54.135'	158°06.758'	33 ± 2.8	*R. stylosa*	-0.8±1	-0.86±0.13
			Palau			
Little Croc Lake	7°09.04'	134°21.33'	10 ± 2.2	*R. apiculata*	-29.4±1	-4.43±0.15
Big Croc Lake	7°09.34'	134°22.12'	22 ± 3.2	*R. mucronata*	-12.5±1	-1.48±0.11
Long Lake 1	**7°14.908'**	**134°24.527'**	32 ± 1.1	*R. mucronata*	-4.64±1	-0.39±0.03
Long Lake 2	**7°14.908'**	**134°24.527'**	32 ± 1.1	*R. mucronata*	-4.64±1	-0.5±0.05
Lagoon 1	7°20.123'	134°29.834'	29 ± 1	*R. mucronata*	1.8±1	-0.16±0.06
Lagoon 2	7°20.80'	134°27.31'	33 ± 1	*R. mucronata*	1.8±1	0.7±0.04
Lagoon 3	7°20.826'	134°27.295'	32 ± 1	*R. apiculata*	1.8±1	0.56±0.02

Table 2: Water and lipid isotope measurements and fractionation factors calculated from those values. Error bars represent one standard deviation.

Site	XW δ^2H (‰)	XW $\delta^{18}O$ (‰)	LW δ^2H (‰)	LW $\delta^{18}O$ (‰)	Tarax δ^2H (‰)	nC_{29} δ^2H (‰)	nC_{31} δ^2H (‰)	$\alpha^2_{XW\text{-}SW}$	$\alpha^{18}_{XW\text{-}SW}$	$\alpha^2_{LW\text{-}XW}$	$\alpha^{18}_{LW\text{-}XW}$	$\alpha_{Tx\text{-}LW}$	$\alpha_{C29\text{-}LW}$	$\alpha_{C31\text{-}LW}$	$\alpha_{Tx\text{-}SW}$	$\alpha_{C29\text{-}SW}$	$\alpha_{C31\text{-}SW}$
							Pohnpei										
Kamar 1	-33.3 ±0.4	-5.2 ±0.2	-31.2 ±0.4	-2.3 ±0.2	-208 ±1	-153 ±3	-148 ±2	0.991± 0.001	0.999 ±0.0002	1.00± 0.001	1.002 ±0.0002	0.822 ± 0.001	0.874 ± 0.003	0.873 ± 0.002	0.811± 0.002	0.868± 0.003	0.851± 0.002
Kamar 2	-27.9 ±0.4	-4.3 ±0.2	-32.2 ±0.4	-3.5 ±0.2	-180 ±3	-142 ±3	-146 ±5	1.01 ±0.001	1.000 ±0.0002	0.996 ±0.001	1.001 ±0.0002	0.850 ±0.003	0.886 ±0.003	0.884 ±0.005	0.852 ±0.003	0.887 ±0.003	0.853± 0.005
Kamar 3	-19.7 ±0.4	-2.3 ±0.2	-22.8 ±0.4	0.4 ±0.2	-188 ±9	-157 ±2		0.992 ±0.001	1.000 ±0.0002	9.997 ±0.001	1.003 ±0.0002	0.834 ±0.009	0.862 ±0.002		0.825 ±0.009	0.853 ±0.002	
Kamar 4	-19.2 ±0.4	-3.1 ±0.2	-22.9 ±0.4	-0.8 ±0.2	-220 ±6	-163 ±5		0.988 ±0.001	0.998 ±0.0002	0.996 ±0.001	1.001 ±0.0002	0.804 ±0.007	0.857 ±0.005		0.792 ±0.006	0.843 ±0.005	
Kamar 5	-19.5 ±0.4	-2.7 ±0.2	-17.8 ±0.4	-0.9 ±0.2	-211 ±10	-176 ±3		0.987 ±0.001	1.000 ±0.0002	1.00 ±0.001	1.002 ±0.0002	0.808 ±0.010	0.839 ±0.003		0.799 ±0.010	0.830 ±0.003	
Sapwalap 1	-28.8 ±0.4	-3.5 ±0.1	-13.7 ±0.4	-1.1 ±0.2	-177 ±1		-179 ±2	0.998 ±0.001	1.002 ±0.001	1.015 ±0.001	0.999 ±0.001	0.834 ±0.001		0.832 ±0.002	0.845 ±0.001		0.843 ±0.002
Sapwalap 2	-28.4 ±0.6	-3.3 ±0.1	-13.3 ±0.4	1.1 ±0.2				0.993 ±0.001	1.001 ±0.001	1.016 ±0.001	1.001 ±0.001	0.774 ±0.003	0.849 ±0.001	0.850 ±0.005			
Sapwalap 3					-210 ±7		-160 ±4								0.806 ±0.008		0.856 ±0.004
Sapwalap 4	-25.7 ±0.7	-3.3 ±0.1	-13.1 ±0.8	1.0 ±0.2				0.991 ±0.001	1.000 ±0.001	1.013 ±0.001	1.001 ±0.001	0.788 ±0.002		0.848 ±0.005			
Sapwalap 5	-23.3 ±0.4	-2.8 ±0.1	-17.9 ±0.9	0.4 ±0.2	-215 ±4		-145 ±4	0.988 ±0.001	1.000 ±0.0004	1.006 ±0.001	1.000 ±0.001	0.799 ±0.004		0.871 ±0.004	0.794 ±0.004		0.865 ±0.004
Sapwalap 6	-24.5 ±0.7	-2.6 ±0.2	-17.7 ±0.4	1.3 ±0.2				0.984 ±0.001	0.999 ±0.001	1.007 ±0.001	1.001 ±0.002	0.793 ±0.004		0.861 ±0.005			
Sapwalap 7 *R. styl*					-219 ±1	-142 ±1									0.787 ±0.001	0.864 ±0.001	
Sapwalap 7 *R. apic*					-218 ±2		-140 ±8								0.788 ±0.002		0.866 ±0.008
Sapwalap 8 *R. styl*					-212 ±1	-131 ±4									0.791 ±0.001	0.872 ±0.004	
Sapwalap 8 *R. apic*					-201 ±3		-145 ±2								0.802 ±0.003		0.858 ±0.002
Sapwalap 9 *R. mucr*	-15.5 ±0.1	-1.6 ±0.2	-13.0 ±0.9	0.1 ±0.1				0.987 ±0.001	0.999 ±0.0001	1.002 ±0.001	1.000 ±0.001	0.788 ±0.005	0.845 ±0.003	0.845 ±0.005			
Sapwalap 9 *R. apic*	-14.8 ±1.0	-1.3 ±0.2	-17 ±1	0.5 ±0.1				0.988 ±0.001	0.999 ±0.001	0.998 ±0.002	1.000 ±0.001	0.814 ±0.006		0.860 ±0.005			

Sapwalap 10	-13.2 ±0.2	-0.8 ±0.2	-12.4 ±0.7	1.6 ±0.2				0.987 ±0.001	1.000 ±0.002	1.001 ±0.001	1.001 ±0.002	0.813 ±0.002	0.840 ±0.002	0.843 ±0.005			
Sapwalap 11	-11.7 ±0.2	-0.8 ±0.2	-11.3 ±0.7	1.4 ±0.2	-204 ±5	-150 ±6	-155	0.988 ±0.001	1.000 ±0.001	1.000 ±0.001	1.001 ±0.002	0.806 ±0.005	0.860 ±0.006	0.855 ±0.005	0.796 ±0.005	0.850 ±0.006	0.845 ±0.005
Soundau 1	-32.8 ±0.8	-4.1 ±0.2	-21.4 ±0.6	-0.5 ±0.2	-227 ±5		-167 ±2	0.990 ±0.001	1.000 ±0.0001	1.012 ±0.001	1.004 ±0.0003	0.790 ±0.005		0.854 ±0.002	0.791 ±0.006		0.856 ±0.002
Soundau 2	-23.8 ±0.6	-3.7 ±0.2	-10.3 ±0.3	2.8 ±0.2	-229 ±1		-161 ±2	0.992 ±0.001	1.000 ±0.0002	1.014 ±0.002	1.007 ±0.0003	0.779 ±0.001		0.850 ±0.001	0.783 ±0.001		0.854 ±0.001
Soundau 3 *R. apiculata*	-21.8 ±0.5	-2.6 ±0.3						0.990 ±0.001	1.000 ±0.0002								
Soundau 3 *R. mucronata*	-28.5 ±0.1	-3.5 ±0.1	-17.4 ±0.8	1.1 ±0.2	-200 ±3		-149 ±1	0.984 ±0.001	1.000 ±0.0002	1.011 ±0.001	1.005 ±0.0002	0.814 ±0.003		.866 ±0.001	0.810 ±0.003		0.864 ±0.001
Soundau 4	-17.9 ±0.9	-1.7 ±0.2	-9 ±1	2.7 ±0.2	-224 ±5	-155 ±1	-150 ±2	0.991 ±0.001	1.000 ±0.0002	1.009 ±0.001	1.005 ±0.0003	0.783 ±0.005	0.852 ±0.001	0.872 ±0.001	0.784 ±0.005	0.852 ±0.01	0.872 ±0.001
Soundau 5	-16.7 ±1.1	-1.6 ±0.1	-8.0 ±0.7	3.0 ±0.2	-225 ±6	-147 ±4		0.989 ±0.002	1.000 ±0.0002	1.009 ±0.001	1.005 ±0.0002	0.781 ±0.006	0.856 ±0.004		0.780 ±0.006	0.854 ±0.004	
Soundau 6	-16.4 ±1.2	-1.5 ±0.1	-2.2 ±0.3	5.7 ±0.2	-227 ±4			0.987 ±0.002	0.999 ±0.0001	1.014 ±0.001	1.007 ±0.0002	0.775 ±0.004	0.845 ±0.003		0.775 ±0.004		
Soundau 7	-15.7 ±2	-1.4 ±0.1	-5.6 ±0.7	4.0 ±0.2	-228 ±5	-155 ±1	-156 ±2	0.985 ±0.001	0.999 ±0.0002	1.010 ±0.001	1.005 ±0.0002	0.776 ±0.005	0.850 ±0.003	0.852 ±0.001	0.773 ±0.005	0.846 ±0.003	0.848 ±0.001
									Palau								
Little Croc *R. apic 1*	-41.4 ±0.4	-4.9 ±0.2	-34.9 ±1.5	-3.2 ±0.3	-235 ±3		-160 ±3	0.986 ±0.001	0.999 ±0.0002	1.007 ±0.002	1.002 ±0.0004	0.792 ±0.003		0.870 ±0.004	0.789 ±0.003		0.866 ±0.004
Little Croc *R. apic 2*	-43.9 ±0.7	-5.1 ±0.2	-37.7 ±0.1	-2.8 ±0.3	-216 ±6	-164 ±2	-167 ±6	0.984 ±0.001	0.999 ±0.0002	1.007 ±0.001	1.002 ±0.0003	0.815 ±0.006	0.868 ±0.002	0.865 ±0.006	0.809 ±0.006	0.862 ±0.002	0.858 ±0.006
Little Croc *R. apic 3*	-45.4 ±1.0	-5.6 ±0.1	-36.7 ±0.7	-3.2 ±0.1	-209 ±5		-179 ±2	0.982 ±0.002	0.999 ±0.0002	1.009 ±0.001	1.002 ±0.0002	0.821 ±0.005		0.852 ±0.002	0.816 ±0.005		0.847 ±0.002
Big Croc *R. mucr 1*	-36.6 ±0.3	-4.0 ±0.1	-8.5 ±0.7	5.3 ±0.1	-226 ±4	-180 ±4	-180 ±10	0.975 ±0.001	0.998 ±0.0002	1.029 ±0.001	1.009 ±0.0001	0.781 ±0.004	0.827 ±0.004	0.826 ±0.010	0.786 ±0.004	0.833 ±0.004	0.832 ±0.010
Big Croc *R. mucr 2*	-36.5 ±0.4	-4.2 ±0.1	-12.7 ±0.7	3.2 ±0.1	-224 ±3	-180 ±10	-180 ±4	0.975 ±0.001	0.997 ±0.0002	1.025 ±0.001	1.007 ±0.0002	0.786 ±0.003	0.831 ±0.010	0.830 ±0.004	0.788 ±0.003	0.833 ±0.010	0.832 ±0.004
Big Croc *R. mucr 3*	-38.2 ±0.6	-4.7 ±0.2	-21.4 ±0.7	-1.1 ±0.2	-221 ±11	-168 ±3	-171 ±12	0.973 ±0.001	0.997 ±0.0002	1.017 ±0.001	1.004 ±0.0003	0.796 ±0.011	0.850 ±0.003	0.847 ±0.012	0.791 ±0.011	0.845 ±0.003	0.842 ±0.012
Long Lake *R. mucr* 1	-21.9 ±0.5	-2.3 ±0.2	-32.7 ±1.1	-4.9 ±0.2	-207 ±4		-169 ±8	0.980 ±0.002	0.998 ±0.0002	0.989 ±0.001	0.997 ±0.0003	0.820 ±0.005		0.859 ±0.009	0.793 ±0.004		0.831 ±0.008
Long	-18.0	-1.7	-16.7	9.8	-206		-158	0.984	0.999	1.001	1.012	0.807		0.856	0.794		0.842

Lake *R. mucr* 2	±0.7	±0.3	±1.2	±0.1	±2		±4	±0.001	±0.0003	±0.001	±0.0003	±0.002		±0.004	±0.002		±0.004
Lagoon *R. mucr* 1	-17.5 ±0.4	-1.2 ±0.2	-8.8 ±1.1	1.5 ±0.1	-208 ±7	-160 ±5	-166 ±4	0.985 ±0.001	0.999 ±0.0002	1.009 ±0.001	1003 ±0.0002	0.799 ±0.007	0.848 ±0.005	0.841 ±0.004	0.793 ±0.007	0.841 ±0.005	0.835 ±0.004
Lagoon *R. mucr* 2	-20.7 ±0.9	-1.7 ±0.2	-27.0 ±1.2	-0.8 ±0.3	-218 ±6	-168 ±4	-171 ±7	0.979 ±0.001	0.999 ±0.0002	0.994 ±0.001	1.001 ±0.0003	0.803 ±0.007	0.855 ±0.005	0.852 ±0.007	0.782 ±0.006	0.832 ±0.005	0.829 ±0.007
Lagoon *R. mucr* 3	-24.7 ±0.3	-1.5 ±0.2	-29.9 ±0.8	-1.0 ±0.1	-230 ±4	-156 ±9	-152 ±4	0.975 ±0.001	0.998 ±0.0002	0.995 ±0.001	1.001 ±0.0002	0.794 ±0.004	0.870 ±0.010	0.875 ±0.004	0.771 ±0.004	0.845 ±0.009	0.849 ±0.004
Lagoon *R. apic* 1	-23.5 ±0.6	-2.3 ±0.2	-30.8 ±0.4	-1.7 ±0.1	-224 ±7		-156 ±4	0.977 ±0.001	0.997 ±0.0002	0.993 ±0.001	1.001 ±0.0002	0.800 ±0.007		0.871 ±0.005	0.776 ±0.007		0.845 ±0.005

4.8 Figure Captions:

Figure 1: Map of field sites in Palau (left panel) and Pohnpei (right panel). Stars indicate locations of lakes sampled on Palau and estuaries sampled on Pohnpei.

Figure 2: Surface (blue), xylem (brown) and leaf (green) water isotopes as a function of salinity. Panel a shows δ^2H values from Pohnpei estuaries and panel b shows δ^2H values from Palau lakes. Panels c and d contain the corresponding $\delta^{18}O$ values.

Figure 3: Relationship between modeled and measured leaf water (a) δ^2H values and (b) $\delta^{18}O$ values for *Rhizophora* spp. in Pohnpei and Palau. Modeled leaf water values are from a Peclet-modified Craig-Gordon model of leaf water enrichment.

Figure 4: Relationship between salinity and fractionation factors between xylem water and surface water. Panel a shows ^2H fractionation in Pohnpei estuaries and b shows ^2H fractionation in Palau lakes. Panels c and d show corresponding relationships for ^{18}O fractionation.

Figure 5: Relationship between salinity and fractionation factors between leaf water and xylem water. Panel a shows ^2H fractionation in Pohnpei estuaries and b shows ^2H fractionation in Palau lakes. Panels c and d show corresponding relationships for ^{18}O fractionation.

Figure 6: Relationship between salinity and net fractionation in mangrove leaf lipids for (a) Pohnpei taraxerol, (b) Palau taraxerol, (c) Pohnpei n-C_{29}-alkanes, (d) Palau n-C_{31}-alkanes, (e) Pohnpei n-C_{31}-alkanes, (f) Palau n-C_{31}-alkanes.

Figure 7: Measured xylem water δ^2H values from Palau *Rhizophora* plotted relative to those predicted by measured xylem water $\delta^{18}O$ values and the relationship between the two isotopes in surface water (LWL = Local Water Line).

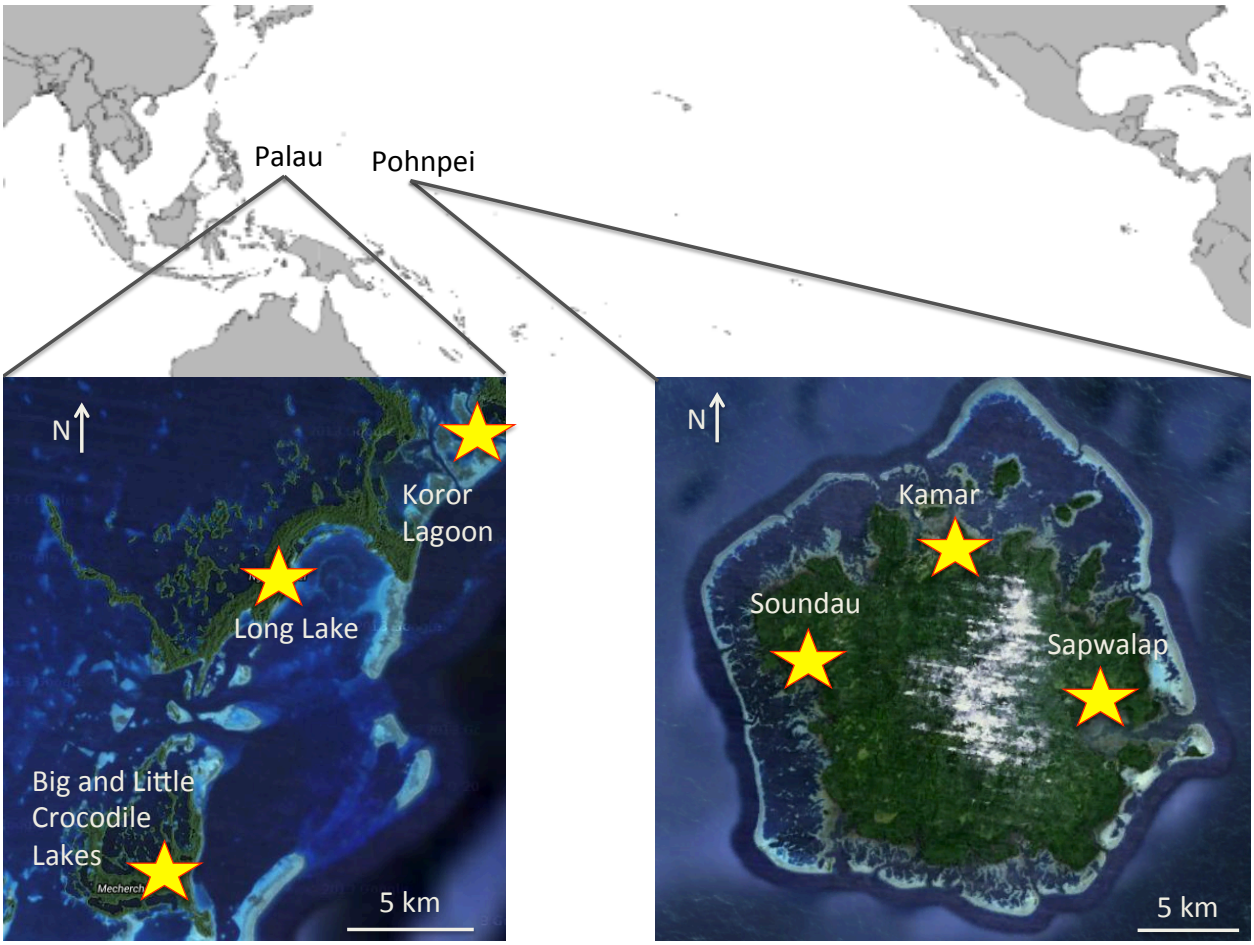

Figure 1: Map of field sites in Palau (left panel) and Pohnpei (right panel). Stars indicate locations of lakes sampled on Palau and estuaries sampled on Pohnpei.

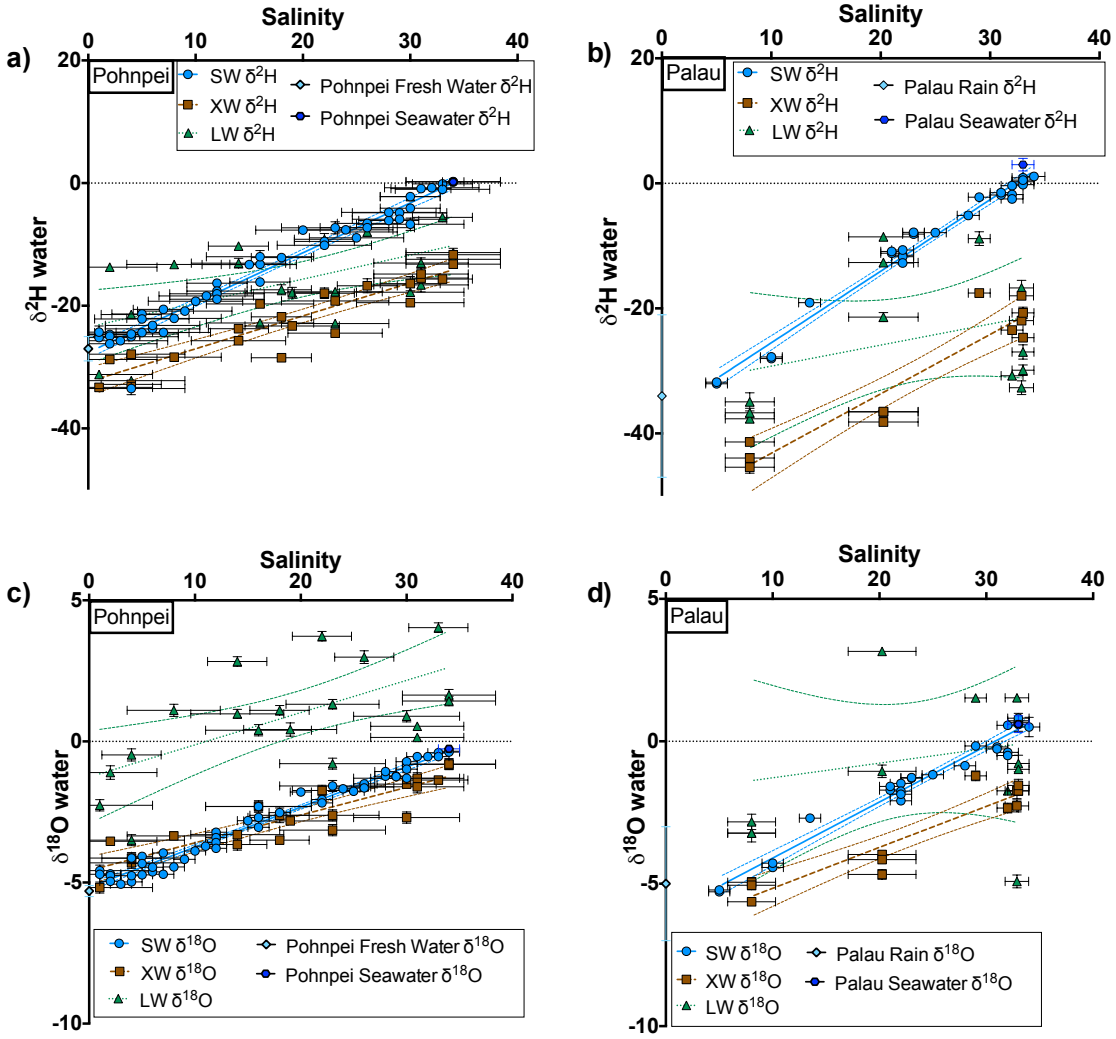

Pohnpei						Palau				
m	**b**	**R^2**	**p**	**n**	**Water δ^2H**	**m**	**b**	**R^2**	**p**	**n**
0.81 ± 0.02	-27.6 ± 0.5	0.96	<0.0001	50	Surface water δ^2H	1.15 ± 2	-36.9 ± 0.9	0.98	<0.0001	26
0.54 ± 0.05	-32 ± 1	0.85	<0.0001	22	Xylem water δ^2H	0.9 ± 0.1	-53 ± 3	0.87	<0.0001	12
0.4 ± 0.1	-23 ± 3	0.34	0.006	21	Leaf water δ^2H	0.3 ± 0.3	-33 ± 8	0.11	0.30	12
m	**b**	**R^2**	**p**	**n**	**Water $\delta^{18}O$**	**m**	**b**	**R^2**	**p**	**n**
0.142 ± 0.003	-5.16 ± 0.07	0.97	<0.0001	50	Surface water $\delta^{18}O$	0.197 ± 0.008	-6.1 ± 0.2	0.96	<0.0001	26
0.10 ± 0.01	-4.6 ± 0.2	0.81	<0.0001	22	Xylem water $\delta^{18}O$	0.14 ± 0.02	-6.6 ± 0.4	0.87	<0.0001	12
0.11 ± 0.03	-1.3 ± 0.8	0.36	0.004	21	Leaf water $\delta^{18}O$	0.1 ± 0.1	-3 ± 3	0.09	0.35	12

Figure 2: Surface (blue), xylem (brown) and leaf (green) water isotopes as a function of salinity. Panel a shows δ^2H values from Pohnpei estuaries and panel b shows δ^2H values from Palau lakes. Panels c and d contain the corresponding $\delta^{18}O$ values.

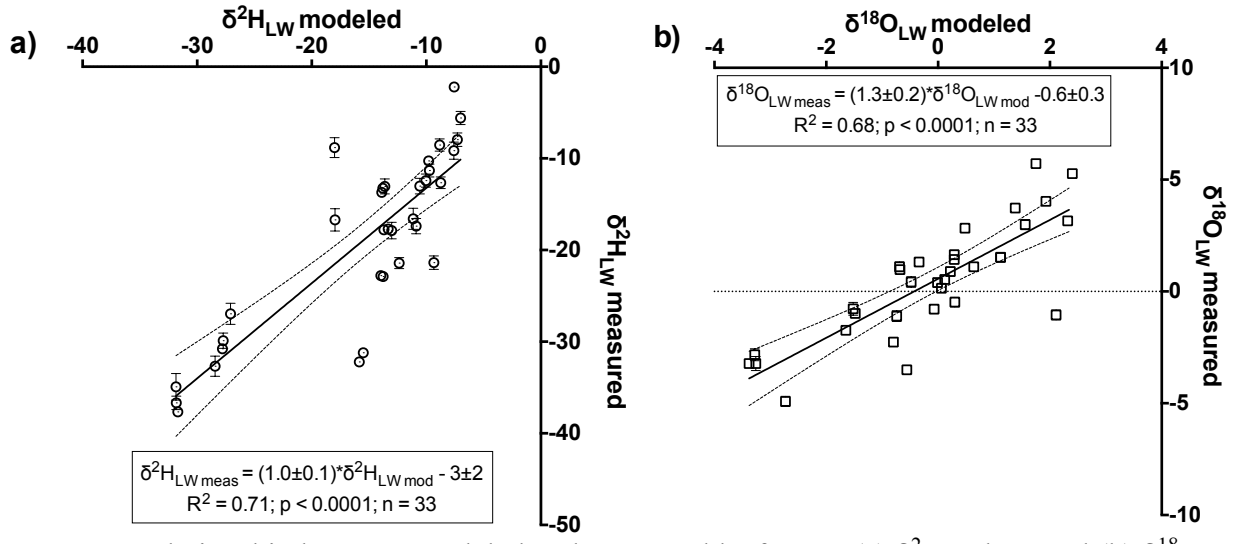

Figure 3: Relationship between modeled and measured leaf water (a) δ^2H values and (b) $\delta^{18}O$ values for *Rhizophora* spp. in Pohnpei and Palau. Modeled leaf water values are from a Peclet-modified Craig-Gordon model of leaf water enrichment.

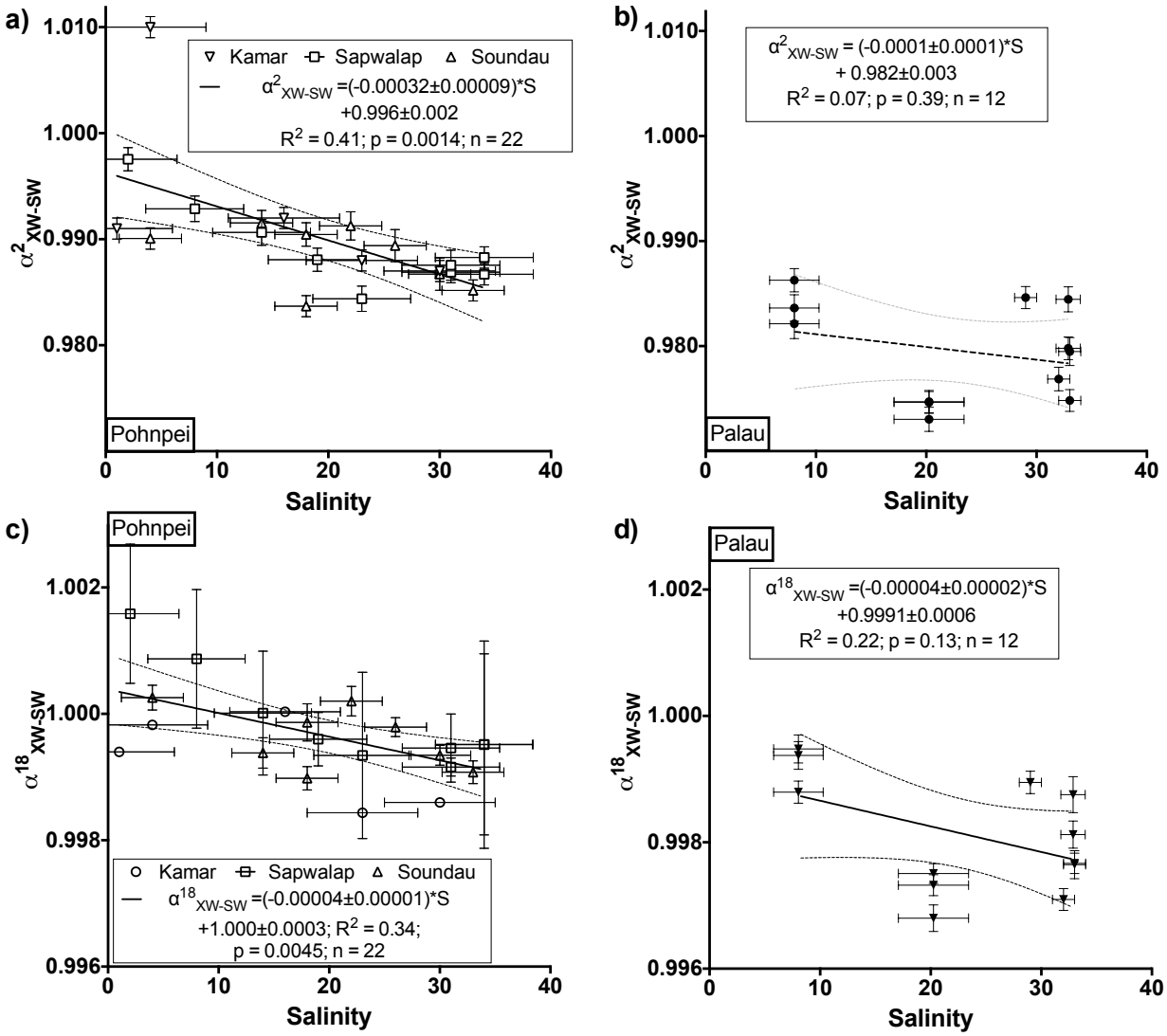

Figure 4: Relationship between salinity and fractionation factors between xylem water and surface water. Panel a shows ^{2}H fractionation in Pohnpei estuaries and b shows ^{2}H fractionation in Palau lakes. Panels c and d show corresponding relationships for ^{18}O fractionation.

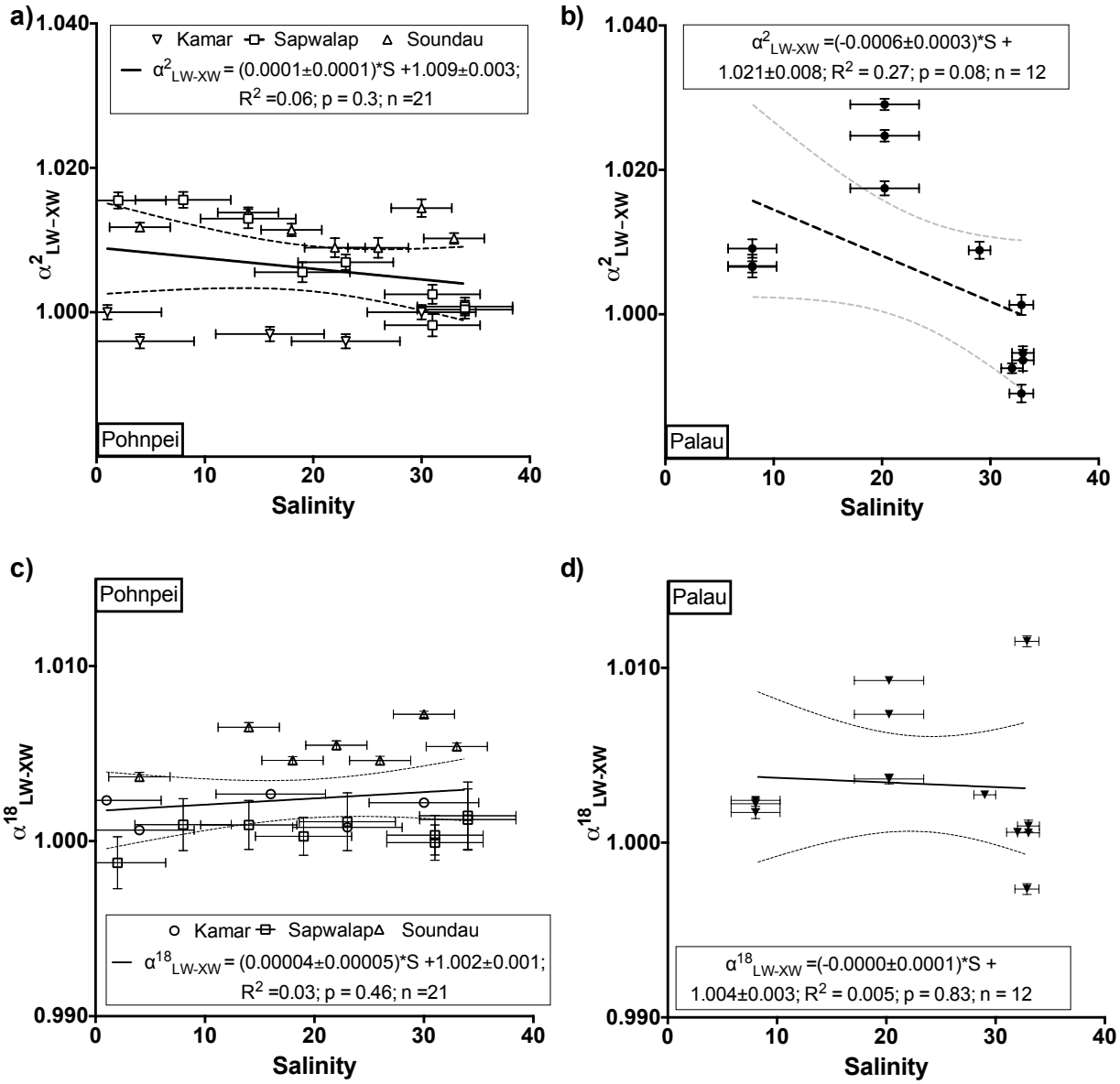

Figure 5: Relationship between salinity and fractionation factors between leaf water and xylem water. Panel a shows ^{2}H fractionation in Pohnpei estuaries and b shows ^{2}H fractionation in Palau lakes. Panels c and d show corresponding relationships for ^{18}O fractionation.

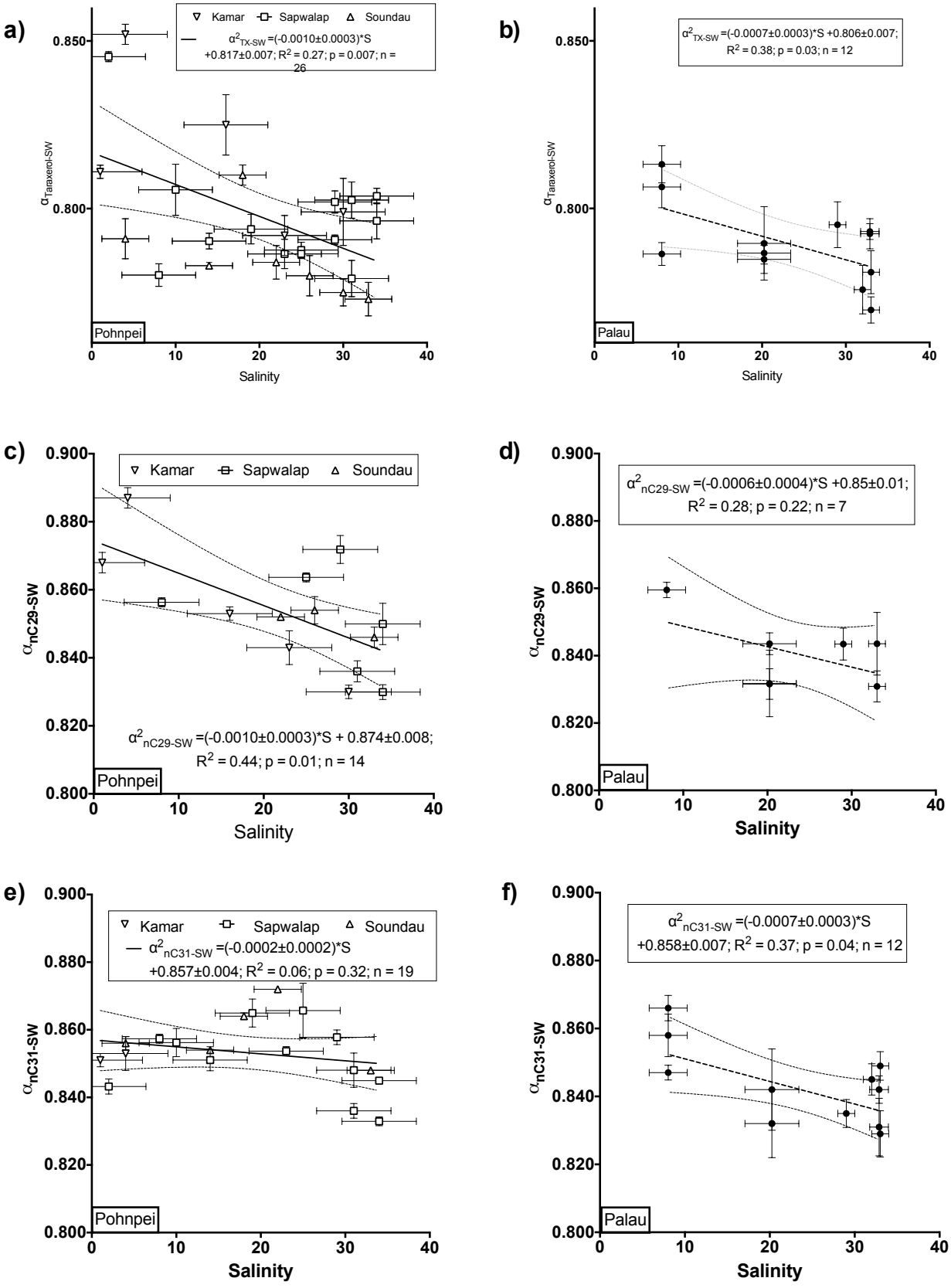
a)
Kamar
Sapwalap
Soundau
$\alpha^2_{TX\text{-}SW}$ =(-0.0010±0.0003)*S +0.817±0.007; R^2 = 0.27; p = 0.007; n = 26
$\alpha_{Taraxerol\text{-}SW}$
Pohnpei
Salinity
b)
$\alpha^2_{TX\text{-}SW}$ =(-0.0007±0.0003)*S +0.806±0.007; R^2 = 0.38; p = 0.03; n = 12
$\alpha_{Taraxerol\text{-}SW}$
Palau
Salinity
c)
Kamar
Sapwalap
Soundau
$\alpha^2_{nC29\text{-}SW}$ =(-0.0010±0.0003)*S + 0.874±0.008; R^2 = 0.44; p = 0.01; n = 14
$\alpha_{nC29\text{-}SW}$
Pohnpei
Salinity
d)
$\alpha^2_{nC29\text{-}SW}$ =(-0.0006±0.0004)*S +0.85±0.01; R^2 = 0.28; p = 0.22; n = 7
$\alpha_{nC29\text{-}SW}$
Palau
Salinity
e)
Kamar
Sapwalap
Soundau
$\alpha^2_{nC31\text{-}SW}$ =(-0.0002±0.0002)*S +0.857±0.004; R^2 = 0.06; p = 0.32; n = 19
$\alpha_{nC31\text{-}SW}$
Pohnpei
Salinity
f)
$\alpha^2_{nC31\text{-}SW}$ =(-0.0007±0.0003)*S +0.858±0.007; R^2 = 0.37; p = 0.04; n = 12
$\alpha_{nC31\text{-}SW}$
Palau
Salinity

Figure 6: Relationship between salinity and net fractionation in mangrove leaf lipids for (a) Pohnpei taraxerol, (b) Palau taraxerol, (c) Pohnpei nC$_{29}$-alkanes, (d) Palau nC$_{31}$-alkanes, (e) Pohnpei nC$_{31}$-alkanes, (f) Palau nC$_{31}$-alkanes.

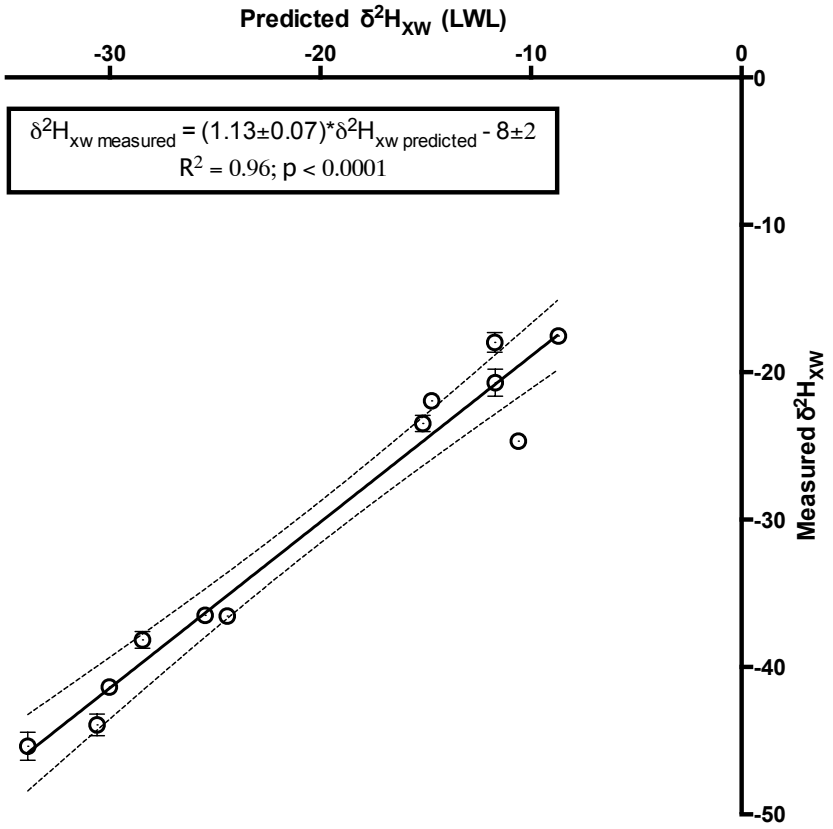

Figure 7: Measured xylem water δ^2H values from Palau *Rhizophora* plotted relative to those predicted by measured xylem water δ^{18}O values and the relationship between the two isotopes in surface water (LWL = Local Water Line).

Chapter 5: Hydrogen isotope response to changing salinity and rainfall in Australian mangroves

5.1 Abstract

Hydrogen isotope ratios ($^2H/^1H$, δ^2H) of leaf waxes covary with those in precipitation and are therefore a useful paleohydrologic proxy. Mangroves are an exception to this relationship because their δ^2H values are also influenced by salinity. The mechanisms underlying this response were investigated by measuring leaf lipid δ^2H and leaf and xylem water δ^2H and $\delta^{18}O$ from three mangrove species over 9.5 months in a subtropical Australian estuary. Net $^2H/^1H$ fractionation between surface water and leaf lipids decreased by 0.5-1.0‰ ppt^{-1} for *n*-alkanes and 0.4-0.8‰ ppt^{-1} for isoprenoids. Xylem water was ^2H depleted relative to surface water, reflecting ^2H discrimination of 4-10‰ during water uptake at all salinities and opportunistic uptake of freshwater at high salinity. However, leaf water ^2H enrichment relative to estuary water was insensitive to salinity and identical for all species. Therefore variations in leaf and xylem water δ^2H values cannot explain the salinity-dependent ^2H depletion in leaf lipids, nor the 30‰ range of leaf lipid δ^2H values among species. Biochemical changes in direct response to salt stress, such as increased compatible solute production or preferential use of stored carbohydrates, and/or the timing of lipid production and subsequent turnover rates, are the likely cause.

5.2 Introduction

Hydrogen isotopes of plant leaf waxes are a valuable source of information about the water cycle, and δ^2H_{Wax} ($\delta^2H = (^2H/^1H_{Sample})/ (^2H/^1H_{VSMOW})$) values are increasingly used as a paleoclimate proxy (*Sachse et al., 2012 and sources therein*). Over large environmental gradients, the primary cause of variability in δ^2H_{Wax} values are the δ^2H values of local

precipitation (*Sachse et al., 2004; Polissar & Freeman, 2010; Sachse et al., 2012; Tipple & Pagani, 2013*), which is directly related to environmental variables such as temperature, rainfall rate, and moisture source (*Dansgaard, 1964; Craig & Gordon, 1965; Gat, 1996*).

However, changes in $\delta^2H_{Precipitation}$ are not the only cause of variability in δ^2H_{Wax} (*Sachse et al., 2012*). Other environmental variables, including relative humidity (*Feakins & Sessions, 2010a; Douglas et al., 2012; Kahmen et al., 2013a; Kahmen et al., 2013b; Tipple et al., 2014*), plant type (*Luo et al., 2006; Smith & Freeman, 2006; Hou et al., 2007; Feakins & Sessions, 2010b*), and light levels (*Luo & Yang, 2008; Yang et al., 2009; Yang et al., 2011*) can affect the offset between δ^2H_{Wax} and δ^2H_{Water}. On tropical and subtropical coastlines where mangroves are present, salinity is another important variable that can affect this offset, which is defined by the fractionation factor $\alpha_{Lipid\text{-}SW}$ ($\alpha_{Lipid\text{-}SW} = (\delta^2H_{Lipid} +1000)/(\delta^2H_{Surface\ Water} +1000)$. Since mangroves contribute 10-15% of total organic material to global marine sediments (*Jennerjahn & Ittekkot, 2002; Dittmar et al., 2006*), and a significantly higher amount to the local coastal sediments in the low-latitude regions where they are found, it is imperative to understand this effect in order to accurately apply the δ^2H_{Lipid} proxy in tropical coastal sediments.

Previous work has investigated the relationship between salinity and apparent isotope fractionation in mangroves growing along spatial salinity gradients at a single point in time (*Ladd & Sachs, 2012; Ladd & Sachs, in prep*). In the Brisbane River, $\alpha_{Lipid\text{-}SW}$ decreased by 1.5±0.3‰ PSU^{-1} for both n-C_{31}- and n-C_{33}-alkanes produced by *Avicennia marina* (gray mangroves) growing along a salinity gradient of 6-35 (*Ladd & Sachs, 2012*). Subsequently, a 0.9±0.2‰ PSU^{-1} decrease in $\alpha_{Lipid\text{-}SW}$ was observed for the pentacyclic tripenoid taraxerol produced by *Rhizophora* spp. (red mangroves) growing along three Micronesian estuaries and

four marine lakes in Palau. For *n*-alkanes produced by the same plants, $\alpha_{Lipid\text{-}SW}$ decreased by1.0±0.3‰ PSU^{-1} (*Ladd & Sachs, in prep*).

The main goal of this study was to investigate how changes in apparent isotope fractionation manifest themselves throughout the year by studying mangroves at a single location with highly seasonal and episodic precipitation. Similar time series of temperate plants have indicated that leaf wax isotopes reflect the environmental conditions during leaf flush (*Sachse et al., 2010; Kahmen et al., 2011; Tipple et al., 2013*), and are thus more likely to reflect spring conditions than the average of the entire summer growth period. Evergreen tropical plants, such as the mangroves studied here, do not have such a well-defined growth period and produce new leaves throughout the year (*Wium-Anderse n& Christensen, 1978; Duke et al., 1984; Coupland et al., 2005*). Mangrove leaves can remain on the tree for up to 18 months (*Wium-Andersen & Christensen, 1978; Coupland et al., 2005*), and their lipids may thus represent aggregate conditions throughout the year.

Another major goal of this study was to better understand the mechanism that results in greater net discrimination against ^{2}H during the synthesis of mangrove lipids at high salinity. It has previously been hypothesized that increased fractionation at high salinity could be due to (1) increased discrimination against ^{2}H during water uptake by roots, (2) increased production of compatible solutes, resulting in different allocations of H within the cell, and (3) salt on the leaf surface, which increases the relative humidity along the leaf boundary layer and decreases the vapor pressure difference between the interior and exterior of the leaf (*Ladd & Sachs, 2012*). This third mechanism should be more pronounced for mangroves that secrete salt, such as *Avicennia* and *Aegicerus,* than for mangroves that lack this function, such as *Rhizophora*.

Analyzing the isotopic composition of intermediate water pools such as xylem water (δ^2H_{XW}) and leaf water (δ^2H_{LW}) is an effective method to assess causes of net fractionation during lipid synthesis (*Feakins & Sessions, 2010a; Romero & Feakins, 2011; Kahmen et al., 2013b; Tipple et al., 2013; Ladd & Sachs, in prep*). This study included weekly measurements of these values from adjacent salt-secreting and non-secreting trees over a 9.5-month period to test the relative likelihood of each of the three hypotheses summarized above.

5.3 Methods

5.3.1 Study site and sample collection

Mobbs Bay (S 28°53.068', E 153°34.211') is located at the mouth of the Richmond River in South Ballina, New South Wales, Australia (**Figure 1**). South Ballina has a humid subtropical climate, with mean maximum temperatures ranging from 19.9°C in July to 28.2°C in January (*Australian Bureau of Meteorology*). Mean annual rainfall is 1768.6 mm/year, with a wet season from January-June and a dry season from July-December. On average, March is the wettest month, with an average of 214.3 mm/month, and September is the driest month with 61.3 mm/month (*Australian Bureau of Meteorology*).

The study period began on October 1, 2012 and lasted until July 17, 2013. During weekly site visits, surface water salinity (1 cm depth) was measured with a refractometer (VeeGee Scientific, Kirkland, WA) with accuracy of ±1 ppt. Salinity varied from 36 ppt on October 24, 2012 to 1 ppt on March 6th, 2013. 4 mL of water was collected from 1 cm below the surface for isotopic analysis.

One *Avicennia marina* individual and one *Rhizophora stylosa* individual growing adjacent to one another on the fringe of the mangrove swamp were selected for study. In March

2013, one *Aegiceras corniculatum* individual was added to the study. The roots of all three trees were fully flooded at high tide. Each week, two sun-exposed branches were collected from each tree. One or two leaves from each branch were stored in an 11 mL glass screw cap vial for leaf water analysis. The remaining leaves from each branch were stored in a Whirlpak plastic bag for lipid analysis. A ~5 cm length of well-suberized stem on each branch was stored in an 11 mL glass screw cap vial for xylem water analysis. All samples were stored on ice and transferred to a -20°C freezer, where they remained prior to analysis.

Rainwater samples were collected regularly throughout the study period in East Ballina, NSW (3.5 km NNE along the coast from Mobbs Bay at S 28°51.623', E 153°35.633'; **Figure 1**). 4 mL of rainwater collected from a rooftop of a single story dwelling (~3-5 m elevation) and transferred to ground level through a downspout was collected once or twice per rain event and stored in a glass screw cap vial sealed with electrical tape.

5.3.2 Leaf and xylem water extraction

Leaf and xylem water samples were cryogenically extracted on a vacuum line in the Agricultural Sciences Institute at ETH-Zurich. Samples were heated to 80°C, while attached to a glass U-tube that was submerged in liquid Nitrogen. The sealed line was kept at a pressure below 60 mTorr for at least two hours. After this time, the U-tubes were removed from the liquid N_2, sealed, and the collected water was allowed to thaw. The water was then filtered through a 0.45 μm PTFE filter to remove any particulate material and transferred to 2mL screw cap vials, which were sealed with Parafilm until analysis.

5.3.3 Water isotope measurements

Leaf and xylem water samples were analyzed by a Total Combustion Elemental Analyzer (TC/EA) coupled to a Delta V Isotope Ratio Mass Spectrometer (IRMS; Thermo Scientific, Waltham, MA) in the Sustainable Land Use Group in the Botany Department of the University of Basel, Switzerland. Each sample and standard was injected six times in sequence. The first three injections of each sample were discarded in order to avoid memory effects. Thermo Isodat 3.0 software normalized raw isotopic ratios to the VSMOW (Vienna Standard Mean Ocean Water) scale using pulses of reference gas before and after the sample injection. Additionally, two in-house water standards of known isotopic composition were analyzed after every six samples throughout each sequence. The slope and intercept of the linear regression between the measured and known δ values of these samples was used to further normalize sample δ^2H and $\delta^{18}O$ values and to correct for any instrumental drift throughout the course of the sequence. An additional laboratory standard was analyzed after every 12 samples. This standard was not used for any of the isotopic corrections, but was used to assess instrument performance over time and the accuracy of the isotope corrections. Average absolute offset from the known value of this standard was 1.0‰ for δ^2H measurements and 0.2‰ for $\delta^{18}O$ measurements. Average precision of triplicate sample injections was 0.9‰ for δ^2H measurements and 0.2‰ for $\delta^{18}O$ measurements**.**

Surface water and rainwater δ^2H and $\delta^{18}O$ values were measured by a Picarro Cavity Ring Down Spectroscopy (CRDS) L2130i Water Isotope Analyzer at the University of Washington. Measurements were normalized to the VSMOW scale using three laboratory standards of known isotopic composition. The suite of standards was analyzed between every six samples throughout the run. All samples and standards were injected six times, and the first three

measurements were discarded in order to avoid memory effects. Average precision of triplicate analyses was 0.2‰ for δ^2H measurements and 0.05‰ for $\delta^{18}O$ measurements**.**

5.3.4 Lipid extraction and purification

Four intact whole leaves from each week (2 from each branch sampled) were selected for analysis and treated as a single sample. Leaves were rinsed with DI water to remove debris, then cut into ~0.5 cm pieces using solvent-washed scissors prior to freeze-drying. Dry leaves were ground with a solvent-cleaned mortar and pestle, and lipids from ~0.5 g of dry leaf were extracted using accelerated solvent extraction (ASE-200, Dionex Corp., Sunnyvale, CA, USA) with 9:1 Dichloromethane:Methanol (DCM:MeOH) at 100 °C and 1500 psi for 3 x 5 min static cycles. The resulting total lipid extract (TLE) was evaporated to dryness under a stream of N_2 on a Turbovap system (Caliper, Hopkinton, MA, USA).

An aliquot of the TLE (~10 mg) was purified using silica gel column chromatography. The stationary phase was 1g of Si gel (5% deactivated with water). Hydrocarbons were eluted with 8 mL hexane, sterols, alcohols and triterpenols with 8 mL 4:1 Hexane:Ethyl Acetate and remaining compounds with 4 mL MeOH.

The alcohol fraction was acetylated at 70°C for 30 minutes with 25 μL of acetic anhydride of known δ^2H composition in 25 μL of pyridine. The alcohol fraction of *R. stylosa* leaves of all species was dominated by taraxerol, with relatively small amounts of β-sitosterol, β-amyrin, and *n*-alkanols. Lupeol was the most abundant compound in the alcohol fraction of *A. marina* leaves, which also contained significant amounts of α-amyrin, β-amyrin, β-sitosterol, and stigmasterol. Although they were not the most abundant alcohols, β-sitosterol and stigmasterol were the best resolved compounds by GC, and were thus targeted for isotopic analyses.

Stigmastanol was the most abundant compound in the alcohol fraction of *A. corniculatum*. Lipids in the alcohol fraction were quantified by Gas Chromatography – Mass Spectrometry (GC-MS) using an Agilent (Santa Clara, CA, USA) 6890N gas chromatograph equipped with an Agilent 7683 autosampler, a split-splitless injector operated in splitless mode and an Agilent VF-17ms capillary column (60 m X 0.32 mm X 0.25 μm) interfaced to an Agilent 5975 quadrupole mass selective detector. The oven temperature was increased from 110°C to 320°C at 4°C/min, then held at 320°C for 10 minutes. Quantification of target compounds was performed by comparing integrated peak areas with a known amount of 5α-cholestane, added to the sample just prior to GC-MS analysis.

The hydrocarbon fraction of leaves of all species was dominated by odd-numbered *n*-alkanes, with chain lengths ranging from C_{27}-C_{33}. In *R. stylosa* and *A. corniculatum* leaves, nC_{29} was the most abundant *n*-alkane, followed by nC_{31}. In *A. marina* leaves nC_{31} and nC_{33} were the most abundant alkanes. The *n*-alkanes were quantified with a GC instrument equipped with flame ionization detection (GC-FID). An Agilent 6890N gas chromatograph equipped with an Agilent 7683 autosampler, programmable temperature vaporization inlet (PTV) operated in splitless mode and an Agilent DB-5ms column (60 m x 0.32 mm x 0.25 μm) was used with He as carrier gas (2.4 mL/min). The oven temperature was increased from 60 to 150°C at 15°C/min, then at 6°C/min to 320°C (held 28 min). Quantification of *n*-alkanes was performed by comparing integrated peak areas with a known amount of nC_{37}-alkane, added to the sample just prior to GC-FID analysis.

These quantifications were used to determine an appropriate amount of solvent in which to dissolve the sample so that it would produce a peak of ~20V*s when analyzed by Gas Chromatrography – Isotope Ratio Mass Spectrometry (GC-IRMS).

5.3.5 Lipid δ^2H analyses

The δ^2H values of individual lipids were measured by GC-IRMS on a Thermo DELTA V PLUS system (Thermo Scientific, Waltham, MA, USA). The gas chromatograph (Trace Ultra, Thermo) was equipped with a split-splitless injector operated in splitless mode at 320°C, a TRIPLUS autosampler (Thermo Scientific), and a VF-17ms capillary column (60 m x 0.25 mm x 0.25 μm, Agilent). For taraxerol and stigmastanol analyses, the GC was heated from 120°C to 260°C at 20 °C/min, then at 1°C/min to 300°C, at 20 °C/min to 325°C and then held at 325°C for 20 min. For β-sitosterol and stigmansterol from *A. marina* the GC was heated from 120°C to 260°C at 20°C/min, then at 1°C/min to 300°C, at 20 °C/min to 325°C and then held at 325°C for 40 min. For *n*-alkane analyses, the GC was heated from 120°C to 250°C at 20°C/min, then at 6°C/min to 325°C and then held at 325°C for 12 min. Helium was used as the carrier gas at a constant flow of 1.1 mL/min. Compounds were pyrolyzed in a ceramic reactor at 1400°C. 1 μL of sample was injected along with 0.5 μL of a mix of *n*-alkanes of known isotopic composition (A. Schimmelmann, Indiana University, Bloomington, Indiana). For isoprenoid analyses, this mix included nC$_{26}$-, nC$_{28}$-, nC$_{32}$-, nC$_{34}$- and nC$_{41}$-alkanes. For *n*-alkane analyses, the co-injection standards were nC$_{21}$ and nC$_{23}$. At the beginning and the end of the sequence, as well as after every 4-6 sample injections, a vial of additional *n*-alkane standards of known isotopic composition was analyzed with the co-injection standards, in place of a sample. For triterpenoid sequences, this external standard was nC$_{38}$, which elutes within 1 minute of taraxerol and β-sitosterol under these GC conditions. For *n*-alkane sequences, nC$_{28}$-, nC$_{32}$- and nC$_{34}$-alkanes were used as external standards.

Thermo ISODAT software V.2.5 was used to control instrumentation and calculate δ^2H values. The slope and intercept of the relationship between measured and known δ^2H values of the *n*-alkane standards was used to correct lipid δ^2H values for instrument bias. Offsets between corrected and known standard δ^2H values were used to further correct for drift, retention time, and peak area for each sequence. Each sample was measured in triplicate. Reported analytical uncertainties are the standard error in the mean of the isotope standards, or the standard deviation of the triplicate sample analyses (whichever value was higher). The H_{3+} factor was determined each day using pulses of a reference gas of varying heights and averaged 1.7‰.

5.4 Results

5.4.1 Relationship between salinity and $\delta^2H/\delta^{18}O$ values of different water pools

There was an 84‰ range in $\delta^2H_{Precipitaion}$ values throughout the study period, from 17.8 ± 0.2‰ to -67.3 ± 0.2‰ (**Table 1**). Values of $\delta^{18}O_{Precipitation}$ varied by ~11‰ throughout the study period, from 0.21 ± 0.05‰ to -10.97 ± 0.05‰ (**Table 1**). Lighter rainwater isotopes corresponded to periods of heavier rainfall in the summer and autumn, with heavier rainwater isotopes predominant in the drier fall. Surface water isotopes in Mobbs Bay varied between -29 ± 0.2‰ and 6 ± 0.2‰ for δ^2H and -5.15 ± 0.05‰ and 0.48 ± 0.05‰ for $\delta^{18}O$, changing in concert with rain events, with lower values during wet episodes and higher values during dry periods (**Figure 2**).

Salinity and water isotopes at the study site were well correlated throughout the year (**Figure 3;** $R^2 = 0.76$ and $p < 0.0001$ for δ^2H; $R^2 = 0.85$ and $p < 0.0001$ for $\delta^{18}O$). A 0.77 ± 0.07‰ increase in δ^2H_{SW} (**Figure 3a**) and 0.14 ± 0.01‰ increase in $\delta^{18}O_{SW}$ (**Figure 3b**) was associated with a 1 ppt increase in salinity.

Xylem water isotopes in *R. stylosa* and *A. marina* were positively correlated with salinity as well, but with significantly shallower slopes than the surface water **(Figure 3**). For *R. stylosa*, δ^2H_{XW} increased by 0.45 ± 0.09‰ ppt^{-1} ($R^2 = 0.39$ and $p < 0.0001$) and $\delta^{18}O_{XW}$ increased by 0.08 ± 0.02‰ ppt^{-1} ($R^2 = 0.40$ and $p < 0.0001$). For *A. marina,* a 1 ppt increase in salinity was associated with a 0.43 ± 0.08‰ increase in δ^2H_{XW} ($R^2 = 0.44$ and $p < 0.0001$) and with a 0.07 ± 0.02‰ increase in $\delta^{18}O_{XW}$ ($R^2 = 0.36$ and $p < 0.0001$). Xylem water isotopes and salinity were not correlated in *A. corniculatum*, which was only sampled for the last 14 weeks of the study period ($p = 0.79$ for δ^2H_{XW} and 0.82 for $\delta^{18}O_{XW}$).

The apparent fractionation factors between surface water and xylem water, $\alpha^2_{XW\text{-}SW}$ and $\alpha^{18}_{XW\text{-}SW}$, were negatively correlated with salinity for *R. stylosa* and *A. marina* (**Figure 4**). For *R. stylosa*, $\alpha^2_{XW\text{-}SW}$ decreased by 0.3 ± 0.1‰ ppt^{-1} ($R^2 = 0.20$ and $p = 0.005$) and $\alpha^{18}_{XW\text{-}SW}$ decreased by 0.06 ± 0.02‰ ppt^{-1} ($R^2 = 0.23$ and $p = 0.002$). For *A. marina*, $\alpha^2_{XW\text{-}SW}$ decreased by 0.3 ± 0.1‰ ppt ($R^2 = 0.28$ and $p = 0.0006$) and $\alpha^{18}_{XW\text{-}SW}$ decreased by 0.06 ± 0.02‰ ($R^2 = 0.23$ and $p = 0.002$). Salinity was not significantly correlated with either $\alpha^2_{XW\text{-}SW}$ or $\alpha^{18}_{XW\text{-}SW}$ in *A. corniculatum* ($p = 0.14$ for $\alpha^2_{XW\text{-}SW}$ and 0.12 for $\alpha^{18}_{XW\text{-}SW}$).

Leaf water isotopes were positively correlated with salinity in *R. stylosa* and *A. marina*, with slopes that were significantly steeper than the relationship between salinity and xylem water, but statistically indistinguishable from the relationship between salinity and surface water isotopes (**Figure 3**). For *R. stylosa*, a 1ppt increase in salinity was associated with a 0.9 ± 0.2‰ increase in δ^2H_{LW} ($R^2 = 0.35$ and $p = 0.0001$) and with a 0.22 ± 0.07‰ increase in $\delta^{18}O_{LW}$ ($R^2 = 0.25$ and $p = 0.002$). For *A. marina,* a 1ppt increase in salinity was associated with a 0.7 ± 0.2‰ increase in δ^2H_{LW} ($R^2 = 0.28$ and $p = 0.0006$) and with a 0.16 ± 0.06‰ increase in $\delta^{18}O_{LW}$ ($R^2 =$

0.17 and p = 0.01). Leaf water isotopes in *A. corniculatum* were not correlated with salinity (p = 0.73 for δ^2H_{LW} and 0.74 for $\delta^{18}O_{LW}$).

No significant correlations existed between salinity and the net isotope fractionation between surface water and leaf water, $\alpha^2_{LW\text{-}SW}$ and $\alpha^{18}_{LW\text{-}SW}$ in any species, (**Figures 5a-b**) Likewise, no significant correlations existed between salinity and the evaporative enrichment of leaf water relative to xylem water, $\alpha^2_{LW\text{-}XW}$ and $\alpha^{18}_{LW\text{-}XW}$ (**Figures 5c-d**).

5.4.2 Temporal variability of lipid δ^2H

Leaf lipid δ^2H values varied throughout the year, and differed significantly between *R. stylosa* and the other two species (**Figure 2**). For *R. stylosa*, *n*C_{29}-alkane δ^2H values ranged from -138‰ to -108‰, and averaged -118 ± 8‰ (1σ). Insufficient lipid quantities precluded analysis in some samples, but from the 25 weeks where δ^2H values of *n*C_{31}-alkane were measured, it varied from -141‰ to -115‰ and averaged -128 ± 7‰. The pentacyclic triterpenoid measured from this plant, taraxerol, had δ^2H values that varied from -192‰ to -154‰, with an average value of -173 ± 10‰.

For *A. marina,* *n*C_{31}-alkane δ^2H values varied from -169‰ to -143‰ and averaged -154 ± 6‰ (**Figure 2**). The δ^2H values of *n*C_{33}-alkanes from this plant ranged from -180‰ to -142‰ with an average value of -158 ± 10‰. Amongst sterols from *A. marina*, δ^2H values of β-sitosterol varied from -218‰ to -185‰, averaging -200 ± 7‰, while for stigmasterol, δ^2H values ranged from -224‰ to -195‰, with an average of -207 ± 7‰.

Finally, *n*C_{29}-alkane δ^2H values from *A. corniculatum*, which were only measured from March 28th onwards, varied from -169‰ to -146‰, and averaged -163 ± 8‰ (**Figure 2**). The *n*C_{31}-alkane δ^2H values from this plant, which were measured for only 11 weeks, ranged from -

168‰ to -148‰, averaging -162 ± 5‰. Stigmastanol δ^2H values from *A. corniculatum* ranged from -242‰ to -218‰, with an average of -230 ± 7‰.

The apparent fractionation factor between surface water and leaf lipids ($\alpha_{Lipid\text{-}SW}$) was negatively correlated with salinity for all lipids from *A. marina* and *R. stylosa*, and for *n*C_{29}-alkane from *A. corniculatum* (**Figure 6**). There was no significant correlation for for *A. corniculatum n*C_{31}-alkane ($p = 0.21$) or stigmastanol ($p = 0.39$) (**Figure 6**). Significant differences in the y-intercept of these linear relationships existed ($p < 0.0001$), but the slopes were not significantly different ($p = 0.10$).

5.5 Discussion

5.5.1 Fractionation during water uptake and transpiration by mangroves

Mangroves and other woody halophytes discriminate against ^2H by as much as 11‰ during water uptake by roots (*Lin & Sternberg, 1993; Ellsworth & Williams, 2007*). They have not been observed to discriminate against ^{18}O, facilitating the use of $\delta^{18}O_{XW}$ in determining the source of environmental water used by mangroves (*Lin & Sternberg, 1994; Ewe et al., 2007; Lambs et al., 2008; Wei et al., 2013*). Assuming the $\delta^{18}O$ values of xylem water from mangroves in Mobbs Bay represent the isotopic composition of the their water source, it seems that surface (-1 cm) water was not the only water source for these trees, since $\delta^{18}O_{XW}$ were usually 2-3‰ depleted in ^{18}O relative to surface water at salinity > ~20ppt (**Figure 3a**).

A negative correlation between salinity and $\alpha^{18}_{XW\text{-}SW}$ implies that the studied mangroves became less dependent on surface water as salinity of that water increased (**Figure 4a**). There was no statistical difference between $\delta^{18}O_{XW}$ and $\delta^{18}O_{SW}$ at salinities below ~20 ppt, but an increasing offset at higher salinities (**Figures 3a, 4a**). The selective use of fresher water sources

at high salinities has been documented previously (*Ewe et al., 2007; Lambs et al., 2008; Wei et al., 2013*) and is consistent with increasingly negative $\delta^{18}O_{XW}$ values of xylem water as salinity increased in Mobbs Bay mangroves.

^{2}H depletion in the xylem water from *R. stylosa* and *A. marina* relative to Mobbs Bay surface water was observed at all salinities, even at times when $\delta^{18}O_{XW}$ values were not depleted relative to surface water (**Figures 3b, 4b**). Furthermore, $\delta^{2}H_{XW}$ values were lower than those predicted from $\delta^{18}O_{XW}$ by the local meteoric water line (**Figure 7**). Discrimination against ^{2}H during water uptake by mangrove roots has been previously reported and is a likely cause for low $\delta^{2}H_{XW}$ values in Mobbs Bay mangroves relative to $\delta^{2}H_{SW}$ (*Lin & Sternberg, 1993; Ellsworth & Williams, 2007; Ladd & Sachs, in prep*). The magnitude of this effect can be determined from the relationships between $\alpha_{XW\text{-}SW}$ and salinity for each isotope. For both *A. marina* and *R. stylosa*, the y-intercept of the regression between $\alpha^{18}_{XW\text{-}SW}$ and salinity is 1.000 (**Figure 4a**), indicating that when surface water is fresh, it is the primary water source for the mangroves. The y-intercepts for the linear regression between $\alpha^{2}_{XW\text{-}SW}$ and salinity are 0.993 ± 0.003 for *R. stylosa* and 0.994 ± 0.002 for *A. marina* (**Figure 4b**). ^{2}H discrimination during water uptake is thus 7 ± 3‰ by *R. stylosa* and 6 ± 2‰ for *A. marina*. These values compare favorably with published reports of 2 - 11‰ ^{2}H depletion in the xylem water of mangroves and other woody halophytes (*Lin & Sternberg, 1993; Ellsworth & Williams, 2007*).

While the xylem water isotope values are informative about the water pools accessed by mangroves growing in Mobbs Bay, and support the past observation that mangroves discriminate against ^{2}H during water uptake, they cannot explain the inverse relationship between salinity and $\alpha_{Lipid\text{-}SW}$ observed here and elsewhere (**Figure 6;** *Ladd & Sachs, 2012; Ladd & Sachs, in prep*). This is because the leaf water isotopes track surface water isotopes much better than xylem water

isotopes (**Figures 3, 5**), and leaf water is the source of at least 96% of the hydrogen for lipids synthesized in the leaves of dicots (*Kahmen et al., 2013b*). In fact, there is no salinity dependence for either $\alpha^{2}_{LW\text{-}SW}$ or $\alpha^{18}_{LW\text{-}SW}$ in any of the three species studied (**Figures 5a-b**). This result suggests that environmental variables such as relative humidity and the isotopic composition of ambient water vapor have a more significant impact on leaf water isotopes in mangroves than the isotopic composition of xylem water.

5.5.2 Differences in biosynthetic fractionation among different species of mangroves

In contrast to the similarity in xylem water and leaf water isotopes among the three species, there were significant differences in the $\delta^{2}H_{Lipid}$ values (**Figure 2**). In particular, the $\delta^{2}H$ values of n-C_{31}-alkane, the one compound that was produced in sufficient abundance for analysis by all three species, was consistently enriched in *R. stylosa* relative to the other two species by ~25-30‰ (**Figure 2**). This interspecies variability highlights a potential complication of using *n*-alkane $\delta^{2}H$ values to reconstruct past hydroclimate, as a large shift in sedimentary n-C_{31}-alkane $\delta^{2}H$ values in a setting such as Mobbs Bay could reflect a change in the dominant mangrove species rather than a change in hydrological conditions.

Significant interspecies $\delta^{2}H$ values were also observed in isoprenoidal lipids. Taraxerol from *R. stylosa* was enriched on average by ~30‰ relative to β-sitosterol and stigmasterol from *A. marina* and by ~60‰ relative to stigmastanol from *A. corniculatum* (**Figure 2**). These differences could be influenced by differences in the biosynthetic pathways from which pentacyclic triterpenols and sterols are produced. For example, pentacyclic triterpenols produced by *Daucus carota* are enriched by 30-60‰ relative to sterols produced by the same plant (*Sessions et al., 1999*), and the pentacyclic triterpenol lupenol is enriched by 30-40 ‰ relative to

β-sitosterol produced by *Spartina alterniflora* (*Sessions, 2006*). The observation that the most enriched nC$_{31}$-alkane is from the plant that also produced the most enriched isoprenoid analyzed may therefore be a coincidence related to the fact that a pentacyclic triterpenol was analyzed from *R. stylosa*, while sterols and a stanol were measured from the other plants.

Differences in biosynthetic fractionation among different plants growing at the same site of up to 70‰ have been observed previously (*Feakins & Sessions, 2010a; Feakins & Sessions, 2010b; Romero & Feakins, 2011; Eley et al., 2013*). It is unlikely that these differences in biosynthetic fractionation are due to changes in the isotopic fractionation associated with individual biosynthetic steps, which are typically consistent with temperature and reaction rate (*Schmidt et al., 2003; Wang et al., 2009*). Rather, variability in $\alpha_{\text{Lipid-LW}}$ is more likely to be caused either by changes in the source of carbohydrate precursors for lipids, or by different timing of lipid production.

Long-chain *n*-alkanes, such as the leaf waxes studied here, are produced by successively adding 2-carbon acetyl groups to a carbon chain (*Kolattukudy, 1965; Samuels et al., 2008*). These acetyl groups are produced from simple sugars, and are either the products of new photosynthesis (current photosynthate) or produced from stored carbohydrates. Sugars produced from stored carbohydrates are enriched in ^{2}H relative to current photosynthate (*Yakir & DeNiro, 1990; Yakir, 1992; Roden & Ehlringer, 2000*), and it seems likely that lipids produced from a greater proportion of stored carbohydrates are also enriched in ^{2}H. Leaf wax δ^2H values from plants that have relatively high respiration to photosynthesis ratios are enriched by as much as 80‰ relative to those that have more active photosynthesis (*Sessions et al., 2006; Cormier et al., 2014*). If lipid synthesis in *R. stylosa* is more reliant on stored carbohydrates than in the other two species, that could account for the observed differences in δ^2H among species. *A. marina* is

more salt tolerant than *R. stylosa* (*Clough, 1984*; *Naidoo, 1985*; *Clough & Sim, 1989*), and consistently has higher photosynthetic rates than *R. stylosa* growing at the same site (*Clough & Sim,* 1989). *A. marina* may therefore have more primary photosynthate available for leaf wax synthesis than *R. stylosa*.

The ^{2}H composition of precursor carbohydrates in each plant could also be affected by the composition and abundance of compatible solutes. In order to maintain favorable water potentials all of the mangroves studied here produce compatible solutes (*Clough, 1985; Ashihara et al., 1997; Hibino et al., 2001; Parida & Jha, 2010*). *A. marina* produces the amino acids asparagine and glycine betaine as its main compatible solutes (*Ashihara et al., 1997; Hibino et al., 2001*) while *A. corniculatum* produces aspartic acid and alanine (*Datta & Ghosh, 2003*). *R. stylosa*, on the other hand, primarily uses the soluble carbohydrates pinitol and manitol (*Hibino et al., 2001*). Because amino acids are relatively enriched in ^{2}H compared to soluble carbohydrates (*Schmidt et al., 2003*) it is possible that the use of amino acid-based compatible solutes in *A. marina* and *A. corniculatum* results in a relative depletion of the hydrogen pool available for lipid synthesis in those two species as compared to *R. stylosa*.

Another possibility is that differences in the timing of lipid production account for the differences in $\delta^{2}H$ values among species. Differences in timing include production of lipids at different points in the diurnal cycle and during different seasons, as well as different lipid residence times within the leaf. All of the leaf water measurements made in this study were from leaves collected in the early-to-mid afternoon, in order to capture the maximum diurnal enrichment of leaf water. However, leaf water isotopes fluctuate throughout the day with changes in relative humidity, temperature and stomatal conductance (*Kahmen et al., 2008; Ferrio et al., 2009*). Relatively ^{2}H-enriched leaf lipids in *R. stylosa* could be explained if it fixes

a larger proportion of carbon during the afternoon than *A. marina* or *A. corniculatum*, thereby incorporating the most ^{2}H-enriched leaf water of the day, while the other species fix a larger fraction of carbon in the morning and/or evening.

Differences in daily water use patterns and photosynthetic activity have been observed for adjacent *R. stylosa* and *A. marina* growing on North Stradbroke Island, ~200 km north of Mobbs Bay on the east coast of Australia (*Vandegehuchte et al., 2014*). Stomatal resistance in *R. stylosa* there was relatively constant throughout daylight hours, while *A. marina* had much higher stomatal resistance rates during the afternoon than in the morning or evening (*Vandegehuchte et al., 2014*). This pattern is consistent with *A. marina* being more photosynthetically active during cooler parts of the day, when leaf water should be less enriched, which would result in the depleted leaf waxes observed in this plant.

Another possibility is that lipids may be produced at different seasons by different species. Temperate plants typically produce their leaf waxes soon after leaf flush in the spring (*Sachse et al., 2010; Kahmen et al., 2011; Tipple et al., 2013).* Mangroves, and other tropical evergreen plants, are not limited to leaf production during one season, and produce leaves throughout the year (*Wium-Andersen & Christensen, 1978; Duke et al., 1984; Coupland et al., 2005*). Afternoon $\delta^{2}H_{LW}$ values at Mobbs Bay varied by more than 60‰ throughout the year in both *A. marina* and *R. stylosa* (**Figure 3**). If *R. stylosa* produced relatively more leaf lipids during drier times of year, when $\delta^{2}H_{LW}$ values are high, it would be expected to have relatively ^{2}H-enriched lipids compared to *A. marina* and *A. corniculatum*.

In studies of leaf longevity from Phuket, Thailand, and Darwin, in the Northern Territories of Australia, *Rhizophora* leaves had a longer average longevity than *A. marina* leaves (*Wium-Andersen & Christensen, 1978; Coupland et al., 2005*). *Rhizophora* leaves persisted on

average for 11.2 ± 0.2 months, as compared to *A. marina* leaves that lasted an average of 6.3 ± 0.1 months. If *R. stylosa* has the longest leaf residence time among Mobbs Bay mangroves, its δ^2H_{Lipid} values might be more reflective of average conditions in Mobbs Bay throughout the year, while lipids in *A. marina* leaves would be more responsive to changing environmental conditions.

Likewise, lipid turnover in leaves that have already been produced could account for differences among species. While most leaf waxes are produced soon after leaf flush, new waxes can form on mature leaves that have been abraded by wind, rain, or fauna, changing the overall δ^2H_{Wax} values (*Sachse et al., 2009; Gao et al., 2012*). If *A. marina* and *A. corniculatum* leaf waxes are more susceptible to abrasion during rain events, and are subsequently regenerated using the relatively fresher, isotopically depleted water associated with those storms, it would result in their lipids being less enriched than those of *R. stylosa*. Lipid turnover rates have not been investigated for sterols and triterpenols, which are not part of the epicuticular wax, but are located in sub-epidermal parts of the leaf. These compounds are likely less susceptible to abrasion than waxes, but may be replaced for other reasons over the leaf's lifespan, contributing to differences in their isotopic composition.

5.5.3 Relationship between salinity and net isotopic fractionation in mangrove lipids

Net fractionation during mangrove lipid synthesis, $\alpha_{Lipid\text{-}SW}$, was inversely related to salinity (**Figure 6**), as has previously been observed for *A. marina* growing along the Brisbane River (*Ladd & Sachs, 2012*) and for *Rhizophora* spp. growing along estuaries in Micronesia and around marine lakes in Palau (*Ladd & Sachs, in prep*). Part of this dependence was driven by changes in δ^2H_{SW} values, which were large and positively correlated with salinity (**Figure 3**),

making it more appropriate to look at lipid δ^2H values in order to assess changes in lipid composition due to variable salinity (**Figure 2**). Changes in δ^2H_{SW} alone do not explain the decreases in $\alpha_{Lipid\text{-}SW}$ at higher salinities, as δ^2H_{Lipid} values decreased for 7 of the 10 lipids studied here even as δ^2H_{SW} values increased **(Figure 2**). These results contribute to the growing body of evidence that mangroves discriminate more strongly against ^2H during lipid synthesis as salinity increases, regardless of species or local climate.

The results of this study make it possible to reevaluate the hypotheses initially proposed to explain the inverse relationship between salinity and net isotopic fractionation in mangroves by Ladd and Sachs (*2012*). One hypothesis was that discrimination against ^2H during water uptake increased with increasing salinity. The data presented here do not support this hypothesis. While there was discrimination against ^2H during water uptake by all three species, there was no systematic change in the magnitude of that fractionation as a function of salinity (**Figure 7**). The decrease in $\alpha^2_{XW\text{-}SW}$ as Mobbs Bay salinity increased was associated with a decrease in $\alpha^{18}_{XW\text{-}SW}$ (**Figure 4**), which has not been observed to be sensitive to water isotope fractionation by roots (*Lin & Sternberg, 1993; Ellsworth & Williams, 2007*), and is thus more plausibly explained by the opportunistic utilization of fresher, and by extension more isotopically depleted, water than that at 1 cm depth in Mobbs Bay.

The utilization of isotopically depleted, fresher water sources at higher salinity cannot explain the inverse correlation between salinity and $\alpha^2_{Lipid\text{-}SW}$ however, because the isotopic depletion in the xylem water is not observed in the leaf water from which leaf lipids are synthesized (**Figure 5)** (*Kahmen et al., 2013b*). Since there is no change in $\alpha^2_{LW\text{-}SW}$ with salinity, the decrease in δ^2H_{XW} values relative to δ^2H_{SW} values, while interesting from the perspective of

salinity tolerance and water use by mangroves, becomes almost irrelevant to the discussion of the mechanism responsible for the inverse relationship between salinity and $\alpha_{Lipid\text{-}SW}$.

Likewise, the fact that there are no systematic decreases in net leaf water enrichment with increasing salinity argues against the third hypothesis proposed by Ladd and Sachs (*2012*), which is based on increased salt secretion by *A. marina* at higher salinity. We hypothesized that hydration of salts on the surfaces of leaves could diminish leaf-water ^{2}H-enrichment by both lowering the vapor-pressure differential across the leaf surface, and by depleting the δ^2H value of water vapor near the leaf surface (since hydration water of salts is ^{2}H-depleted relative to water vapor (*Matsuo et al.,1972*)). Both of these hypotheses were based on increased salt on the leaf surface at high salinity. As such, they would likely be more pronounced for salt secreting mangroves such as *A. marina* and *A. corniculatum.* Since there was no difference in $\alpha^2_{LW\text{-}SW}$ between the salt secreting mangroves that had salt-coated leaves and the non-secreting tree that did not have visible salt deposits on its leaves, and since there was no relationship between salinity and $\alpha^2_{LW\text{-}SW}$ in any of the three species (**Figure 5**), it seems unlikely that the hypothesis relating salt on the leaf surface to reduced leaf water enrichment is correct.

Ultimately, the entire variability in apparent fractionation between leaf lipids and source water in Mobbs Bay mangroves can be explained by variability in biosynthetic fractionation, $\alpha_{Lipid\text{-}LW}$. Salinity dependent changes in $\alpha_{Lipid\text{-}LW}$ can account for differences among species and for differences within an individual tree. The second hypothesis posed by Ladd and Sachs (*2012*) to explain the Brisbane River data, that increased compatible solute production at high salinity results in changes in H-isotope partitioning among different metabolic products, is the only hypothesis that would manifest itself as changes in $\alpha_{Lipid\text{-}LW}$. However, the other processes described in section 5.5.2 that could result in differences in $\alpha_{Lipid\text{-}LW}$ among species – variability

in the amount of stored carbohydrates used for lipid synthesis, or variability in the timing of lipid production and turnover rates – could also explain differences in $\alpha_{Lipid\text{-}LW}$ within a species over time, as in this study, or over spatial salinity gradients (*Ladd & Sachs, 2012; Ladd & Sachs, in prep*). While the data here does not definitively explain why there would be more biosynthetic discrimination against ^{2}H at higher salinity, it does suggest that this is the most promising avenue for further investigation of the mechanisms responsible for the inverse relationship between salinity and $\alpha_{Lipid\text{-}SW}$.

5.6 Conclusions

$\delta^{2}H$ values of leaf lipids and $\delta^{2}H$ and $\delta^{18}O$ values of surface, xylem, and leaf, water were measured weekly in *R. stylosa, A. marina* and *A. corniculatum* mangroves in Mobbs Bay, New South Wales, Australia over 9.5 months. When salinity exceeded 20 ppt, xylem water $\delta^{18}O$ values decreased relative to surface water, suggesting that the mangroves relied more on non-surface water sources, such as groundwater, episodic rain events and/or foliar water uptake. Even at times when there was no ^{18}O-depletion, xylem water $\delta^{2}H$ was depleted by 4-10‰ relative to estuary surface water in all three species, implying discrimination against ^{2}H during water uptake.

Although xylem water became more ^{2}H- and ^{18}O-depleted relative to surface water as salinity increased from 1-36 ppt, there were no systematic changes in leaf water $\delta^{2}H$ or $\delta^{18}O$ relative to surface water. Leaf water $\delta^{2}H$ values were also similar among species. In all three species, the ^{2}H-depletion in leaf lipids relative to estuary and leaf water increased with salinity by 0.5-1.0‰ in *n*-alkanes and by 0.4-0.8‰ in isoprenoids. Since there were no systematic changes in leaf water enrichment with salinity, changes in leaf and xylem water $\delta^{2}H$ values

cannot explain the salinity-dependence of ^{2}H-depletion in leaf lipids. More likely causes are (i) increased compatible solute production at high salinity causing changes in H-isotope partitioning among different metabolic products, (ii) reduced utilization of stored carbohydrates for lipid synthesis as salinity increases, or (iii) variability in the timing of lipid production and turnover rates. A ~30‰ ^{2}H enrichment of *n*-alkanes and isoprenoids in *R. stylosa* leaves relative to the other two species can be explained by either different classes of compatible solutes, a different proportional reliance on stored carbohydrates in lipid synthesis, a different timing of leaf lipid production, or different turnover rates of leaves compared to *A. marina* and *A. corniculatum*.

Further investigation into the causes of biosynthetic fractionation in leaf lipids will better constrain the use of δ^2H_{lipid} values from mangroves as a paleohydrologic proxy, and offer improved understanding of carbon and lipid metabolisms within trees.

5.7 References

Ashihara, H., Adachi, K., Otawa, M., Yasumoto, E., Fukushima, Y., Kato, M., Sano, H., Sasamoto, H. & Baba, S. (1997) Compatible solutes and inorganic ions in the mangrove plant *Avicennia marina* and their effects on the activities of enzymes. *Zeitschrift für Naturforschung* 52, 433-440.

Clough B.F. (1984) Growth and salt balance of the mangroves. Avicennia marina (Forsk.) Vierh. and Rhizophora stylosa Griff. in relation to salinity. *Australian Journal of Plant Physiology* 11, 419–430

Clough B.F. & Sim, R.G. (1989) Changes in gas exchange characteristics and water use efficiency of mangroves in response to salinity and vapour pressure deficit. *Oecologia* 79, 38–44.

Cormier M.-A. & Kahmen, A. (2014) Biochemical hydrogen isotope Fractionation during *n*-alkanes biosynthesis in higher plants. Goldschmidt Conference, Sacramento, CA.

Coupland, G.T., Paling, E.I. & McGuinness, K.A. (2005) Vegetative and reproductive phenologies of four mangrove species from northern Australia. *Australian Journal of Botany* 53, 109-117.

Craig, H. & Gordon, L. (1965) Deuterium and oxygen 18 variations in the ocean and the marine atmosphere. In: Tongiori, E. (Ed.), Proceedings of a Conference on Stable Isotopes in Oceanographic Studies and Paleotemperatures. CNR-Laboratorio di Geologia Nucleare, Pisa, pp. 9-130.

Dansgaard, W. (1964) Stable isotopes in precipitation. *Tellus* 16, 436-468.

Datta, P.N. & Ghose, M. (2003) Estimation of osmotic potential and free amino acids in some mangroves of the Sundarbans, India. *Acta Botanica Croatica* 62, 37-45.
Dittmar T., Hertkorn N., Kattner G. & Lara R.J. (2006) Mangroves, a major source of dissolved organic carbon to the oceans. *Global Biogeochemical Cycles* 20:GB1012, doi:10.1029/2005GB002570.
Douglas, P.J.M., Pagani M., Brenner M., Hodell D.A. & Curtis J.H. (2012) Aridity and 754 vegetation composition are important determinants of leaf-wax δD values in 755 southeastern Mexico and Central America. *Geochimica et Cosmochimica Acta*, 756 97, 24-45.
Duke N.C., Bunt J.S. & Williams W.T. (1984) Observations of the floral and vegetative phenologies of north-eastern Australian mangroves. *Australian Journal of Botany* 32, 87–99.
Eley, Y., Dawson, L., Black, S., Andrews, J. & Pedentchouk, N. (2013) Understanding 2H/1H systematics of leaf wax n-alkanes in coastal plants at Stiffkey saltmarsh, Norfolk, UK. *Geochimica et Cosmochimica Acta* 128, 13–28
Ellsworth, P. & Williams, D. (2007) Hydrogen isotope fractionation during water uptake by woody xerophytes. *Plant and Soil* 291, 93-107.
Ewe, S., Sternberg, L. & Childers, D. (2007) Seasonal plant water uptake patterns in the saline southeast Everglades ecotone. *Oecologia* 152, 607-616.
Feakins, S.J. & Sessions, A.L. (2010a) Controls on the D/H ratios of plant leaf waxes in an arid ecosystem. *Geochimica Cosmochimica Acta* 74, 2128-2141.
Feakins, S.J. & Sessions, A.L. (2010b) Crassulacean acid metabolism influences D/H ratio of leaf wax in succulent plants. *Organic Geochemistry* 41, 1269-1276.
Ferrio J.P., Cuntz M., Offermann C., Siegwolf R., Saurer M. & Gessler A. (2009) Effect of water availablility on leaf water isotopic enrichment in beech seedlings shows limitations of current fractionation models. *Plant, Cell and Environment*, 32, 1285-1296.
Gao L., Burnier A. & Huang Y. (2012) Quantifying instantaneous regeneration rates of plant leaf waxes using stable hydrogen isotope labeling. *Rapid Communications in Mass Spectrometry*, 26, 115-122.
Gat, J.R. (1996) Oxygen and hydrogen isotopes in the hydrologic cycle. *Annual Review in Earth and Planetary Sciences* 24, 225-262.
Hibino, T., Meng, Y.L., Kawamitsu, Y., Uehara, N., Matsuda, N., Tanaka, Y., …, Takabe, T., 2001. Molecular cloning and functional characterization of two kinds of betaine-aldehyde dehydrogenase in betaine-accumulating mangrove *Avicennia marina* (Forsk.) Vierh. *Plant Molecular Biology* 45, 353-363.
Hou, J., D' Andrea, W., MacDonald, D. & Huang, Y.S. (2007) Hydrogen isotopic variability in leaf waxes among terrestrial and aquatic plants around Blood Pond, Massachusetts (USA). *Organic Geochemistry* 38, 977-984.
Jennerjahn T.C. & Ittekot V. (2002) Relevance of mangroves for the production and deposition of organic matter along tropical continental margins. *Naturwissenschaften* 89, 23-30.
Kahmen, A., Dawson, T.E., Vieth, A. & Sachse, D. (2011) Leaf wax *n*-alkane δD values are determined early in the ontogeny of *Populus trichocarpa* leaves when grown under controlled environmental conditions. *Plant, Cell and Environment* 34, 1639-1651.
Kahmen A., Hoffmann B., Schefuss E., Arndt S.K., Cernusak L.A., West J.B. & Sachse D. (2013a) Leaf water deuterium enrichment shapes leaf wax n-alkane dD values of angiosperm plants II: Observational evidence and global implications. *Geochimica et*

Cosmochimica Acta 111, 50-63.
Kahmen A., Schefuss E. & Sachse D. (2013b) Leaf water deuterium enrichment shapes leaf wax n-alkane dD values of angiosperm plants I: Experimental evidence and mechanistic insights. *Geochimica et Cosmochimica Acta* 111, 39-49.
Kahmen, A., Simonin, K., Tu, K.P., Merchant, A. & Callister, A. (2008) Effects of environmental parameters, leaf physiological properties and leaf water relations on leaf water delta ^{18}O enrichment in different Eucalyptus species. *Plant, Cell & Environment* 31, 738-751.
Kolattukudy P.E. (1965) Biosynthesis of wax in Brassica oleracea. *Biochemistry* 4, 1844–1855.
Ladd, S.N. & Sachs, J.P. (2012) Inverse relationship between salinity and *n*-alkane δD values in the mangrove *Avicennia marina*. *Organic Geochemistry* 48, 25-36.
Ladd, S.N. & Sachs, J.P. (in prep.) Influence of salinity on hydrogen isotope fractionation in *Rhizophora* mangroves from Micronesia.
Lambs, L., Muller, E. & Fromard, F. (2008) Mangrove trees growing in a very saline condition but not using seawater. *Rapid Communications in Mass Spectrometry* 22, 2835-2843.
Lin, G. & Sternberg, L. (1993) Hydrogen isotopic fractionation by plant roots during water uptake in coastal wetland plants. In *Stable Isotopes and Plant Carbon/Water Relations* (eds Ehleringer, J., Hall, A. & Farquhar, G.), pp. 497-510. Academic Press, Inc., San Diego.
Lin, G. & Sternberg, L. (1994) Utilization of surface water by red mangrove (*Rhizophora mangle* L.): An isotopic study. *Bulletin of Marine Science* 54, 94-102.
Liu, W.G. & Yang, H. (2008) Multiple controls for the variability of hydrogen isotopic compositions in higher plant *n*-alkanes from modern ecosystems. *Global Change Biology* 14, 2166-2177.
Liu, W.G., Yang, H. & Li, L. (2006) Hydrogen isotopic composition of *n*-alkanes from terrestrial plants correlate with their ecological life form. *Oecologia* 150, 330-338.
Matsuo, S., Friedman, I. & Smith, G.I. (1972) Studies of quaternary saline lakes – I. Hydrogen isotope fractionation in saline minerals. *Geochimica et Cosmochimica Acta* 36, 427-435.
Naidoo, G. (1985) Effects of waterlogging and salinity on plant-water relations and on the accumulation of solutes in three mangrove species. *Aquatic Botany* 22, 133-143.
Parida, A. & Jha, B. (2010) Salt tolerance mechanisms in mangroves: a review. *Trees - Structure and Function* 24, 199-217.
Polissar, P.J. & Freeman, K.H. (2010) Effects of aridity and vegetation on plant-wax δD in modern lake sediments. *Geochimica et Cosmochimica Acta* 74, 5785-5797.
Roden J.S., Lin G. & Ehleringer J.R. (2000) A mechanistic model for interpretation of hydrogen and oxygen isotope ratios in tree-ring cellulose. *Geochimica et Cosmochimica Acta* 64, 21-35.
Romero, I.C. & Feakins, S.J. (2011) Spatial gradients in plant leaf wax D/H across a coastal salt marsh in southern California. *Organic Geochemistry* 42, 618-629.
Sachse, D., Billault, I., Bowen, G.J., Chikaraishi, Y., Dawson, T.E., Feakins, S.J., … Kahmen, A. (2012) Molecular paleohydrology: interpreting the hydrogen-isotopic composition of lipid biomarkers from photosynthesizing organisms. *Annual Review of Earth and Planetary Science* 40, 212-249.
Sachse, D., Gleixner, G., Wilkes, H. & Kahmen, A. (2010) Leaf wax *n*-alkane δD values of field-grown barley reflect leaf water δD values at the time of leaf formation. *Geochimica et Cosmochimica Acta* 74, 6741-6750.

Sachse, D., Kahmen, A. & Gleixner, G. (2009) Significant seasonal variation in the hydrogen isotopic composition of leaf-wax lipids for two deciduous tree ecosystems (*Fagus sylvativa* and *Acer pseudoplatanus*). *Organic Geochemistry* 40, 732-742.

Sachse, D., Radke, J. & Gleixner, G. (2004) Hydrogen isotope ratios of recent lacustrine sedimentary *n*-alkanes record modern climate variability. *Geochimica et Cosmochimica Acta* 68, 4877-4889.

Samuels L., Kunst L. & Jetter R. (2008) Sealing plant surfaces: cuticular wax formation by epidermal cells. *Annual Review of Plant Biology* 59, 683–707.

Schmidt, H.L., Werner, R.A. & Eisenreich, W. (2003) Systematics of ^{2}H patterns in natural compounds and its importance for the elucidation of biosynthetic pathways. *Phytochemistry Reviews* 2, 61-85.

Sessions, A. (2006) Seasonal changes in D/H fractionation accompanying lipid biosynthesis in Spartina alterniflora. *Geochima et Cosmochimica Acta* 70, 2153-2162.

Smith, F.A. & Freeman, K.H. (2006) Influence of physiology and climate on δD of leaf wax *n*-alkanes from C_3 and C_4 grasses. *Geochimica et Cosmochimica Acta* 70, 1172-1187.

Tipple B.J., Berke M.A., Doman C.E., Khachaturyan S. & Ehleringer J.R. (2013) Leaf n- alkane record the plant-water environment at leaf flush. *Proceedings of the National Academy of Science* 110, 2659-2664.

Tipple, B.J., Berke, M., Hambach, B., Roden, J.S. & Ehleringer, J.R. (In Press) Predicting leaf wax n-alkane (2) H/(1) H ratios: controlled water source and humidity experiments with hydroponically grown trees confirm predictions of Craig-Gordon model. *Plant, Cell and Environment*. doi: 10.1111/pce.12457.

Tipple, B.J. & Pagani, M. (2013) Environmental control on eastern broadleaf forest species' leaf wax distributions and D/H ratios. *Geochimica et Cosmochimica Acta* 111, 64-77.

Vandegehuchte M.W., Guyot A., Hubau M., DeGroote, S.R.E., De Baerdemaeker, N.J.F., Hayes, M., …, Steppe, K. (2014) Long-term versus daily stem diameter variation in co-occurring mangrove species: environmental versus ecophysiological drivers. *Agricultural and Forest Meteorology* 192–193, 51-58.

Wang Y, Sessions A.L., Nielsen R.J. & Goddard W.A. (2009) Equilibrium $^{2}H/^{1}H$ fractionations in organic molecules. II. Linear alkanes, alkenes, ketones, carboxylic acids, esters, alcohols and ethers. *Geochimica et Cosmochimica Acta* 73, 7076-7086.

Wei L., Lockington D.A., Poh S.C., Gasparon M. & Lovelock C.E. (2013) Water use patterns of estuarine vegetation in a tidal creek system. *Oecologia* 172: 485-494.

Wium-Andersen S. & Christensen B. (1978) Seasonal growth of mangrove trees in southern Thailand. II. Phenology of *Brugueira cylindrica, Ceriops tagal, Lumnitzera littoria* and *Avicennia marina. Aquatic Botany* 5, 383-390.

Yakir D. (1992) Variations in the natural abundance of ^{18}O and deuterium in plant carbohydrates. *Plant, Cell and Environment* 15, 1005-1020.

Yakir D. & DeNiro M.J. (1990) Oxygen and hydrogen isotope fractionation during cellulose metabolism in *Lemna gibba* L. *Plant Physiology* 93, 325-332.

Yang, H., Pagani, M., Briggs, D.E.G., Equiza, M.A., Jagels, R., Leng, Q. & LePage, B.A. (2009) Carbon and hydrogen isotope fractionation under continuous light: implications for paleoenvironmental interpretations of the High Arctic during Paleogene warming. 160, 461-470.

Table 1: Rainwater isotopes from East Ballina, NSW

Rain date	Rain δ^2H	Rain $\delta^{18}O$
September 24, 2012	15.7±0.2	3.9±0.2
September 30, 2012	7.9±0.2	-2.1±0.2
October 2, 2012	12.9±0.2	-1.9±0.2
October 11, 2012	5.9±0.2	-1.3±0.2
October 30, 2012	7.9±0.2	-2.1±0.2
November 9, 2012	-12.3±0.2	-3.7±0.2
November 10, 2012	-12.5±0.2	-3.5±0.2
December 7, 2012	2±0.2	-2.8±0.2
December 10, 2012	-5.3±0.2	-3.7±0.2
December 19, 2012	7.1±0.2	-0.2±0.2
December 21, 2012	-26.8±0.2	-4.5±0.2
December 23, 2012	2±0.2	-1.4±0.2
December 26, 2012	-14.9±0.2	-3.9±0.2
December 26, 2012	-15.4±0.2	-4.1±0.2
December 28, 2012	-13.4±0.2	-2.8±0.2
January 28, 2013	-13.8±0.2	-3.4±0.2
February 5, 2013	-0.6±0.2	-1.9±0.2
February 18, 2013	2.5±0.2	-1.4±0.2
February 19, 2013	-51.6±0.2	-8±0.2
February 20, 2013	-43.3±0.2	-7±0.2
February 21, 2013	-44±0.2	-7.1±0.2
February 22, 2013	-56.7±0.2	-8.8±0.2
February 26, 2013	-11.3±0.2	-3.6±0.2
March 7, 2013	-1.4±0.2	-2.7±0.2
March 29, 2013	-8.1±0.2	-3.5±0.2
March 31, 2013	-9.8±0.2	-3.5±0.2
April 3, 2013	-20.3±0.2	-4.8±0.2
April 4, 2013	-21.9±0.2	-5.3±0.2
April 8, 2013	0.5±0.2	-2.8±0.2
April 10, 2013	-18.4±0.2	-4.8±0.2
May 11, 2013	-10.1±0.2	-4.2±0.2
May 13, 2013	-3.8±0.2	-3.2±0.2
May 24, 2013	-67.3±0.2	-11±0.2
May 27, 2013	-9.6±0.2	-4.3±0.2
May 30, 2013	-7.2±0.2	-3.4±0.2
June 8, 2013	-15.8±0.2	-4.2±0.2
June 8, 2013	-1.9±0.2	-2.4±0.2
June 10, 2013	17.8±0.2	-0.3±0.2
June 11, 2013	3.2±0.2	-1.8±0.2
June 12, 2013	3±0.2	-2±0.2
June 20, 2013	-8.9±0.2	-3.7±0.2
June 21, 2013	2.4±0.2	-1.2±0.2
June 23, 2013	-25.5±0.2	-6.7±0.2
June 28, 2013	1.8±0.2	-2.5±0.2
June 30, 2013	-16.3±0.2	-4.9±0.2
July 1, 2013	-50.5±0.2	-9.3±0.2
July 2, 2013	-7.3±0.2	-2.9±0.2
July 11, 2013	11.9±0.2	-1.4±0.2

5.8 Figure Captions

Figure 1 Study site in Ballina, New South Wales and sampled trees

Figure 2: Rainfall amount, salinity, δ^2H and $\delta^{18}O$ of surface (SW), xylem (XW), and leaf (LW) water, and δ^2H of *n*-alkanes and isoprenoidal lipids from October 1, 2012 to July 17, 2013. In all panels, Rs stands for *R. stylosa*, Am is *A. marina*, and Ac represents *A. corniculatum*

Figure 3 Surface (SW, blue), xylem (XW) and leaf (LW) water $\delta^{18}O$ values (panel a) and δ^2H values (panel b) for *R. stylosa* (Rs, red), *A. marina* (Am, grey) and *A. corniculatum* (Ac, brown) growing in Mobbs Bay as a function of salinity.

Figure 4 Fractionation factors between xylem water and surface water for oxygen isotopes (panel a) and hydrogen isotopes (panel b) for *R. stylosa* (Rs, red), *A. marina* (Am, gray) and *A. corniculatum* (Ac, brown) growing in Mobbs Bay as a function of salinity.

Figure 5 Fractionation factors between leaf water and different water pools xylem for *R. stylosa* (Rs), *A. marina* (Am) and *A. corniculatum* (Ac) growing in Mobbs Bay as a function of salinity. Panel a shows leaf water fractionation relative to surface water for hydrogen isotopes; panel b is leaf water fractionation relative to xylem water. Panels c and d so equivalent plots for oxygen isotopes.

Figure 6 Net fractionation factors between leaf lipids and surface water for *n*-alkanes (panel a) and isoprenoids (panel b) for *R. stylosa* (Rs, red), *A. marina* (Am, gray) and *A. corniculatum* (Ac, brown) growing in Mobbs Bay as a function of salinity.

Figure 7 Predicted and measured xylem water δ^2H values for *R. stylosa* (Rs, upper panel), *A. marina* (Am, middle panel) and *A. corniculatum* (Ac, lower panel) growing in Mobbs Bay from October 1, 2012 to July 17, 2013. Predicted xylem water δ^2H values are based on measured $\delta^{18}O$ values of xylem water and the local water line.

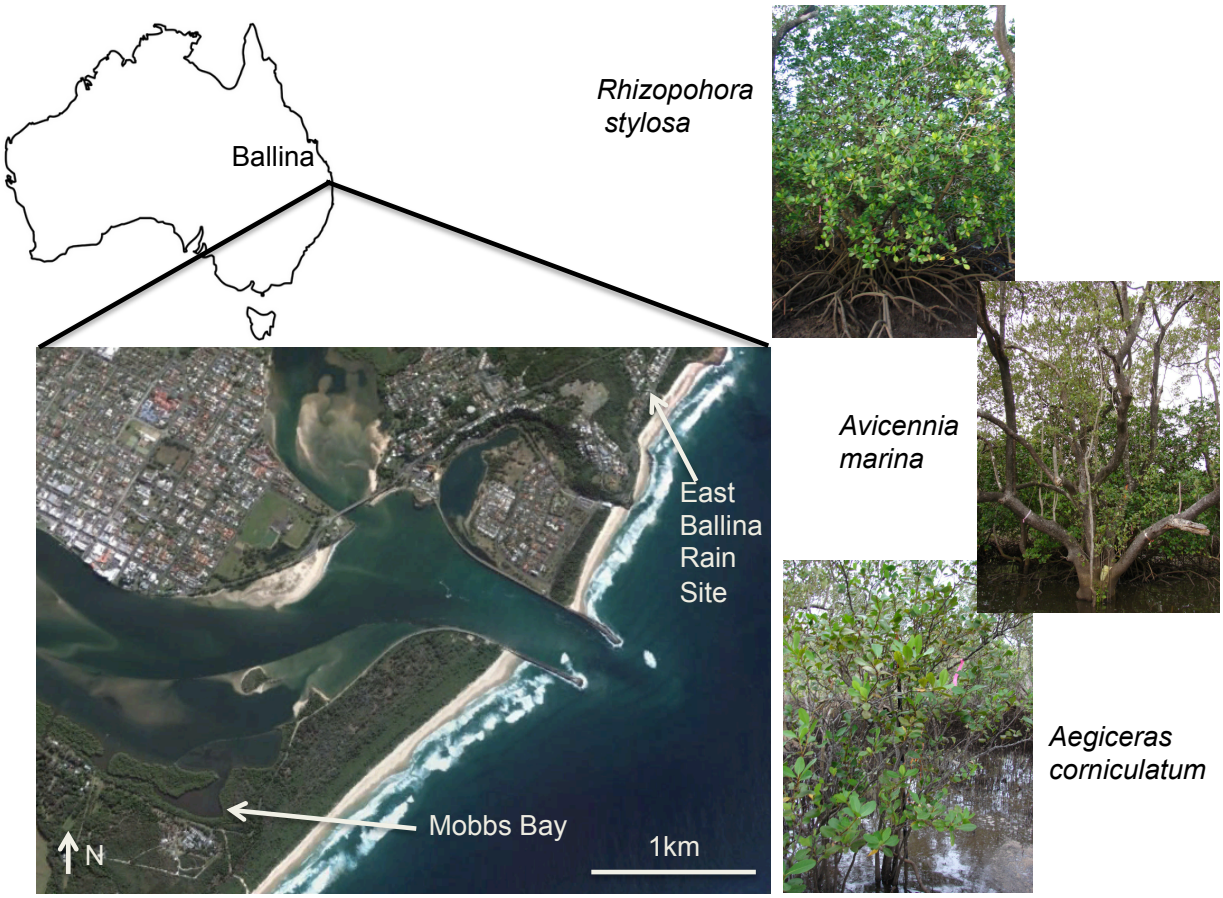

Figure 1 Study site in Ballina, New South Wales and sampled trees

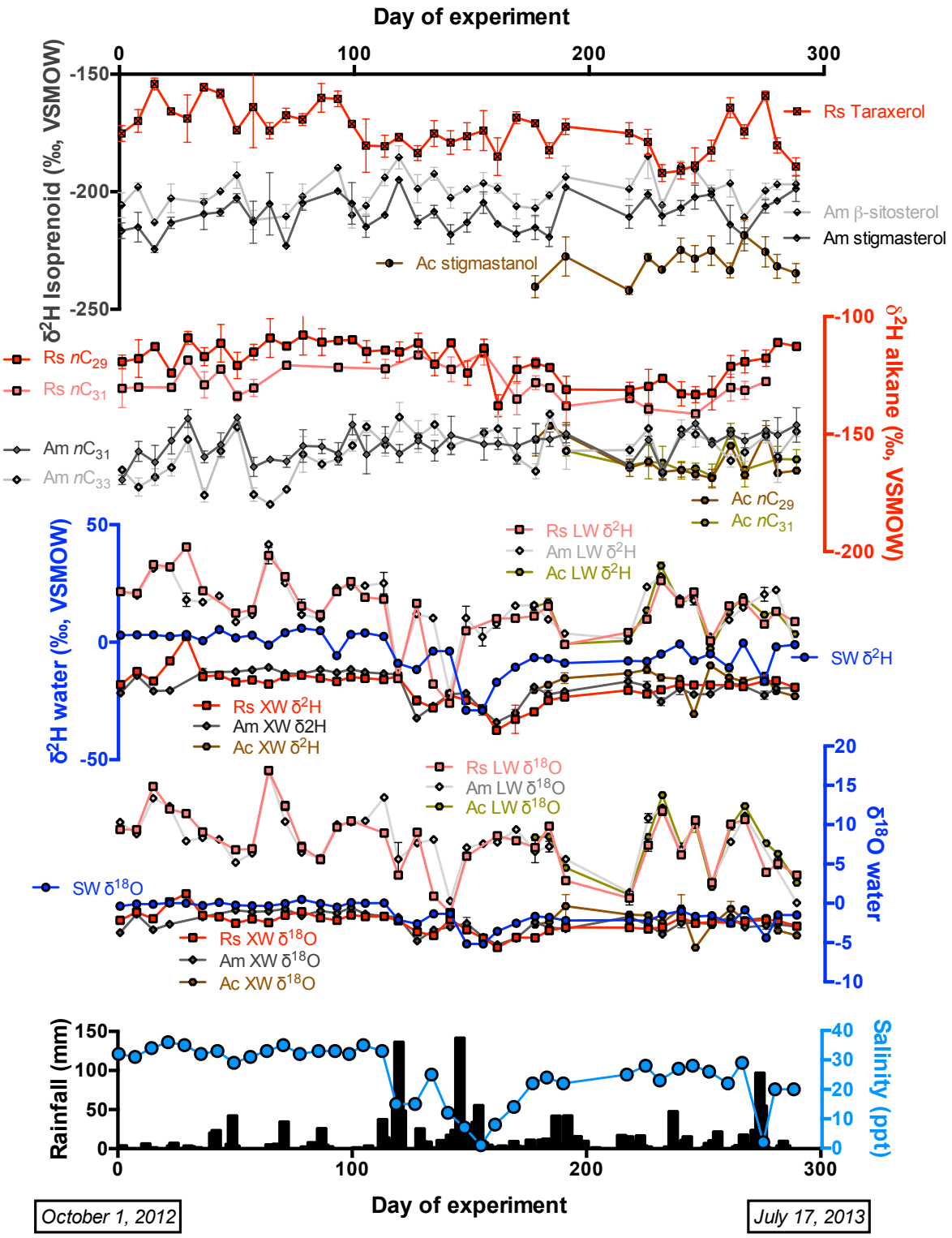

Figure 2: Rainfall amount, salinity, δ^2H and $\delta^{18}O$ of surface (SW), xylem (XW), and leaf (LW) water, and δ^2H of *n*-alkanes and isoprenoidal lipids from October 1, 2012 to July 17, 2013. In all panels, Rs stands for *R. stylosa*, Am is *A. marina*, and Ac represents *A. corniculatum*

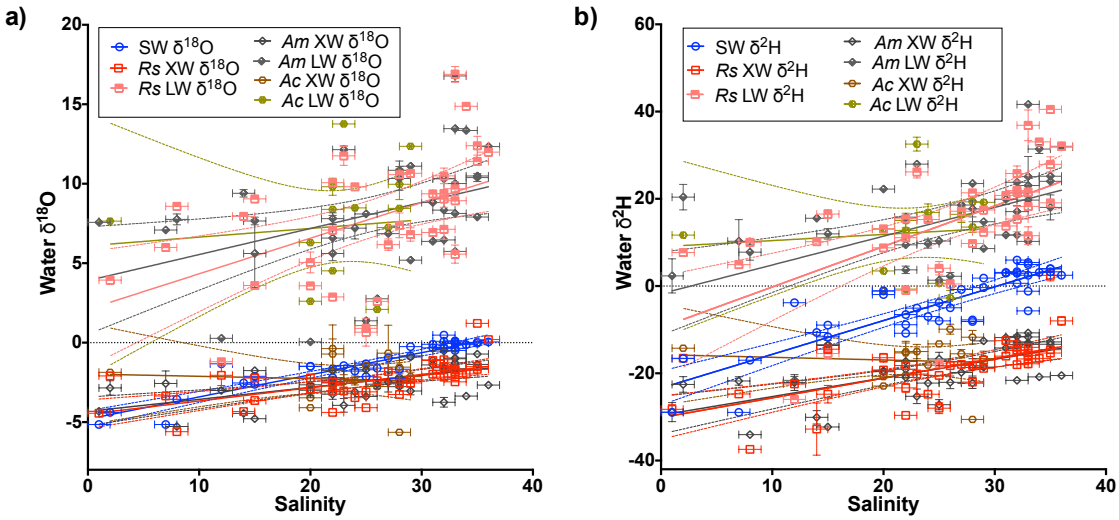

δ18O						δ2H				
m	**b**	**R^2**	**p**	**n**	**Water**	**m**	**b**	**R^2**	**p**	**n**
0.14±0.01	4.8±0.3	0.85	<0.0001	39	Surface (SW)	0.77±0.07	-23±2	0.76	<0.0001	39
0.08±0.02	4.5±0.4	0.40	<0.0001	39	*R. stylosa* xylem (*Rs* XW)	0.45±0.09	-30±2	0.39	<0.0001	39
0.22±0.07	2±2	0.25	0.002	36	*R. stylosa* leaf (*Rs* LW)	0.9±0.2	-9±6	0.35	0.0001	36
0.08±0.02	4.3±0.4	0.36	<0.0001	37	*A. marina* xylem (*Am* XW)	0.43±0.08	-29±2	0.44	<0.0001	37
0.16±0.06	4±2	0.17	0.01	37	*A. marina* leaf (*Am* LW)	0.7±0.2	-2±5	0.28	0.0006	37
-0.01±0.06	2±1	0.005	0.82	14	*A. corniculatum* (*Ac* XW)	0.1±0.2	-15±5	0.006	0.79	14
0.1±0.01	6±4	0.01	0.74	14	*A. corniculatum* leaf (*Ac* LW)	0.1±0.4	9±10	0.01	0.73	14

Figure 3 Surface (SW, blue), xylem (XW) and leaf (LW) water $\delta^{18}O$ values (panel a) and $\delta^{2}H$ values (panel b) for *R. stylosa* (Rs, red), *A. marina* (Am, grey) and *A. corniculatum* (Ac, brown) growing in Mobbs Bay as a function of salinity.

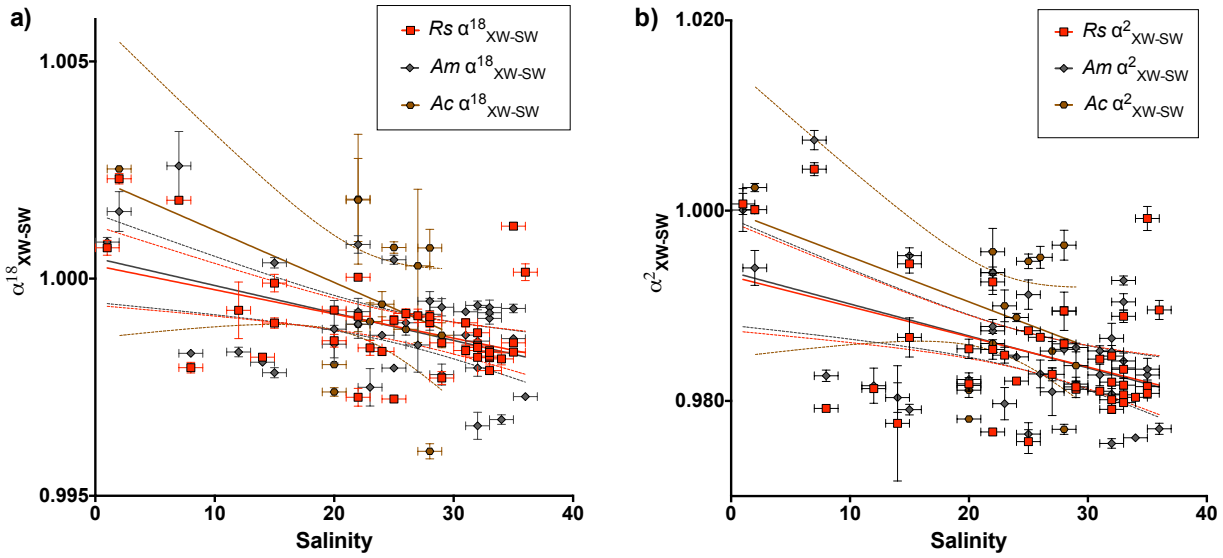

$\alpha^{18}_{XW\text{-}SW}$						$\alpha^{2}_{XW\text{-}SW}$				
m (x10^{-4})	b	R^2	p	n	Species	m (x10^{-4})	b	R^2	p	n
-0.6 ± 0.2	1.000 ± 0.001	0.23	0.002	39	*R. stylosa* (*Rs*)	-3 ± 1	0.993 ± 0.003	0.20	0.005	39
-0.6 ± 0.2	1.000 ± 0.001	0.24	0.002	37	*A. marina* (*Am*)	-3 ± 1	0.994 ± 0.002	0.28	0.0006	37
-1.2 ± 0.7	1.002 ± 0.002	0.19	0.12	14	*A. corniculatum* (*Ac*)	-5 ± 2	0.999 ± 0.007	0.17	0.14	14

Figure 4 Fractionation factors between xylem water and surface water for oxygen isotopes (panel a) and hydrogen isotopes (panel b) for *R. stylosa* (Rs, red), *A. marina* (Am, gray) and *A. corniculatum* (Ac, brown) growing in Mobbs Bay as a function of salinity.

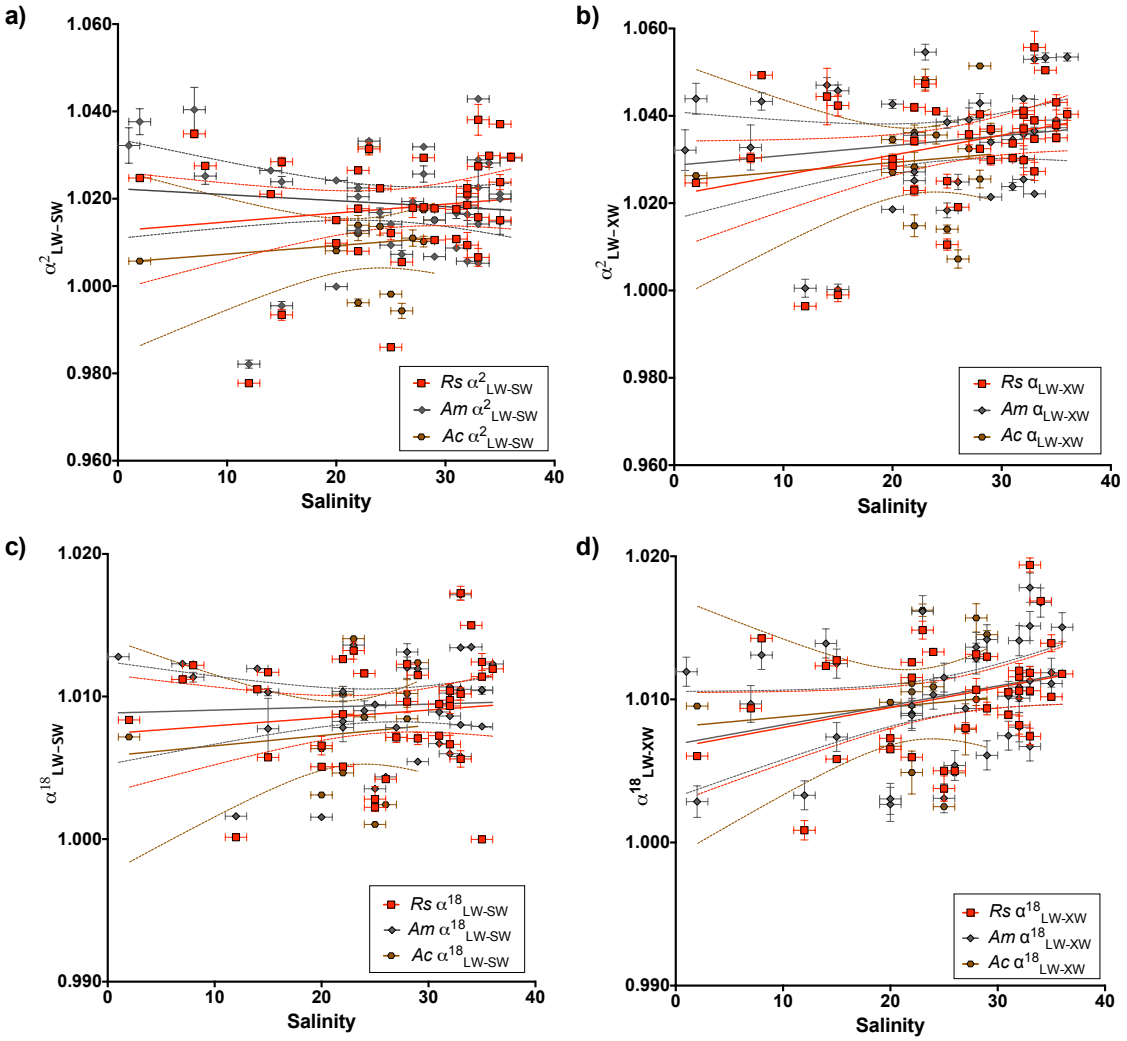

α^2_{LW-SW}						α^2_{LW-XW}				
m (x10^{-4})	**b**	**R^2**	**p**	**n**	**Species**	**m (x10^{-4})**	**b**	**R^2**	**p**	**n**
2 ± 2	1.013 ± 0.007	0.02	0.42	39	*R. stylosa* (*Rs*)	-5 ± 2	1.022 ± 0.006	0.10	0.05	37
-1 ± 2	1.022 ± 0.006	0.01	0.52	37	*A. marina* (*Am*)	-2 ± 2	1.029 ± 0.006	0.03	0.33	35
2 ± 4	1.005 ± 0.009	0.02	0.65	14	*A. corniculatum* (*Ac*)	-2 ± 5	1.03 ± 0.01	0.01	0.70	14
α^{18}_{LW-SW}						α^{18}_{LW-XW}				
m (x10^{-4})	**b**	**R^2**	**p**	**n**	**Species**	**m (x10^{-4})**	**b**	**R^2**	**p**	**n**
0.6 ± 0.8	1.007 ± 0.002	0.002	0.48	36	*R. stylosa* (*Rs*)	1.4 ± 0.7	1.007 ± 0.002	0.09	0.07	37
0.2 ± 0.7	1.009 ± 0.002	0.003	0.75	37	*A. marina* (*Am*)	1.4 ± 0.7	1.007 ± 0.002	0.10	0.06	37
1 ± 2	1.006 ± 0.004	0.02	0.66	14	*A. corniculatum* (*Ac*)	1 ± 2	1.008 ± 0.004	0.01	0.7	14

Figure 5 Fractionation factors between leaf water and different water pools xylem for *R. stylosa* (Rs), *A. marina* (Am) and *A. corniculatum* (Ac) growing in Mobbs Bay as a function of salinity. Panel a shows leaf water fractionation relative to surface water for hydrogen isotopes; panel b is leaf water fractionation relative to xylem water. Panels c and d so equivalent plots for oxygen isotopes.

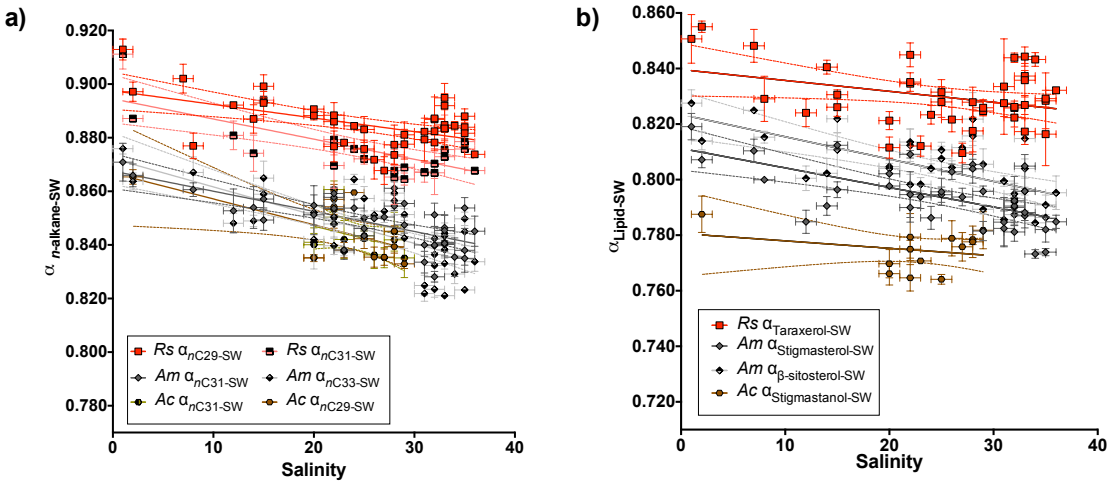

$\alpha_{Lipid-SW}$	m ($x10^4$)	b	R^2	p	n
R. stylosa nC_{29} (Rs $\alpha_{nC29-SW}$)	-5 ± 1	0.898 ± 0.003	0.30	0.003	39
R. stylosa nC_{31} (Rs $\alpha_{nC31-SW}$)	-8 ± 2	0.895 ± 0.004	0.50	0.0001	24
A. marina nC_{31} (Am $\alpha_{nC31-SW}$)	-8 ± 1	0.868 ± 0.003	0.52	<0.0001	38
A. marina nC_{33} (Am $\alpha_{nC33-SW}$)	-11 ± 2	0.872 ± 0.005	0.50	<0.0001	38
A. corniculatum nC_{29}(Ac $\alpha_{nC29-SW}$)	-10 ± 4	0.867 ± 0.009	0.35	0.03	14
A. corniculatum nC_{31} (Ac $\alpha_{nC31-SW}$)	-9 ± 7	0.87 ± 0.02	0.17	0.21	11
R. stylosa taraxerol (Rs $\alpha_{Taraxerol-SW}$)	-4 ± 2	0.840 ± 0.005	0.12	0.03	36
A. marina stigmasterol (Am $\alpha_{Stigmasterol-SW}$)	-7 ± 1	0.811 ± 0.004	0.40	<0.0001	37
A. marina β-sitosterol (Am $\alpha_{β-sitosterol-SW}$)	-8 ± 1	0.824 ± 0.004	0.44	0.0001	36
A. corniculatum stigmastanol (Ac $\alpha_{stigmastanol-SW}$)	-3 ± 3	0.781 ± 0.007	0.07	0.39	13

Figure 6 Net fractionation factors between leaf lipids and surface water for *n*-alkanes (panel a) and isoprenoids (panel b) for *R. stylosa* (Rs, red), *A. marina* (Am, gray) and *A. corniculatum* (Ac, brown) growing in Mobbs Bay as a function of salinity.

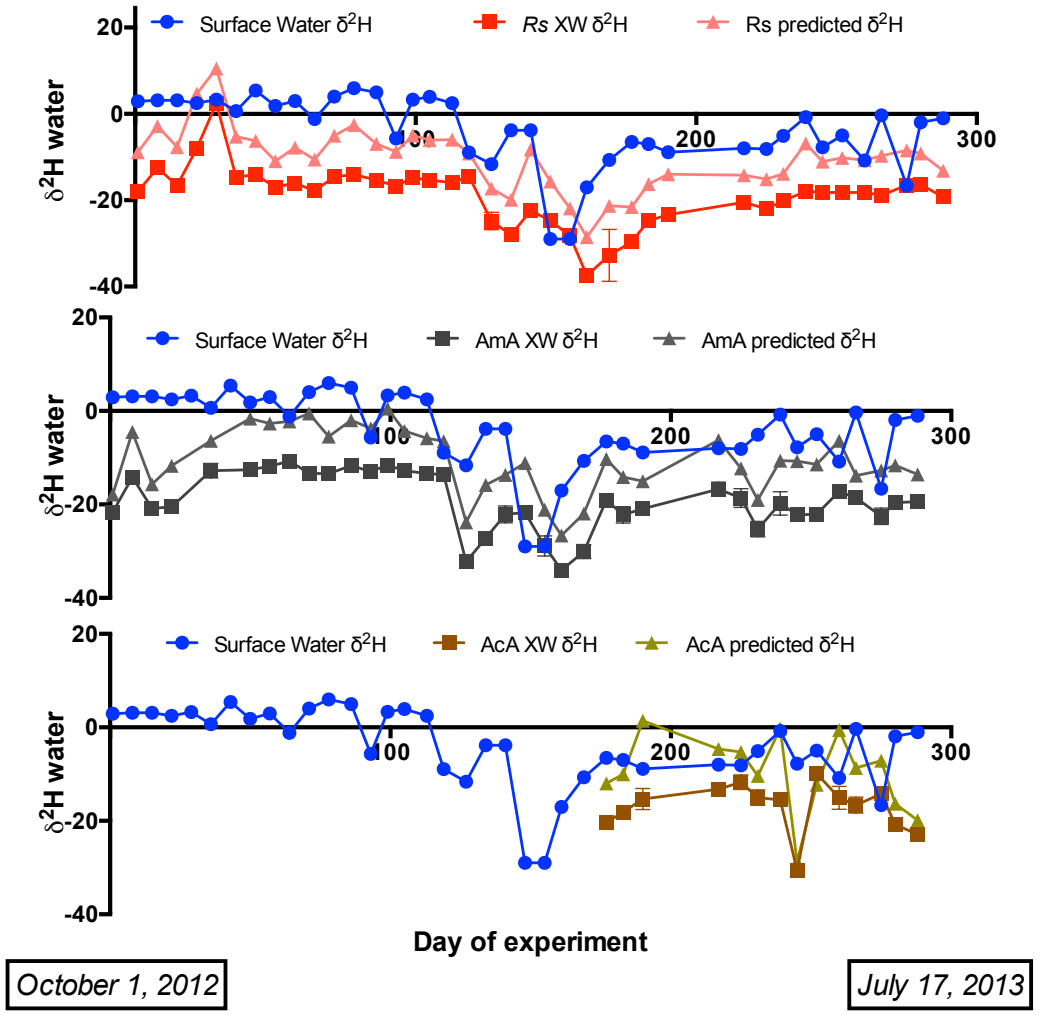

Figure 7 Predicted and measured xylem water δ^2H values for *R. stylosa* (Rs, upper panel), *A. marina* (Am, middle panel) and *A. corniculatum* (Ac, lower panel) growing in Mobbs Bay from October 1, 2012 to July 17, 2013. Predicted xylem water δ^2H values are based on measured $\delta^{18}O$ values of xylem water and the local water line.

Chapter 6: Changing rainfall rates in the western tropical Pacific from hydrogen isotopes of paired lipid biomarkers in Clear Lake, Palau

6.1 Abstract

The Western Pacific Warm Pool (WPWP) is a dynamically important region that is sensitive to changes in the El Niño Southern Oscillation (ENSO) and the migration of the Intertropical Convergence Zone (ITCZ). Past hydrologic change over the past millennium is poorly constrained, and results of the limited proxy reconstructions that exist are not always consistent with each other. We present an 800-year sedimentary record of paired dinosterol and taraxerol hydrogen isotope measurements ($^2H/^1H$ or δ^2H) from Clear Lake, a brackish lake in Palau, in the heart of the WPWP. During the Little Ice Age (~1400 C.E. to ~1800 C.E.) dinosterol $^2H/^1H$ increases by ~35‰ while taraxerol $^2H/^1H$ decreases by ~ 20‰. These values are most consistent with mixed, varying contributions of taraxerol to sediment from terrestrial and mangrove sources and indicate that surface salinity and water $^2H/^1H$ ratios in Clear Lake increased throughout the LIA. This is consistent with a general drying trend in Palau over this interval, and may indicate either reduced ENSO activity or a southward shift in the mean annual position of the ITCZ.

6.2 Introduction

The Western Pacific Warm Pool (WPWP) plays a central role in the global climate as a massive source of latent heat to the atmosphere. Deep convection in this region provides the ascending branch of both the zonal Walker Circulation (*Bjerknes, 1969; Julian & Chervin, 1978; Chiang, 2009*) and the meridional Hadley Cell, transporting moisture, heat and momentum poleward (*Wang & Enfield, 2003; Chiang, 2009*). Small changes in WPWP sea surface

temperature (SST) have a strong impact on both of these circulations (*Trenberth et al., 1998; Pierrehumbert, 2000; Wang & Mehta, 2008*).

Annual precipitation variability in the WPWP is primarily controlled by the seasonal migration of the Intertropical Convergence Zone (ITCZ), which fluctuates from ~10°N in boreal summer to ~3°N in boreal winter, and produces some of the heaviest precipitation rates on the planet (*Legates & Willmott, 1990; Spencer, 1993; Xie & Arkin, 1997*). Interannual precipitation variability in the WPWP is highly correlated with the Southern Oscillation Index (SOI) (*Xie & Arkin, 1997*). During positive phases of the SOI (El Niño events) SSTs in the WPWP are anomalously cool and precipitation amount decreases. The inverse is true of negative phases of the SOI, or La Niña conditions (*Xie & Arkin, 1997*).

Large-scale reorganizations of hydroclimate in the WPWP and the rest of the tropical Pacific have far-reaching, global impacts (*Wallace & Gutzler, 1981; Pierrehumbert, 2000; Wang & Mehta, 2008; Chiang, 2009*). Climate models suggest that global warming will lead to a weakening of Pacific Walker Circulation (*Vecchi et al., 2006*). However, many of the features of modern precipitation patterns in the Pacific are not fully captured by Global Climate Models. Robust reconstructions of past climate variability in the WPWP can improve our understanding of the dynamics in the region. Hydrologic change on decadal to centennial timescales remain poorly constrained, in part because of a historical lack of suitable climate proxies. Records that do exist tend to be from locations near continents (e.g. *Oppo et al., 2009; Tierney et al., 2010; Yan et al., 2011; Konecky et al., 2013; Niedermeyer et al., 2014*) and may be strongly influenced by orographic effects and monsoonal dynamics.

6.2.1 Quantitative hydroclimate reconstructions from paired δ^2H values of algal and mangrove lipids

Hydrogen isotope ratios (typically expressed as $\delta^2H = ({}^2H/{}^1H_{Sample})/({}^2H/{}^1H_{VSMOW})-1$) of lipid biomarkers preserved in sediment are a promising paleoclimate proxy (*Sachse et al., 2012*). At its most fundamental level, this proxy works because the δ^2H values of lipids produced by photoautotrophs are typically strongly correlated with the δ^2H values of the organism's source water. Environmental water isotopes are in turn driven by climatic variables such as temperature, precipitation rate, and moisture sources (*Dansgaard, 1964; Craig & Gordon, 1965; Gat, 1996*).

Because of strong biosynthetic discrimination against ^2H, lipid δ^2H values are typically depleted relative to source water (*Sessions et al., 1999; Sauer et al., 2001; Chikaraishi & Naraoka, 2003; Sachse et al., 2012*). The magnitude of this depletion is expressed by the apparent fractionation factor, $\alpha_{Lipid\text{-}Water} = ({}^2H/{}^1H_{Lipid})/({}^2H/{}^1H_{Water})$. A number of variables can influence the magnitude of $\alpha_{Lipid\text{-}Water}$ in both phytoplankton and higher plants. In algae, $\alpha_{Lipid\text{-}Water}$ is sensitive to salinity (*Schouten et al., 2006; Sachse & Sachs, 2008; Sachs & Schwab, 2011; Nelson & Sachs, 2014*), temperature (*Zhang et al., 2009; Wolhowe et al., 2009*), growth rate (*Schouten et al., 2006; Zhang et al., 2009; Sachs & Kawka, in review*), and growth stage (*Wolhowe et al., 2009; Chivall et al., 2014*).

In vascular plants, lipid δ^2H values can be influenced by relative humidity (*Feakins & Sessions, 2010; Kahmen et al., 2013a; Kahmen et al., 2013b; Tipple et al., 2014*), plant type (*Liu et al., 2006; Smith & Freeman, 2006; Hou et al., 2007*), and light levels (*Liu & Yang, 2008; Yang et al., 2009*). Despite the complications introduced by these variables, on large spatial scales δ^2H values of terrestrial plant lipids typically covary with precipitation δ^2H values (*Sachse et al., 2004; Polissar & Freeman, 2010; Sachse et al., 2012; Tipple & Pagani, 2013*).

Several paleoclimate reconstructions from the tropical Pacific and elsewhere have used δ^2H values of either algal lipid biomarkers (*Huang et al., 2002; Huang et al., 2004; van der Meer et al., 2007; Pahnke et al., 2007, Sachs et al., 2009; Smittenberg et al., 2011; Vasiliev et al., 2013; Atwood & Sachs, 2014; Kasper et al., 2014; Zhang et al., 2014*) or terrestrial plant biomarkers (*Tierney et al., 2010; Feakins et al., 2012; Konecky et al., 2013; Feakins et al., 2014; Niedermeyer et al., 2014*). These studies have only been able to provide qualitative information about changes in water isotopes and climate.

Recently, *Rach et al*. (*2014*) used co-occuring δ^2H values of terrestrial plants and aquatic plants from a German lake to distinguish between changes in water isotopes and changes in relative humidity during the Younger Dryas event, demonstrating the potential of paired lipid isotopes to provide more information than one class of biomarker on its own. Likewise, *Atwood & Sachs* (*2014*) were able to use δ^2H values of lipids produced by two different classes of algae to distinguish between precipitation changes more likely driven by El Niño activity from those more likely caused by shifts in the mean annual position of the ITCZ. Records of δ^2H values of multiple biomarkers from different sources in the same sediment core have thus demonstrated promise for providing richer information about past climate than δ^2H records from a single source.

In this study, we paired δ^2H values of dinosterol, a sterol produced primarily by dinoflagellates (*Volkmann, 2003*) with those of taraxerol, a pentcyclic triterpenoid produced in high abundance by *Rhizophora* spp. (Red mangroves; *Killops & Frewin, 1994; Koch et al., 2003; Versteegh et al., 2004*) in a sediment core from Clear Lake, Palau. Pairing lipid δ^2H values from an algal and a mangrove source is especially promising as a paleohydrologic proxy because of the strong, but opposing, influence of salinity on $\alpha_{Lipid\text{-}Water}$ in both life forms.

In algae, $\alpha_{Lipid\text{-}Water}$ is positively correlated with salinity, meaning that lipids are less depleted in ^2H relative to their source water as salinity increases (*Schouten et al., 2006; Sachse & Sachs, 2008; Sachs & Schwab, 2011; Nelson & Sachs, 2014*). In mangroves, on the other hand, $\alpha_{Lipid\text{-}Water}$ is negatively correlated with salinity, meaning that lipids become more depleted in ^2H relative to source water as salinity increases (*Ladd & Sachs, 2012; Ladd & Sachs, in prep*). These opposite responses mean that algae and mangroves using the same water source will have opposite hydrogen isotope responses to a change in the salinity. Both salinity and the source water δ^2H composition will influence the final δ^2H value of each lipid.

6.3 Site description

The Republic of Palau (N 7°-8°, E 134.5°) is located in the heart of the modern ITCZ (**Figure 1**). In the latter half of the 20th century, mean annual precipitation in Palau exceeded 3,700 mm/year (*Western Regional Climate Center*). As long-term (monthly and longer) precipitation rates increase in Palau and other tropical island locations, average $\delta^2H_{Precipitation}$ values decrease, the so-called "amount effect" (*Dansgaard, 1964; Bowen, 2008; Kurita et al., 2009; Smittenberg et al., 2011*).

Clear Lake (N 7° 09.19', E 134° 21.62') is located on Mecherchar Island, an uninhabited island south of Koror (**Figure 2**). Mecherchar and the other rock islands of Palau are heavily forested, low-lying islands consisting of karst topography. Several basins on Mecherchar contain highly stratified, meromictic lakes, of which Clear Lake is one (*Hamner & Hamner, 1998; Smittenberg et al., 2011*). Smittenberg et al. (*2011*) have previously published depth profiles of temperature, salinity, and surface water isotopes from Clear Lake.

The modern lake has a surface salinity of 22, which gradually increases with depth in the upper 8m. At this depth, there is a layer of purple sulfur bacteria, below which the lake is anoxic with little or no light penetration (*Smittenberg et al., 2011*). Photosynthesizing dinoflagellates are therefore limited to the upper portion of the water column. The lack of oxygen at depth means that the sediments are protected from bioturbation.

Surface water δ^2H values were -13‰ in June of 2004 (*Smittenberg et al., 2011*) and -11‰ during a repeat visit to the site in October 2013. Water δ^2H values increase with depth, along with salinity, in Clear Lake and neighboring Spooky and OTM lakes (*Smittenberg et al., 2011*). The relationship between these two variables in depth profiles from the three lakes was δ^2H_{Water} = 1.05 x Salinity – 36 in June 2004. In October 2013, a similar relationship between surface water and salinity was observed in the surface water of 14 marine lakes from Palau, where δ^2H_{Water} = (1.16±0.04) x Salinity + (-37±1). Because of the limited volume of the brackish surface water in the lakes, surface water δ^2H values are more sensitive to changes in precipitation amount than surrounding seawater δ^2H values (*Smittenberg et al., 2011*)

6.4 Methods

6.4.1 Core description

A 90cm sediment core with an intact mud-water interface was collected from a water depth of 11 m in 2004. 1-cm intervals of sediment were extruded into Whirlpak bags on site. Sediment was kept frozen at -20°C until subsequent analysis.

9 terrestrial macro-fossils were analyzed by AMS for radiocarbon ages. These ages were used to construct an age model for the core. An analysis of surface material from the core indicates that it is modern (post-1950). The overall accumulation rate of Clear Lake sediment is

~1 m/kyr. The 1cm increments of sectioned material therefore each correspond to an ~10 year interval.

6.4.2 Taraxerol purification

Freeze dried sediment was extracted using accelerated solvent extraction (ASE-200, Dionex Corp., Sunnyvale, CA, USA) with 9:1 Dichloromethane:Methanol (DCM:MeOH) at 100 °C and 1500 psi for 3 x 5 min static cycles. The resulting total lipid extract (TLE) was evaporated to dryness under a stream of N_2 on a Turbovap system (Caliper, Hopkinton, MA, USA).

The TLE was purified using two-step column chromatography. In the first round, neutral compounds were separated from acids using 0.5g of aminopropyl Si gel. The neutral fraction was further purified into alkane, wax ester, alcohol and more polar fractions using a stationary phase of 1 g of Si gel (5% deactivated with water). The alcohol fraction was acetylated at 70°C for 30 minutes with 25 µL of acetic anhydride of known δ^2H composition in 25 µL of pyridine. Taraxerol and dinosterol were then purified from the alcohol fraction using reverse-phase HPLC following the method of Nelson and Sachs (*2013*).

Taraxerol abundance in the HPLC-purified fractions were quantified by Gas Chromatography – Mass Spectrometry (GC-MS) using an Agilent (Santa Clara, CA, USA) 6890N gas chromatograph equipped with an Agilent 7683 autosampler, a split-splitless injector operated in splitless mode and an Agilent VF-17ms capillary column (60 m X 0.32 mm X 0.25 µm) interfaced to an Agilent 5975 quadrupole mass selective detector. The oven temperature was increased from 110°C to 320°C at 4°C/min, then held at 320°C for 10 minutes. Quantification of taraxerol was performed by comparing integrated peak areas with a known amount of 5α-

cholestane, added to the sample just prior to GC-MS analysis. These quantifications were used to determine an appropriate amount of solvent in which to dissolve the sample so that it would produce a peak of ~20V*s when analyzed by Gas Chromatrography – Isotope Ratio Mass Spectrometry (GC-IRMS).

6.4.3 Taraxerol δ^2H analyses

The δ^2H values of taraxerol were measured by GC-IRMS on a Thermo DELTA V PLUS system (Thermo Scientific, Waltham, MA, USA). The gas chromatograph (Trace Ultra, Thermo) was equipped with a split-splitless injector operated in splitless mode at 320 °C, a TRIPLUS autosampler (Thermo Scientific), and a VF-17ms capillary column (60 m x 0.25 mm x 0.25 μm, Agilent). The GC was heated from 120 °C to 260 °C at 20 °C/min, then at 1 °C/min to 300 °C, at 20 °C/min to 325 °C and then held at 325 °C for 20 min. Helium was used as the carrier gas at a constant flow of 1.1 mL/min. Compounds were pyrolyzed in a ceramic reactor at 1400°C. 1 μL of sample was injected along with 0.5 μL of a mix of nC$_{26}$-, nC$_{28}$-, nC$_{32}$-, nC$_{34}$- and nC$_{41}$-alkanes of known isotopic composition (A. Schimmelmann, Indiana University, Bloomington, Indiana). At the beginning and the end of the sequence, as well as after every 4-6 sample injections, a vial of additional nC$_{38}$-alkane standards of known isotopic composition was analyzed with the co-injection standards, in place of a sample.

Thermo ISODAT software V.2.5 controlled the instrumentation and was employed to calculate δ^2H values. The slope and intercept of the relationship between measured and known δ^2H values of the *n*-alkane standards was used to correct lipid δ^2H values for instrument bias. Offsets between corrected and known standard δ^2H values were used to further correct for drift, retention time, and peak area for each sequence. Each sample was measured in triplicate.

Reported analytical uncertainties are the standard error in the mean of the isotope standards, or the standard deviation of the triplicate sample analyses (whichever value was higher).

6.4.4 Salinity and δ^2H_{water} reconstructions from a mangrove taraxerol source

Taraxerol δ^2H measurements were paired with those of dinosterol, reported by Richey and Sachs (in prep.) from the same sediment sample. From Nelson & Sachs (*2014*) the empirical relationship between salinity (*S*) and $\alpha_{Dino\text{-}Water}$ in tropical Pacific lakes is:

$$\alpha_{Dino\text{-}Water} = (0.0008 \pm 0.0003‰) \text{ x } S + (0.725 \pm 0.009) \quad (1)$$

while the equivalent relationship for $\alpha_{Tarax\text{-}Water}$ is:

$$\alpha_{Tarax\text{-}Water} = (-0.0009 \pm 0.0002‰) \text{ x } S + (0.814 \pm 0.006) \quad (2)$$

(*Ladd & Sachs, in prep*). The definitions of $\alpha_{Dino\text{-}Water}$ and $\alpha_{Tarax\text{-}Water}$ are:

$$\alpha_{Dino\text{-}Water} = ({}^2H/{}^1H)_{Dino}/({}^2H/{}^1H)_{Water} = (\delta^2H_{Dino} + 1000)/(\delta^2H_{Water} + 1000) \quad (3)$$

and

$$\alpha_{Tarax\text{-}Water} = ({}^2H/{}^1H)_{Tarax}/({}^2H/{}^1H)_{Water} = (\delta^2H_{Tarax} + 1000)/(\delta^2H_{Water} + 1000) \quad (4)$$

Combining equations 1-4 and solving for *S* and δ^2H_{Water} yields:

$$S = \left[\frac{(0.814 \pm 0.006) - R \cdot (0.725 \pm 0.009)}{R \cdot (0.0008 \pm 0.0003) + (-0.0009 \pm 0.0002)}\right], \text{ where } R = \left(\frac{\delta^2 H_{tarax} + 1000}{\delta^2 H_{dino} + 1000}\right) \quad (5)$$

$$\delta^2 H_{water} = \left[\frac{\delta^2 H_{tarax} + 1000}{(0.814 \pm 0.006) - (-0.0009 \pm 0.0002) \cdot S}\right] - 1000 \quad (6)$$

For each sedimentary interval in which both δ^2H_{Tarax} and δ^2H_{Dino} were measured, salinity and δ^2H_{Water} were solved for using equations 5 and 6. Uncertainty associated with each reconstructed salinity and δ^2H_{Water} was assessed using a 1000 iteration Monte Carlo analysis, which took into account uncertainty associated with the slope and intercept of each calibration curve and the instrumental uncertainty of each δ^2H_{Tarax} and δ^2H_{Dino} measurement. Average 1σ uncertainties from the Monte Carlo analysis were 5 for salinity and 7‰ for δ^2H_{Water}.

6.4.5 Sedimentary δ^2H_{Tarax} model for variable mangrove inputs

A simple mixing model based on expected δ^2H_{Tarax} values for mangroves and terrestrial plants under a range of rainfall rates from 3mm/day to 16mm/day was developed in order to assess the potential impact of non-mangrove inputs on sedimentary δ^2H_{Tarax} values. Precipitation δ^2H values were defined using the local amount effect relationship of *Kurita et al.* (*2009*):

$$\delta^2 H_{Precip} = -3.4r + 2.0 \quad (7)$$

where *r* is the rainfall rate in mm/day. Terrestrial plants were assumed to use only precipitation, and to have a constant $\alpha_{Tarax\text{-}Water} = 0.814$, the y-intercept of the *Rhizophora* salinity- $\alpha_{Tarax\text{-}Water}$

relationship (that is, the $\alpha_{Tarax\text{-}Water}$ of *Rhizophora* growing in freshwater). The *Rhizophora* contribution was assumed to come from trees that were only using lake water, and whose $\alpha_{Tarax\text{-}Water}$ varied with salinity according to equation 2. The relationship between lake surface water salinity and rainfall rate was defined using modern conditions (S = 22 and r = 10mm/day) and assumed surface water salinity would be that of surrounding seawater (34) when rainfall rates were zero. The analysis was repeated with a stronger S dependence on r, such that a 1mm/day reduction in r resulted in a salinity increase of 3. Corresponding surface water δ^2H values were calculated assuming a two-end member mix between precipitation and seawater, and seawater salinity and δ^2H were held constant at modern conditions. Salinity and δ^2H_{Water} for each scenario are shown in **Figure 3**.

6.5 Results

6.5.1 Trends in δ^2H_{Tarax} in Clear Lake sediments

There was a 33‰ range in δ^2H_{Tarax} values, spanning -209 to -176‰ (**Figure 4**). In the early part of the record, δ^2H_{Tarax} values were relatively high, remaining above ~ -190‰. Starting in the early 15th century, δ^2H_{Tarax} values followed a gradually decreasing trend until the mid-18th century, when they reached a minimum of -209‰. They subsequently increased through most of the 20th Century, reaching a maximum of -187‰ around 1980 C.E. The two measurements of younger material are more depleted, with a core top δ^2H_{Tarax} value of -198‰ (**Figure 4**).

While δ^2H_{Tarax} values declined throughout the Little Ice Age (LIA), δ^2H_{Dino} values increased by ~35‰ (**Figure 4**). In the 20th century, the two values moved in tandem with each other, both rising until a few decades before the end of the century, and declining in the most recently deposited samples (**Figure 4**).

6.5.2 Trends in salinity and δ^2H_{water} calculated from a mangrove taraxerol source

Salinity values calculated using the paired isotope approach described in section 6.4.4 are -8 ± 5 for the in the 13th century, and decrease to -26 ± 5 in the late 14th century (**Figure 5**). Reconstructed salinity values trend upwards to a maximum of 9 ± 5 in late 18th century, and then decline to -16 ± 5 in the late 19th century. There is a subsequent increase to 10 ± 5 in the mid 20th century, followed by a decline to 3 ± 5 at the core top.

Reconstructed δ^2H_{Water} values vary from -38 ± 7‰ to 1 ± 7 (**Figure 5**). There is a general upward trend from the late 14th century value of -31 ± 7‰ to the late 18th century value of -2 ± 7‰. The highest δ^2H_{Water} values are from the late 20th century, and the core top value is -11 ± 7‰.

Reconstructed salinity and δ^2H_{Water} values were positively correlated with each other (**Figure 6a;** $R^2 = 0.17$; $p = 0.006$). The slope of this relationship was 0.4 ± 0.1‰ PSU^{-1} (**Figure 6a**). This slope is significantly shallower ($p < 0.0001$) than that of the relationship between salinity and δ^2H_{Water} in modern surface water in lakes on Palau's rock islands (**Figure 6b;** m = 1.16 ± 0.04).

6.5.3 Sedimentary δ^2H_{Tarax} model for variable mangrove inputs

Terrestrial δ^2H_{Tarax} values in the model decrease linearly from -174‰ to -221‰ as precipitation rate increases from 3-16 mm/day (**Figure 7**). For modern rainfall of 10 mm/day, the terrestrial δ^2H_{Tarax} is -199‰, within the analytical error of the coretop δ^2H_{Tarax} measurement (-198‰). The relationship between rainfall rate and expected mangrove δ^2H_{Tarax} is quadratic rather than linear. For the first scenario, where surface water salinity never exceeds that of seawater,

and increases by 1.2 for a 1 mm/day decrease in rainfall rate, mangrove $\delta^2H_{Tarax} = -0.11r^2 + 1.654r - 220.45$. Mangrove δ^2H_{Tarax} are highest at 6-9mm/day (-214‰) and lowest at 16mm/day (-220‰). In the high sensitivity scenario, where lake surface water is more sensitive to changes in rainfall rates, mangrove $\delta^2H_{Tarax} = -0.278r^2 + 5.359r - 240.85$. The range of mangrove δ^2H_{Tarax} values is larger in this scenario, and varies from -227‰ (r = 3 mm/day) to -216‰ (r = 8.5 – 11 mm/day) (**Figure 7**).

6.6 Discussion

6.6.1 Taraxerol sources in Clear Lake

Quantitative reconstructions of salinity and δ^2H_{Water} from paired dinosterol and taraxerol δ^2H values are only possible if the source of taraxerol is *Rhizophora* spp. mangroves. Terrestrial plants are incapable of using brackish lake water, and thus do not share their source water with the dinosterol-producing dinoflagellates. It is possible that the taraxerol in Clear Lake sediment was derived from a terrestrial, non-mangrove source.

No *Rhizophora* trees were present around Clear Lake during a repeat visit to the site in 2013, 9 years after the sediment core analyzed here was collected. *Rhizophora* was present at nearby Big Crocodile Lake, Spooky Lake, and Little Crocodile Lake. In a 2013 survey of 89 plants growing adjacent to Ongael Lake (Ongael Island, **Figure 2**), T Lake (Ngeruktabel Island, **Figure 2**), and Big Crocodile Lake (Mecherchar Island, **Figure 2**), 5 non-mangrove plants were found to produce significant quantities of taraxerol. None of these plants have been confirmed to be present at Clear Lake.

However, the measured core top δ^2H_{Tarax} value of -198 ± 10‰ indicates that terrestrial plants are the most likely source of sedimentary taraxerol in Clear Lake surface sediment, as

terrestrial plants are expected to have taraxerol values of ~199‰ under modern conditions, while *Rhizophora* should produce taraxerol with a δ^2H value of ~ -215‰, regardless of the sensitivity of surface water salinity to rainfall rates (**Figure 7**).

If taraxerol in the entire 800-year record was exclusively derived from non-mangrove sources, the ~20‰ decrease in δ^2H_{Tarax} throughout the LIA (**Figure 4**) would be best explained by an increase in rainfall rate of 4 – 6 mm/day rainier conditions in Palau (**Figure 7**). This increase in rainfall rate would be expected to make surface water in Clear Lake fresher (by 5-18, depending on the sensitivity) and more isotopically depleted (**Figure 3**). Lighter $\delta^2H_{Precipitation}$ values, increased freshwater input, and reduced evaporative enrichment would all combine to decrease δ^2H_{Water} values in the lake (**Figure 3**; *Smittenberg et al., 2011*). Lower δ^2H_{Water} values and lower salinity result in lower δ^2H_{Dino} values (*Sachs & Schwab, 2011; Smittenberg et al, 2011; Nelson & Sachs, 2014*). If rainfall rates increased by 4mm/day and salinity in Clear Lake increased by 5 (the low end of the estimates needed to produce the δ^2H_{Tarax} signal from terrestrial sources alone), surface water δ^2H values in Clear Lake would have decreased by ~11‰ This expectation contrasts with the ~35‰ increase in δ^2H_{Dino} in Clear Lake during the LIA (**Figure 4**).

Other variables can influence δ^2H values of algal lipids, but it seems unlikely that any known effect could account for the ~45‰ increase in $\alpha_{Dino\text{-}Water}$ that would be needed to overcome an 11‰ decrease in δ^2H_{Water} and produce a 35‰ increase in δ^2H_{Dino}. A decrease in temperature of 1°C causes $\alpha_{Lipid\text{-}Water}$ in phytoplankton to increase by about 0.5-5‰ (*Schouten et al., 2006; Wolhowe et al., 2009*; *Zhang et al., 2009*). Assuming a similar relationship for dinoflagellates, a minimum cooling of 9 °C would be necessary to produce the observed trend in

δ^2H_{Dino} values. Given that tropical SSTs only change by ~3°C on glacial-interglacial cycles (*Lea et al., 2006; Herbert et al., 2010*), a temperature shift of this magnitude is unlikely in Palau.

Isotope fractionation in algae is more sensitive to growth rate than to temperature (*Schouten et al., 2006; Zhang et al., 2009; Sachs & Kawka, in review*). In alkenones, fatty acids, and brasicasterol produced by the coccolithophorid *Emiliania huxleyi*, a 24-79‰ increase in $\alpha_{Lipid\text{-}Water}$ was associated with a reduction in growth rate of 1 division per day. Assuming a similar response in dinoflagellates, a reduction in growth rate of 0.5-1 division per day could result in the necessary 45‰ increase in $\alpha_{Dino\text{-}Water}$. It is unclear what mechanism could result in such a dramatic decrease in dinoflagellate growth rate in Clear Lake. Wetter conditions would be expected to bring more nutrient-rich run-off to the lake, which should stimulate growth. And any cause of decreased growth in Clear Lake would have had to result in a similar impact on growth in nearby Spooky Lake, where δ^2H_{Dino} increased at a similar rate during the LIA (*Sachs et al., 2009; Smittenberg et al., 2011*; **Figure 4**).

The magnitude of biosynthetic fractionation can vary among different types of algae (*Sauer et al., 2001; Zhang & Sachs, 2007*). Therefore, it is possible that a change in the dominant dinosterol producers from Clear Lake could produce a significant change in δ^2H_{Dino} values. However, similar relationships between salinity and $\alpha_{Dino\text{-}water}$ have been observed in a wide range of marine and lacustrine settings (*Sachs & Schwab, 2011; Nelson & Sachs, 2014*), which presumably encompass a correspondingly large range of dinosterol producers. As such, species-specific responses to salinity seem an unlikely mechanism to explain the time-varying δ^2H_{Dino} values. Additionally, the marine lakes of Palau's rock islands have been relatively stable ecosystems over the timeframe in question (*Hamner & Hamner, 1998*). Given the similarity between the Clear Lake and Spooky Lake δ^2H_{Dino} records, any change in species composition

would have to have taken place simultaneously in both lakes. Since the lakes are not physically connected to each other, this seems unlikely.

Based on current understanding of isotope fractionation in algae, therefore, the increase in δ^2H_{Dino} values throughout the LIA are most consistent with a trend towards drier conditions. In this context, the decrease in δ^2H_{Tarax} can be best explained by time-varying taraxerol contributions from terrestrial and *Rhizophora* sources. Mixing curves for different ratios of taraxerol sources are shown in **Figure 7**, and decreases in δ^2H_{Tarax} during relatively dry periods can be attributed to larger contributions from *Rhizophora*. This effect would be amplified if lower runoff rates during drier periods resulted in less delivery of organic material from higher in the catchment to the lake.

At times when the taraxerol source was mostly terrestrial trees, δ^2H_{Tarax} and δ^2H_{Dino} would be expected to covary. This is the case in the upper portion of the core (after ~1850 C.E.) (**Figure 8a**; $R^2 = 0.58$, $p = 0.02$). Prior to ~1850 C.E., δ^2H_{Tarax} and δ^2H_{Dino} are not correlated in Clear Lake sediment (**Figure 8b**; $R^2 = 0.05$, $p = 0.1$), which would be consistent with a less straightforward relationship between the two variables if taraxerol was derived from a mix of mangrove and terrestrial sources.

Carbon isotope fractionation in mangroves is also sensitive to salinity (*Ladd & Sachs, 2013*). Since mangrove lipid $\delta^{13}C$ values are positively correlated with salinity, they would be expected to increase at times when salinity increases. $\delta^{13}C$ measurements of Clear Lake taraxerol would thus be useful to help establish the likelihood of a mangrove source in this setting. These measurements are currently in progress, and will aid in the interpretation of this record.

6.6.2 Clear Lake, Palau salinity and δ^2H_{water} trends over the last millennium

The reconstruction of salinity and δ^2H_{Water} values shown in **Figure 5** argues against an exclusive *Rhizophora* source of sedimentary taraxerol in Clear Lake. To begin with, modern salinity is ~22, rather than the ~3 derived from the paired lipids, although modern δ^2H_{Water} values -13‰ are consistent with the calculated value of -11‰ (and the calculated value is identical to that of surface water during the repeat visit in 2013). Calculated salinity values are consistently too low, often less than 0, which is not physically possible. Even the positive salinity values seem implausibly low. If Clear Lake surface salinity is strongly dependent on rainfall rates, precipitation rates would have to increase to 16mm/day, higher than those observed anyway over the modern tropical Pacific (**Figure 1**), in order for surface water salinity to decrease to 4. Nearly all of the calculated salinity values fall below this threshold (**Figure 5**). Given these results and the lack of *Rhizophora* around the modern lake, it seems most likely *Rhizophora* was not the sole source of sedimentary taraxerol in Clear Lake over the past century, and that it is inappropriate to reconstruct salinity and δ^2H_{Water} values using equations 5 and 6 in this setting.

However, for reasons outlined in section **6.6.2**, the best explanation for increasing δ^2H_{Dino} values from 1400-1800 C.E. is saltier, ^{2}H-enriched surface water. All environmental changes that would result in saltier, ^{2}H-enriched water are ones that would correspond to a drier climate. As demonstrated in **Figure 7** it would be possible to explain decreasing δ^2H_{Tarax} values during drying in this interval by shifting contributions from mangrove and non-mangrove taraxerol sources. As such, the simplest climate explanation for the lipid isotope data presented here is a drying trend through the LIA.

6.6.3 Tropical Pacific hydrology in the Little Ice Age

There are two large-scale hydrologic reorganizations that could have produced drier conditions in Palau during the LIA: (1) a southward shift of the Intertropical Convergence Zone (ITCZ) or (2) a shift towards stronger El Niño activity (defined here as either more frequent or more intense El Niño events). Distinguishing between these two possibilities requires viewing the Clear Lake record in the context of the broader tropical Pacific basin. A southward shift in the ITCZ would be expected to manifest itself as a meridional change, with latitudes in the heart of the modern ITCZ becoming drier, and southern latitudes near the equator becoming wetter. Stronger El Niño activity, on the other hand, should manifest itself zonally, with drier conditions throughout the Indo-Pacific Warm Pool (IPWP) and increased precipitation in the central and eastern tropical Pacific.

A southwards shift in the ITCZ during the LIA is consistent with modeling results that indicate the mean annual position of the ITCZ is sensitive to northern hemisphere temperature forcings (*Chiang & Bitz, 2005; Broccoli et al., 2006*). It is also consistent with previously published biomarker data from Palau and Washington Islands (5°N), showing that these locations were dry during the LIA (*Sachs et al., 2009; Smittenberg et al., 2011*). At the same time, botryococcene δ^2H values from El Junco Lake on San Cristóbal Island in the Galapagos (1°S, just south of the modern range of the ITCZ) were relatively depleted, consistent with wetter conditions (*Sachs et al., 2009*). A grain size analysis from El Junco indicates that there was reduced frequency of high intensity precipitation events during the LIA, which was interpreted as reduced El Niño activity (*Conroy et al., 2008*). Together, these two records from El Junco are consistent with a wetter mean state for the lake due to a southward shift of the mean annual position of the ITCZ, with reduced ENSO driven precipitation variability.

The history of precipitation changes in El Junco is complicated by the relatively high elevation (670 m.a.s.l) of the lake. ~25% of annual precipitation in the Galapagos highlands is from Garua fog cloud interception during winter (*Pryet et al., 2012*). Therefore controls on precipitation in El Junco may be different than at low-elevation sites, which should be more indicative of marine conditions. A recent paired algal and mangrove biomarker reconstruction of salinity and δ^2H_{Water} from three coastal lakes on Isabella Island in the Galapagos indicates that both parameters decreased during the LIA, and is interpreted as wetter mean annual conditions without an El Niño driven increase local sea level (*Nelson & Sachs, in prep*). Such a hydrologic change is also consistent with a southward shift in the mean annual position of the ITCZ.

Decreases in terrestrial runoff in the northern hemisphere Cariaco Basin during the LIA have also been interpreted as the result of a southward shift in the ITCZ (*Haug et al., 2001*). Likewise, increased precipitation in Indonesia, as evidenced by decreases in leaf wax δ^2H values (*Tierney et al., 2010; Konecky et al., 2013*) and decreased sea surface salinity inferred from paired Mg/Ca and $\delta^{18}O$ values of foraminifera (*Newton et al., 2006; Oppo et al, 2009*), is also consistent with a southward shifted ITCZ.

Despite many lines of evidence that would support the hypothesis that the ITCZ shifted southward during the LIA, there is not unambiguous agreement from all existing tropical Pacific climate records. For example, Mg/Ca derived SSTs in the Makassar Straight indicate local cooling during the LIA (*Oppo et al., 2009*). Cooler SSTs support less deep convection and would not be expected to coincide with ITCZ driven rainfall. Cooler SSTs in the IPWP are also consistent with more El Niño like conditions, which also produce drier conditions in Palau (*Xie & Arkin, 1997*). However, these cooler SSTs coincide with wetter conditions in Indonesia (*Newton et al., 2006; Oppo et al., 2009; Tierney et al., 2010; Konecky et al., 2013*), suggesting

that a straightforward link between SST and precipitation rates is not appropriate, and that orographic effects from Indonesia may complicate interpretations in this region.

A precipitation record that is inconsistent with a southward shift in the ITCZ comes from Cattle Pond in the South China Sea, where lithogenic and isotopic proxies indicate a trend towards wetter conditions throughout the LIA (*Yan et al., 2011*). Since Cattle Pond is on the northern edge of the modern range of the ITCZ (**Figure 1**), a southward shift in the mean annual position of the ITCZ would be expected to result in drying conditions. However, rainfall rates in the South China Sea might be influenced by the East Asian Monsoon, and therefore not indicative of precipitation changes in the WPWP as a whole. Since Palau is further from the Asian landmass, the LIA drying trend from Clear Lake is more likely to indicate marine hydrologic conditions.

6.7 Conclusions

Paired taraxerol and dinosterol δ^2H values have the potential to allow quantitative reconstructions of salinity and water δ^2H values, which can help untangle the competing influence of changes in ENSO or the ITCZ (*Ladd & Sachs, in prep, Nelson & Sachs, in prep*). However, quantitative reconstructions of this nature are only possible in settings where mangroves are the major source of sedimentary taraxerol.

We measured taraxerol δ^2H values from a sediment core spanning 800 years in Clear Lake, Palau. An exclusive mangrove taraxerol source in this setting is not supported, as no *Rhizophora* is found around the modern lake, at least 5 terrestrial trees in the region produce taraxerol, and reconstructing salinity assuming a mangrove source results in unrealistically low values. However, taraxerol δ^2H values increased by ~20‰ during the Little Ice Age (LIA; ~1400

C.E. - ~1800 C.E.), while dinosterol δ^2H values decreased by ~35‰. These divergent trends are difficult to explain if all sedimentary taraxerol came from terrestrial sources, suggesting variable mangrove contributions to the sediment over time.

The most plausible interpretation of the paired lipid isotopes from this record is that salinity and water δ^2H values in Clear Lake increased throughout the LIA, indicating drying conditions in Palau throughout this time. This drying trend corresponds to wetter conditions in southern hemisphere sites in Indonesia and the Galapagos, and supports the hypothesis that the ITCZ shifted south during the LIA. However, drying due to changes in ENSO activity cannot be ruled out using this data. Higher spatial density of climate reconstructions from the tropical Pacific will help disentangle the competing influence variability due to ENSO and the ITCZ's mean annual position.

6.8 References

Atwood, A. R. & Sachs, J. P. (2014) Separating ITCZ- and ENSO-related rainfall changes in the Galápagos over the last 3 kyr using D/H ratios of multiple lipid biomarkers. *Earth and Planetary Science Letters* 404, 408-419.

Bjerknes, J. (1969) Atmospheric teleconnections from the equatorial Pacific. *Mon.Weather Rev.* 97:163–72.

Bowen, G. J. (2008) Spatial analysis of the intra-annual variation of precipitation isotope ratios and its climatological corollaries. *J. Geophys. Res*. 113. doi:10.1029/2007JD009295 D05113.

Broccoli, A. J., Dahl, K. A., & Stouffer, R. J. (2006) Response of the ITCZ to Northern Hemisphere cooling. *Geophysical Research Letters, 33*(1). doi: 10.1029/2005gl024546

Chiang, J. C. H. (2009) The tropics in paleoclimate. *Annual Review of Earth and Planetary Sciences* 37, 263-297.

Chiang J. C. H., Bitz C. M. (2005) Influence of high latitude ice cover on the marine Intertropical Convergence Zone. *Clim. Dyn*. 25, 477–96

Chikaraishi Y. & Naraoka H. (2003) Compound-specific δD- δ13C analyses of *n*-alkanes extracted from terrestrial and aquatic plants. *Phytochemistry* 63, 361-371.

Chivall, D., M'Boule, D., Sinke-Schoen, D., Sinninghe Damsté, J.S., Schouten, S. & van der Meer, M. T. J. (2014) The effects of growth phase and salinity on the hydrogen isotopic composition of alkenones produced by coastal haptophyte algae. *Geochimica et Cosmochimica Acta* 140, 381-390.

Conroy, J. L., Overpeck, J. T., Cole, J. E., Shanahan, T. M. & Steinitz-Kannan, M. (2008)

Holocene changes in eastern tropical Pacific climate inferred from a Galápagos lake sediment record. *Quaternary Science Reviews, 27* 1166-1180.
Craig H. & Gordon L. (1965) Deuterium and oxygen 18 variations in the ocean and the marine atmosphere. In *Proceedings of a Conference on Stable Isotopes in Oceanographic Studies and Paleotemperatures* (ed E. Tongiori). CNR-Laboratorio di Geologia Nucleare, Pisa. pp. 9-130.
Dansgaard W. (1964) Stable isotopes in precipitation. *Tellus* 16, 436-468.
Feakins, S. J., Kirby, M. E., Cheetham, M. I., Ibarra, Y. & Zimmerman, S. R. H. (2014) Leaf wax D/H reconstructions of late Holocene hydroclimate from Zaca Lake, California, *Organic Geochemistry* 66, 48-59.
Feakins S. J. & Sessions A. L. (2010) Controls on the D/H ratios of plant leaf waxes in an arid ecosystem. *Geochimica Cosmochimica Acta* 74, 2128-2141.
Feakins, S. J., Warny, S. & Lee, J. E. (2012) Hydrologic cycling over Antarctica during the Middle Miocene warming, *Nature Geoscience*, doi:10.1038/NGEO1498.
Gat, J. R. (1996) Oxygen and hydrogen isotopes in the hydrologic cycle. *Annual Review in Earth and Planetary Sciences* 24, 225-262.
Hamner W. M. and Hamner P. P. (1998) Stratified marine lakes of Palau (Western Caroline Islands). *Physical Geography* 19, 175-220.
Haug, G. H., Hughen, K. A., Sigman, D. M., Peterson, L. C. & Röhl, U. (2001) Southward Migration of the Intertropical Convergence Zone Through the Holocene. *Science* 293, 1304-1308.
Herbert, T. D., Peterson, L. C., Lawrence, K. T. & Liu, Z. (2010) Tropical ocean temperatures over the past 3.5 million years. *Science* 328, 1530-1534.
Hou J., D'Andrea W., MacDonald D. & Huang Y. S. (2007) Hydrogen isotopic variability in leaf waxes among terrestrial and aquatic plants around Blood Pond, Massachusetts (USA). *Organic Geochemistry* 38, 977-984.
Huang, Y., Shuman, B., Wang, Y. & Webb III, T. (2002) Hydrogen isotope ratios of palmitic acid in lacustrine sediments record late Quaternary climate variations. *Geology* 30, 1103-1106.
Huang, Y., Shuman, B., Wang, Y. & Webb, T. (2004) Hydrogen isotope ratios of individual lipids in lake sediments as novel tracers of climatic and environmental change: a surface sediment test. *Journal of Paleolimnology* 31, 363-375.
Julian, P. R. & Chervin R. M. (1978), A study of the Southern Oscillation and Walker circulation phenomenon, *Mon. Weather Rev*. 106, 1433–1451.
Kahmen A., Hoffmann B., Schefuss E., Arndt S.K., Cernusak L. A., West J. B. & Sachse D. (2013a) Leaf water deuterium enrichment shapes leaf wax n-alkane dD values of angiosperm plants II: Observational evidence and global implications. *Geochimica et Cosmochimica Acta* 111, 50-63.
Kahmen A., Schefuss E. & Sachse D. (2013b) Leaf water deuterium enrichment shapes leaf wax *n*-alkane dD values of angiosperm plants I: Experimental evidence and mechanistic insights. *Geochimica et Cosmochimica Acta* 111, 39-49.
Kasper, S., van der Meer, M. T. J., Mets, A., Zahn, R., Sinninghe Damsté, J. S. & Schouten, S., (2014) Salinity changes in the Agulhas leakage area recorded by stable hydrogen isotopes of C37 alkenones during Termination I and II. *Clim. Past* 10, 251-260.
Killops S. D. & Frewin N. L. (1994) Triterpenoid diagenesis and cuticular preservation. *Organic Geochemistry* 21, 1193-1209.

Koch B. P., Rullkotter J., & Lara R. J. (2003) Evaluation of triterpenols and sterols as organic matter biomarkers in a mangrove ecosystem in northern Brazil. *Wetlands Ecology and Management* 11, 257-263.

Konecky, B. L., Russell, J. M., Rodysill, J. R., Vuille, M., Bijaksana, S. & Huang, Y. (2012). Intensification of southwestern Indonesian rainfall over the past millennium. *Geophysical Research Letters*. doi: 10.1029/2012gl054331

Kurita N., Ichiyanagi K., Matsumoto J., Yamanaka M. D. & Ohata T. (2009) The relationship between the isotopic content of precipitation and the precipitation amount in tropical regions. *Journal of Geochemical Exploration* 102, 113-122.

Ladd S. N. & Sachs J. P. (2012) Inverse relationship between salinity and *n*-alkane δD values in the mangrove *Avicennia marina*. *Organic Geochemistry* 48, 25-36.

Ladd S. N. & Sachs J. P. (2013) Positive correlation between salinity and *n*-alkane d13C values in the mangrove *Avicennia marina*. *Organic Geochemistry* 64, 1-8.

Ladd, S. N. & Sachs, J. P. (in prep.) Influence of salinity on hydrogen isotope fractionation in *Rhizophora* mangroves from Micronesia.

Lea, D. W., Pak, D. K., Belanger, C. L., Spero, H. J., Hall, M. A., Shackleton, N. J. (2006) Paleoclimate history of Galapagos surface waters over the last 135,000 yr. *Quaternary Science Reviews* 25, 1152-1167.

Legates, D. R. & Willmott, C. J. (1990) Mean seasonal and spatial variability in gauge-corrected, global precipitation. *Int. J. Climatol*. 10, 111-127

Liu W. G. & Yang H. (2008) Multiple controls for the variability of hydrogen isotopic compositions in higher plant *n*-alkanes from modern ecosystems. *Global Change Biology* 14, 2166-2177.

Liu W. G., Yang H. & Li L. (2006) Hydrogen isotopic composition of *n*-alkanes from terrestrial plants correlate with their ecological life form. *Oecologia* 150, 330-338.

Nelson, D. B. & Sachs, J. P. (2013) Concurrent Purification of Sterols, Triterpenols and Alkenones from Sediments for Hydrogen Isotope Analysis using High Performance Liquid Chromatography. *Organic Geochemistry* 64, 19-28.

Nelson, D. B. & Sachs, J. P. (2014) The influence of salinity on D/H fractionation in dinosterol and brassicasterol from globally distributed saline and hypersaline lakes. *Geochimica et Cosmochimica Acta*, 133, 325-339.

Nelson, D. B. & Sachs, J. P. (In prep) "Galapagos rainfall changes in the Common Era."

Newton, A., Thunell, R. & Stott, L. (2006). Climate and hydrographic variability in the Indo-Pacific Warm Pool during the last millennium. *Geophysical Research Letters, 33* doi: 10.1029/2006gl027234

Niedermeyer, E., Sessions, A. L., Feakins, S. J. & Mohtadi, M., 2014. Hydroclimate of the western Indo Pacific Warm Pool during the past 24,000 years, *Proceedings of the National Academy of Sciences* 111, 9402-9406.

Oppo, D. W., Rosenthal, Y. & Linsley, B. K. (2009). 2,000-year-long temperature and hydrology reconstructions from the Indo-Pacific warm pool. *Nature* 460, 1113-1116.

Pahnke, K., Sachs, J. P., Keigwin, L. D., Timmermann, A. & Xie, S. P. (2007) Eastern tropical Pacific hydrologic changes during the past 27,000 years from D/H ratios in alkenones. *Paleoceanography* 22, PA4214, 15pp.

Pierrehumbert R. T. (2000) Climate change and the tropical Pacific: The sleeping dragon wakes. *Proc. Natl. Acad. Sci.* 97, 1355–1358

Polissar P. J. & Freeman K. H. (2010) Effects of aridity and vegetation on plant-wax δD in modern lake sediments. *Geochimica et Cosmochimica Acta* 74, 5785-5797.

Pryet, A., Dominguez, C., Tomai, P. F., Chaumont, C., d'Ozouville, N., Villacis, M. & Violette, S. (2012) Quantification of cloud water interception along the wind- ward slope of Santa Cruz Island, Galápagos (Ecuador). *Agric. For. Meteorol*. 161, 94–106

Rach, O., Brauer, A., Wilkes, H. & Sachse, D. (2014) Delayed hydrological response to Greenland cooling at the onset of the Younger Dryas in western Europe. *Nature Geosci* 7, 109-112

Richey, J. N. & Sachs, J. P. (in prep) "Precipitation in the western tropical Pacific over the past millenium."

Sachs, J. P. & Kawka, O. (in review) "The influence of nitrogen-limited growth rate on hydrogen isotope fractionation in the coccolithophorid *Emiliania huxleyi*."

Sachs, J. P., Sachse, D., Smittenberg, R. H., Zhang, Z., Battisti, D. S. & Golubic, S. (2009) Southward movement of the Pacific intertropical convergence zone AD 1400–1850. *Nature Geoscience* 2, 519-525.

Sachs, J. P. & Schwab, V. F. (2011) Hydrogen isotopes in dinosterol from the Chesapeake Bay estuary. *Geochimica et Cosmochimica Acta* 75, 444-459.

Sachse D., Billault I., Bowen G. J., Chikaraishi Y., Dawson T. E., Feakins S. J., Freeman K. H., Magill C. R., McInerney F. A., van der Meer M. T. J., Polissar P., Robins R. J., Sachs J. P., Schmidt H. L., Sessions A. L., White J. W. C., West. J. B. & Kahmen A. (2012) Molecular paleohydrology: interpreting the hydrogen-isotopic composition of lipid biomarkers from photosynthesizing organisms. *Annual Review of Earth and Planetary Science* 40, 212-249.

Sachse D., Radke J. & Gleixner G. (2004) Hydrogen isotope ratios of recent lacustrine sedimentary *n*-alkanes record modern climate variability. *Geochimica et Cosmochimica Acta* 68, 4877-4889.

Sachse, D., & Sachs, J. P. (2008) Inverse relationship between D/H fractionation in cyanobacterial lipids and salinity in Christmas Island saline ponds. *Geochimica et Cosmochimica Acta, 72*(3), 793-806.

Sauer P. E., Eglinton T. I., Hayes J. M., Schimmelmann A., Sessions A. L. (2001) Compound-specific D/H ratios of lipid biomarkers from sediments as a proxy for environmental and climatic conditions. *Geochimica et Cosmochimica Acta* 65, 213-222.

Schouten, S., Ossebaar, J., Schreiber, K., Kienhuis, M. V. M., Langer, G., Benthien, A., Bijma & J. (2006) The effect of temperature, salinity and growth rate on the stable hydrogen isotopic composition of long chain alkenones produced by *Emiliania huxleyi* and *Gephyrocapsa oceanica*. *Biogeosciences* 3, 113-119.

Sessions A. L., Burgoyne T. W., Schimmelmann A. & Hayes J. M. (1999) Fractionation of hydrogen isotopes in lipid biosynthesis. *Organic Geochemistry* 30, 1193-1200.

Smith F. A. & Freeman K. H. (2006) Influence of physiology and climate on δD of leaf wax *n*-alkanes from C_3 and C_4 grasses. *Geochimica et Cosmochimica Acta* 70, 1172-1187.

Smittenberg, R. H., Saenger, C., Dawson, M. N. & Sachs, J. P. (2011). Compound-specific D/H ratios of the marine lakes of Palau as proxies for West Pacific Warm Pool hydrologic variability. *Quaternary Science Reviews* 30, 921-933.

Spencer, R.W. (1993) Global oceanic precipitation from the MSU during 1979-91 and comparisons to other climatologies. J. Clim. 6, 1301-1326.

Tierney, J. E., Oppo, D. W., Rosenthal, Y., Russell, J. M., & Linsley, B. K. (2010) Coordinated

hydrological regimes in the Indo-Pacific region during the past two millennia. *Paleoceanography* 25, doi: 10.1029/2009pa001871

Tipple B. J., Berke M., Hambach B., Roden J. S. & Ehleringer J. R. (In Press) Predicting leaf wax *n*-alkane (2) H/(1) H ratios: controlled water source and humidity experiments with hydroponically grown trees confirm predictions of Craig-Gordon model. *Plant, Cell and Environment*. doi: 10.1111/pce.12457.

Tipple, B. J. & Pagani, M. (2013) Environmental control on eastern broadleaf forest species' leaf wax distributions and D/H ratios. *Geochimica et Cosmochimica Acta* 111, 64-77.

Trenberth K. E., Branstator G.W., Karoly D., Kumar A., Lau N.-C. & Ropelewski C. (1998) Progress during TOGA in understanding and modeling global teleconnections associated with tropical sea surface temperatures. *J. Geophys. Res*. 103, 14291–14324

van der Meer, M., Baas, M., Rijpstra, W., Marino, G., Rohling, E., Damste, J. S. S. & Schouten, S. (2007) Hydrogen isotopic compositions of long-chain alkenones record freshwater flooding of the Eastern Mediterranean at the onset of sapropel deposition. *Earth and Planetary Science Letters* 262, 594-600.

Vasiliev, I., Reichart, G.-J. & Krijgsman, W. (2013) Impact of the Messinian Salinity Crisis on Black Sea hydrology—Insights from hydrogen isotopes analysis on biomarkers. *Earth and Planetary Science Letters* 362, 272-282.

Vecchi, G. A., Soden, B. J., Wittenberg, A. T., Held, I. M., Leetmaa, A. & Harrison, M. J. (2006) Weakening of tropical Pacific atmospheric circulation due to anthropogenic forcing. *Nature* 441, 73-76

Versteegh, G. J. M, Schefub, E., Dupont, L., Marret, F., Sinninghe Damaste, J. & Jansen, J. H. F. (2002) Taraxerol and *Rhizophora* pollen as proxies for tracking past mangroves ecosystems. *Geochimica et Cosmochimica Acta* 68, 411-422.

Volkman, J. K. (2003) Sterols in microorganisms. *Applied Microbiology and Biotechnology* 60, 495-506.

Wallace, J. M. & Gutzler, D. S. (1981) Teleconnections in the geopotential height field during the Northern Hemisphere winter. *Mon. Weather Rev*. 109, 784–812.

Wang, C. & D. B. Enfield (2003) A Further Study of the Tropical Western Hemisphere Warm Pool. *Journal of Climate* 16, 1476-1493.

Wang, H. & Mehta, V. M. (2008) Decadal Variability of the Indo-Pacific Warm Pool and Its Association with Atmospheric and Oceanic Variability in the NCEP–NCAR and SODA Reanalyses. *Journal of Climate* 21, 5545-5565.

Wolhowe, M., Prahl, F., Probert, I. & Maldonado, M. (2009) Growth phase dependent hydrogen isotopic fractionation in alkenone-producing haptophytes. *Biogeosciences* 6, 4165-4200.

Xie P. P. & Arkin P. A. (1997) Global precipitation: A 17-year monthly analysis based on gauge observations, satellite estimates, and numerical model outputs. *Bull. Am. Meteorol. Soc.* 78, 2539–2558.

Yan, H., Sun, L., Wang, Y., Huang, W., Qiu, S. & Yang, C. (2011). A record of the Southern Oscillation Index for the past 2,000 years from precipitation proxies. *Nature Geoscience* 4, 611-614

Yang H., Pagani, M., Briggs, D. E. G., Equiza, M. A., Jagels, R., Leng, Q. & LePage, B. A. (2009) Carbon and hydrogen isotope fractionation under continuous light: implications for paleoenvironmental interpretations of the High Arctic during Paleogene warming. *Oecologia* 160, 461-470.

Zhang, Z., Leduc, G. & Sachs, J. P. (2014) El Niño evolution during the Holocene revealed by a biomarker rain gauge in the Galápagos Islands. *Earth and Planetary Science Letters* 404, 420-434.
Zhang, Z. & Sachs, J. P. (2007). Hydrogen isotope fractionation in freshwater algae: I. Variations among lipids and species. *Organic Geochemistry* 38, 582-608.
Zhang Z., Sachs J. P. & Marchetti A. (2009) Hydrogen isotope fractionation in freshwater and marine algae: II. Temperature and nitrogen limited growth rate effects. *Organic Geochemistry* 40, 428-439.

Figure captions:

Figure 1 Mean annual precipitation in the tropical Pacific from 1979-2010 in mm/day. Palau and other site mentioned in the text are indicated by numbers 1-4. Precipitation data is from the Global Precipitation Climatology Project (GPCP) and provided by the NOAA/OAR/ESRL PSD, Boulder, Colorado, USA, from their Web site at http://www.esrl.noaa.gov/psd/

Figure 2 Map of Palau and lake referenced in the text. The vegetation survey included plants from Ongael and Ngeruktabel islands. Figure adapted from Smittenberg et al. (*2011*).

Figure 3 Predicted salinity, lake water δ^2H values and precipitation δ^2H values for different rainfall rates. Precipitation δ^2H values are based on the local amount effect, described by Kurita et al. (*2009*). Dark, solid lines represent the scenario where surface water is less sensitive to changes in rainfall rates; light, dashed lines represent the high sensitivity scenario.

Figure 4 Measured taraxerol and dinosterol δ^2H values from Clear and Spooky Lake. Error bars represent one standard deviation of triplicate measurements.

Figure 5 Salinity and water δ^2H values in Clear Lake over time, as reconstructed from taraxerol and dinosterol δ^2H values and assuming an exclusive mangrove source for taraxerol. Error bars represent average standard deviations from a 1000 iteration Monte Carlo that took into account instrumental errors and uncertainty in the calibration curves for the relationships between salinity and isotope fractionation for both dinosterol and mangrove derived taraxerol.

Figure 6 (a) Calculated water δ^2H values versus salinity in Clear Lake, compared to the relationship between the two variables in surface water in modern Palau marine lakes (b).

Figure 7 Modeled taraxerol δ^2H values as a function of rainfall rate for low (a) and high (b) sensitivity scenarios shown in figure 3. Plotted curves represent a 100% terrestrial source for taraxerol (dark green), a 0% terrestrial source (100% mangrove; dark blue), and representative sedimentary values for a mix of the two sources (green = 70% terrestrial; teal = 50% terrestrial; light blue = 30% terrestrial). Dashed lines represent measured sedimentary taraxerol δ^2H values for the core top, late 18^{th} century, and late 14^{th} century.

Figure 8 Linear regression of measured δ^2H_{Tarax} values versus δ^2H_{Dino} values for (a) pre- and (b) post-1850 C.E.

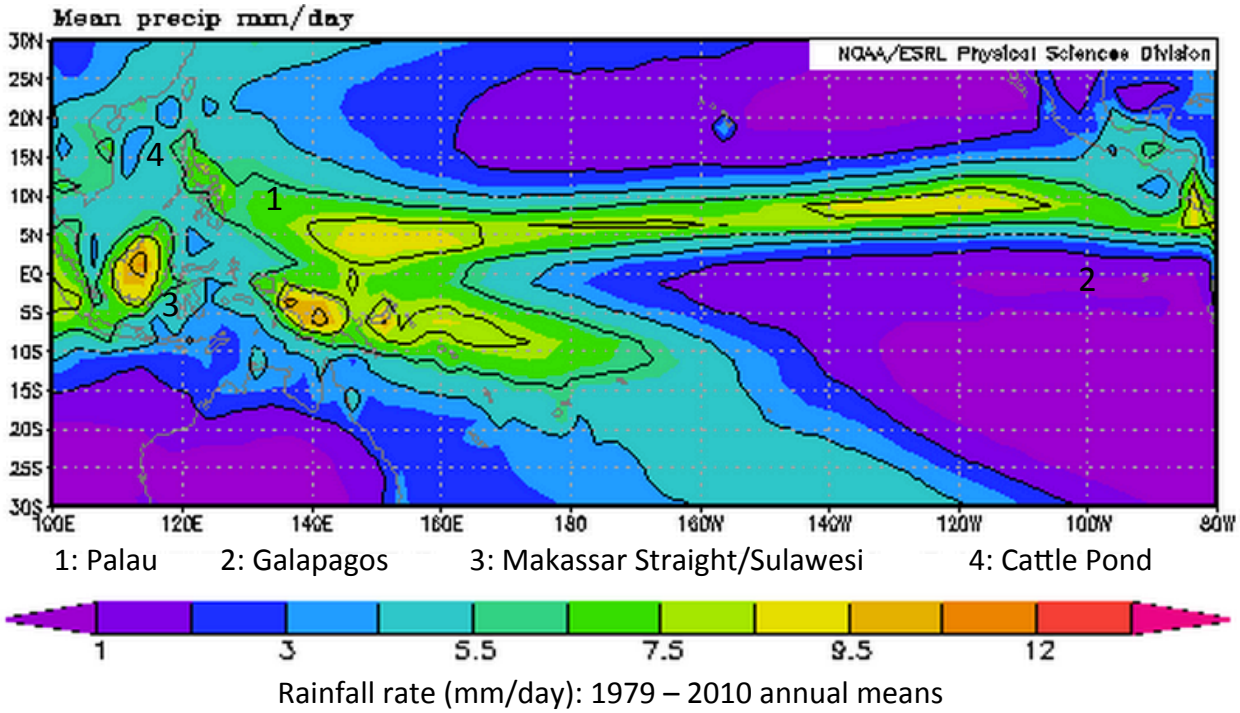

Figure 1 Mean annual precipitation in the tropical Pacific from 1979-2010 in mm/day. Palau and other site mentioned in the text are indicated by numbers 1-4. Precipitation data is from the Global Precipitation Climatology Project (GPCP) and provided by the NOAA/OAR/ESRL PSD, Boulder, Colorado, USA, from their Web site at http://www.esrl.noaa.gov/psd/

Figure 2 Map of Palau and lake referenced in the text. The vegetation survey included plants from Ongael and Ngeruktabel islands. Figure adapted from Smittenberg et al. (*2011*).

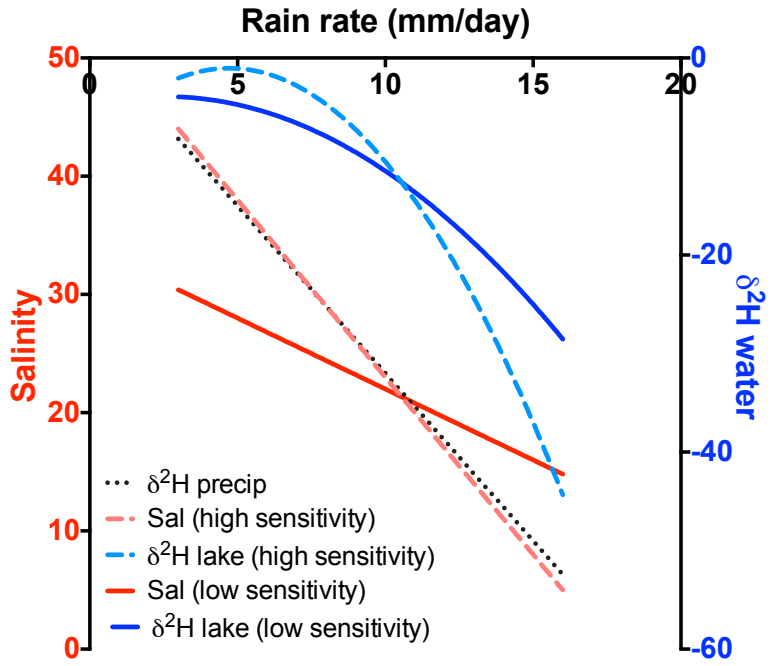

Figure 3 Predicted salinity, lake water δ^2H values and precipitation δ^2H values for different rainfall rates. Precipitation δ^2H values are based on the local amount effect, described by Kurita et al. (*2009*). Dark, solid lines represent the scenario where surface water is less sensitive to changes in rainfall rates; light, dashed lines represent the high sensitivity scenario.

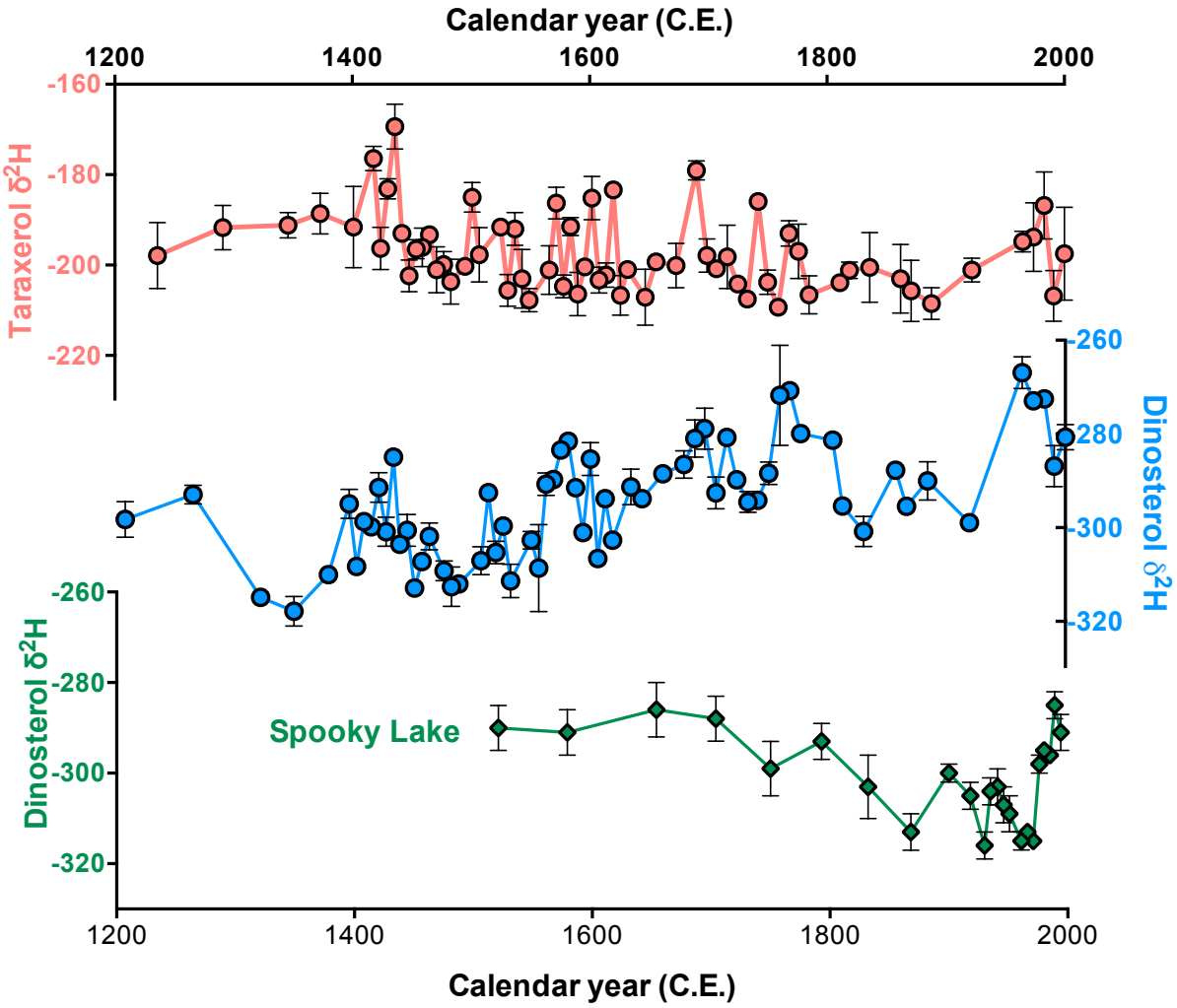

Figure 4 Measured taraxerol and dinosterol δ^2H values from Clear and Spooky Lake. Error bars represent one standard deviation of triplicate measurements.

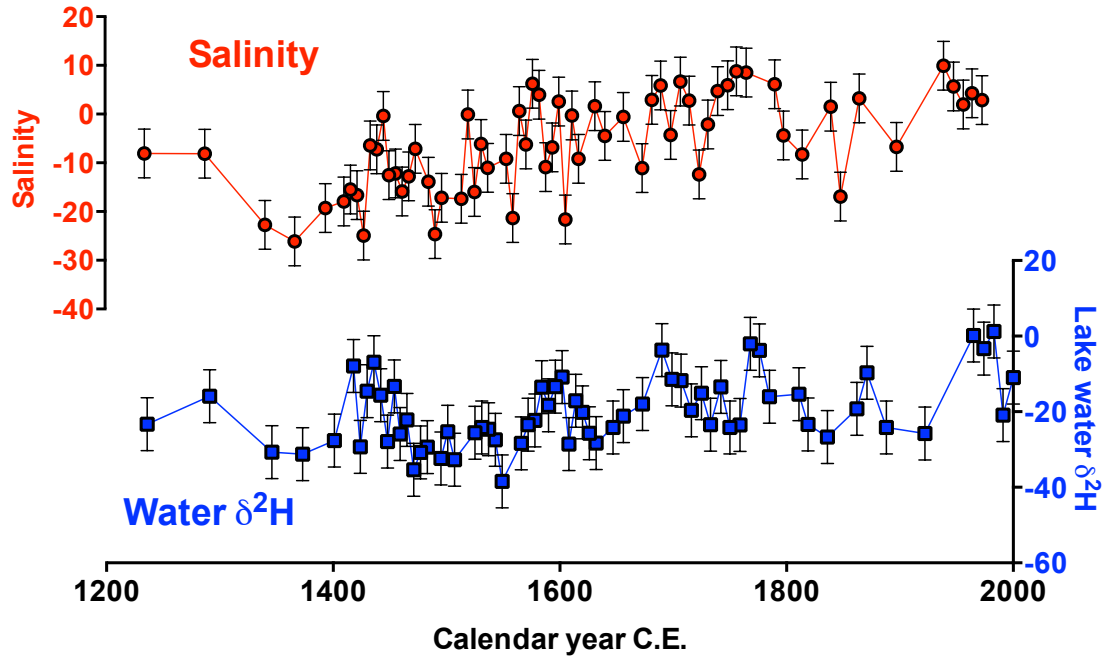

Figure 5 Salinity and water δ^2H values in Clear Lake over time, as reconstructed from taraxerol and dinosterol δ^2H values and assuming an exclusive mangrove source for taraxerol. Error bars represent average standard deviations from a 1000 iteration Monte Carlo that took into account instrumental errors and uncertainty in the calibration curves for the relationships between salinity and isotope fractionation for both dinosterol and mangrove derived taraxerol.

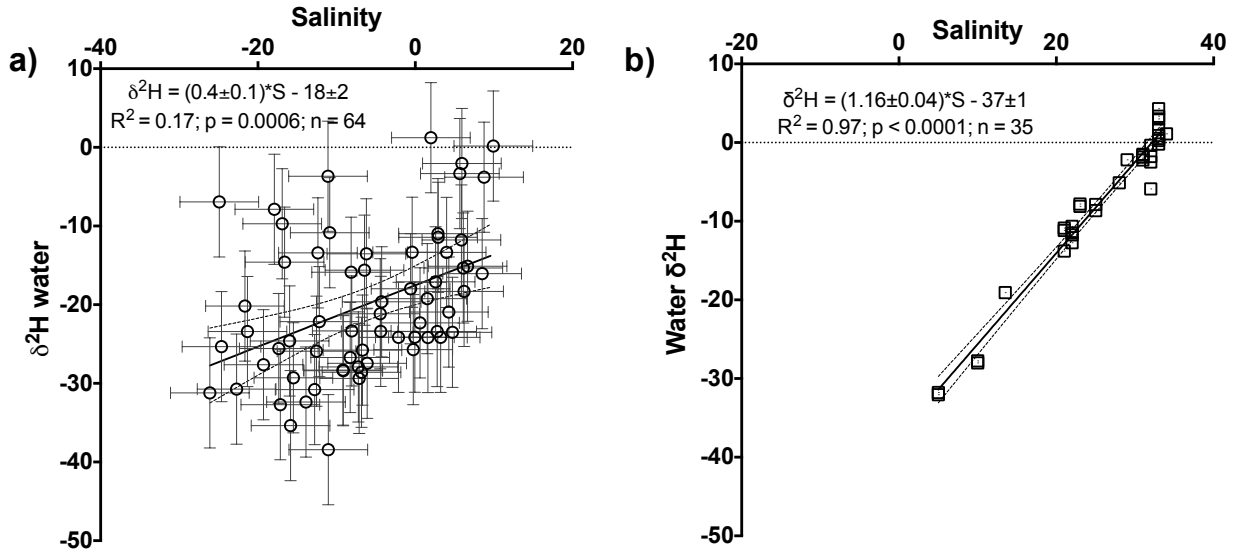

Figure 6 (a) Calculated water δ^2H values versus salinity in Clear Lake, compared to the relationship between the two variables in surface water in modern Palau marine lakes (b).

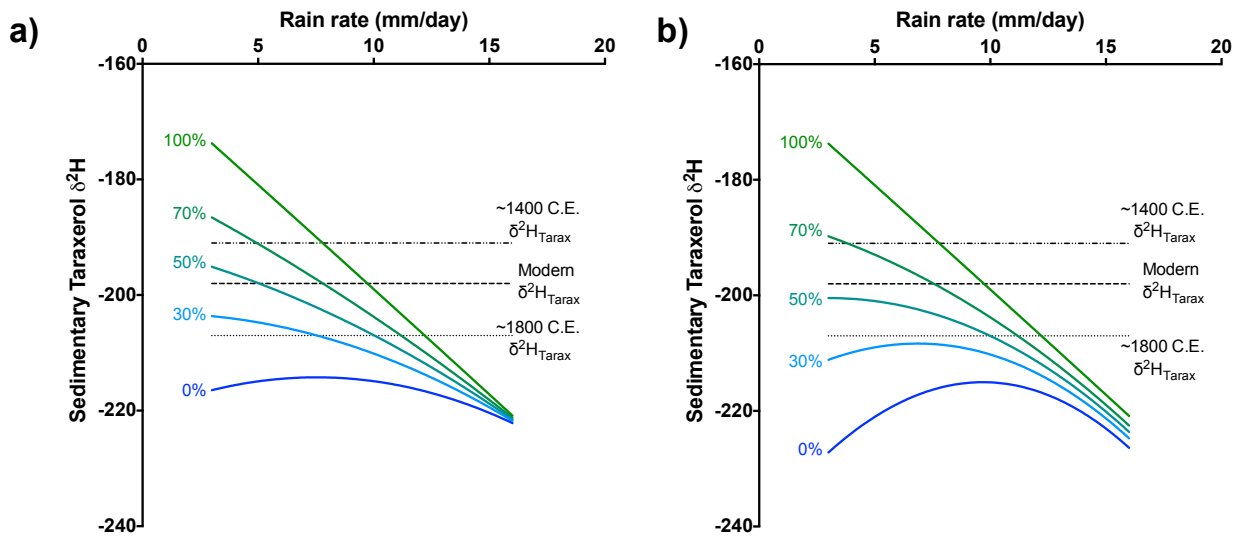

Figure 7 Modeled taraxerol δ^2H values as a function of rainfall rate for low (a) and high (b) sensitivity scenarios shown in figure 3. Plotted curves represent a 100% terrestrial source for taraxerol (dark green), a 0% terrestrial source (100% mangrove; dark blue), and representative sedimentary values for a mix of the two sources (green = 70% terrestrial; teal = 50% terrestrial; light blue = 30% terrestrial). Dashed lines represent measured sedimentary taraxerol δ^2H values for the core top, late 18th century, and late 14th century.

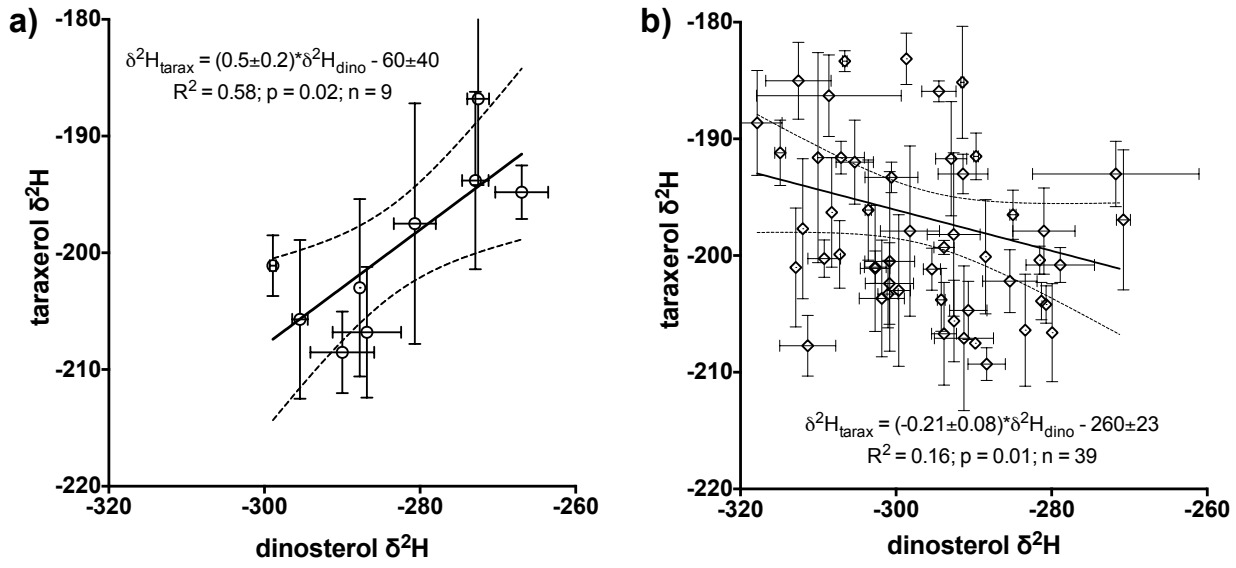

Figure 8 Linear regression of measured δ^2H_{Tarax} values versus δ^2H_{Dino} values for (a) pre- and (b) post-1850 C.E.